Nuclear export and cytoplasmic localisation of mRNA in *Drosophila melanogaster*

Gavin S. Wilkie

PhD Thesis

The University of Edinburgh

May, 2001

For Margaret

ABSTRACT

The genetic material in all eukaryotic cells is stored in the nucleus, a distinct compartment separated from the cytoplasm by the nuclear envelope. Consequently, an essential step in gene expression is the export of mRNA from the nucleus to the cytoplasm. There is also increasing evidence that asymmetric transcript localisation in the cytoplasm is an important mechanism for intracellular protein targeting and for the generation of cellular polarity. However, the factors involved in mRNA export are only beginning to be characterised in detail and the mechanism of mRNA localisation is poorly understood in most cases.

This thesis defines the entire pathway of mRNA movement in *Drosophila* embryonic blastoderm nuclei, from intranuclear sites of synthesis to final sites of localisation in the cytoplasm. It shows that transcription of individual genes can take place in all parts of the nucleus and that genes are not significantly redistributed to new positions when they become active. Furthermore, mRNA export intermediates in the nucleus are evenly distributed, consistent with their movement occurring by unconstrained diffusion within the nucleoplasm.

In order to identify proteins involved in intracellular mRNA transport, a genetic screen was designed to isolate mutations disrupting the correct cytoplasmic distribution of mRNA. It was found that *small bristles* is required for the nuclear export of mRNA in *Drosophila*, and that this gene encodes a homologue of the human and yeast nuclear mRNA export factors TAP/NXF1 and Mex67p, respectively.

Finally, the localisation of pair-rule and *wingless* transcripts to the apical cytoplasm of *Drosophila* embryos is shown to occur by active transport of mRNA in the cytoplasm, rather than diffusion and anchoring or asymmetric nuclear export. Apical mRNA localisation is mediated by the transport of RNA particles to the minus ends of microtubules by the molecular motor cytoplasmic dynein.

It is very likely that these findings in *Drosophila* will be applicable to other organisms. There is evidence that mRNA moves through the nucleoplasm by diffusion in other systems, and the machinery of mRNA export appears to be conserved throughout evolution from yeast to humans. Dynein is involved in the transport of many different cytoplasmic cargoes and is also a good candidate for the transport of mRNA in the oocyte and in other organisms.

PREFACE

This thesis is my own work, and the experiments described in it were performed by myself (unless otherwise stated) while working at the Institute of Cell and Molecular Biology, University of Edinburgh. I would like to thank my supervisor, Ilan Davis, for encouraging me to become a PhD student instead of a technician, and for the enormous amount of training, support and encouragement he has invested during my time in the lab. I would also like to thank Ilan for introducing me to the amazing world of very small things via our DeltaVision microscope, which has been both a source of inspiration and an essential tool for this work. I would like to acknowledge David Finnegan, my second supervisor, for advice and encouragement. I am indebted to the Medical Research Council for their generous financial support.

I am grateful to my fellow lab members Nina MacDougall and Hille Tekotte for help with numerous tasks, especially fly work. I would also like to thank other members of the institute who have contributed to this research or my general state of happiness, including Andrew Jarman, David Prentice, Paul Taylor, Sarah Goulding, Petra zur Lage, Bridget Lovegrove, Neil White, Ifat Ahmed, Adrian Bird, Andreas Merdes, Joe Lewis, Liz Thompson, Yiota Kafasla, Lubna Arif, Hiro Okhura, Chris Jeffrey and John Findlay.

Furthermore, I am indebted to my colleagues in other institutes who have generously shared data and reagents. I would particularly like to thank David Ish-Horowicz, Simon Bullock, Sabbi Lall, David Van Vactor, Christopher Korey, William Sullivan, Helen Francis-Lang, David Sharp, Tom Hays, Elena Kiseleva and Ludmilla Mamon.

Finally, I would like to thank Anna for her selfless support and coffee-making abilities, and Margaret for her smiles.

OCTOBER 2001.

TABLE OF CONTENTS

ABBREVIATIONS

3'UTR	3' untranslated region
5'UTR	5' untranslated region
bcd	*bicoid*
BDGP	Berkeley *Drosophila* Genome Project
bp	base pair
BR	Balbiani ring
CCD	charge coupled device
CTE	constitutive transport element
cy3	cyanine 3
cy5	cyanine 5
DIC	diffraction interference contrast
DAPI	4,6-diamidino-2-phenylindole
dhc	dynein heavy chain
DIG	Digoxygenin
EDGP	European *Drosophila* Genome Project
EMS	ethyl methane sulphate
en	*engrailed*
EST	expressed sequence tag
FISH	fluorescence *in situ* hybridisation
FITC	fluorescein isothiocyanate
ftz	*fushi tarazu*
GFP	green fluorescent protein
GST	glutathione-S-transferase
grk	*gurken*
h	*hairy*
hb	*hunchback*
HSP	heat shock protein
HYB	hybridisation buffer
hkb	*huckebein*
kb	kilobase
kni	*knirps*
kDa	kilo Dalton
kr	*kruppel*
lacZ	β-galactosidase
MBP	myelin basic protein
mRNA	messenger RNA
MTOC	microtubule organising centre
NA	numerical aperture
NE	nuclear envelope
nls	nuclear localisation signal
NPC	nuclear pore complex
ORF	open reading frame
osk	*oskar*
PBS	phosphate buffered saline
PBT	PBS + 0.1% Tween 20
P*CR*	*po*lymerase chain re*action*
prd	*paired*
*R*T-PCR	reverse transcription PCR
run	*runt*
sbr	*small bristles*
stg	*string*
STS	sequence tagged site
ts	temperature sensitive
TSA	tyramide signal amplification
TGFα	transforming growth factor alpha
Ubx	*Ultrabithorax*
VE-DIC	video enhanced DIC
wg	*wingless*

LIST OF FIGURES

LIST OF TABLES

1

INTRODUCTION

A key aspect of the function and diversity of eukaryotic cells is regional specialisation within the cytoplasm. This is achieved by compartmentalisation of the cell into organelles and other specialised regions, and by the sorting of proteins and nucleic acids to different subcellular locations. Such a system requires transport between different compartments, for example the export of newly synthesised mRNA from the nucleus, or the targeting of specific proteins for import into mitochondria or the endoplasmic reticulum. Furthermore, some proteins are localised to regions of the cytoplasm outwith membrane bound compartments. One mechanism by which this is achieved is the asymmetric distribution of mRNA in the cytoplasm, which targets proteins to their site of function and is an important mechanism for the generation of polarity in single cells and multicellular organisms.

In the current work, the mechanism of intracellular mRNA movement was analysed during all stages of its motion from sites of synthesis within the nucleus to final sites of localisation in the cytoplasm. Although the organisation of organelles and other cytoplasmic compartments is relatively well understood, the extent to which the nucleus is compartmentalised is still a matter of debate. Gaining a detailed understanding of how nuclear processes such as replication, transcription and transport of nucleic acids are arranged in space and regulated remains a major goal for cell biology today.

The Organisation of the Interphase Nucleus

During mitosis, the chromosomes become visible as they are condensed and aligned on the spindle. However, during interphase the decondensed chromosomes are much more difficult to visualise. The spatial arrangement of interphase chromosomes and the organisation of transcription and processing of RNA within the nucleus have become subjects of great interest. Furthermore, a debate has continued over whether the nucleus is compartmentalised into specialised domains with specific functions (like the cytoplasm), or whether the nucleus is more simply a "bag of genes" in which specific factors are recruited to active loci as required.

The most conspicuous substructure within the nucleus is the nucleolus, which appears as a very distinct region of the nucleoplasm. The nucleolus forms around ribosomal DNA (rDNA) repeats that are found in clusters on several different chromosomes, depending on the organism. The nucleolus functions as a factory for the transcription and processing of rRNA and in the assembly of ribosomal subunits from rRNA and ribosomal proteins. Electron microscopy has shown that there are three distinct subregions within the nucleolus, which are thought to have specific functions. The fibrillar centre contains rDNA, RNA polymerase I and associated transcription factors. The dense fibrillar component is the site of processing of some rRNA transcripts while ribosomal subunits are assembled in the granular component of the nucleolus (Lamond and Earnshaw, 1998). Unlike cytoplasmic organelles, the nucleolus is not bounded by a membrane, but appears to form by the binding of ribosomal precursors to each other, forming a large network (Alberts et al., 1989). However, correctly processed rRNA can be produced from a plasmid containing a single rDNA gene (Nierras et al., 1997) suggesting that the higher order structure of the nucleolus may be a consequence of the

transcription and processing of rRNA rather than the result of a requirement for specialised compartments.

Outside the nucleolus, it is less clear whether the rest of the nucleoplasm has an underlying structure and organisation. One compartment which has been described is the pattern of 20-50 "speckles" visualised throughout mammalian cell nuclei by antibodies to a range of splicing factors (Spector, 1993). The speckles were proposed to be sites of active splicing, and have been reported to be associated with the site of transcription of several genes (Huang and Spector, 1996; Lawrence et al., 1993; Xing et al., 1993; Xing et al., 1995). However, the speckles may be exaggerated by antibody labeling conditions and thresholding during digital image processing (Neugebauer and Roth, 1997; Singer and Green, 1997). For example, the signal intensity for the essential splicing factor SC35 within speckles is only twice the intensity of the nucleoplasmic average (Fay et al., 1997). Furthermore, a more recent study showed that the nuclear distribution of splicing and transcription factors was much more diffuse in cells with high transcriptional activity. RNA polymerase II and splicing factors were only found in speckles in cells with reduced transcriptional activity (Zeng et al., 1997). These results suggest that speckles are not active sites of RNA synthesis and processing, but rather act as storage areas for transcription and splicing factors (Lewis and Tollervey, 2000). GFP-tagged splicing factors have been visualised moving rapidly in and out of speckles in living cells (Phair and Misteli, 2000) and speckles are associated with some highly active genes (Smith et al., 1999) providing further clues that transcription and processing factors may be recruited to active genes from nearby speckles.

A number of other distinct structures have been visualised within nuclei, including coiled (or Cajal) bodies, PML nuclear bodies and cleavage bodies. The existence of

these structures has been taken as further evidence that the nucleus has specialised compartments, but in most cases the functions of these bodies are not known. Coiled bodies are highly dynamic structures that have been shown to contain high concentrations of splicing snRNP's and other proteins, but lack nascent or newly synthesised RNA. Under the electron microscope, coiled bodies appear as a tangle of coiled threads 0.15-1.5μm in diameter, to which they owe their name. Coiled bodies are found in both plant and animal cells, and occasionally associate with the nucleolus, histone loci and U snRNA genes (Lamond and Earnshaw, 1998). They have been proposed to have a function in the assembly of large complexes containing transcription, splicing and polyadenylation components (transcriptosomes) because these factors pass through coiled bodies after they enter the nucleus in *Xenopus* oocytes (Gall et al., 1999). A typical mammalian cell nucleus also contains 10-20 PML nuclear bodies which are visualised as electron dense, spherical structures with a diameter of around 0.3μm (Stuurman et al., 1992). These bodies are labelled by antibodies to PML, a RING-finger protein discovered during studies of human acute promyelocytic leukaemia (APL). APL patients commonly have a chromosome translocation which fuses the PML gene to the retinoic acid receptor, blocking differentiation of erythropoietic stem cells and leading to leukaemia (Warrell et al., 1993). In mutant APL cells, PML bodies are dispersed into many smaller foci. PML bodies are also disrupted during some viral infections, but despite this the function of PML bodies in the nucleus is unknown. PML bodies are not thought to participate in splicing or gene expression as they lack snRNP's and splicing factors, and do not contain nascent RNA (Lamond and Earnshaw, 1998). A third type of structure that has been described in the nucleus are cleavage bodies. These were identified using antibodies to the 3' cleavage and polyadenylation factors CstF and CPSF which are found throughout the nucleoplasm but are also highly concentrated in a

few foci, some of which also contain newly synthesised RNA (Schul et al., 1996). Intriguingly, some of these cleavage bodies are closely associated with coiled bodies and PML bodies. However, the significance of this is not understood and the function of cleavage bodies is not known.

One view of the compartmentalised nucleus which is becoming more accepted is a division of the nucleoplasm into the chromatin compartment consisting of all the chromosomes, and the interchromatin space which is a network of channels between the chromosomes. Within the chromatin compartment, interphase chromosomes are thought to occupy discrete territories that do not overlap significantly. The giant polytene chromosomes in *Drosophila* larval tissues are separated into distinct spatial domains and different chromosome arms are not extensively intertwined (Hochstrasser et al., 1986; Mathog et al., 1984). Fluorescent *in situ* hybridisation (FISH) techniques have revealed the compact organisation of interphase chromosomes in specific non-overlapping territories in different cell types (Cremer et al., 1993; Leitch et al., 1990). Furthermore, it has been shown that some chromosomes adopt specific positions inside the nucleus which are maintained throughout the cell cycle (Croft et al., 1999). It has been proposed that active genes are localised on open loops of chromatin at the periphery of chromosome territories, and that this might enhance access to transcription factors and allow nascent RNA to be shed into the interchromatin space. However, this has only been demonstrated in a few cases (Clemson et al., 1996; Kurz et al., 1996; Nogami et al., 2000; Zirbel et al., 1993). Consistent with this is the idea that the interchromatin space might act as a channel through which newly synthesised mRNA could move to reach the nuclear envelope (Zachar et al., 1993). Previous work has shown that the interchromatin space forms a continuous network of channels between the chromosomes which end at nuclear pores (Bridger et al., 1998). Furthermore, fluorescent dextrans have been shown

to have very similar diffusion characteristics in the cytoplasm and nucleus, which are only slightly retarded compared to those measured in free solution (Seksek et al., 1997). These results suggest that the interchromatin space consists of aqueous channels through which macromolecules can diffuse freely.

In order to maintain chromosome territories, it would seem likely that chromosomes might be attached or anchored to some structural component in the nucleus. Indeed, measurements of chromosome dynamics in living cells have indicated that specific loci or chromosomal domains normally diffuse freely only within a confined space, suggesting that they are tethered to an immobile structure (Bornfleth et al., 1999; Marshall et al., 1997). The nuclear matrix, or nucleoskeleton, has been suggested to provide such a role. The nuclear matrix is defined as the structure remaining in the nucleus after DNAaseI digestion and extensive extraction have removed the chromatin and all the soluble components (Bornfleth et al., 1999). Varying procedures have been used in matrix preparations with comparable results, namely a fibrogranular structure extending throughout the nucleoplasm (Mirkovitch et al., 1984; Nickerson et al., 1997). Newly synthesised RNA and transcribed DNA sequences have been shown to be associated with this nuclear matrix (Nelson et al., 1986). Furthermore, specific DNA sequences (scaffold/matrix attachment regions) have been identified which are thought to attach loops of chromatin to the nuclear matrix (Cockerill and Garrard, 1986; Mirkovitch et al., 1984). Despite this, the existence of the nuclear matrix remains highly controversial. Matrix filaments are not observed in standard ultrastructural studies, and it has been suggested that the matrix structure is an artefact induced by non-physiological extraction conditions which could precipitate RNA and proteins into strands and clusters (Singer and Green, 1997). Almost exclusively, proteins isolated from nuclear matrix preparations have been found to be hnRNP proteins or RNA polymerase (Mattern et al.,

1997), and structural proteins which might contribute to the matrix have remained elusive – a fact which has led many researchers to question the existence of the matrix at all (Pederson, 2000). Alternative possibilities are that the nuclear matrix is composed of lamins which may extend into the nucleoplasm from the inner surface of the nuclear envelope (Neri et al., 1999), or from filaments that extend from the nucleoplasmic face of nuclear pores (Cordes et al., 1997). The existence of intranuclear filaments is a controversial issue, but some groups have isolated proteins that may form filaments extending into the nucleus from nuclear pores (Kosova et al., 2000; Strambio-de-Castillia et al., 1999).

Another possible anchoring site for chromosomes could be provided by the nuclear envelope. Previous work has shown that polytene chromosomes make specific contacts with the nuclear envelope (Hochstrasser et al., 1986) and interactions between chromatin and the nuclear envelope were found in an extensive study of the 3-D position of specific sequences along the 2nd chromosome in *Drosophila* embryonic nuclei. This study estimated that as many as 15 loci on each chromosome arm are consistently associated with the nuclear envelope (Marshall et al., 1996). It is therefore likely that interactions between chromatin and the nuclear envelope could play a significant role in nuclear organisation, although the proteins and DNA sequences involved in binding are unknown at this time.

Taken together, these results suggest that the nucleus does have some level of higher organisation, although the function and organisation of different nuclear compartments is still highly debated. Nevertheless, the division of the cell into nuclear and cytoplasmic compartments and the trafficking of molecules between the two is an important aspect of

eukaryotic biology. In the last few years, there has been considerable progress in identifying the machinery required for transport between these two compartments.

Nucleocytoplasmic Transport

The evolution of eukaryotic cells and their nuclei required the formation not only of the nuclear envelope, but also of a new set of proteins to regulate and facilitate the transport of different cargoes across it. For example, tRNA and mRNA are synthesised in the nucleus and must be exported to the cytoplasm to function in translation. In contrast, proteins that function in the nucleus, such as histones and DNA polymerase, must be selectively imported into the nucleus after their synthesis. Furthermore, the biogenesis of ribosomes and U snRNP complexes requires multiple transport events between the nucleus and cytoplasm (Mattaj and Englmeier, 1998).

All transport in and out of the nucleus occurs through the nuclear pore complexes (NPC) which span the nuclear membrane. The NPC is a large complex with a molecular weight of around 125MDa, which is composed of 50-100 distinct proteins termed nucleoporins or nups (Doye and Hurt, 1997; Fabre and Hurt, 1994). The NPC appears to be a highly conserved structure, which is found in all eukaryotic cells. Ultrastructural studies have shown that the NPC has a basic framework with eightfold radial symmetry, organised around a putative central gated channel which is sandwiched between distinct cytoplasmic, nuclear membrane and nucleoplasmic ring structures. Eight long fibrils extend into the cytosol from the cytoplasmic ring, while the nucleoplasmic ring is capped by a basket structure consisting of eight fibres joined distally by a smaller terminal ring (Fahrenkrog et al., 1998; Goldberg et al., 1997; Stoffler et al., 1999). A powerful combination of genetics and biochemical analysis has identified over 30 nucleoporins in yeast (Fabre and Hurt, 1997). Many nucleoporins have characteristic

amino acid repeats with sequence GLFG, FxFG or FG which are able to bind some of the soluble factors essential for nucleocytoplasmic transport. Some nucleoporins have been localised to distinct sites on the NPC such as the cytoplasmic ring or nuclear basket (Rout et al., 2000). The asymmetric nature of NPC structure and nucleoporin distribution across the nuclear membrane is likely to reflect the specific directionality of nuclear import and export.

While ions and small molecules up to approximately 40KDa in size are able to diffuse through aqueous channels associated with nuclear pores, proteins and RNA are actively transported through the NPC by a receptor-mediated process that is poorly understood. The existence of the central transporter has been controversial, since it is not always visualised depending on sample preparation. The emerging consensus is that of a central gated channel with a resting diameter of 10nm, which can expand to at least 26nm to translocate large cargoes such as ribosomal subunits and mRNP complexes (Feldherr et al., 1984; Kiseleva et al., 1998). However, many aspects of NPC structure and function remain unresolved, such as the question of the existence of specialised NPC's which might transport specific cargoes (Iborra et al., 2000).

In addition to nucleoporins, there are soluble factors that are required for the transport of different molecules across the nuclear envelope. In the last few years, many of the key receptor and adapter proteins that control nucleocytoplasmic transport have been identified, and this has led to a greater understanding of the general mechanisms of nuclear import and export (Mattaj and Englmeier, 1998). Different classes of cargo destined for nuclear import or export contain a transport signal that is recognised by a specific receptor protein. The cargo/receptor complex is targeted to the NPC and translocated through the central gated channel by a poorly understood process, which is

capable of carrying the cargo against a concentration gradient in many cases. Once translocation is completed, the cargo is released and the receptor must be recycled back to the original compartment to take part in more transport events. In some cases, specific adapter proteins recognise transport signals and mediate interactions with the receptor protein. In such cases, the entire cargo/adapter/receptor complex is translocated through the NPC, and both adapters and receptors must be recycled. Proteins that are involved in nucleocytoplasmic transport therefore shuttle continuously between the nucleus and cytoplasm.

The asymmetric nature of translocation through the NPC is an intriguing and essential aspect of nucleocytoplasmic transport. Cargoes that have completed translocation must not bind receptors, or they would risk being transported back to their original compartment. As the nuclear localisation and exclusion of factors must be re-established after each round of mitosis, the transport signals cannot be removed as found after translocation into the endoplasmic reticulum or mitochondria. Instead, it has become clear that the directionality of nuclear transport events is dependent on the small GTPase Ran and its associated factors. RanGTP is only produced in the nucleus due to the asymmetric distribution of the proteins that regulate its nucleotide exchange and GTP hydrolysis activity. The nucleotide exchange factor RCC1 is localised in the nucleus, where it is stably bound to chromatin (Ohtsubo et al., 1989) whilst the GTPase activating proteins are excluded from the nucleus and deplete RanGTP from the cytoplasm (Gorlich, 1997; Koepp and Silver, 1996). In the nucleus, RanGTP interacts with transport receptors but has opposite effects on the ability of import and export receptors to interact with their cargoes. Import receptors release their cargo when bound to RanGTP in the nucleus. In contrast, export receptors only bind their cargoes when

associated with RanGTP, and therefore dissociate from their cargo in the cytoplasm where RanGTP is hydrolysed to RanGDP (Gorlich and Kutay, 1999).

The Importin-β family of nuclear transport receptors

Import receptors (importins) and export receptors (exportins) make up the importin-β superfamily of related Ran-binding proteins which has 14 members in yeast and at least 21 family members in humans (Gorlich and Kutay, 1999). Specific transport functions have been assigned to a number of these proteins. Importin-β was the first member of the family to be identified, and was found to be required for the nuclear import of proteins bearing a classic basic nuclear localisation signal (nls). The nls is recognised by the adapter protein Importin-α (srp1p in yeast) which in turn recruits Importin-β, targeting the entire complex for nuclear import (Gorlich et al., 1995). Higher eukaryotes have a family of importin-α adapter proteins, and at least six members of this family have been identified in the human genome (Kohler et al., 1999). In higher eukaryotes, importin-β can interact with these additional adapter proteins to increase its substrate specificity. For example, importin-β associates with snurportin for import of U snRNP's (Huber et al., 1998) or with XRIPα for import of replication protein A (Jullien et al., 1999).

Another import receptor is transportin, which is responsible for the nuclear import of hnRNP proteins with an M9 nuclear import signal (Pollard et al., 1996). Interestingly, M9 also acts as an export signal, so targets proteins to shuttle between the nucleus and cytoplasm (Michael et al., 1997). Transportin also recognises a different import signal, the BIB domain, which is required for the import of the ribosomal protein rpL23a (Jakel and Gorlich, 1998).

The importin-β superfamily also contains members that are involved in nuclear protein export. For example, Crm1 is required for the nuclear export of proteins containing a leucine-rich nuclear export signal (NES) (Fornerod et al., 1997). CAS (known as Cse1p in yeast) is the nuclear export receptor for importin-α which must be efficiently recycled to the cytoplasm after each round of nuclear protein import (Hood and Silver, 1998; Kunzler and Hurt, 1998; Kutay et al., 1997; Solsbacher et al., 1998).

It has long been thought that the nuclear export of RNA is also mediated by class-specific receptors, because the export pathways of tRNA, mRNA, 5S rRNA, U snRNA and rRNA (as ribosomal subunits) are uniquely saturable. Thus, when excess mRNA is injected into *Xenopus* oocyte nuclei, the import of other mRNA transcripts is inhibited whilst export of 5S rRNA, tRNA, U snRNA and ribosomal subunits is not affected (Jarmolowski et al., 1994; Pante et al., 1997). However, the only exportin known to bind directly to RNA is exportin-t (Los1p in yeast) which is responsible for the export of mature tRNA to the cytoplasm (Arts et al., 1998; Hellmuth et al., 1998; Kutay et al., 1998). Nuclear export of other classes of RNA may be mediated by factors other than exportins. For example, the export of U snRNA depends upon the recognition of their monomethyl guanosine cap structure by the nuclear cap binding complex (CBC) (Izaurralde et al., 1995). In contrast, binding of CBC to the cap of mRNA only has a minor role in nuclear mRNA export, which is currently one of the least understood of all nucleocytoplasmic transport events.

Nuclear Export of mRNA

The nuclear mRNA export pathway remains poorly characterised compared to the transport of proteins in and out of the nucleus. The many thousands of different transcripts synthesised in the nucleus are exported as RNA/protein (RNP) complexes,

which are highly variable in size, sequence and composition. It is thought that multiple features of mRNP complexes such as the cap structure, poly(A) tail and specific bound proteins may contribute to efficient nuclear export. A great deal has been learned about mRNA export by the study of giant transcripts synthesised in the salivary glands of the insect *Chironomus tentans*. The Balbiani ring (BR) genes encode large secreted proteins, and the BR transcripts, 30-40kb in size, are large enough to visualise directly in the electron microscope as they are transcribed and exported from the nucleus (Daneholt, 1997). It has been shown that hnRNP proteins bind to the BR pre-mRNA during transcription, producing a tightly packed mRNP complex, which is released into the nucleoplasm after completion of processing. The BR mRNP particle is then unwound at the NPC and can be visualised during different stages of transit through the NPC to the cytoplasm (Kiseleva et al., 1998). The 5' end of the BR mRNP always leads the way during translocation to the cytoplasm. Whilst the *C. tentans* homologues of hnRNPA1 and the nuclear cap binding complex remain bound to the BR mRNP during translocation and are exported to the cytoplasm (Visa et al., 1996; Visa et al., 1996), a different hnRNP protein is released from the BR mRNP complex at the moment of reaching the NPC (Sun et al., 1998). A homologue of the splicing factor SF2/ASF is released from the BR mRNP as the particle enters the central transporter of the NPC (Alzhanova-Ericsson et al., 1996). The protein composition of the mRNP particle therefore changes during different stages of export from the nucleus.

Early indications were that mRNA export might also be mediated by members of the importin-β superfamily of nuclear transport receptors, as it was found that disruption of the RanGTP gradient across the nuclear membrane inhibits mRNA export (Cheng et al., 1995; Izaurralde et al., 1997; Kadowaki et al., 1993; Schlenstedt et al., 1995). Consistent with this, mutants in the yeast transport receptors Crm1p, Pse1p, Mtr10p, Yrb4p and

Sxm1p were found to be defective in mRNA export. However, it is now thought that importins and exportins are not likely to have a direct role in mRNA export, and that disruption of the Ran system or importin-β transport receptors can lead to a defect in mRNA export by inhibiting the import of other shuttling factors that are essential for nuclear export of mRNA (reviewed in (Gorlich and Kutay, 1999).

Many factors essential for mRNA export have been identified by genetic screens in the budding yeast *Saccharomyces cerevisiae*. Homologues of a number of these proteins have been found in higher eukaryotes and have been proposed to have similar functions in mRNA export in many cases. These discoveries have progressed at a startling rate, so that our knowledge of the factors involved in mRNA export have increased dramatically over the last 3-4 years (i.e. during the time this work was being carried out). The different mRNA export factors will be reviewed below, as they are directly relevant to this thesis.

In yeast, *in situ* hybridisation with poly(T) probes was used to identify conditional temperature sensitive *RAT* (mRNA trafficking) and *MTR* (mRNA transport) mutants with defects in poly(A)$^+$ RNA export at the restrictive temperature (Amberg et al., 1992; Kadowaki et al., 1992). These strains were later found to have mutations in various components required for nucleocytoplasmic transport, such as components of the Ran system, RNA processing factors, nucleoporins or factors involved in membrane biogenesis (Strasser and Hurt, 1999; Stutz and Rosbash, 1998). These results are consistent with the known functions of nuclear pores in mRNA export and with the fact that unspliced or incorrectly processed mRNA is retained in the nucleus and not exported to the cytoplasm (Brodsky and Silver, 2000; Legrain and Rosbash, 1989). However, some *RAT/MTR* mutants were also found to have defects in nuclear protein

import, or structural defects in the nuclear envelope, making it difficult to assess whether the nuclear accumulation of poly(A)$^+$ RNA is the primary defect in such strains (Doye and Hurt, 1997).

Additional candidate mRNA export factors in yeast were identified in synthetic lethal screens with nucleoporin mutants. The *GLE1* gene has been cloned independently in a number of such screens (Del Priore et al., 1996; Murphy and Wente, 1996; Stutz and Rosbash, 1998) and was also identified in a screen of conditional cold sensitive mutants for splicing defects (Noble and Guthrie, 1996). The Gle1p protein is localised at nuclear pores, where it is found predominantly on the cytoplasmic side of the NPC, although it can also be detected on the nucleoplasmic face (Rout et al., 2000). While *gle1* mutants have a defect in poly(A)$^+$ RNA export, the precise role of Gle1p in mRNA export is not understood. The Gle1p protein has a sequence that resembles a NES, but this has not yet been shown to have a function in nuclear export. Furthermore, Gle1p is not known to bind mRNA, and it has been proposed to be a stable component of nuclear pores rather than a shuttling factor (Rout et al., 2000; Stutz and Rosbash, 1998). Gle1p may therefore have an important role in the transport of mRNA through the NPC, but is not likely to represent a true transport receptor. A human homologue of Gle1p has been identified which is also located at the NPC. Microinjection of antibodies against hGle1 leads to nuclear accumulation of poly(A)$^+$ RNA in HeLa cells, suggesting that the function of this protein in mRNA export may have been conserved through evolution (Watkins et al., 1998).

Gle2p and Rae1p, its homologue in *Schizosaccharomyces pombe*, have been implicated in mRNA export (Brown et al., 1995; Murphy et al., 1996). Inactivation of Gle2p leads to a block in poly(A)$^+$ RNA export and also causes NPC defects. In *S. cerevisiae*, Gle2p

interacts with the nucleoporin Nup116p through a binding domain that is functionally conserved in the vertebrate nucleoporin NUP98. The interaction between human RAE1 and NUP98 is independent of mRNA but has been shown to be required for poly(A)$^+$ RNA export in cultured human cells (Bailer et al., 1998; Pritchard et al., 1999). Furthermore human RAE1 shuttles between the nucleus and cytoplasm and can be crosslinked to poly(A)$^+$ RNA (Kraemer and Blobel, 1997; Pritchard et al., 1999). The human *RAE1* gene can partially suppress the poly(A)$^+$ export defect of the *rae1-1* mutant in *S. pombe*, suggesting that the human and yeast genes are functional homologues (Bharathi et al., 1997). The binding of RAE1 to mRNA has been studied in the salivary glands of *C. tentans*. The *C. tentans* homologue of RAE1 does not bind to nascent or nucleoplasmic Balbiani ring transcripts, but only becomes associated with BR mRNP particles at the nucleoplasmic side of the NPC (Sabri and Visa, 2000). Taken together, these results suggest that binding of RAE1 to the NPC is an important event for mRNA export, which might confer competence on the NPC or the mRNA for translocation.

Another gene essential for mRNA export in yeast is *DBP5/RAT8*, which encodes a DEAD box RNA helicase that has ATP-dependent RNA unwinding activity (SnayHodge et al., 1998; Tseng et al., 1998). Dbp5p also shuttles between the nucleus and cytoplasm and interacts with Gle1p (Hodge et al., 1999). The role of this protein in mRNA export is not clear, but it has been proposed to function in the unwinding of the mRNP particle before or during translocation through the NPC, or in removal of nuclear export proteins from the translocated mRNP in the cytoplasm. A human Dbp5 protein homologue was recently identified which displays similar nucleotide-dependent RNA unwinding activity to the yeast protein (Schmitt et al., 1999). Mutant forms of hDbp5 inhibit mRNA export when microinjected into *Xenopus* oocytes, suggesting that Dbp5 also plays an important role in nuclear mRNA export in higher eukaryotes.

One of the best candidates for an mRNA export factor is the yeast protein Mex67p, which was originally isolated in a synthetic lethal screen with the nucleoporin Nup85p (Segref et al., 1997). Temperature sensitive alleles of *mex67* display an extremely rapid onset of nuclear poly(A)$^+$ RNA accumulation at the restrictive temperature. Mex67p forms a complex with Mtr2p, and this complex is able to bind directly to RNA *in vitro* via Mex67p (Santos-Rosa et al., 1998). Furthermore, the Mex67p/Mtr2p complex binds to nuclear pores via the FG repeats of nucleoporins (Strasser et al., 2000). There is mounting evidence that TAP, the vertebrate homologue of Mex67p, also has a role in nuclear export of mRNA. TAP is the cellular co-factor necessary for the nuclear export of unspliced retroviral RNA containing a signal known as the constitutive transport element, or CTE (Gruter et al., 1998). Microinjection of surplus CTE RNA inhibits mRNA export in *Xenopus* oocytes, suggesting that mRNA and CTE RNA export occurs by the same pathway. TAP can overcome this block in mRNA export when provided in excess, suggesting that TAP also has a role in nuclear export of mRNA. TAP can be U.V. crosslinked to poly(A)$^+$ RNA in cultured cells, demonstrating that the protein is directly associated with mRNA *in vivo*. Furthermore, TAP has been shown to shuttle between the nucleus and cytoplasm (Katahira et al., 1999). The C-terminal domain of TAP mediates the interaction of the protein with nucleoporins, and also acts as an efficient nuclear export signal (Bachi et al., 2000). The residues upstream of this NES mediate the interaction of TAP with its co-factor p15, a homologue of the nuclear transport factor NTF2 (Bachi et al., 2000; Katahira et al., 1999). Although p15 has no sequence homology to yeast Mtr2p, the proteins may perform similar roles as the TAP-p15 complex can rescue the growth defect of a *mex67,mtr2* double knockout yeast strain, suggesting that the TAP-p15 has similar functions in nuclear export of mRNA as Mex67p/Mtr2p (Katahira et al., 1999). Recently, it was shown that disruption of TAP

function in *C. elegans* by RNA interference leads to nuclear accumulation of poly(A)$^+$ RNA (Tan et al., 2000). Taken together, these results suggest that TAP-p15 and Mex67p/Mtr2p are suitable candidates for the transport receptor responsible for the nuclear export of cellular mRNA.

Further evidence that Mex67p/TAP is involved in an important step in mRNA export comes from work linking pre-mRNA processing to mRNA export. It has long been known that incorrectly spliced or processed RNA is not exported from the nucleus (Brodsky and Silver, 2000; Chang and Sharp, 1989; Custodio et al., 1999; Legrain and Rosbash, 1989) and it has been suggested that correctly processed mRNA might receive an "export license" targeting it to the nuclear export pathway (Cullen, 2000). This proposal was based on evidence that splicing can target injected pre-mRNA's efficiently for nuclear export, whereas corresponding transcripts with no introns are retained in the nucleus after injection (Luo and Reed, 1999). The recent identification of vertebrate ALY, yeast Yra1p (REF family) and also Y14 as factors that specifically associate with spliced transcripts in the nucleus may explain this observation (Kataoka et al., 2000; Rodrigues et al., 2001; Strasser and Hurt, 2000; Stutz et al., 2000; Zhou et al., 2000). The REF proteins ALY and Yra1p are essential for mRNA export, and interact strongly with TAP and Mex67p, respectively. Furthermore, the nuclear export of inefficiently spliced pre-mRNA or microinjected intron-free transcripts can be stimulated by excess TAP or REF proteins (Braun et al., 2001; Rodrigues et al., 2001). It therefore appears likely that pre-mRNA processing recruits REF proteins to the mRNP complex, which then target the mature mRNP for nuclear export by recruiting TAP/Mex67p. This model places TAP/Mex67p at the penultimate step in nuclear export of mRNA, as the receptor which receives processed mRNA and sends it through the NPC.

ASYMMETRIC LOCALISATION OF mRNA IN THE CYTOPLASM

Localised Transcripts and their functions

It is well recognised that, once exported from the nucleus, many transcripts become localised to specific regions of the cytoplasm. It has been estimated that as many as 10% of all transcripts in *Drosophila* oocytes, and possibly in other organisms, are localised asymmetrically (Dubowy and Macdonald, 1998). To date, over 100 cytoplasmically localised mRNA's have been identified (Bashirullah et al., 1998; Lipshitz and Smibert, 2000). Transcript localisation is an important mechanism for targeting proteins to their subcellular site of function, as localising an mRNA that can be translated many times is inherently more efficient than transporting many protein molecules from sites of synthesis throughout the cytoplasm to a specific region of the cell (St Johnston, 1995).

Localisation of mRNA to specific subcellular regions plays a major role in generating cellular asymmetry, and in many cases localised transcripts are essential to create polarised cells. For example, the lamellipodia of migrating chicken embryo fibroblasts undergo rapid polymerisation of actin filaments. It has been shown that the localisation of *β-actin* mRNA to the leading edge of lamellipodia is required for the maintenance of cell polarity, and is also essential for cell motility (Kislauskis et al., 1997; Kislauskis et al., 1994; Sundell and Singer, 1990).

Transcript localisation also has an important role during asymmetric cell division. In *S. cerevisiae*, the localisation of *Ash1* mRNA to the bud of a dividing cell is required to suppress mating-type switching in the daughter cell (Bobola et al., 1996; Long et al.,

1997). During the division of *Drosophila* neuroblasts, the asymmetric segregation of Numb and Prospero proteins into only one of the daughter cells is required to specify different cell fates. *prospero* mRNA and protein are localised basally during mitosis and are inherited only by one daughter cell which differentiates to become a ganglion mother cell (Li et al., 1997). However, it is thought that *prospero* mRNA localisation is not essential for the asymmetric localisation of the protein it encodes.

It has become increasingly clear that transcript localisation plays an important role in development. The study of *Xenopus* and *Drosophila* oocytes has shown that localised transcripts establish spatial cues to polarise the major body axes during early stages of development. In *Xenopus* oocytes, the animal-vegetal axis is thought to be defined by the localisation of *Vg1* and TGFβ-5 mRNA to the vegetal hemisphere, where the proteins encoded by these transcripts have a role in the induction of mesoderm fate (Bashirullah et al., 1998; Joseph and Melton, 1998; Weeks and Melton, 1987). Furthermore, the localisation of *Xwnt11* mRNA is thought to have a role in the formation of the dorsoventral axis of the oocyte after fertilisation, although this is poorly understood (Ku and Melton, 1993).

In *Drosophila*, the powerful genetic screens have uncovered more of the molecules that are involved in the polarisation of the body axes during development. Notably, the localisation of *gurken* (*grk*), *bicoid* (*bcd*) and *oskar* (*osk*) transcripts to specific regions of the oocyte are essential symmetry-breaking events that define the dorsoventral and anteroposterior axes of the embryo. *grk* mRNA is localised at the posterior of early oocytes, in a crescent between the oocyte nucleus and overlying follicle cells (Neuman-Silberberg and Schüpbach, 1993). *grk* encodes a TGFα-like signalling molecule which is received by the EGFR receptor in the adjacent follicle cells, inducing them to adopt a

posterior fate (Gonzalez-Reyes and St Johnston, 1998; Schüpbach and Roth, 1994). The posterior follicle cells respond by sending a signal back to the oocyte, thus bringing about the repolarisation of the oocyte cytoskeleton. Although the nature of this signal is not known, the ERM protein Merlin is required in the posterior follicle cells to target the signal to the oocyte (MacDougall et al., 2001) inducing the posterior MTOC to break down and reform along the anterior margin of the oocyte, reversing the polarity of the oocyte microtubules (Clark et al., 1994; Clark et al., 1997; Theurkauf et al., 1992). The correct localisation of *bcd*, *osk*, and *nanos* transcripts, which define the co-ordinates of the anteroposterior axis, are dependent on the reorganisation of the oocyte cytoskeleton. *bcd* mRNA becomes localised at the anterior of the oocyte, and is translated in the early embryo to produce a morphogenetic gradient of Bcd protein which defines the anteroposterior axis (Driever and Nüsslein-Volhard, 1988). Correctly localised *osk* mRNA is required to specify the formation of pole cells at the posterior of the embryo which form the future germ cells (Ephrussi et al., 1991; Kim-Ha et al., 1991). Posterior Osk is also required to recruit other factors to the posterior pole plasm, including *nanos* mRNA which encodes an essential determinant of the abdominal body segments (Gavis and Lehmann, 1994; Lehmann and Ephrussi, 1994).

The localisation of *grk* mRNA is also required to initiate the formation of the dorsoventral axis after the oocyte nucleus migrates from the posterior to the dorsoanterior corner of the oocyte later in oogenesis. *grk* transcripts become tightly localised above the oocyte nucleus, resulting in a second localised TGFα signal which induces the overlying follicle cells to adopt a dorsal fate (Gonzalez-Reyes et al., 1995; Neuman-Silberberg and Schüpbach, 1994; Neuman-Silberberg and Schüpbach, 1993).

Transcript localisation therefore plays a major role during axis specification in *Drosophila*. The discovery of localised transcripts in the early embryos of ascidian, echinoderm and zebrafish species suggests that this may be a widely deployed mechanism to generate asymmetry during development (Bashirullah et al., 1998). However, it is still not clear whether early patterning in mammalian embryos also involves mRNA localisation.

Transcript localisation is also important in the syncitial blastoderm embryo. At this stage of development, *Drosophila* embryos contain a layer of nuclei under the plasma membrane which divide the cortical cytoplasm into apical and basal compartments, joined only by a thin layer of cytoplasm between nuclei (see section on "*Drosophila* Development", below). Different transcripts become localised in the apical or basal cytoplasm, and these alternate patterns of apical, basal or unlocalised mRNA are thought to serve distinct functions. The transcripts of the *wingless* gene and the pair rule genes (including *hairy*, *fushi tarazu*, *even-skipped*, *runt* and *paired*) are localised in the apical cytoplasm above the cortical nuclei (Baker, 1988; Davis and Ish-Horowicz, 1991; Edgar et al., 1987; Gergen and Butler, 1988; Kilchherr et al., 1986; Macdonald et al., 1986). Correct localisation of *wingless* (*wg*) transcripts is required for Wg signalling function, as the apical localisation of *wg* mRNA targets the Wg protein to the apical membrane for secretion (Simmonds et al., 2001). The apical localisation of pair-rule transcripts may function to restrict the lateral diffusion of the transcription factors they encode, maintaining the sharp boundaries of pair-rule gene expression necessary to define segment limits (Davis and Ish-Horowicz, 1991). In contrast, the transcripts of the gap genes (including *hunchback* and *kruppel*) are unlocalised (Davis and Ish-Horowicz, 1991) which is thought to allow these proteins to diffuse and form short-range gradients in the syncitial embryo (Hulskamp et al., 1990; Hulskamp and Tautz, 1991). A different

pattern of localisation has been observed for *string*, the *Drosophila* homologue of CDC25 (Edgar and O'Farrell, 1990). *string* mRNA is mainly localised in the basal cytoplasm, although the function of this localisation in not known.

In some cases, localisation of mRNA may provide a mechanism to prevent ectopic expression of a protein in a part of the cell where it could have toxic or deleterious effects. An example of this may be the transcripts encoding myelin basic protein (MBP), which are localised to sites of myelin sheath formation in oligodendrocytes (Trapp et al., 1987). The MBP protein reacts strongly with membranes causing a change in their structure, and it would be difficult to transport MBP from the cell body to sites of myelination in the distal processes without the protein contacting any membranes. This problem appears to be circumvented by localising the *MBP* mRNA and producing the protein only at sites where it is required.

It would not be possible to produce proteins exclusively at sites of transcript localisation unless mRNA in the process of localisation was translationally repressed. The links between localisation and translation of mRNA have been investigated for several *Drosophila* transcripts in the oocyte and early embryo, and in these cases unlocalised transcripts were indeed found to be translationally repressed. Repression of unlocalised *osk* mRNA has been shown to depend on several *trans*-acting factors including Bruno and Apontic, which bind to elements in the *osk* 3'UTR (Castagnetti et al., 2000; Kim-Ha et al., 1995; Lie and Macdonald, 1999; Webster et al., 1997). When *osk* mRNA reaches its correct site of localisation at the posterior of the oocyte, translation is activated by a mechanism which involves sequences in the 5'UTR of the *osk* mRNA (Gunkel et al., 1998). Translation of *osk* mRNA is dependent on Staufen protein and may also require the gene products of *vasa* and *orb* ***reviewed in (Lipshitz and Smibert, 2000). The

molecular mechanisms that activate translation at the site of localisation are not fully understood, but are thought to involve removal of repressors, recruitment of translational initiation factors and modification of *osk* poly(A) tail length (Lipshitz and Smibert, 2000).

Bruno, Orb, Vasa and Aubergine also play a role in translational regulation during the localisation of *grk* mRNA in the *Drosophila* oocyte, suggesting that some mechanisms for translational repression and activation during localisation may be conserved (Lipshitz and Smibert, 2000). However, a different mechanism appears to regulate the translation of *nanos* mRNA, which is localised inefficiently to the posterior of oocytes and early embryos (Bergsten and Gavis, 1999). Translational repression of unlocalised *nanos* mRNA requires the novel protein Smaug, whilst the translation of correctly localised *nanos* mRNA is activated by Oskar protein at the posterior (Dahanukar et al., 1999; Gavis and Lehmann, 1994; Smibert et al., 1999). The underlying molecular mechanisms by which these factors repress and activate mRNA translation are poorly understood. However, the development of *in vitro* assays which reproduce translational repression of *osk* and *nanos* in *Drosophila* extracts will provide a useful tool to investigate the mechanisms linking localisation and translation of mRNA (Castagnetti et al., 2000; Lie and Macdonald, 1999; Smibert et al., 1999).

Mechanisms of mRNA localisation

Although the asymmetric distribution of different transcripts has been shown to have a variety of important functions, the precise mechanism and path of localisation taken by most transcripts is poorly understood. Four models were previously proposed for the apical localisation of pair-rule transcripts in *Drosophila* blastoderm embryos (Davis et al., 1993; Francis-Lang et al., 1996) and for all other asymmetrically localised

transcripts (Lipshitz and Smibert, 2000). A major aim of this thesis is to test these models, and they are therefore reviewed below.

Selective degradation of unlocalised transcripts, or selective stabilisation of transcripts at the site of localisation is one mechanism which could lead to the asymmetric distribution of transcripts in the cytoplasm. An example of this is *Hsp83* mRNA in *Drosophila*, which is initially found in high levels throughout the oocyte. However, after fertilisation *Hsp83* transcripts are degraded in all parts of the embryo except the posterior pole plasm, where they are protected from degradation (Bashirullah et al., 1999). Selective stabilisation also refines the localisation of *nanos* mRNA in the early embryo. *nanos* localisation is inefficient, and only 4% of the *nanos* mRNA in the embryo is correctly localised to the posterior (Bergsten and Gavis, 1999). Degradation of the large cytoplasmic pool of unlocalised transcripts therefore restricts the localisation of *nanos* mRNA to the posterior (Bashirullah et al., 1999).

A different mechanism for mRNA localisation is selective anchoring of transcripts at the site of localisation following their random diffusion through the cytoplasm. This mechanism has been shown to function in the localisation of fluorescently labelled *osk* RNA microinjected into living *Drosophila* oocytes. Time-lapse microscopy revealed that ooplasmic streaming causes vigorous mixing of the oocyte cytoplasm during later stages of oogenesis, allowing injected *osk* RNA to reach the posterior where it accumulates in a similar pattern to endogenous *osk* mRNA (Glotzer et al., 1997). Although *osk* mRNA also becomes localised to the posterior during earlier stages of oogenesis, these results demonstrate that selective anchoring is able to contribute to posterior *osk* mRNA localisation in late stage oocytes.

An alternative mechanism which could generate asymmetric distribution of transcripts in the cytoplasm is vectorial export of mRNA from the nucleus. This model suggests that mRNA could be exported exclusively from one side of the nucleus, and a number of different mechanisms have been proposed by which this could occur (Davis et al., 1993). In the direct gene gating model, transcripts are directionally exported due to the presence of DNA sequences that target genes to localise near nuclear pores on one side of the nuclear envelope, so that transcripts are exported directly by a these nuclear pores. This idea was originally proposed in the gene gating hypothesis by Gunter Blobel (Blobel, 1985). Indirect gene gating is a variation of this idea, in which transcription occurs in the nuclear interior, but transcripts are targeted to specific NPC's by diffusing through the nucleoplasm and being selectively exported only by a subset of specialised NPC's on one side of the nucleus. Alternatively, indirect gene gating could involve active transport of mRNA within the nucleoplasm to NPC's on one side of the nucleus. Although conclusive demonstrations of a transcript localised by vectorial nuclear export are currently lacking, this model has been proposed to account for the apical localisation of pair-rule transcripts in *Drosophila* blastoderm embryos (Davis et al., 1993; Francis-Lang et al., 1996). Vectorial nuclear export has also been suggested as a mechanism for the localisation of *grk* mRNA in a crescent on one side of the oocyte nucleus, although it is a matter of debate whether *grk* is transcribed in the oocyte or nurse cells (Lipshitz and Smibert, 2000; Norvell et al., 1999; Saunders and Cohen, 1999; Thio et al., 2000). Furthermore, a vectorial localisation mechanism could potentially explain other localised transcripts that are in close proximity to one cytoplasmic face of the nuclear envelope.

A fourth mechanism for the asymmetric localisation of mRNA in the cytoplasm is active transport along the cytoskeleton. There is increasing evidence that microtubules and

microfilaments are required for the localisation of different transcripts. For example, the localisation of *β-actin* mRNA to the distal lamellae of chicken embryo fibroblasts requires actin microfilaments (Sundell and Singer, 1991) whereas microtubules are required for the localisation of *Vg1* mRNA to the vegetal hemisphere of *Xenopus* oocytes (Yisraeli et al., 1990) and for the localisation of *bcd* and *osk* transcripts in *Drosophila* oocytes (Clark et al., 1994; Pokrywka and Stephenson, 1995; Pokrywka and Stephenson, 1991; Theurkauf et al., 1993). It is interesting to note that microfilaments also have a role in *osk* mRNA localisation (Erdelyi et al., 1995; Lantz et al., 1999; Tetzlaff et al., 1996) consistent with suggestions that microtubules are required for long-range transport of mRNA whereas microfilaments are involved in short-range transport and anchoring of transcripts at the site of localisation (Lipshitz and Smibert, 2000; Yisraeli et al., 1990).

Recently, the identity of some molecular motors responsible for the transport of mRNA along polarised cytoskeletal filaments have been reported. The localisation of *Ash1* mRNA to the daughter cell bud in *S. cerevisiae* requires the actin-based myosin motor Myo4p (Long et al., 1997; Munchow et al., 1999; Takizawa et al., 1997) and other gene products including She3p which acts as an adapter linking *Ash1* mRNA to the Myo4p motor (Takizawa and Vale, 2000). The localisation of *osk* transcripts to the posterior of *Drosophila* oocytes has been shown to depend on the plus end directed microtubule motor Kinesin I (Brendza et al., 2000). Kinesin is also required for the translocation of *MBP* mRNA from the cell body to the distal processes of cultured oligodendrocytes (Carson et al., 1997). The localisation of *bcd* mRNA to the anterior of the oocyte requires *swallow* (Stephenson, 1988) which encodes a putative linker to the minus end directed microtubule motor cytoplasmic dynein (Schnorrer et al., 2000). However, dynein has not been shown to be required for *bcd* localisation and although many

transcripts such as *bcd* are localised to microtubule minus ends, the minus end directed motor(s) involved in this transport have not been identified.

In some cases, transcript localisation has been shown to depend on *cis*-acting RNA elements which are necessary and sufficient to localise reporter transcripts. Localisation assays using transgenic fusion constructs (Davis and Ish-Horowicz, 1991) or microinjection of RNA (Ferrandon et al., 1994; Glotzer et al., 1997) have allowed these localisation elements to be mapped to discrete sequences, often less than 100 nucleotides in length ***reviewed in (Bashirullah et al., 1998). In almost all cases, these localisation signals are found in the 3'UTR of the transcript, although some exceptions have been identified where sequences in the coding region or 5'UTR may be involved in localisation (Gonzalez et al., 1999; Thio et al., 2000).

In order to identify the RNA localisation machinery, biochemical methods such as U.V. crosslinking have been used to isolate factors which bind to RNA localisation elements. The results of these experiments suggest that some factors involved in mRNA localisation may be conserved across species, since the Vg1RBP/Vera protein which binds the localisation element of *Vg1* mRNA in *Xenopus* is homologous to the zipcode binding protein (ZBP-1) involved in *β-actin* mRNA localisation in chicken embryo fibroblasts (Deshler et al., 1998; Havin et al., 1998; Ross et al., 1997). However, the precise roles that Vg1RBP and ZBP perform in localisation are poorly understood.

Genetical analysis has also been used to identify factors involved in mRNA localisation. A number of mutations that disrupt the localisation of specific transcripts have been isolated in *Drosophila* and *S. cerevisiae*. In *Drosophila*, these genes include *staufen*, *exuperantia*, *swallow*, *vasa*, *homeless*, *orb*, *squid*, *K10*, *Bicaudal-C*, *Bicaudal-D*, *egalitarian* and *bullwinkle* (reviewed in (Bashirullah et al., 1998). Although many of

these genes have been cloned and sequenced, the functions played by the majority these proteins in transcript localisation are poorly characterised. The best understood examples are *squid* and *staufen* which encode an hnRNP protein and a dsRNA binding protein, respectively. Mutations in *squid* (*sqd*) cause mislocalisation of *grk* mRNA in the oocyte, leading to dorsoventral patterning defects (Kelley, 1993; Neuman-Silberberg and Schüpbach, 1993). Different isoforms of Sqd protein produced by alternative splicing perform distinct roles in *grk* mRNA localisation and translational activation (Norvell et al., 1999). *staufen* is required for the localisation and anchoring of *bcd* and *osk* transcripts in the oocyte and early embryo (Ferrandon et al., 1994; St Johnston et al., 1991). The Staufen protein has five dsRNA binding domains, which have specific functions in the transport and translational control of localised transcripts to which it binds (Micklem et al., 2000; Ramos et al., 2000).

In summary, mRNA localisation is an important mechanism for targeting proteins to their site of function and generating cellular polarity. In recent years, some of the mechanisms by which transcripts become asymmetrically localised in the cytoplasm have been identified. These include selective protection from degradation, anchoring at specific sites in the cytoplasm and motor-driven transport along microtubules and microfilaments. These models are not mutually exclusive, and could function in concert during the localisation of some transcripts (e.g. *osk* localisation by kinesin driven transport and selective anchoring during cytoplasmic streaming). It remains to be demonstrated whether vectorial nuclear export also contributes to mRNA localisation. Furthermore, in most cases the factors which anchor transcripts at the site of localisation or link mRNA to specific motors have not been identified, and these will be important areas for future study.

DROSOPHILA DEVELOPMENT

Drosophila melanogaster is an excellent model system for the study of cytoplasmic mRNA localisation and nuclear mRNA export as it combines excellent genetics with the ability to detect the intracellular location of mRNA at several developmental stages.

Overview of oogenesis

Female *Drosophila* have a pair of ovaries, each composed of 16-20 ovarioles which represent independent egg production lines. Ovarioles usually contain 6-7 developing egg chambers which become sequentially more mature as they move posteriorly within the ovariole. The egg chambers are produced in a specialised region at the anterior of the ovariole which contains somatic and germline stem cells. Within this germarium region, the progeny of the germline stem cells each undergo four rounds of mitosis with incomplete cytokinesis at each division. This forms a cyst of 16 cells which are interconnected with cytoplasmic bridges known as ring canals. Each cyst becomes surrounded by a layer of somatic follicle cells to produce an egg chamber which moves into the ovariole and eventually matures into an egg (Mahowald and Kambysellis, 1980).

The developmental events of oogenesis have been intensively studied, and will not be extensively reviewed here. In summary, one of the 16 cells in the cyst is chosen to become the oocyte, while the other 15 cells develop as nurse cells which become polyploid and perform nutritive roles for the oocyte. Proteins and mRNA's synthesised in the nurse cells are transported into the oocyte through the ring canals, and the developing oocyte expands to take up an increasing proportion of the egg chamber. Eventually, the nurse cells become confined to a small volume at the anterior of the egg

chamber as the contents of their cytoplasm are dumped into the enlarging oocyte. The nurse cells then break down. Meanwhile, the follicle cells migrate to cover the entire oocyte and secrete specialised layers of eggshell consisting of a waxy vitelline membrane under a layer of chorion. The eggshell protects the embryo after it is laid, preventing it from drying out. The chorion also contains several distinct structures with specialised functions. These include the dorsal appendages which function in gas exchange, and the micropyle which provides a route for sperm entry before the egg is laid (Spradling, 1993).

Early development of the embryo

The first 13 nuclear divisions of the *Drosophila* embryo occur rapidly and synchronously in a syncitium. Following fertilisation, cell cycles proceed from replication to mitotic phases with no gaps, and nuclear divisions take place every 8-12 minutes. Mitosis occurs almost synchronously throughout the early embryo, initiating in waves that spread out from the poles of the embryo and meet in its midregion (Foe and Alberts, 1983). During each of the early cycles the nuclei migrate outwards in a stepwise fashion towards the edge of the embryo, reaching the cortex at the beginning of cycle 10. The nuclei remain at the cortex of the embryo during the next three divisions, known as the syncitial blastoderm stages. The yolk is cleared from the peripheral cytoplasm (periplasm) surrounding the blastoderm nuclei, so that by the interphase of cycle 14 the embryo contains a monolayer of 6000 nuclei beneath the cortex and yolk particles are confined to the centre of the embryo, at least 40μm below the plasma membrane (Foe et al., 1993). Cycle 14 is the first cell cycle with a prolonged interphase. During the first 50 minutes of interphase 14, cleavage furrows progress inwards from the plasma membrane and enclose each nucleus in a separate cell. The nuclei change shape dramatically during

this phase of cellularisation. At the start of cycle 14 the cortical nuclei are roughly spherical, with a diameter of around 5μm, but they elongate progressively to become more cylindrical in shape and reach a height of over 15μm by the time cellularisation has completed (Fung et al., 1998). The process of gastrulation then begins the complex series of morphological events which elaborate the larval body.

It has been shown that no zygotic gene expression is required for normal progression through the first 13 mitotic cycles, development to this point being programmed largely by factors provided during oogenesis. Although the translation of some maternally derived transcripts (such as *bcd*) begins as soon as the embryo is fertilised, zygotic transcription does not begin appreciatively until cycle 10. Embryonic gene expression then increases during cycles 11-13 and reaches a high level by cycle 14 (reviewed in (Foe et al., 1993). During cycle 14, many maternal transcripts are specifically targeted for digestion (Bashirullah et al., 1999) allowing the control of development to pass from maternal to zygotic control.

Many of the genes expressed during the syncitial blastoderm stage are involved in setting up the segmented body pattern of the larva, in response to the maternal signals that specify the body axes. Every point along the anteroposterior (AP) axis encounters a unique concentration of maternal determinants such as Bicoid and Nanos, which are translated from localised transcripts and diffuse to form gradients through the syncitium. The expression of the gap genes (which include *hunchback*, *kruppel*, *knirps*, *giant*, *huckebein*, *tailless*, *orthodenticle*, *buttonhead* and *empty spiracles*) depends on the local concentration of maternal determinants, resulting in broad overlapping domains of gap gene expression along the AP axis. The gap genes are amongst the earliest zygotic products, and were originally isolated as mutations in which blocks of larval segments

are deleted or defective (Nüsslein-Volhard and Wieschaus, 1980). The gap gene products act as transcription factors which activate and repress the expression of individual pair-rule genes, leading to a complex striped pattern of pair-rule gene expression during cycle 14 (Pankratz and Jackle, 1993). The pair-rule genes (which include *hairy*, *fushi tarazu*, *even-skipped*, *runt*, *paired*, *odd-paired*, *sloppy paired* and *odd-skipped*) are expressed in a pattern of seven stripes, each offset slightly along the AP axis. Unlike the gap genes, the domains of pair-rule gene expression are very sharp, and each stripe is only about 4-5 nuclei in width. This is significant because the stripes of pair-rule gene expression define the pattern of larval segments by controlling the expression of the segment polarity genes (e.g. *wg* and *engrailed*) in single cell stripes, which define the exact parasegment boundaries.

The apical localisation of pair-rule transcripts is thought to suppress the diffusion of their products, since the invaginating membrane furrows block the transfer of components between the apical cytoplasm of adjacent nuclei as cellularisation progresses (Davis and Ish-Horowicz, 1991). By the time the pattern of segment polarity gene expression is established, cellularisation of the embryo is complete and the process of gastrulation is underway. However, by refining the patterns of gene expression from broad gradients to progressively narrower domains, every cell along the AP axis has received the information necessary for the segmented body plan of the larva and adult fly to be defined. The result of this cascade is the activation of the homeotic genes (such as *Ultrabithorax* and *Antennapedia*) which control the development and identity of different segments destined to produce adult structures such as wings or abdomen (Martinez-Arias, 1993).

The asymmetric distribution of mRNA in the cytoplasm plays an important role in multiple steps of this developmental pathway. The localisation of maternal transcripts to the anterior and posterior of the oocyte and early embryo define the co-ordinates which polarise the body axes. Apical localisation of mRNA in the blastoderm embryo may act to sharpen the stripes of pair-rule proteins (Davis and Ish-Horowicz, 1991) and is essential for the correct targeting and signalling function of the secreted Wg protein (Simmonds et al., 2001).

Aims of this study

The aims of this work were to investigate the mechanisms of intracellular trafficking of mRNA, and isolate factors involved in the nuclear export and cytoplasmic localisation of transcripts in the blastoderm embryo.

The first two results Chapters describe investigations into the movement of mRNA in the nucleus, by defining the sites of mRNA synthesis in embryonic nuclei and analysing the distribution of mRNA export intermediates in the nucleoplasm and nuclear envelope.

The following Chapters describe the isolation of a mutation which disrupts the nuclear export of mRNA, and the cloning and characterisation of the corresponding wild type gene *small bristles* which encodes a homologue of the TAP/Mex67p protein proposed to function in nuclear mRNA export.

In the final results Chapters, the models of cytoplasmic mRNA localisation are tested for apically-targeted pair-rule and *wg* transcripts, and the mechanism and molecular motors functioning in apical mRNA localisation are identified.

2

MATERIALS AND METHODS

MOLECULAR BIOLOGY

Solutions and Reagents

All solutions used were as described in Molecular Cloning – A Laboratory Manual (Sambrook et al., 1989). All reagents used to prepare buffers and solutions were from Sigma or BDH unless otherwise stated. Restriction enzymes were purchased from Roche (formerly Boerhinger Mannheim) or New England Biolabs, and were used according to the manufacturers instructions.

Purification of plasmid DNA

Minipreps of plasmid DNA were performed using a Qiagen turbo miniprep kit and vacuum manifold according to the manufacturers instructions. Where more DNA was required, a Qiagen midiprep kit was used to purify larger amounts plasmid DNA according to the manufacturers instructions.

Purification of genomic DNA from P1 and cosmid clones

The modified Qiagen protocol from Ali Moshrefi at the BDGP (available at http://www.fruitfly.org/methods) was used to purify DNA from genomic P1 and cosmid clones using a Qiagen maxi kit.

Purification of genomic DNA from adult flies

30-50 flies were placed in an eppendorf tube and frozen at –70°C. Frozen flies were homogenised with a pellet mixer (Treff) in 350µl of a solution containing 0.1M Tris (pH9), 0.1M EDTA (pH8) and 1% SDS and incubated at 70°C for 30 minutes. 50µl of 8M Potassium Acetate was added and the tube was incubated on ice for 30 minutes. The tube was spun in a microfuge at maximum speed for 15 minutes at 4°C, and the supernatant was removed to a new tube. Centrifugation was repeated to obtain a clear supernatant. 175µl of isopropanol was added and the tube was placed at –70°C for 10 minutes then spun for 5 minutes at maximum speed. The supernatant was discarded and the pellet was washed in 70% ethanol, air-dried and dissolved in 50µl T.E.

Where required, genomic DNA was further purified by addition of RNAaseA followed by 2 phenol/chloroform extractions. After an extraction with chloroform to remove all traces of phenol, genomic DNA was precipitated with Sodium Acetate and Ethanol. The pellet was washed with 70% Ethanol, air dried and dissolved in 50µl of T.E.

Isolation of total RNA from flies

An RNeasy mini kit (Qiagen) was used to prepare total RNA from flies according to the manufacturers instructions. 30 well-fed flies were frozen in liquid nitrogen and homogenised in 350µl of RLT buffer (Qiagen) using a Polytron (Kinematica) at maximum speed. Elution volume was 30µl and the concentration of RNA obtained was typically 1.0-3.0 µg/µl.

PCR

Standard conditions for a 50µl reaction were : 50ng template DNA, 5µl 10x PCR buffer containing 15mM $MgCl_2$ (Roche), 0.2mM Ultrapure dNTPs (Amersham), 1µM each forward and reverse primers, 2.5 Units Taq Polymerase (Roche).

The standard PCR program used was a 94°C hot start before 35 cycles of melting at 94°C for 30 seconds, annealing at 55°C for 30 seconds and elongation at 72°C for 30 seconds. A final elongation step at 72°C was carried out for 8 minutes.

Primers used are listed in Appendix B. Cycle conditions varied for certain primers. The extension time was increased up to 2 minutes for longer products, and the annealing temperature was raised to increase specificity. For amplifying larger products from genomic DNA, TaqPlus Long (Stratagene) was used with High Salt Buffer, and 1µl of DMSO was added to the reaction. A personal thermal cycler (Biometra) was used for all PCR reactions and the lid temperature was set to 105°C.

RT-PCR

A Titan One-tube RT-PCR kit (Roche) was used for RT-PCR. 10 Units of RNasin RNAase inhibitor (Promega) was added to the reaction and reverse transcription was carried out at 50°C for 30 minutes using 1ng of fly total RNA as a template, before switching to thermal cycling according to the manufacturers instructions

DNA Sequencing

A Big Dye DNA sequencing kit (Perkin Elmer Applied Biosystems) was used according to the manufacturers instructions in a 10µl reaction containing 4µl of Big Dye mix and 1.6 pmols of primer. The amounts of template DNA used for sequencing was typically

50-100ng for PCR products, 200ng for plasmid DNA and 2μg for cosmid and P1 DNA. To eliminate the chances of mistakes arising due to inaccuracy of Taq polymerase, PCR products were always sequenced on both strands and from two independent PCR reactions.

Cycle conditions used for sequencing reactions were 25 cycles of melting at 96°C for 30 seconds, annealing at 50°C for 15 seconds followed by elongation at 60°C for 4 minutes. Sequencing reactions were precipitated with 1μl of 3M NaOAc (pH 4.6) and 25μl of 100% Ethanol on ice for 20 minutes. Samples were then centrifuged at 14kprm for 30 minutes at 4°C and the supernatant was removed. Pellets (not always visible) were washed with 70% Ethanol and air dried. Sequencing reactions were analysed on an ABI377 sequencer by the sequencing service at ICMB, University of Edinburgh. Primers used are listed in Appendix B

Synthesis of Dig labelled RNA probes

DIG labelled RNA probes were synthesised by *in vitro* transcription using an RNA DIG labelling kit (Roche) according to the manufacturers instructions. 1μg of linearised plasmid DNA containing the appropriate cDNA sequence was used as a template for transcription by T3, T7 or SP6 polymerase in the presence of 20 Units of RNasin RNAase inhibitor (Promega). The resulting DIG labelled RNA was not purified further before use.

Plasmids containing cDNA were gifts from David Ish-Horowicz: *even-skipped, hairy, paired, fushi tarazu.* Elizabeth Gavis: *giant, knirps, huckebein.* Bruce Edgar: *string, hunchback, Kruppel.* Peter Gergen: *runt.* Ira Clark: *LacZ.* Patrick O'Farrell: *Ultrabithorax* (exon 1.2), *engrailed.* Jean-Paul Vincent: *Wingless.* Ilan Davis: *pBSX44.* The *hairy* intron probe was synthesised by transcription directly from a purified 0.8Kb

PCR product amplified from genomic DNA with primers containing T7 and T3 promoters.

Synthesis of fluorescently labelled, capped RNA

Fluorescently labelled, capped RNA was synthesised by *in vitro* transcription using an mCAP RNA capping kit (Stratagene). 2-3μg of linearised plasmid DNA was transcribed by T3, T7 or SP6 RNA polymerase for 2 hours at 37°C in a 50μl reaction containing 0.4mM ATP, 0.4mM CTP, 0.36mM UTP, 0.04mM AlexaFluor 488 or 546-UTP (Molecular Probes), 0.12mM GTP, 0.3mM ^{7}mG(5')ppp(5') CAP analogue and 40 Units of RNasin (Promega). The reaction was incubated for 15 minutes with DNAaseI to digest template DNA. Unincorporated nucleotides were removed using a Sephadex G50 RNA spin column (Roche) and the RNA was extracted with phenol/$CHCl_3$, precipitated with NH_4OAc/EtOH and re-suspended in water.

The quality of the resulting RNA was assessed by electrophoresis and the yield and incorporation by spectrophotometry. Each molecule of *run* RNA was labelled by 16 molecules of AlexaFluor546 dye. This is equivalent to incorporation of 6.5 fluorochromes per kb of RNA, or one fluorochrome every 154 nucleotides on average.

Southern Blotting

After visualisation with Ethidium bromide, the agarose gel was soaked in 0.1M HCl for 10 minutes to depurinate the DNA. The DNA was then transferred to a Hybond N+ membrane overnight by alkaline capillary transfer using 0.4M NaOH as a transfer buffer. After transfer, the membrane was washed briefly in 2x SSC, then baked at 65°C for 1 hour. The membrane was then moistened in 2x SSC, rolled in a mesh and placed in a Hybaid bottle (all subsequent steps performed in Hybaid bottle). The membrane was

prehybridised for at least 2 hours at 50°C in Southern HYB solution containing 50% formamide, 5x SSC, 1x Dernhardts reagent, 1% SDS, 20mM $Na_4P_2O_7$ (pH7) and 4% Blocking reagent (Roche). The membrane was then hybridised overnight at 50°C in 15ml of Southern HYB containing 150µl of 10mg/ml denatured herring sperm DNA and 1.5µl (approx 0.75ng) of the appropriate DIG labelled RNA probe.

Northern Blotting

30µg of fly total RNA was electrophoresed in denaturing agarose gels containing formaldehyde and 1x MOPS buffer. Gels were then rinsed in 3 changes of water to remove the formaldehyde before being soaked in 20x SSC for 20 minutes. The RNA was transferred to a Hybond N membrane overnight by capillary transfer using 20x SSC as a transfer buffer. After transfer, the membrane was rinsed in 6x SSC and the RNA was crosslinked to the membrane with U.V. light. The membrane was then stained with 0.04% Methylene Blue in 0.5M NaOAc to visualise the RNA markers and rRNA bands. The membrane was then moistened in 2x SSC, rolled in a mesh and placed in a Hybaid bottle (all subsequent steps performed in Hybaid bottle). The membrane was prehybridised for at least 2 hours at 65°C in Northern HYB solution containing 50% formamide, 5x SSC, 1x Dernhardts reagent, 1% SDS, 20mM $Na_4P_2O_7$ (pH7) and 4% Blocking reagent (Roche). The membrane was then hybridised overnight at 65°C in 15ml of Northern HYB containing 150µl of 10mg/ml *E. coli* tRNA and 1.5µl (approx 0.75ng) of the appropriate DIG labelled RNA probe.

Detection of DIG labelled nucleic acid probes on membranes

After hybridisation, the probe was removed and the membrane was rinsed twice at 65°C in a solution containing 2x SSC and 0.1% SDS. The membrane was then washed twice

in this solution at 65°C for 30 minutes each. A final wash was performed at 65°C in 0.1x SSC with 0.1% SDS for 30 minutes, before incubation in blocking buffer (1% w/v blocking reagent in 0.1M Maleic Acid Buffer, pH7.5) at room temperature for 30 minutes. The probe was detected by incubating the membrane in 20ml of blocking buffer containing 2µl of Alkaline Phosphatase-conjugated sheep anti-DIG antibody (FAB fragment, Roche) for 1 hour at room temperature. The membrane was then washed twice for 15 minutes each in washing buffer (0.1M Maleic Acid Buffer, pH7.5 with 0.3% v/v Tween 20) at room temperature. The membrane was rinsed in detection buffer containing 100mM Tris (pH9.5), 100mM NaCl, 50mM $MgCl_2$ before chemiluminescent detection of Alkaline Phosphatase by incubation for 5 minutes in 10ml detection buffer containing 100µl CSPD (Roche). Membranes were sealed into plastic bags whilst still wet and incubated at 37°C for 15 minutes before autoradiography.

Computer Analysis of DNA and protein sequences

Small scale manipulation, translation and alignment of DNA sequences was carried out using Gene Jockey 2 (P.L. Taylor, Biosoft, UK). Larger scale analyses of DNA and protein sequences were carried out using the facilities at the MRC Human Genome Mapping Project Resource Centre (available at http://www.hgmp.mrc.ac.uk/). NIX was used to predict ORF's and other features in genomic DNA sequences. MAGI was used to create multiple alignments of protein and DNA sequences using ClustalW, Dialign or Alien algorythms. ExIsT was used to predict the intron/exon structure of genes by comparing genomic and cDNA sequences.

ClustalX (Jeanmougin et al., 1998) was used to generate final alignments for protein sequences, and MacBOXSHADE 2.15 (Michael D. Baron, Institute for Animal Health,

Pirbright Surrey UK) was used illustrate multiple sequence alignments in colour according to consensus identical or conserved residues.

BLAST searches were run either at the HGMP, the Berkeley *Drosophila* Genome project (available at http://www.fruitfly.org/blast/index.html) or at the NCBI (available at http://www.ncbi.nlm.nih.gov/BLAST/).

DROSOPHILA SPECIFIC PROTOCOLS

Drosophila strains

All fly stocks were raised on standard cornmeal-agar medium at 18°C, 21°C, 25°C or 29°C depending on the experiment. *OregonR* and *y,Df(1)w*^{67} were used as the wild type strains. Other fly stocks used in this study are listed in Appendix A.

Collection and fixation of embryos

Embryos were collected, dechorionated and fixed rapidly in a two phase mixture of 37% formaldehyde and heptane as described previously (Wilkie and Davis, 1998; Wilkie et al., 1999). Fixed embryos were devitellinised in methanol and stored in methanol at -20°C.

To shift embryos from the t.s. collection to 33°C, the collection plate was wrapped in parafilm then completely immersed in a water bath at 33°C for the desired time. Embryos were then dechorionated and fixed as above, except all solutions including fix were preheated to 33°C.

Microinjected embryos were washed from coverslips using heptane, then fixed as above before being transferred to double-sided sticky tape, immersed in PBS and devitellinised by hand using a fine hypodermic needle.

mRNA in situ hybridization with fluorescent tyramide detection

In situ hybridisation to detect mRNA with fluorescent tyramides (NEN LifeSciences) was performed as described previously (Wilkie and Davis, 1998; Wilkie et al., 1999). Briefly, embryos were rehydrated then post-fixed and rinsed five times in 1x PBT (1x PBS + 0.1% Tween20) and prehybridized for at least one hour at 70°C in mRNA HYB buffer (50% formamide, 5x SSC, 100µg/ml *E. coli* tRNA, 50µg/ml heparin and 0.1% Tween20, adjusted to pH6.5 with HCl). DIG labelled antisense RNA probes were typically used at a concentration of 0.5ng/ml in mRNA HYB buffer and hybridised to embryos overnight at 70°C. Hybridised embryos were extensively washed at 70°C in mRNA HYB buffer and PBT, then incubated in a horse radish peroxidase (HRP) conjugated anti-DIG antibody (sheep anti-DIG-POD Fab fragment, Roche) and washed in PBT. The HRP coupled antibody was visualised by adding Cyanine-3 (Cy3) or FITC tyramides according to the manufacturer's instructions (TSA Direct, NEN Life Sciences, UK). The reaction was allowed to proceed for 2-10 minutes before washing with PBT to remove unreacted tyramides.

Immunofluoresence

The nuclear envelope was labelled in the green fluorescent channel using AlexaFluor488-conjugated Wheat Germ Agglutinin (Molecular Probes). For triple labelling experiments, the nuclear envelope was labelled with a monoclonal anti-lamin antibody (Yosef Gruenbaum) and visualised using Cy5 coupled donkey anti mouse

antibodies (Jackson). Microtubules were detected using a monoclonal antibody against β-tubulin (Amersham) and visualised using Alexa568 coupled goat anti mouse antibodies (Molecular Probes) or Cy5 coupled donkey anti mouse antibodies (Jackson). Alternatively, microtubules were labelled with a rat antibody against α-tubulin (Clone YL1/2, Oxford Biotechnology Limited) and visualised with goat anti rat AlexaFluor488 coupled antibodies (Molecular Probes) or Cy5 coupled goat anti rat antibodies (Jackson).

Microinjection of living *Drosophila* embryos.

Dechorionated embryos were aligned in rows on agar blocks and transferred onto number 1 thickness coverslips coated with lines of embryo glue (prepared by dissolving double sided sellotape in heptane overnight). The embryos were then dehydrated for 10 minutes over silica gel and overlayed with series 700 halocarbon oil (KMZ Chemicals Ltd). Embryos were microinjected through the anterior or posterior using Eppendorf femtotip needles with 100μg/ml Colcemid (Sigma) in water or 500μg/ml Cytochalasin B (Sigma) in injection buffer (0.1mM Sodium Phosphate buffer, Ph7.8 and 5mM KCl) with 10% DMSO. Monoclonal antibodies: P1H4 from Tom Hays against a fragment of *Drosophila* dhc from residues 128-422 near the N-terminus (McGrail and Hays, 1997), anti-dhc antibody from David Sharp against the HUV fragment of *Drosophila* dhc (Sharp et al., 2000a) and 12CA5 anti-HA (Yiota Kafasla and Joe Lewis) were spot dialysed into injection buffer using Millipore 0.025 micron VSWP filters before injection. GST-p50/dynamitin or control GST protein was expressed in bacteria and purified over a glutathione-agarose column as previously described (Sharp et al., 2000b) and concentrated to 18 mg/ml in injection buffer using an Ultrafree protein concentrator (Millipore). Final intracellular concentration of drugs and proteins is approximately 50

times lower than the injected concentration. Colcemid was inactivated by 10 seconds of illumination under the DAPI channel, which excites the sample with U.V. light. Similar techniques have previously been used to inactivate colcemid in the oocyte (Theurkauf and Hazelrigg, 1998). Pre-injection of embryos with water, 10% DMSO or 50% DMSO did not disrupt the ability of injected *run* RNA to localise correctly to the apical cytoplasm (data not shown). A second injection with fluorescent RNA was typically made through the same point in the embryo within ten minutes after the first injection. Injected embryos were either imaged *in vivo*, or fixed and devitellinised by hand using a fine hypodermic needle and stored in Methanol at –20°C.

MICROSCOPY

4-D Fluorescence imaging and deconvolution

Fixed embryos were mounted in Vectashield (Vector Laboratories) or 80% glycerol and viewed using a Sedat/Agard DeltaVision widefield microscope (Applied Precision Inc.) based on an Olympus IX70 inverted microscope. 3-D image stacks were acquired with a cooled 12 bit PXL CCD camera (Photometrics) as previously described (Davis, 2000; Wilkie et al., 1999). Immersion oil with the appropriate refractive index was used to minimise spherical aberration in thick samples viewed by oil immersion lenses (Davis, 2000). Combined DIC and green fluorescent images were captured using a dedicated dual DIC/GFP filter cube (Olympus) with a diachroic mirror that polarises light for the DIC in the red spectrum only. DeltaVision software was used to control the movement of the motorised stage in 3 dimensions, and also to control the filter wheels governing the excitation and emission filters and the shutters controlling light sources and camera exposure. Each image in a Z-series was obtained by moving the Z position by 0.2μm

(100X/1.4NA lens) or 1.0μm increments (20X/0.75NA lens). At every focal position, an image was captured for each fluorochrome, typically DAPI (blue), FITC or AlexaFluor488 (green), Rhodamine, Cyanine 3 or AlexaFluor546 (red) and Cyanine 5 (far-red). Each Z-series from the same experiment was taken with an identical objective lens and camera settings (exposure, gain and degree of pixel binning) so that different images from the same sample could be compared. Living embryos were imaged directly on coverslips, and 3-D image stacks were typically captured every 10 seconds to construct time-lapse movies. Out-of-focus light was reassigned to its original point source in image stacks (from each time point in time-lapse movies) using Sedat/Agard 3-D constrained iterative deconvolution algorithms (DeltaVision software) after empirical determination of the point spread function of each lens.

Data analysis

Nuclei were imaged at the surface of embryos at similar ages in interphase 14. The age of embryos was estimated from the progression of the cellularisation membranes and the average length of nuclei (Fung et al., 1998). The distances from the top of the nucleus to the position of nascent transcript foci and RNA export intermediates were measured, and this data was plotted onto a 12μm scale with 0.5μm increments, representing the nucleus in an embryo 20 minutes after the start of interphase 14.

All analysis of microscope images was carried out using DeltaVision 3-D image analysis software running on Silicon Graphics workstations. To measure the fluorescence intensity of RNA particles, 2-D polygons were defined in deconvolved image stacks using the appropriate threshold intensity to identify nascent transcript foci and mRNA export and localisation intermediates. Subsequently, 3-D objects were created from the 2-D stacks of polygons and the integrated fluorescence intensity, volume and position of

each object were calculated. Identical threshold intensities were used to define objects within equivalent image stacks so that calculated intensity values were comparable between image stacks captured from the same sample of embryos. Nascent transcript foci were usually identified as one or two very intense and highly localised fluorescent signals within nuclei. The number of foci was determined by viewing a series of focal planes through the entire nucleus. The average speed of RNA particles was determined by tracking individual particles in time-lapse movies and measuring the distance moved between in different time points.

Thin section transmission electron microscopy

Dechorionated embryos were fixed in a two phase mixture of freshly prepared 2% paraformaldehyde and 0.5% gluteraldehyde in 0.1M Phosphate Buffer (pH7.5) under heptane for 1 hour. They were then devitellinised by hand using a needle, and post fixed for 3 hours. Embryos were then fixed in Osmium tetroxide and dehydrated in an ethanol series before infiltration through a series of propylene oxide and Spurrs' resin. Embryos were embedded and dried in Spurrs' resin overnight at 70°C. 90nm sections were cut on a Reichart Jung Ultracut microtome, collected on specimen grids and stained in uranyl acetate and lead citrate. Specimens were viewed with a Philips CM120 Biotwin transmission electron microscope (Biological Sciences Electron Microscope Facility, ICMB) operated at an accelerating voltage of 100kV.

3

THE INTRANUCLEAR POSITION OF TRANSCRIBED GENES

INTRODUCTION

The spatial arrangement of interphase chromosomes and the way in which transcription and processing of mRNA are organised within the nucleus are subjects of great interest. Although the genomes of several organisms have now been sequenced, yielding new insights into the higher level organisation of genes on chromosomes, much less is understood about the architecture of the nucleus and the spatial arrangement of chromosomes during interphase. In particular, the relationship between the intranuclear position of genes and their transcriptional state is poorly characterised. Some inactive genes in mammalian cells and *Drosophila* embryos specifically associate with centromeric heterochromatin (Brown et al., 1997; Dernburg et al., 1996), and association with the nuclear envelope has been shown to enhance transcriptional silencing in yeast (Andrulis et al., 1998). Although these results demonstrate that transcriptional silencing can involve movement of a gene to a different part of the nucleus, it is less clear whether genes generally move to new positions upon activation of their transcription. The use of *in situ* nick-translation to infer the location of transcriptionally active chromatin based on its increased sensitivity to DNAaseI has suggested that transcription might occur largely around the nuclear periphery (Degraaf et al., 1990; Hutchison and Weintraub, 1985; Krystosek and Puck, 1990). These results support the "Gene Gating" hypothesis

which proposes that active genes could associate with nuclear pores to facilitate efficient mRNA export or directional nuclear export (Blobel, 1985; Davis et al., 1993). In contrast RNA polymerase II, Poly(A)$^+$ RNA and nascent RNA are found in many discrete sites throughout the nucleus, rather than being enriched at the nuclear periphery (Fay et al., 1997; Singer and Green, 1997; Zeng et al., 1997). When transcription sites are labelled in living cells by incorporation of ribonucleotide analogues, the number of intranuclear sites detected is frequently fewer than the number of transcripts synthesised in the cell. These results led to the proposal that transcription sites are clustered together in a relatively small number of regions, each containing many active genes (Iborra et al., 1996; Jackson et al., 1993; Pombo and Cook, 1996). This model predicts that genes would move to specialised transcription sites when they became active, which has yet to be observed. It is therefore controversial whether transcription can occur in any part of the nucleus, or whether it is localised to specific nuclear sites.

The *Drosophila* blastoderm embryo provides a particularly suitable model system for analysing the intranuclear position of genes and for testing the relationship between their transcription and their intranuclear distribution. Within each blastoderm nucleus, chromosomes are aligned with the centromeres clustered within the apical hemisphere and the telomeres localising within the basal hemisphere, an arrangement known as Rabl conformation. Other parts of the chromosomes are known occupy intermediate positions in the apical-basal axis depending on their cytological location (Marshall et al., 1996). rDNA genes are located at the apical pole of the nucleus, where the nucleolus is positioned. The interphase Rabl orientation of chromosomes is thought to result from the movement of chromosomes during the previous mitotic division, which leaves centromeres and telomeres on opposite sides of the cell following anaphase. Rabl orientation of chromosomes has been observed in many tissue types including plant and

mammalian cells in addition to *Drosophila* (Marshall et al., 1997) and was first described by the microscopist Carl Rabl in 1885 (Rabl, 1885).

The nuclear positions of randomly selected loci were previously mapped by FISH to chromosomes in blastoderm embryos, demonstrating that some loci consistently localise at the periphery or interior, while others occupy random positions within the nucleus (Marshall et al., 1996). This study reported the average position of chromosomal DNA in nuclei throughout the embryo, and would therefore not necessarily reveal variations in the position of genes that are expressed at different levels (such as stripes of pair rule gene activity). Furthermore, although Poly(A)$^+$ and nascent RNA have been detected throughout the nucleus (Singer and Green, 1997), the position of specific transcribed genes has only been studied in a few cases in *Drosophila* (Kopczynski and Muskavitch, 1992; Shermoen and O' Farrell, 1991).

To address the relationship between the intranuclear position of genes and their transcriptional state, the location and intensity of nascent transcripts detected by RNA *in situ* hybridisation was analysed in blastoderm nuclei.

RESULTS

Sensitive, high resolution detection of mRNA *in situ* using fluorescent tyramide signal amplification

Nascent transcripts can be visualised by mRNA *in situ* hybridisation because large amounts of nascent RNA, pre-mRNA and splicing intermediates are concentrated in a small region around the gene. These foci have been shown to contain nascent RNA as they disappear upon RNAase treatment and 5' sequences are detected prior to 3' sequences after induction of transcription (Shermoen and O' Farrell, 1991). Furthermore, the number of foci depends on the state of DNA replication and the pairing of homologous chromosomes. A suitable method of studying the position of individual transcribed genes is therefore to determine the nuclear position of nascent transcripts. The most widely used method for the detection of mRNA is *in situ* hybridisation with Digoxygenin labelled probes, followed by highly sensitive alkaline phosphatase histochemical detection (Lehmann and Tautz, 1994; Tautz and Pfeifle, 1989). However, the resulting dark stains are incompatible with fluorescent labelling and are visualised with much poorer spatial resolution than fluorescent markers. To overcome this problem, a new *in situ* hybridisation protocol was developed which uses tyramide signal amplification (TSA) for the fluorescent detection of mRNA (Wilkie and Davis, 1998). The detection is highly sensitive as it relies on enzymatic amplification of signal by Horse Radish Peroxidase (HRP) to deposit fluorochrome labelled tyramides at the location of the probe (Raap et al., 1995). High resolution is maintained as the reaction produces tyramide radicals which covalently react with proteins at the site of HRP activity, preventing appreciable diffusion of the signal (Speel et al., 1997). Furthermore,

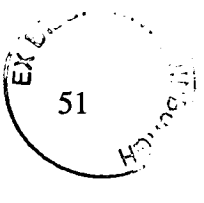

Figure 3-1

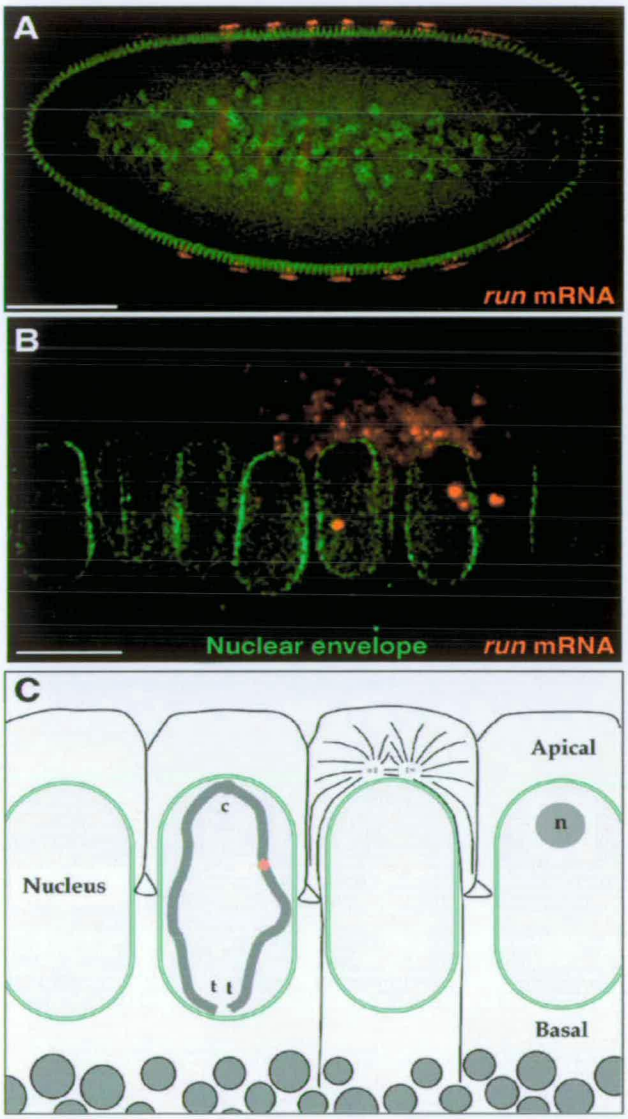

Figure 3-1 Detection of mRNA and architecture of the blastoderm embryo. (**A**) Low power optical section through the middle of a cycle 14 blastoderm embryo. The nuclear envelope is labelled with WGA-AlexaFluor488, shown in green. mRNA of the *ftz* gene, detected by *in situ* hybridisation, is shown in red. *ftz* is expressed in seven stripes along the anterior-posterior axis, and the *ftz* mRNA is localised on the apical side of the peripheral nuclei. Bar = 100μm. (**B**) High power image of peripheral nuclei, showing *ftz* mRNA in the apical cytoplasm, and bright nascent transcript foci within nuclei in expression stripes. Bar = 10μm. (**C**) Diagram of the polarised cytology of a blastoderm embryo. The elongated nuclei are arranged along the periphery of the embryo, dividing the cortical cytoplasm into apical and basal compartments. Cell membrane furrows move down between the nuclei to cellularise the embryo. The polarised nuclei contain an apical nucleolus (n) and Rabl-oriented chromosomes with apical centromeres (c) and basal telomeres (t). The red circle represents a transcribed gene. A pair of centrosomes in the apical cytoplasm nucleate a basket of microtubules, which form an apical cap around the nucleus with a few microtubules trailing down into the yolk.

the use of fluorescence allows quantitative, high resolution detection in addition to double and triple labelling of different transcripts and other cell components.

Nascent transcript foci adopt a consistent position in the apical-basal nuclear axis

In situ mRNA hybridisation with fluorescent TSA detection was used to covisualise the nascent transcript foci of 15 different genes with the nuclear envelope at high magnification. Nascent transcript foci were identified as one or two very bright fluorescent signals within nuclei, depending on the pairing of homologous chromosomes and the state of DNA replication (Figure 3-1). Optical sections were acquired through the middle of the embryo allowing the nuclei aligned along the edge of the embryo to be imaged in the apical-basal axis, with the apical side nearest the plasma membrane (Figure 3-1). The location of nascent transcript foci from each gene were mapped in nuclei from 2-3 different embryos of similar ages, and these positions were plotted onto the outline of a single representative nucleus, defining the area where each gene is transcribed within the nucleus.

The results show that the position of each transcribed gene is restricted to a specific plane along the apical-basal nuclear axis. The nuclear position of this plane is directly related to the cytological position of the gene and the Rabl orientation of chromosomes. Genes such as *kruppel* (*kr*), *giant* (*gt*) and *string* (*stg*) which are located near a telomere are transcribed in the basal part of the nucleus whereas genes positioned midway along a chromosome arm such as *runt* (*run*), *engrailed* (*en*) and *hunchback* (*hb*) are transcribed in the middle of the nucleus (Figure 3-2). Tandemly repeated rDNA genes which are located in the heterochromatin nearest the centromere are found in the most apical position (Anthony Shermoen, see Figure 3.2 and (Wilkie et al., 1999). All the genes that

Figure 3-2

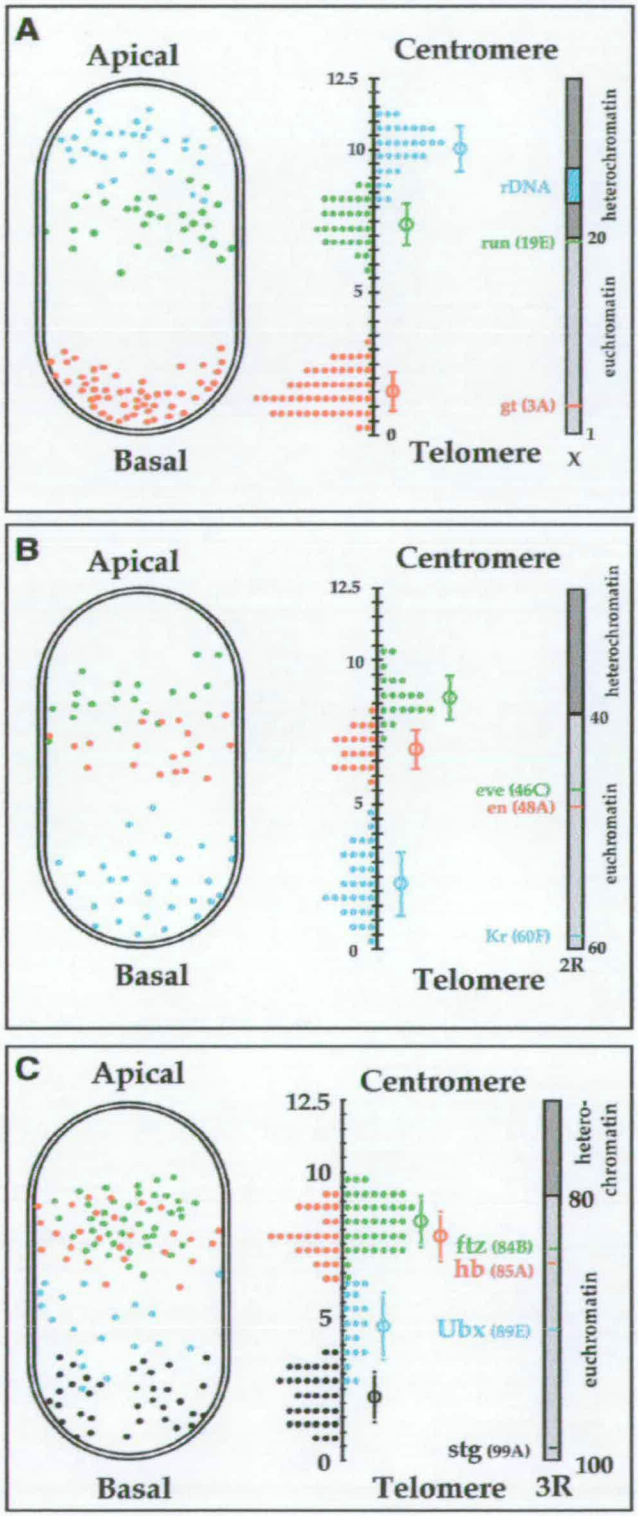
A
Apical
Centromere
12.5
10
5
0
rDNA
run (19E)
gt (3A)
heterochromatin
20
euchromatin
1
Basal
Telomere
X
B
Apical
Centromere
12.5
10
5
0
heterochromatin
40
eve (46C)
en (48A)
euchromatin
Kr (60F)
60
Basal
Telomere
2R
C
Apical
Centromere
12.5
10
5
0
hetero-
chromatin
80
ftz (84B)
hb (85A)
Ubx (89E)
euchromatin
stg (99A)
100
Basal
Telomere
3R

were analysed were found to occupy distinct positions within the apical-basal nuclear axis. Even closely linked genes such as *ftz* and *hb* (separated by only 0.5 centimorgans or 1/100 of a chromosome arm) have overlapping but distinguishable positions (Figure 3-2).

These results suggest that transcriptional activation of a gene does not radically change its position in the nucleus, as the positions measured for the all the genes that were analysed are exactly as predicted by the known orientation of chromosomes in blastoderm nuclei (Marshall et al., 1996). Furthermore, these results demonstrate that direct gene gating of pair-rule genes does not occur. Pair-rule transcripts are localised in the apical cytoplasm, but pair-rule genes such as *ftz*, *run*, and *eve* are not transcribed in the apical region of the nucleus. Direct gene gating is still a possibility in the case of *stg*, which is transcribed in the basal part of the nucleus and has mRNA that is localised to the basal cytoplasm.

Figure 3-2 Apical-Basal Position of Transcribed genes on the X chromosome, the left arm of chromosome 2 and the right arm of chromosome 3. The observed nuclear positions are plotted into average-shaped nuclei, 12.5 μm in length. The cytological positions of the genes on metaphase chromosome arms are drawn to scale on the right of each panel. In the centre of each panel, a histogram is drawn from the distribution of the nascent transcript foci that lie within 0.5 μm intervals along the apical–basal axis of the nucleus. The average position is indicated by an open circle and the standard deviation by an error bar in each case. (**A**) The *gt* gene (red) is located relatively near the telomere of the X chromosome and is transcribed in the basal region of the nucleus, whereas *run* (green) is located near the middle of the chromosome and is transcribed in the middle of the nucleus. Tandemly repeated rDNA genes (blue) are located in a more apical position in accordance with their more proximal cytological position. (**B**) *Kr* (blue) is located very near the telomere of chromosome 2R, and is transcribed in the basal region of the nucleus. In contrast, *en* (red) and *eve* (green) are situated nearer the middle of the chromosome arm and are transcribed in more apical regions of the nucleus in correspondence with their order on the chromosome. (**C**) *stg* (black) is positioned near the telomere of chromosome 3R, and is transcribed basally. *Ubx* (blue), *hb* (red) and *ftz* (green) are transcribed in successively more apical domains, in accordance with their cytological positions.

Figure 3-3

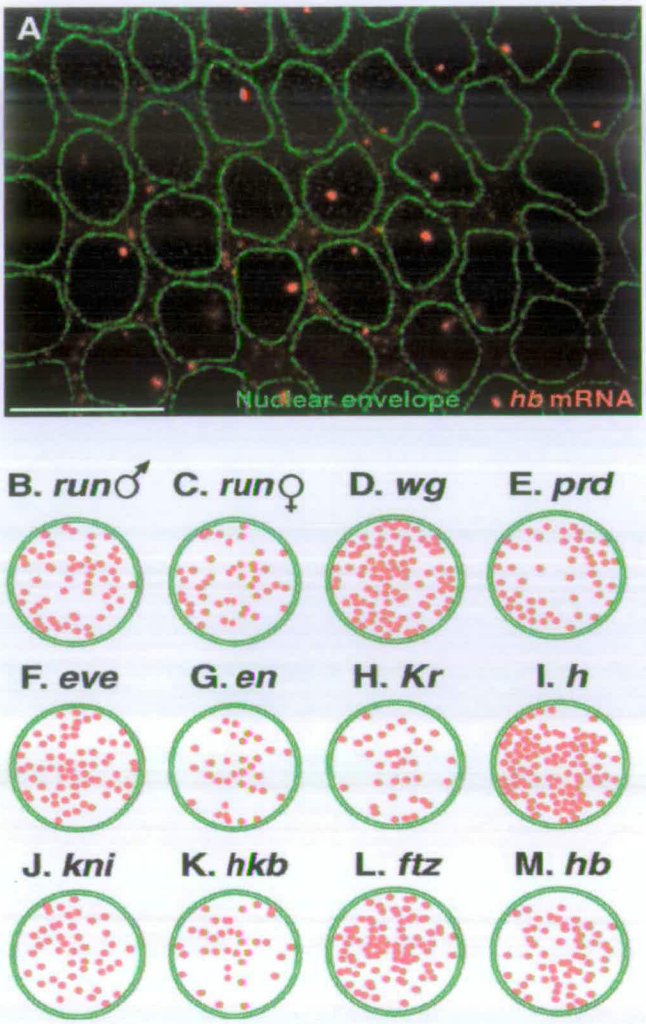

Figure 3-3 Radial Position of Transcribed genes. (**A**) Optical section through the layer of nuclei at the surface of a blastoderm embryo. The nuclear envelope is labelled in green. *hb* mRNA, detected by *in situ* hybridisation, is shown in red. Bright nascent transcript foci are visible within nuclei, representing sites of active transcription of the *hb* gene. Bar = 10μm. (**B-M**) The radial distribution of nascent transcript foci of 11 different genes, plotted into average nuclear outlines. No difference was observed between (**B**) male and (**C**) female embryos expressing *run*, despite the different number of copies of the gene in the two sexes. The nascent transcripts of most genes are located in random radial positions, but (**E**) *prd* showed some preference for the nuclear envelope, in accordance with its location near a nuclear envelope attachment site.

Although these results do not show the positions of transcribed genes in 3 dimensional space, they show that nascent transcripts are not specifically associated with the nuclear envelope, suggesting that genes are often transcribed in the interior of the nucleus.

Transcribed genes do not adopt consistent radial positions within their apical-basal domains

To define the relationship between transcribed genes and the nuclear envelope more precisely, optical sections were acquired at the surface of the embryo allowing nuclei to be visualised in cross section, in a plane perpendicular to the apical-basal axis. Nascent transcript foci from 11 different genes were covisualised with the nuclear envelope in 2-3 embryos of similar age, and their positions were plotted onto a profile of a typical nucleus.

Nascent transcript foci were not found to adopt any particular radial position within their apical-basal domain. In all but one case, nascent transcript foci adopted random positions inside the nucleus, and did not display any consistent association or exclusion from the nuclear envelope (Figure 3-3). For example, *ftz* nascent transcript foci are randomly positioned with respect to the nuclear envelope. This finding is in agreement with previous studies showing that genomic DNA from the 84A6-B2 region which includes the *ftz* gene is situated at random locations in the nucleus (Marshall et al., 1996). This result demonstrates that the position of the *ftz* gene is not altered in regions of the embryo where it is transcribed. *ftz* is not specifically associated or excluded from the nuclear envelope in the expression stripes, but is localised randomly in all regions of the embryo. In contrast to the random radial positions found for 10 of the transcribed genes which were studied, the *paired* (*prd*) gene was consistently transcribed near the nuclear envelope (Figure 3-3). This can be explained by the fact that *prd* is located in

close proximity to a nuclear envelope attachment site in polytene region 32E-33D. A P1 probe from 33C1-6 containing the *prd* gene was previously shown to associate with the nuclear envelope (Marshall et al., 1996).

Together, these results indicate that active genes are not specifically associated or excluded from the nuclear envelope. The locations of the transcribed genes investigated here are consistent with the known arrangement of chromosomes and the position of loci previously described inside the nucleus. Furthermore, the results suggest that effective transcription of genes can take place throughout the nucleus.

The level of transcription does not influence the intranuclear position of active genes

The use of *in situ* nick translation to infer the location of active chromatin has suggested that transcription takes place mainly at the periphery of the nucleus (Hutchison and Weintraub, 1985; Krystosek and Puck, 1990). Although the results described above show that it is possible for genes to be transcribed in all parts of the nucleus, these experiments do not address whether genes positioned in different parts of the nucleus are expressed at different levels. For example, the most strongly expressed genes might be associated with the nuclear envelope or localised in the interior of the nucleus. In order to determine whether the level of transcription is related to the nuclear position of a given gene, the amount of RNA at individual nascent transcripts was compared to their distance from the nuclear envelope.

The amount of RNA at a nascent transcript focus should be directly related to its fluorescent intensity, which can be reliably measured providing a CCD camera with a linear response is used to capture images. To demonstrate that the fluorescence intensity

Table 3a. Fluorescence intensity of *run* nascent transcript foci

Region of embryo	Intensity of nascent transcripts
Stripe 1	648,771 ± 70,300 (N=17)
Head Patch	144,680 ± 28,236 (N=12)
Interstripe	15,124 ± 5,326 (N=4)

The fluorescence intensity of nascent transcript foci within nuclei in different expression domains of *run* in a single male embryo. Total integrated fluorescence intensity is measured in arbitrary units ± standard error. N = number of foci measured.

Table 3b. Fluorescence intensity of nascent transcripts

Gene	Intensity at nuclear periphery	Intensity at nuclear interior
run	246,692 ± 30,915 (N = 8)	272,175 ± 51,896 (N =7)
h	119,369 ± 7,851 (N = 35)	126,828 ± 10,579 (N = 31)
Ubx	600,795 ± 109,538 (N = 7	588,316 ± 131,285 (N =7)
X44N	1,442,708 ± 202,842 (N = 14)	1,501,704 ± 225,728 (N = 15)

A comparison of the fluorescence intensity of nascent transcript foci within individual nuclei, in which one focus is at the periphery and the other in the nuclear interior. The data was collected from a single embryo for each gene. Peripheral nascent transcripts were within 0.2μm of the nuclear envelope. Total integrated fluorescence intensity is measured in arbitrary units ± standard error. N = number of foci measured.

of a nascent transcript focus is a measure of its transcriptional activity, the intensity of *run* nascent transcript foci was measured in different regions of the embryo known to express the gene at different levels. *run* nascent transcript foci in stripe one were found to have a fluorescence intensity 4.5 times higher than nascent transcript foci in the head patch of the same embryo (Table 3a) where expression begins later and is not as strong (Klingler et al., 1996). In addition to this, very rare nuclei in the interstripes which express *run* at low levels were found to have faint nascent transcript foci which were 43 times less bright than those found in the expression stripes. These results show that the intensity of fluorescent signal in the nascent transcript is related to the level of expression of a gene.

To determine whether genes are transcribed more heavily at the nuclear envelope or the nuclear interior, the intensity of nascent transcripts within 0.5μm of the nuclear envelope were compared with foci from the interior of the nucleus. Intensity data for each gene was obtained from many nuclei from a single embryo, as there are sometimes variations in intensity between different embryos in the same experiment. The results show that the total fluorescence intensity of nascent transcript foci at the periphery and the interior of the nucleus are not significantly different (Table 3b).

To further investigate the relationship between transcriptional activity and nuclear position of different genes, the intensity of nascent transcripts was plotted against their distance from the nuclear envelope. In the case of *run*, the transcriptional level was found to be independent of the distance from the nuclear envelope, both in the head patch and in the stronger expression stripes (Figure 3-4). The intensities of *wg*, *ftz* and *hairy* (*h*) nascent transcript foci were also unrelated to their distance from the nuclear envelope (Figure 3-4) as the plots clearly show a scatter of intensities at all positions

(Wilkie et al., 1999). In every case, linear regression analysis demonstrated that the gradient of the best-fit line was not significantly different to zero, confirming that the amount of RNA contained in a nascent transcript is not related to distance from the nuclear envelope (Ilan Davis, data not shown).

Taken together, these results show that genes are not transcribed more heavily when they are near the nuclear envelope or in the nuclear interior. Rather, the level of expression of active genes is independent of their position in the nucleus.

The intranuclear position of transcribed genes is not affected by abnormally abundant nascent mRNA.

It could be argued that large genes with highly abundant nascent mRNA might be transcribed at different nuclear positions from the relatively small genes examined above. If this were the case, it could account for the compartmentalisation of transcription factors and nascent RNA which have been reported in some cases (Smith et al., 1999). Two different approaches were used to test this idea.

First, the position of a large gene with highly abundant nascent RNA was investigated. *Ubx* is a complex gene with multiple exons spread over 77kb of genomic DNA. The primary transcript takes approximately 55 minutes to complete (Shermoen and O' Farrell, 1991). A large number of RNA polymerase II complexes are therefore likely to be transcribing *Ubx* at any one time. The radial positions of *Ubx* nascent transcripts were

Figure 3-4

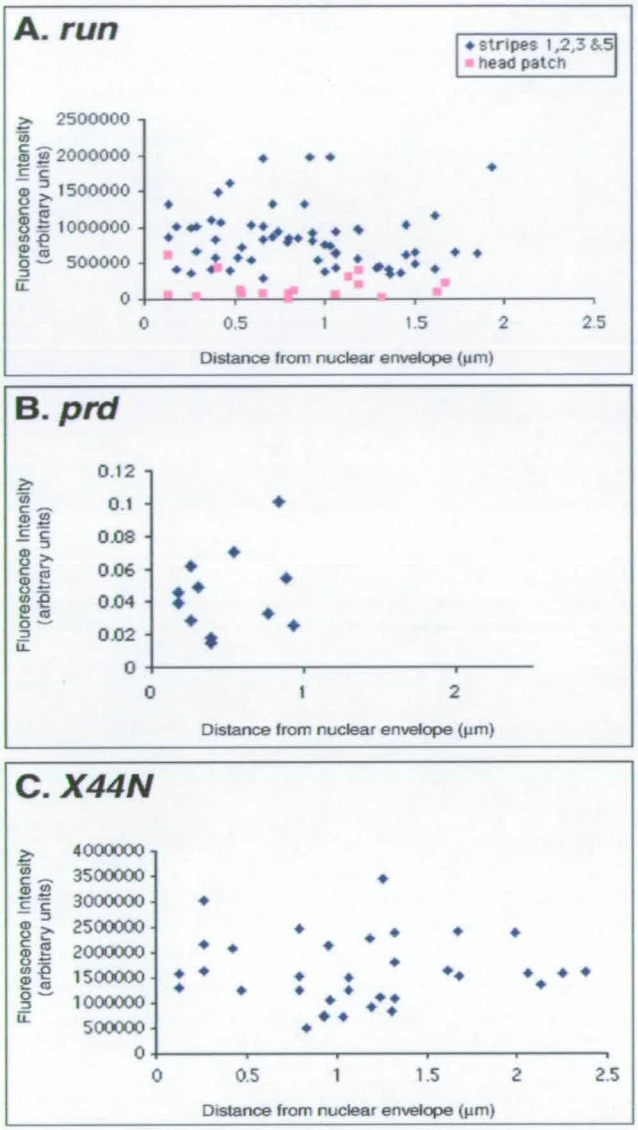
A. run
stripes 1,2,3 &5
head patch
Fluorescence Intensity (arbitrary units)
2500000
2000000
1500000
1000000
500000
0
0
0.5
1
1.5
2
2.5
Distance from nuclear envelope (µm)
B. prd
Fluorescence Intensity (arbitrary units)
0.12
0.1
0.08
0.06
0.04
0.02
0
0
1
2
Distance from nuclear envelope (µm)
C. X44N
Fluorescence Intensity (arbitrary units)
4000000
3500000
3000000
2500000
2000000
1500000
1000000
500000
0
0
0.5
1
1.5
2
2.5
Distance from nuclear envelope (µm)
D. Ubx
E. Xho25
F. en
G. X44I
H. X44P
I. X44V
J. X44H
K. X44N

determined and were found to adopt random positions in the nucleus (Figure 3-4). Previous work using FISH to detect the DNA of the *Bithorax-Complex* (*BX-C*) locus which includes the *Ubx* gene demonstrated that *BX-C* is localised at random positions in the nucleus and is not associated with the nuclear envelope (Gemkow et al., 1998). These experiments detected the *BX-C* DNA in nuclei throughout the embryo, including most regions where *Ubx* is not transcribed. The similar arrangement of *Ubx* nascent transcripts described here demonstrate that *Ubx* is not specifically relocalised to the nuclear envelope or the nuclear interior in regions of the embryo where the gene is transcribed.

To further investigate whether genes might move to new positions when associated with abundant nascent mRNA, the nuclear position of transgenes lacking polyadenylation signals were determined. Functional polyadenylation signals are known to be required for effective transcriptional termination (Connelly and Manley, 1988; Hansen et al., 1998; Logan et al., 1987; Osheim et al., 1999) and the lack of a polyadenylation signal in these constructs causes transcription of flanking sequences downstream of the gene, due to read-through by RNA polymerase II. The lack of termination leads to a large increase in the number of nascent transcripts decorating the locus, producing very bright nascent transcript foci.

Figure 3-4 Relationship between Intensity and Radial Position of Nascent Transcript Foci. (**A**) Intensity of *run* nascent transcripts is not related to distance from the nuclear envelope, whether in the expression stripes (blue diamonds) or weaker head patch (pink squares). (**B**) *prd* nascent transcript foci of all intensities are located near to the nuclear envelope. (**C**) The position of *X44N* nascent transcript foci are independent of fluorescence intensity. (**D-K**) The distribution of nascent transcript foci of heavily transcribed genes, plotted into average nuclear outlines. No difference was observed between *Xho25* embryos stained with (**E**) *LacZ* and (**F**) *en*, compared to the distribution of *en* foci in wild type embryos (Fig. 3-3G). (**G-K**). The nascent transcripts of five independent *X44* transgenic lines are located in random radial positions, despite containing large amounts of nascent RNA.

Xho25 is a transgenic *Drosophila* line which was generated by targeted insertion of an *engrailed-lacZ* fusion construct into a site 250bp upstream of the *engrailed* (*en*) gene (Hama et al., 1990). The *en-lacZ* transgene lacks a polyadenylation signal and is transcribed in the opposite orientation to the nearby *en* gene. Transcription from *en-lacZ* has been shown to extend into genomic DNA at least 20kb upstream of *en* (M. Stark and P. O'Farrel, unpublished data). Detection of *en-lacZ* nascent transcript foci with a *lacZ* probe in *Xho25* embryos showed that the large *en-lacZ* foci have a similar nuclear distribution to *en* nascent transcript foci in wild type embryos (Figure 3-4). This result demonstrates that increasing the number of nascent transcripts decorating the *en* locus does not significantly alter its nuclear position, and does not lead to specific relocalisation to the nuclear interior or the nuclear envelope.

To test whether this result was also true for other locations in the genome, transgenes at other cytological positions were investigated. The *hbX44* construct (Ilan Davis) consists of 4.8kb of non-coding tandem DNA repeats with no polyadenylation signal, driven by a fragment of the *hb* promoter (Wilkie et al., 1999). 30 independent *hbX44* transgenic lines with insertions at different cytological positions were produced by germline-mediated transformation of *hbX44* inserted in the P-element transformation vector pCaSpeR4 (Ilan Davis). mRNA *in situ* hybridisation with an *X44* probe shows that the *hbX44* lines are expressed in a *hb*-like pattern and have extremely bright nascent transcript foci, consistent with failure to terminate due to the lack of a polyadenylation signal (Wilkie et al., 1999). The position of *hbX44* nascent transcript foci from 5 different lines with the strongest expression of the transgene were determined and found to be localised throughout the nucleus (Figure 3-4). Specific association or exclusion of *hbX44* nascent transcript foci with the nuclear envelope was not observed, and the

intensity of *hbX44* foci was not related to their position in the nucleus (Figure 3-4 and Table 3b).

These results indicate that heavily transcribed genes are not associated with the nuclear envelope or specifically localised in the nuclear interior. Furthermore, artificially increasing the number of nascent mRNA molecules decorating a gene does not alter its position in the nucleus or cause relocalisation to the nuclear interior or the periphery of the nucleus.

CONCLUSIONS

Taken together, these results indicate that transcribed genes are not specifically positioned at the nuclear envelope or the nuclear interior in *Drosophila* embryonic nuclei. Rather, the position of transcribed genes is consistent with the known arrangement of chromosomes and the proximity of genes to nuclear envelope attachment sites in blastoderm nuclei. The level of expression of active genes is independent of their position within the nucleus and proximity to the nuclear envelope. Furthermore, highly transcribed genes with large amounts of nascent mRNA are not specifically localised to the periphery or interior of the nucleus. Therefore, in *Drosophila* embryos genes do not move large distances to new sites in the nucleus when they become active, and effective transcription can occur in all parts of the nucleoplasm. If active genes do migrate to new positions, then these sites must be numerous and evenly distributed in the nucleoplasm. In addition, these results show that pair-rule genes are not transcribed in the apical part of the nucleus, complementing previous results (Davis et al., 1993) and demonstrating that direct gene gating cannot be responsible for the localisation of these transcripts to the apical cytoplasm.

These conclusions are likely to be applicable to other organisms, since the nuclear organisation of active genes and transcriptional components are not thought to have unique or specialised roles in during early *Drosophila* development. Furthermore, there is evidence that nuclei have a similar organisation in other systems (Marshall and Sedat, 1999).

4

THE PATH OF INTRANUCLEAR mRNA MOVEMENT AND NUCLEAR EXPORT

INTRODUCTION

Links between nuclear export and cytoplasmic mRNA localisation

Vectorial nuclear export was previously proposed as a mechanism to explain the localisation of pair-rule transcripts to the apical cytoplasm in *Drosophila* blastoderm embryos (Davis et al., 1993). In this model, transcripts are targeted to the apical cytoplasm by directional export exclusively from the apical side of the nucleus. This was proposed because other localisation mechanisms, such as degradation of unlocalised mRNA or active transport along the cytoskeleton were shown to be unlikely (Francis-Lang et al., 1996). Recent work has shown a transport mechanism in the cytoplasm can apically localise microinjected *ftz* RNA (Lall et al., 1999). However, these results do not exclude the possibility that vectorial nuclear export is responsible, or contributes to, the apical localisation of pair-rule transcripts *in vivo*.

Four different models were proposed for the mechanism of vectorial nuclear export (Davis et al., 1993). In the direct gene gating model, genes whose transcripts are targeted to the apical cytoplasm would be transcribed in the apical part of the nucleus, allowing newly synthesised mRNA to be exported by nearby apical nuclear pores. However, it was previously reported that *h* and *ftz* are transcribed in the middle rather than the apical

part of the nucleus (Davis et al., 1993). The mapping of nascent transcript foci described in Chapter 3 confirms this result and additionally shows that *run* and *eve* are also transcribed nearer the middle rather than the apical part of the nucleus. Therefore, direct gene gating cannot be responsible for the localisation of pair-rule transcripts. An indirect gene gating model where DNA signals included in the gene target transcripts to apical NPC's was also proposed. However, *lacZ* enhancer trap insertions in the *h* gene demonstrate that localisation depends on signals in the transcript rather than the chromatin, as *lacZ* mRNA from transgenes inserted within 12bp of the site of *h* transcript initiation are unlocalised in the cytoplasm (Davis et al., 1993).

These results suggest that gene gating mechanisms are not responsible for vectorial nuclear export of pair-rule mRNA. An alternative mechanism for vectorial nuclear export is that transcripts could diffuse through the nucleus after release from their site of synthesis, but be exported exclusively by apical NPC's. The final possibility is that transcripts are actively transported through the nucleoplasm to apical NPC's. Neither of these last two models have been tested, as standard *in situ* hybridisation techniques are not sensitive enough to detect intermediates in the nuclear export of pair-rule mRNA (Davis et al., 1993; Francis-Lang et al., 1996).

Intranuclear transport of mRNA

In the *Drosophila* embryo, nascent transcript foci are not specifically localised at the nuclear periphery, but are found throughout the nucleoplasm. Therefore, many genes are transcribed in the interior of the nucleus and newly synthesised transcripts must travel distances of up to 3μm through the nucleoplasm to reach the nearest NPC. Two alternative mechanisms have been proposed to describe how mRNA travels between its

site of synthesis and processing and the nuclear envelope – active transport along intranuclear tracks or random diffusion in the nucleoplasm.

Evidence for active intranuclear transport of mRNA includes *in situ* hybridisation data revealing "tracks" of mRNA leading away from the site of transcription towards the nuclear envelope (Lawrence et al., 1989; Xing et al., 1993; Xing et al., 1995). These results suggest that an active mechanism might transport mRNA to the nuclear surface along an organised path, possibly defined by the nuclear matrix or fibres extending from nuclear pores (Lawrence et al., 1989). Transport of mRNA through the nucleoplasm on defined tracks might provide an elegant mechanism for indirect gene gating which could target pair-rule mRNA to apical nuclear pores, resulting in vectorial export from the apical side of the nucleus (Davis et al., 1993). However, it has been proposed that tracks may be an artefact due to decondensation of target DNA sequences caused by hybridisation conditions and hypotonic swelling of nuclei (Zachar et al., 1993). Tracks have mainly been visualised for heavily transcribed viral genes which synthesise pre-mRNA that is inefficiently processed and exported from the nucleus. Another problem with the concept that tracks represent transport pathways to nuclear pores is that the tracks seldom extend to the nuclear envelope (Xing and Lawrence, 1993) and often point towards the nuclear interior, or run in parallel with the nuclear envelope rather than towards it (Melcak et al., 2000). In cases where tracks have been detected for cellular genes, these have exclusively been large and complex genes which are extensively spliced. Since intron RNA has also been detected in tracks, it has been proposed that tracks represent splicing intermediates associated with the nuclear matrix, from which mature mRNA molecules might be released on completion of processing (Xing and Lawrence, 1993). Indeed, the nascent transcripts of smaller genes containing few introns are detected as a distinct focus or spot in the nucleus whereas in similar cells the

transcripts of large genes with high requirements for splicing are found in a track (Dirks et al., 1995; Smith et al., 1999).

The alternative model of intranuclear diffusion is supported by *in situ* hybridisation and microinjection experiments. Both poly(A)$^+$ RNA and a specific pre-mRNA have been detected throughout the interchromatin channels in *Drosophila* polytene nuclei, suggesting that RNA released from its site of transcription diffuses through the spaces between chromosomes until the nuclear envelope is reached (Zachar et al., 1993). This has been supported by studies demonstrating that globin mRNA (Wang et al., 1991) and gold labelled RNA (Pante et al., 1997) rapidly reach all parts of the nucleoplasm after microinjection into the nucleus. Furthermore, giant Balbiani ring mRNP particles (35-40kb in size) synthesised in the salivary glands of *Chironomus tentans* are visible by electron microscopy and have been observed to move randomly to all parts of the nucleoplasm before export, at rates consistent with free or slightly retarded diffusion through the interchromatin space (Singh et al., 1999). *In situ* hybridisation has detected faint signals radiating away from the nascent transcript foci of some genes, possibly representing intermediates in the export of mRNA. These intermediates appeared to diffuse away from the site of transcription towards the nuclear envelope (Dirks et al., 1995). More recently, the sensitivity of *in situ* hybridisation techniques has improved, allowing quantitative detection of small amounts of mRNA (Femino et al., 1998). These authors reported that single molecules of *β-actin* mRNA often appeared to diffuse away from the site of transcription in cultured cells. In addition to this, two different studies investigating the intranuclear movement of poly(A)$^+$ RNA recently showed that a large fraction of nuclear poly(A)$^+$ RNA moves through the nucleoplasm by free diffusion (Politz et al., 1998; Politz et al., 1999).

To distinguish between these possibilities and examine the mechanism by which transcripts travel from their site of synthesis to the nuclear envelope, sensitive TSA detection was used to visualise transcripts in the export pathway. The intranuclear position of these export intermediates was mapped for both apically targeted transcripts and also non-localised mRNA's to determine if there is any directionality in the export of specific transcripts or in the movement of mRNA through the nucleus in *Drosophila* embryos.

Figure 4-1

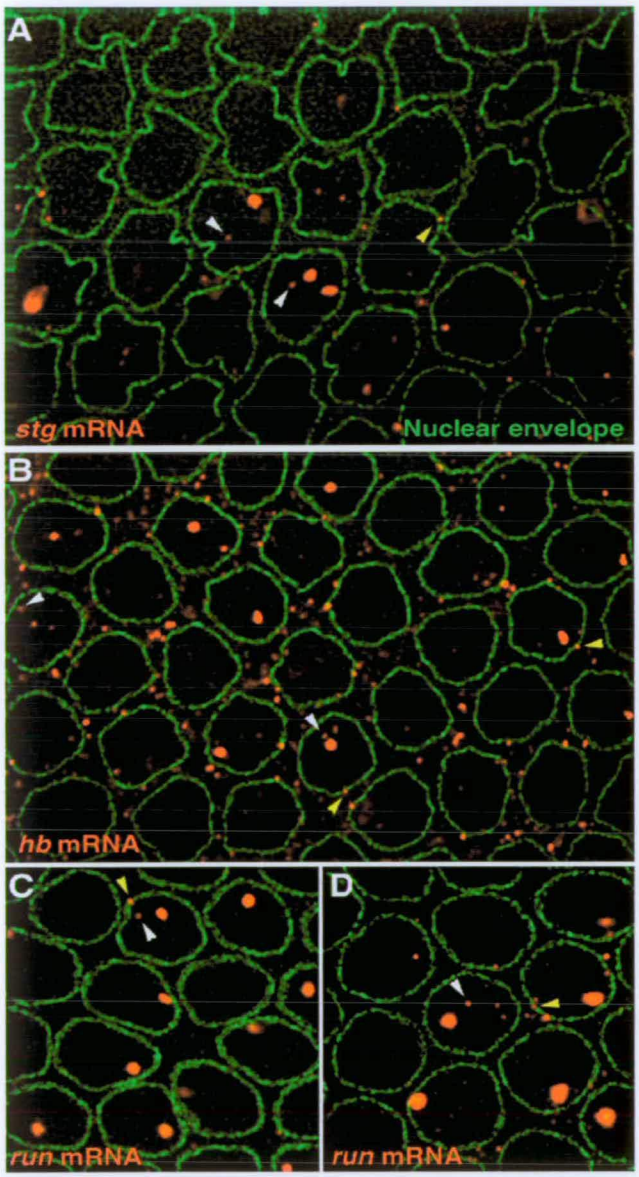

Figure 4-1 Nuclear mRNA export intermediates. Export intermediates visualised within the nucleoplasm (white arrowheads) or nuclear envelope (yellow arrowheads) of blastoderm embryos, by *in situ* hybridisation to detect (**A**) *stg* mRNA (**B**) *hb* mRNA and (**C-D**) *run* mRNA. C and D are projections of 5 consecutive 0.2μm sections, representing 1μm of focal depth. The nuclear envelope is labelled in green.

RESULTS

Visualisation of mRNA export intermediates.

Using probes against a number of different transcripts, faint sites of hybridisation were detected within the nucleus in addition to nascent transcript foci (Figure 4-1). These signals are likely to represent nuclear export intermediates since their fluorescence intensity is an order of magnitude above general background, and they have a similar intensity to many particles of mRNA in the cytoplasm (Table 4a). This is significant as an independent study recently demonstrated that nuclear *β-actin* export intermediates have identical intensity values to cytoplasmic *β-actin* mRNA in cultured rat NRK cells, and that these signals represent single molecules of mRNA (Femino et al., 1998).

Additional evidence that the faint hybridisation signals represent true mRNA export intermediates, rather than background fluorescence, is that the signals are absent from embryos that genetically lack the RNA (Figure 4-2). Furthermore, the export intermediates are predominantly found in nuclei within regions of the embryo that express a gene strongly (Figure 4-2), and their frequency is related to the level of gene expression. In regions with poor expression, occasional nuclei show much fainter nascent transcript foci and fewer additional sites of hybridisation. For example, within the expression stripes of the *run* gene, each nucleus contains an average of 4.3 ± 2.2 *run* export intermediates, whereas rare nuclei in the interstripe with fainter nascent transcripts had only 1.2 ± 1.1 export intermediates on average. Taken together, these results strongly support the conclusion that these signals represent particles of mRNA in the export pathway.

Figure 4-2

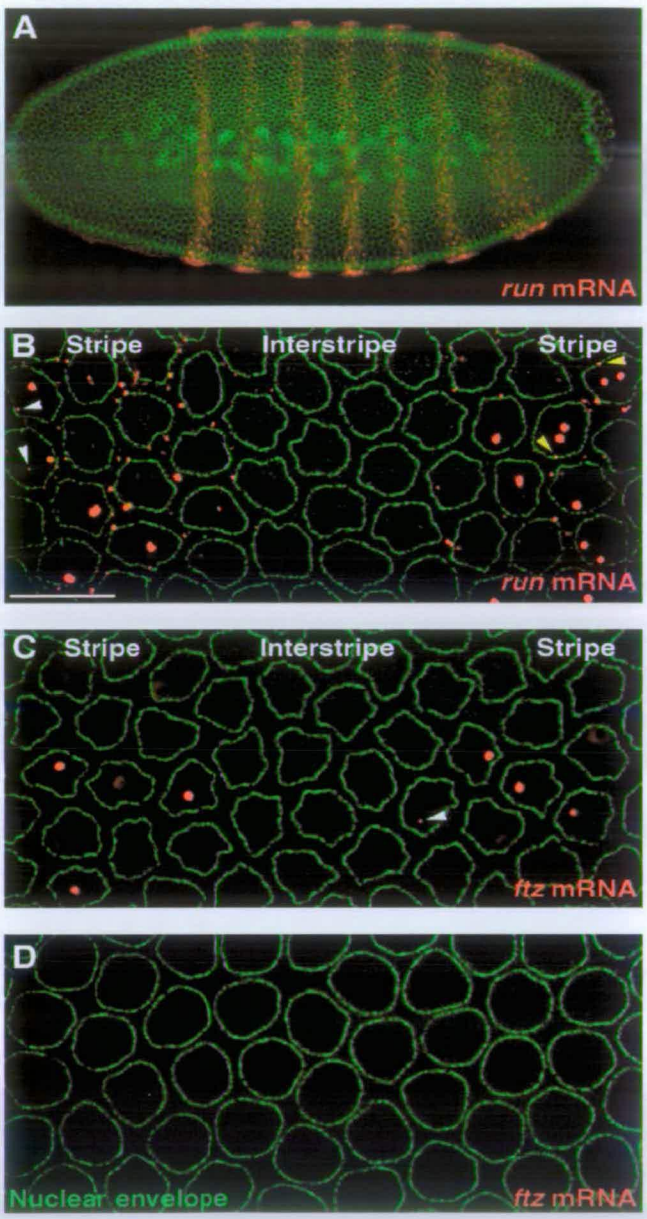

Figure 4-2 mRNA particles are not background fluorescence. (**A**) Low power image of stripes of *run* mRNA expression in nuclei at the surface of a blastoderm embryo. (**B**) High power section of stripes 1-2 from (A) showing that *run* mRNA (red) is not detected in interstripe regions. Bar = 10μm (**C-D**) *ftz* mRNA imaged at a similar position in deficiency embryos lacking (**C**) one copy, or (**D**) both copies of the *ftz* gene. No mRNA hybridisation signals are detected in embryos that lack the *ftz* gene. The nuclear envelope is labelled in green.

Table 4a. Fluorescence intensity of nuclear and cytoplasmic mRNA

Gene	Nascent transcripts	Nuclear mRNA	Cytoplasmic mRNA
hb	324,462 ± 37,498 (N=26)	14,384 ± 1,983 (N=40)	17,339 ± 2,352 (N=22)
kr	3,112,872 ± 239,195 (N=28)	165,730 ± 24,090 (N=46)	201,086 ± 29,261 (N=24)
run	591,632 ± 119,315 (N=10)	11,884 ± 1,376 (N=36)	20,243 ± 3,152* (N=15)

The fluorescence intensity of nascent transcript foci and other particles of RNA in the nucleus and cytoplasm. Total integrated fluorescence intensity is measured in arbitrary units ± standard error. N = number of foci measured. * Rare unlocalised *run* mRNA particles in the basal cytoplasm had intensity 9,899 ± 1,859 (N=15).

The TSA detection technique does not allow the number of molecules of mRNA in these export intermediates to be directly calculated. However previous work describing the density of RNA polymerase II on active genes (Alberts et al., 1989; Femino et al., 1998; McKnight and Miller, 1976; Osheim et al., 1985) has shown that the spacing between polymerase complexes can vary between as little as 60bp to over 750bp, suggesting that the nascent transcript foci of these relatively short *Drosophila* genes (2-3kb in size) are likely to contain between 4 and 50 nascent RNA chains.

This estimate is compatible with the finding that faint *run* nascent transcripts in the interstripe regions are 40 times less bright than those in the expression stripes, while the head patch nascent transcripts contain 4 times less fluorescence than expression stripes (Table 3a). The mRNA export intermediates described here for different *Drosophila* genes have a range of intensities, but generally contain between 15-50 times less fluorescence than nascent transcript foci in strongly expressing regions (Table 4a). These results are therefore are therefore consistent with a composition of between 1-3 molecules of mRNA for export intermediates.

Specific transcripts diffuse through the nucleus from their site of synthesis

To study the movement of mRNA from the site of transcription to the nuclear envelope, the positions of nuclear export intermediates from different genes were mapped in serial optical sections captured through blastoderm nuclei at 0.2μm intervals. Individual nuclei were found to have varying numbers of export intermediates – some nuclei did not have any signals apart from nascent transcripts while other nuclei contained as many as 10 mRNA export intermediates. In nuclei with multiple mRNA export intermediates, the intermediates were found to be positioned randomly throughout the nucleus. Among all

Figure 4-3

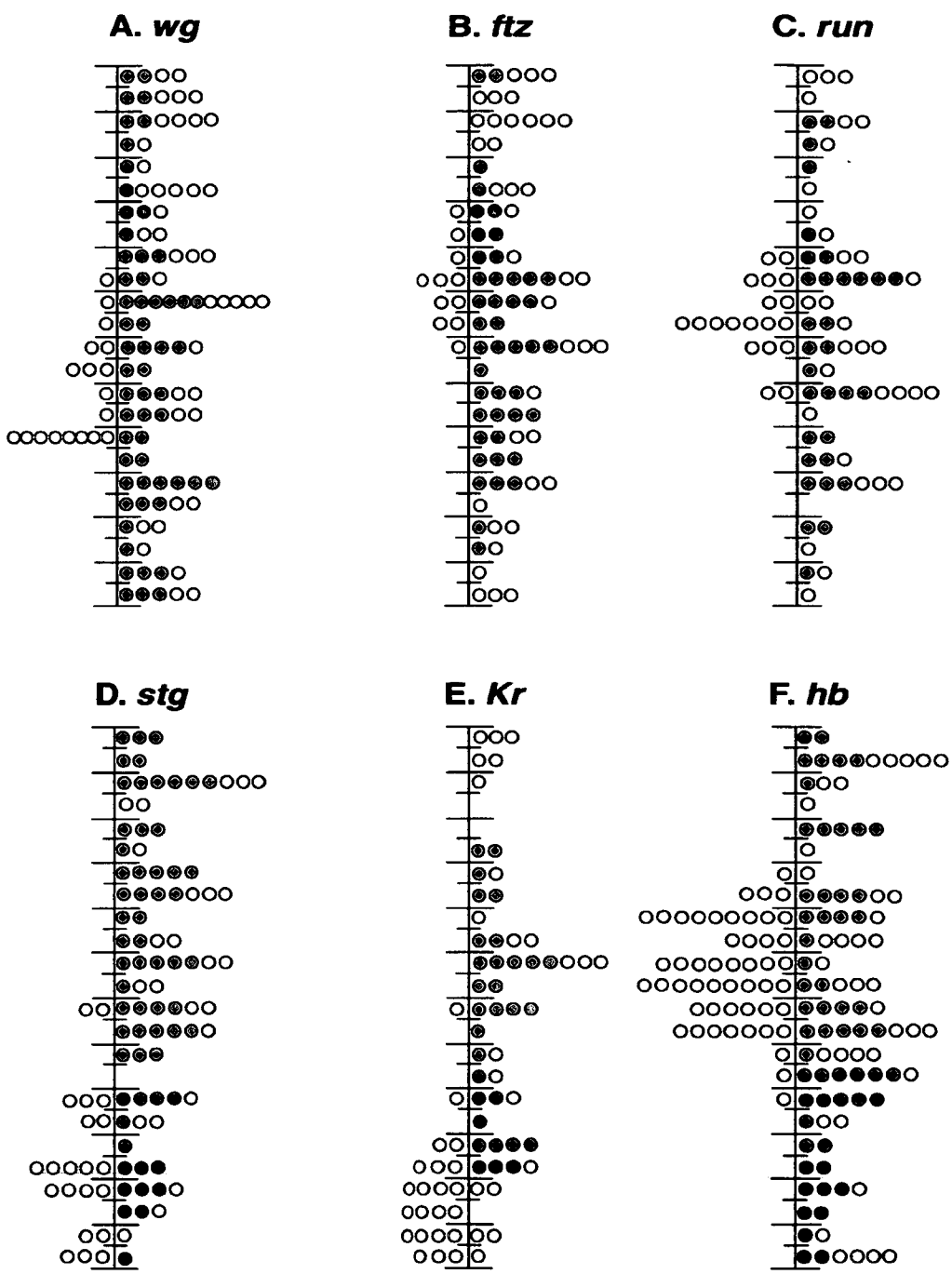

the cases which were examined, there was no consistent evidence of tracks or any organised transport of mRNA through the nucleoplasm (Figure 4-1 and data not shown).

In order to determine whether transcripts with different cytoplasmic destinations are differentially and directionally transported within the nucleoplasm, the positions of mRNA export intermediates from many nuclei were mapped with respect to the apical-basal nuclear axis. In all cases studied, export intermediates were evenly distributed throughout the entire nucleoplasm. These results are more consistent with random movement of transcripts through the nucleoplasm after release from their site of synthesis, rather than any directed transport between nascent transcripts and the nuclear surface. For example, *kr* is transcribed in the basal part of the nucleus, due to the location of the gene near the telomere on chromosome arm 2R. However, *kr* mRNA export intermediates have a more ubiqitous distribution in the nucleus, and are often found in more apical positions than *kr* nascent transcript foci (Figure 4-3). *hb* is transcribed nearer the middle of the nucleus, yet *hb* mRNA export intermediates are found in all parts of the nucleoplasm (Figure 4-3).

To test whether transcripts destined for localisation in different parts of the cytoplasm are transported through the nucleus in a vectorial fashion *stg*, *ftz*, *run* and *wg* mRNA export intermediates were mapped in blastoderm nuclei. *stg* mRNA is mainly found in the basal cytoplasm and the *stg* gene is positioned in the basal part of the nucleus due to its location near the end of chromosome arm 3R. In contrast, *stg* mRNA nuclear export

Figure 4-3 Distribution of intermediates in mRNA export. The positions of nascent transcripts and mRNA nuclear export intermediates were mapped onto a linear scale representing the apical-basal nuclear axis. Each graduation represents 0.5μm. (**A-F**) For six different genes, nascent transcripts (open red circles) are localised according to chromosomal position, whereas nucleoplasmic mRNA particles (red circles) and export intermediates within the nuclear envelope (yellow circles) are randomly distributed.

intermediates are found throughout the nucleus (Figure 4-3). Apically targeted transcripts were also found to have a similar random distribution of mRNA export intermediates, similar to genes with unlocalised mRNA. *ftz*, *run* and *wg* mRNA export intermediates are not enriched in the apical part of the nucleus, but rather are randomly dispersed along the apical-basal nuclear axis (Figure 4-3). Therefore, it can be concluded that localised transcripts are not transported vectorially to one side of the nucleus.

Taken together, these results demonstrate that mRNA export intermediates are not found in tracks and are not transported through the nucleus in a directional manner in *Drosophila* embryos. The positions of nuclear export intermediates are more consistent with random movement of transcripts through the nucleoplasm after release from the site of synthesis. These results also demonstrate that the asymmetric cytoplasmic localisation of *stg*, *ftz, run* and *wg* transcripts does not result from the directional transport of mRNA within the nucleoplasm.

Transcripts are exported through all parts of the nuclear envelope

The results described above fail to address whether some localised transcripts are exported by specialised pores on one side of the nucleus. Such a mechanism could account for vectorial nuclear export of localised transcripts with intermediates which are found throughout the nucleoplasm (Davis et al., 1993). To test this, the distribution of mRNA export intermediates which colocalise with the nuclear envelope were examined to determine whether transcripts are asymmetrically exported from one side of the nucleus. The resolution of this technique is physically limited by the wavelength of light to just under 0.2μm (200nm), and is not sufficiently high to resolve individual nuclear pores or to determine whether transcripts are actually in transit through the NPC. Therefore *Drosophila* mRNA export intermediates located within 0.2μm of the nuclear

envelope were classed as undergoing export. A similar classification of 200nm on either side of the nuclear envelope has also been adopted in other studies of mRNA export complexes using immunogold labelling and T.E.M. (Visa, RNA 2000).

The results show that transcripts are exported from all sides of the nucleus in the *Drosophila* blastoderm embryo. mRNA export intermediates for *hb* and *kr* are found in all parts of the nuclear envelope (Figure 4-3). *stg* mRNA is also exported from all sides of the nucleus, despite being transcribed in the basal part of the nucleus and localised to the basal cytoplasm (Figure 4-3). Apically targeted transcripts such as *run*, *ftz* and *wg* are not selectively exported through the apical side of the nucleus, but rather are exported equally through all parts of the nuclear envelope (Figure 4-3). Together, these results show that transcripts are exported in a similar pattern from all sides of the nucleus, irrespective of their final cytoplasmic destinations.

CONCLUSIONS

Intermediates in the nuclear transport and nuclear export of specific transcripts were visualised in *Drosophila* blastoderm nuclei. These intermediates are likely to consist of a small number of molecules of mRNA, in the range of 1-3 transcripts. mRNA export intermediates for 6 different genes were found at random positions in the nucleus, consistent with their diffusion through the interchromatin space after release from their site of synthesis. No evidence of tracks or any ordered transport of mRNA through the nucleus was observed. In all the cases which were examined, transcripts reach the nuclear envelope at random positions which are often far from nascent transcripts, and appear to be exported to the cytoplasm through nuclear pores on all sides of the nucleus.

These results show that vectorial nuclear export does not occur by directed transport of mRNA export intermediates within the nucleus or by export from one side of the nucleus. Instead, transcripts are exported to all parts of the cytoplasm and then sorted to their appropriate destinations. This is consistent with the observation of rare particles of pair-rule mRNA in the basal cytoplasm of wild type embryos (Wilkie and Davis, 2001). Furthermore, fluorescently labelled *ftz* RNA can localise apically after microinjection into the basal cytoplasm if it is preincubated with nuclear extracts or Squid protein (Lall et al., 1999). Taken together, these results imply that localisation of pair-rule transcripts is carried out exclusively by a mechanism that operates in the cytoplasm.

The results of experiments which address the localisation mechanism are described in Chapter 8. Before this, work is presented on the identification of the machinery required for exporting transcripts from the nucleus to the cytoplasm.

5

ISOLATION OF NUCLEAR mRNA EXPORT AND CYTOPLASMIC LOCALISATION MUTANTS

INTRODUCTION

The results described in Chapters 3 and 4 demonstrate that apical localisation of pair-rule mRNA depends on an unknown mechanism that acts in the cytoplasm. These transcripts appear to diffuse randomly through the nucleus after release from their site of synthesis, and are exported from the nucleus in all directions. In order to characterise the export and localisation pathway in more detail, a screen was designed to isolate mutant lines which cause mislocalisation of transcripts in the nucleus or cytoplasm. Such mutants would allow genes involved in the nuclear export and cytoplasmic localisation of mRNA to be identified. Furthermore, the phenotypes of mutations causing mislocalisation of transcripts in the nucleus or cytoplasm are likely to reveal new information about the mechanisms of export or localisation.

mRNA export in higher eukaryotes

Although many components of the mRNA export machinery have been identified in yeast, mRNA export is less well characterised in higher eukaryotes. Many homologues of the yeast proteins required for mRNA export have been identified, but it has proved

difficult to conclusively demonstrate their role in mRNA export in higher eukaryotes. This has been hindered by the lack of an *in vitro* nuclear mRNA export assay, and by the lack of genetic analysis techniques in mammalian cell culture systems.

Proteins which are thought to have a direct role in mRNA export in higher eukaryotes are RAE1, hGLE1, DBP5 and TAP (Gruter et al., 1998; Kraemer and Blobel, 1997; Pritchard et al., 1999; Schmitt et al., 1999; Watkins et al., 1998). However, the functions of these proteins have mainly been tested by overexpression and microinjection experiments in cultured cells and *in vitro* binding assays. For example, the only evidence that hGLE1 is required for mRNA export is that microinjection of anti-hGLE1 antibodies into cultured cells causes nuclear accumulation of poly(A)$^+$ RNA, which is not a conclusive experiment (Watkins et al., 1998). Similarly, human DBP5 is thought to function in mRNA export because the export efficiency of some transcripts is reduced when mutant forms of the DBP5 protein are injected into *Xenopus* oocytes (Schmitt et al., 1999).

RAE1 is the homologue of yeast Gle2p in higher eukaryotes, and has been demonstrated to shuttle between the nucleus and cytoplasm in *Xenopus* oocytes. The vertebrate nucleoporin NUP98 has a domain that binds to RAE1, reminiscent of the interaction between Nup116p and Gle2p required for mRNA export in yeast. Overexpression of this domain causes nuclear accumulation of poly(A)$^+$ RNA, which can be abrogated by excess RAE1 protein (Pritchard et al., 1999). This data suggests that RAE1 plays an important role in mRNA export in higher eukaryotes.

The most thoroughly-characterised RNA export factor in higher eukaryotes is TAP, the cellular co-factor necessary for the nuclear export of unspliced retroviral RNA containing the CTE (Constitutive Transport Element). Viral RNA is thought to be

exported by the same pathway as cellular mRNA, because excess CTE RNA inhibits mRNA export in *Xenopus* oocytes (Gruter et al., 1998). TAP was initially implicated in mRNA export because it can overcome the mRNA export block caused by saturating amounts of CTE RNA when it is provided in excess (Gruter et al., 1998). TAP heterodimerises with p15 (an orthologue of yeast Mtr2p) and also interacts with RAE1 and multiple nucleoporins, including NUP98, CAN/NUP214, NUP88 and NUP93, suggesting that these proteins share a role in the mRNA export pathway (Bachi et al., 2000; Katahira et al., 1999; Suyama et al., 2000). Furthermore, TAP can be crosslinked to Poly(A)$^+$ RNA and shuttles between the nucleus and cytoplasm, its nuclear import being mediated by transportin and its export stimulated by direct binding to nucleoporins (Bear et al., 1999; Kang and Cullen, 1999). Additional evidence that TAP is involved in nuclear mRNA export was recently provided by the discovery of its interaction with REF proteins, which are recruited to pre-mRNA processing complexes and target mature mRNA for export (Stutz et al., 2000; Zhou et al., 2000). Taken together, these results suggest a model where TAP acts as a receptor for nuclear mRNA export, receiving processed mRNP complexes and targeting them to the NPC for export to the cytoplasm.

However, the elegant simplicity of this model was recently broken by the discovery that TAP is just one member of a family of related proteins in higher eukaryotes. The NXF family of putative nuclear export factors has two members in *C. elegans* and four members in *Drosophila*. The human genome contains five NXF proteins, TAP being defined as NXF1 (Herold et al., 2000). Furthermore, an additional p15 homologue (p15-2, or NXT2) has been identified in humans which is able to bind TAP and other NXF proteins, raising the possibility that different combinations of NXF and p15 proteins could have specific substrate or tissue specificities. Therefore, the TAP(NXF1)-p15 complex may not be the export receptor for all cellular mRNA, unlike Mex67p-Mtr2p

which is thought to be required for all mRNA export in yeast (Hurt et al., 2000; Segref et al., 1997). Indeed, the human protein NXF2 displays similar CTE RNA export and nucleoporin binding properties to TAP/NXF1, whereas NXF3 does not (Herold et al., 2000).

In the absence of genetic analysis techniques in higher eukaryotic cell culture systems, RNA interference (RNAi) may provide an extremely valuable tool to test the functions of individual genes. In a recent study, RNAi was used to deplete levels of both TAP homologues in *C. elegans*. It was found that functional knockout of one of these genes had no effect, while depleting levels of the other NXF was lethal in both adult and embryonic stages and caused nuclear accumulation of poly(A)$^+$ RNA (Tan et al., 2000). This represents the strongest evidence to date that a TAP-like protein (Ce-NXF1) functions in the nuclear export of mRNA in a higher eukaryote. However, this study did not analyse the specific defect caused by disruption of Ce-NXF1 by RNAi, and in particular did not determine whether pre-mRNA splicing or nuclear protein import pathways were also defective after RNAi treatment.

In summary, the results described above suggest that RAE1, hGLE1 and DBP5 are involved in mRNA export, but do not conclusively show that these proteins actually function in the nuclear export of mRNA *in vivo*. There is a larger body of evidence which implicates TAP/NXF in mRNA export, but questions remain over the functions of other NXF proteins and whether TAP/NXF1 acts as the receptor for the export of all mRNA transcripts from the nucleus.

To study the mechanisms of mRNA export in a multicellular, genetically tractable higher eukaryote, a screen was carried out to isolate genes required for mRNA export in *Drosophila*.

The Francis-Lang and Sullivan collection of temperature sensitive (t.s.) lethal *Drosophila* lines.

There were no known mutations which affected mRNA export or pair-rule mRNA localisation in *Drosophila* before this work was initiated. Furthermore, previous analysis of aneuploid embryos lacking each of the major chromosome arms demonstrated that zygotic gene expression is not required for the correct export and localisation of pair-rule transcripts at the syncitial blastoderm stage, suggesting that the mRNA export and localisation machinery must be maternally provided (Francis-Lang et al., 1996). Because mRNA export is an essential cellular process, the use of conventional mutations to study export in the highly tractable blastoderm embryo is difficult due to early lethality. Although the FRT-FLP system has made it possible to screen zygotic lethals mutants for maternal effects by creating germline clones (Chou and Perrimon, 1992) it is likely that mutations in genes required for RNA export and localisation would interfere with early oogenesis or cause an arrest at an early preblastoderm stage of embryonic development. These potential problems could be overcome by using conditional temperature sensitive (t.s.) mutations, which allow the phenotype to be exerted at any time in development by shifting to the restrictive temperature. This approach has been successfully used in the budding yeast *S. Cerevisiae* to screen for nuclear mRNA export mutants (Amberg et al., 1992; Kadowaki et al., 1994). Screens for conditional mutants have also been carried out in *Drosophila*, mainly in the 1970's (Arking, 1975; Suzuki, 1970) but problems with reversion meant that this approach has not been very popular since then.

A collection of t.s. lethal mutations was recently created in an EMS mutagenesis screen carried out by Helen Francis-Lang and William Sullivan during work to identify novel factors involved in the regulation of the cell cycle and the cytoskeleton in the embryo. The t.s. lethal flies were isolated in a scheme designed to recover X-linked conditional

lethal mutations which are lethal at 29°C and viable at 21°C (see Appendix A). Over 10,000 EMS-treated lines were screened to isolate 180 lines with lethal t.s. mutations (Sullivan and Francis-Lang, unpublished data). The collection was kindly given to a number of different laboratories before its publication, allowing other investigators to screen for different phenotypes. It is difficult to perform a saturating screen with this approach since only around 10% of lethal mutations are temperature sensitive. Therefore, a very large number of mutagenised lines would have to be screened to isolate more t.s. mutations.

Using the t.s. lethal collection to screen for mRNA export and localisation mutants.

The basic components of the mRNA export machinery were originally identified in the budding yeast *S. cerevisiae* using genetic approaches. One successful approach has been to screen banks of conditional lethal mutants for accumulation of excess poly(A)$^+$ RNA in the nucleus using poly(T) probes (Amberg et al., 1992; Kadowaki et al., 1994). Other genes essential for mRNA export in yeast have been identified in synthetic lethal screens with nucleoporin mutants, on the basis of their nuclear poly(A)$^+$ RNA accumulation phenotypes (Murphy et al., 1996; Segref et al., 1997).

The detection of poly(A)$^+$ RNA is a sensitive assay for the bulk location of mRNA, but it represents an average of all polyadenylated transcripts and cannot be used to test the effect of mutants on individual transcripts. Although it has recently become possible to detect the transcripts of single genes in yeast and mammalian cells using fluorescent oligonucleotides (Femino et al., 1998; Long et al., 1997) this technique would be a difficult and expensive assay for a screen. In contrast, this approach was feasible in *Drosophila* as the transcripts of individual genes can be readily detected by *in situ*

hybridisation. This approach was used to design a screen for mutations affecting nuclear export or cytoplasmic localisation of mRNA in the embryo. *In situ* hybridisation was used to detect the transcripts of the pair-rule gene *ftz*, which are localised apically in the blastoderm embryo (Edgar et al., 1986). Mutations with either unlocalised or nuclear *ftz* mRNA could potentially be identified in such a screen. *ftz* was chosen in preference to other localised transcripts because *ftz* mRNA has a half-life of only 6 minutes (Edgar et al., 1986). Changes in the pattern of *ftz* mRNA accumulation therefore rapidly become apparent, rather than being masked by mRNA correctly exported and localised at the permissive temperature before the temperature shift.

In order to screen the t.s. lethal *Drosophila* collection for these defects, it was necessary to create temporary homozygous lines from the balanced t.s. stocks. This was achieved by maintaining the lines at the permissive temperature (18°C) and selecting against the *FM7c* balancer chromosome, which is marked with the dominant eye shape mutation *Bar*. 100 homozygous t.s. lines were created in this way (Ruth Kirby and Gavin Wilkie). The other lines showed some degree of female or male sterility or were not homozygous viable at the permissive temperature. This was not unexpected, since the original mutagenesis scheme only tested for survival of males at 21°C, therefore these types of defects were not screened out.

To screen the homozygous t.s. lines for nuclear export and cytoplasmic localisation of *ftz* mRNA, the lines were temporarily expanded at the permissive temperature and embryos were collected from each line and shifted to the restrictive temperature. A shift of 1 hour to 33°C was used in the screen to induce severe phenotypes in the mutant embryos, and increase the chance of identifying mutants. The embryos were then fixed at the restrictive temperature, and *ftz* mRNA was detected by *in situ* hybridisation using

standard alkaline phosphatase histochemical detection (Tautz and Pfeifle, 1989). Embryos from each line were examined under the microscope for abnormal accumulation of *ftz* mRNA in the nucleus or basal cytoplasm.

Figure 5-1

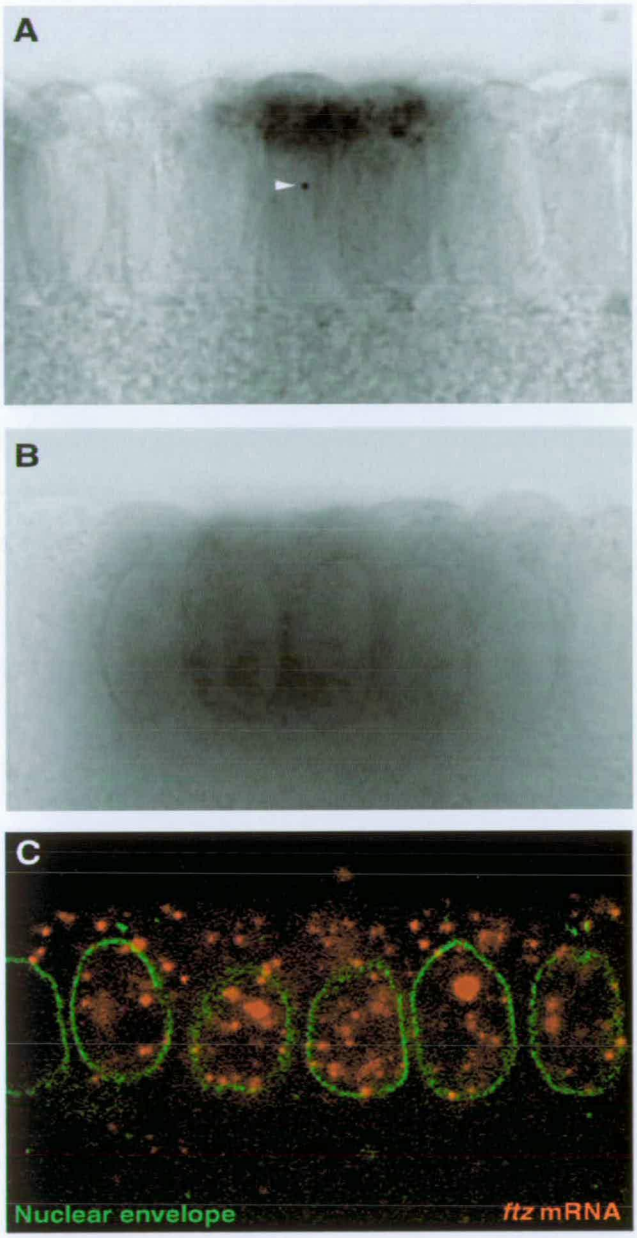

Figure 5-1 *l(1)ts148* Disrupts Nuclear Export of *ftz* mRNA at the Restrictive Temperature. (**A**) *ftz* mRNA, visualised by *in situ* hybridisation with histochemical detection, is localised correctly to the apical cytoplasm in *l(1)ts148* embryos at the permissive temperature (18°C). White arrowhead indicates nascent transcript. (**B**) After a 60 minute shift to 33°C, *ftz* is abnormally localised in *l(1)ts148* embryos. (**C**) Fluorescent detection of mRNA demonstrates that *ftz* mRNA (red) accumulates in the nucleus of *l(1)ts148* embryos after shifting to 33°C for 30 minutes. The nuclear envelope is labelled in green.

RESULTS

ftz mRNA accumulates in the nuclei of *l(1)ts148* embryos at the restrictive temperature

After screening all 100 t.s. lethal lines for defects in *ftz* mRNA nuclear export and cytoplasmic localisation, no lines were identified with unlocalised *ftz* mRNA. Thus, no mutations affecting apical localisation of *ftz* mRNA were found.

However, one line was identified which showed a dramatic excess of *ftz* mRNA in the nucleus at the restrictive temperature. In line *l(1)ts148*, *ftz* mRNA was found to accumulate in many discrete particles throughout the nucleus after a 60 minute shift to the restrictive temperature, and the amount of *ftz* mRNA in the apical cytoplasm was reduced (Figure 5-1). This phenotype was not visible in *l(1)ts148* embryos at the permissive temperature (18°C). Furthermore, the phenotype was not observed in yw^{67} embryos after 60mins at 33°C, or in any of the other t.s. lines after 60 minutes at 33°C (data not shown). These results show that the nuclear mRNA accumulation phenotype is specific to the *l(1)ts148* line.

l(1)ts148 inhibits the nuclear export of many different transcripts

To test whether *l(1)ts148* has a defect specifically in the nuclear export of *ftz* mRNA, *in situ* hybridisation was used to determine the intracellular location of many other transcripts in *l(1)ts148* embryos. In all the cases which were tested, mRNA was found to accumulate in the nuclei of *l(1)ts148* embryos at the restrictive temperature. A number of different classes of genes were tested, including the gap genes *hunchback* and *kruppel*, the pair-rule genes *hairy*, *runt*, *even-skipped* and *paired*, the segment polarity

Figure 5-2

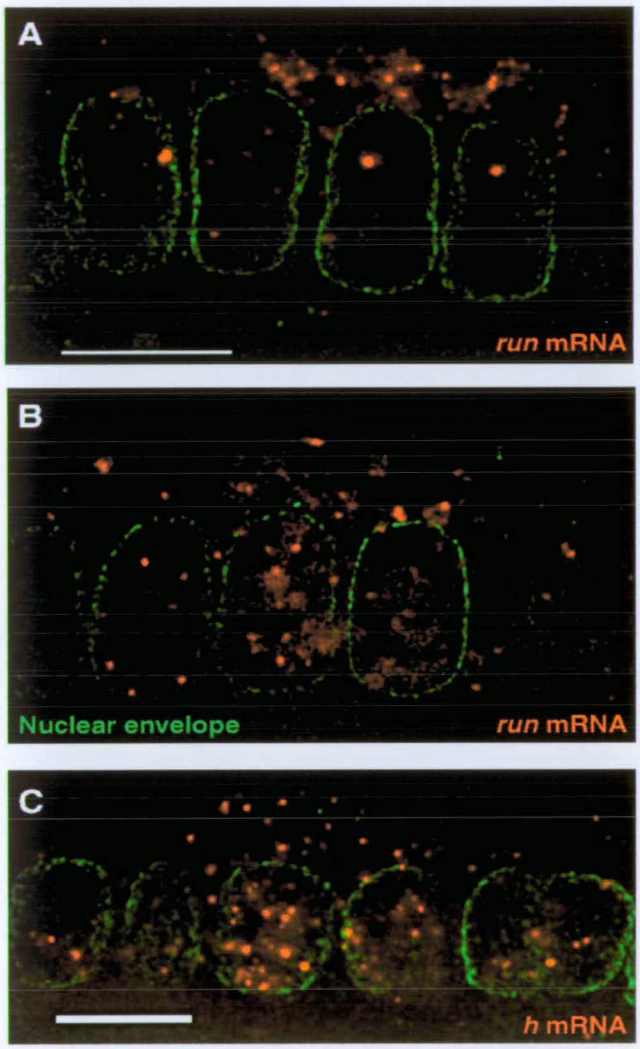

Figure 5-2 *l(1)ts148* Inhibits Nuclear mRNA Export at the restrictive temperature. (**A**) In wild type embryos, *run* mRNA (red) is localised to the apical cytoplasm. Bright nascent transcripts are visualised within nuclei, together with a small number of export intermediates. Bar = 10μm (**B**) *run* mRNA (red) accumulates throughout the nucleus of *l(1)ts148* embryos after shifting to 33°C for 30 minutes, and mRNA levels in the apical cytoplasm are reduced. (**C**) Many particles of *h* mRNA (red) are detected within nuclei of *l(1)ts148* embryos after 30 minutes at 33°C. The nuclear envelope is labelled in green.

genes *wingless, ultrabithorax* and *engrailed*, and the *cdc25* homologue *string* (Figure 5-2 and data not shown). Furthermore, it was found that *l(1)ts148* inhibits the nuclear export of *wg* and *atonal* mRNA at other developmental stages, such as late stage embryos and larval imaginal discs (Ilan Davis, data not shown and experiments in progress). A similar pattern of nuclear mRNA accumulation was observed for all transcripts tested at the restrictive temperature, with multiple particles of mRNA scattered throughout the nucleoplasm.

l(1)ts148 is required at all stages of development

To test whether *l(1)ts148* is required at all stages of development or causes a specific phenotype at a certain stage in the life cycle, the effects of the *l(1)ts148* mutation were investigated at different stages of development at the restrictive temperature.

To test the requirement of *l(1)ts148* in the embryo, embryos were collected from *l(1)ts148* and yw^{67} flies at 18°C for 8 hours. Hatch rates of 50 embryos were then measured at different temperatures. These results indicate that *l(1)ts148* is lethal in the embryo at 23°C or over (Table 5a). To test if *l(1)ts148* embryos die at any specific stage of development at the restrictive temperature, mutant embryos were collected as described above, then shifted to 29°C for up to 18 hours before they were fixed and investigated under the microscope. It was found that *l(1)ts148* embryos do not die at any specific stage of embryogenesis at the restrictive temperature. Instead embryos were found at a range of different stages of development in these collections, consistent with an arrest in development soon after the temperature shift. No specific defects in the pattern of the cuticle were observed in *l(1)ts148* embryos - the cuticle was either normal or development was arrested before cuticle formation at 29°C (data not shown).

Figure 5-3

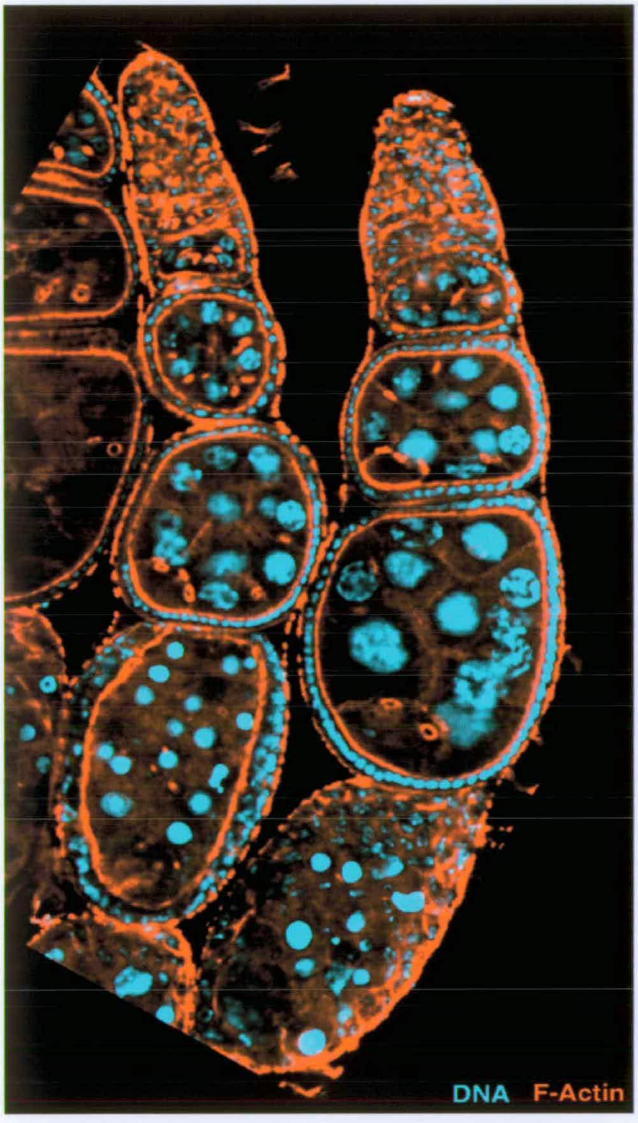

Figure 5-3 *l(1)ts148* Disrupts Oogenesis at the Restrictive Temperature. Ovarioles dissected from *l(1)ts148* mutant flies after 3 days at 29°C. DNA (stained with DAPI) is shown in cyan, while actin filaments (detected with Rhodamine-Phalloidin) are shown in red. The nurse cells fail to dump their cytoplasm into the oocyte, and egg chambers break down after stage 7. Image aquired by Ilan Davis.

To test the effect of *l(1)ts148* at other stages of the *Drosophila* life cycle, larvae, pupae and adult flies were shifted to 29°C. It was found that *l(1)ts148* larvae failed to pupate at 29°C, but rather died and turned black after several days at 29°C. Similarly, no adult flies were found to eclose from *l(1)ts148* pupae at 29°C. Adult flies are very inactive at the restrictive temperature, and do not attempt to fly or even crawl far up the wall of culture vials. Male *l(1)ts148* flies die after approximately 3 days at 29°C, whereas females flies survive for around a week at 29°C but lay fewer and fewer embryos which are around 30% smaller than wild type and do not develop cuticle or hatch (data not shown). Oocytes from *l(1)ts148* females shifted to 29°C for 3 days show a severe defect in oogenesis after stage 7. The nurse cells fail to transfer their cytoplasm into the oocyte and egg chambers after this stage degrade (Figure 5-3). This phenotype could explain the smaller embryos laid by *l(1)ts148* flies after several days at 29°C.

Despite extensive efforts, it was not possible to detect a nuclear mRNA export defect in *l(1)ts148* mutant ovaries. It was found that *l(1)ts148* ovaries were extremely small and undeveloped after more severe temperature shifts. After shorter shifts to the restrictive temperature, maternal transcripts such as bcd, grk and osk were correctly localised in *l(1)ts148* mutant ovaries (where egg chambers at the correct stages were present), and excess mRNA was not detected in the oocyte or nurse cell nuclei (Nina Ehrenberg, data not shown). This result may be due to reduced sensitivity of mRNA detection in the oocyte, or could reflect the slower rate of ovarian development, with transcription, export and localisation of maternal transcripts taking place over many hours or several days, compared to the short interphase cycles of the early embryo.

Table 5a. Hatching rates of *l(1)ts148* and yw^{67} embryos

Temperature	yw^{67} hatch rate	*l(1)ts148* hatch rate
18°C	94%	82%
21°C	88%	80%
22°C	92%	96%
23°C	86%	0%
25°C	98%	0%
29°C	90%	0%

Hatching rates of y,w^{67} and $y,w^{67},l(1)ts148$ embryos measured at different temperatures. For each measurement, 50 embryos were aligned on agar blocks and incubated at the temperature indicated. Hatching was indicated by empty eggshells.

Taken together, these results demonstrate that *l(1)ts148* is lethal during all stages of development at the restrictive temperature, suggesting that *l(1)ts148* encodes an essential gene.

CONCLUSIONS

A screen of 100 conditional t.s. lethal mutant lines was performed to identify mutations which disrupt nuclear export or cytoplasmic localisation of *ftz* mRNA. One mutant line was identified in which mRNA accumulates in the nucleus at the restrictive temperature. *l(1)ts148* is likely to be required for the nuclear export of all mRNA, since all transcripts tested accumulate in the nucleus at the restrictive temperature, and the mutation is lethal at all stages of development.

This type of screen has not been attempted previously in *Drosophila*, and represents a novel method of screening for essential maternal-effect genes involved in mRNA localisation and export from the nucleus. The numbers screened were low, due to the fact that this was a pilot screen designed to test the approach, and also because the generation of large numbers of t.s. lethal mutant lines in *Drosophila* is a labour-intensive process. In previous screens of t.s. yeast strains for poly(A)$^+$ RNA export defects, 1-2% of the mutants screened were found to have excess nuclear poly(A)$^+$ RNA (Amberg et al., 1992; Kadowaki et al., 1994). Only one mutation disrupting nuclear mRNA export was identified in this screen of 100 t.s. lethal *Drosophila* mutants. While it is not possible to extrapolate from such small numbers, these results are consistent with the frequency of mRNA export mutations isolated in the yeast screens. Although not all genes can be mutated to give conditional alleles, the screen could be repeated on a larger scale by isolating more t.s. lethal mutations. The mutagenesis scheme could also be adapted to isolate conditional mutations on the autosomes, although it is not likely that enough mutations could be found to come close to saturating the genome.

6

l(1)ts148 CAUSES A DEFECT IN NUCLEAR mRNA EXPORT

INTRODUCTION

Although the isolation of yeast mutations with nuclear accumulation of poly(A)$^+$ RNA was a successful approach which led to the identification of many mRNA export factors, several other classes of genes were identified with excess nuclear poly(A)$^+$ RNA. Many of these genes encode proteins which are not part of the mRNA export machinery, such as factors involved in RNA turnover or membrane biogenesis. In addition to this, some mRNA export mutants display defects in nuclear structure, such as clustering of NPC's on one side of the nucleus, or nucleolar fragmentation. Furthermore, disruption of the nuclear protein import pathways can indirectly cause an mRNA export phenotype due to cytoplasmic accumulation of the shuttling proteins required for mRNA export (Gorlich and Kutay, 1999). Mutations which disrupt the splicing of pre-mRNA also lead to nuclear accumulation of RNA, because transcripts containing introns are not normally exported from the nucleus (Custodio et al., 1999; Legrain and Rosbash, 1989).

Therefore, in order to test whether *l(1)ts148* disrupts a gene directly involved in mRNA export, a number of assays were used to determine whether mRNA export, nuclear protein import, pre-mRNA splicing or nuclear ultrastructure were disrupted in *l(1)ts148* mutant embryos.

Figure 6-1

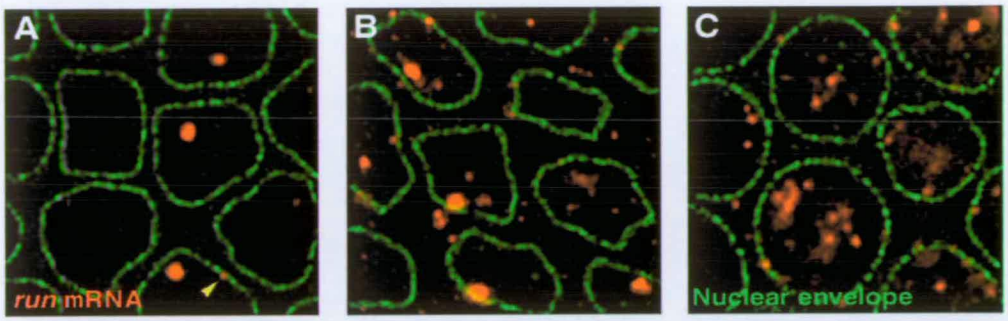

Figure 6-1 Nuclear mRNA Levels Increase with Time at the Restrictive Temperature (**A**) *l(1)ts148* embryos resemble wild type at 18°C, with bright nascent transcripts and few export intermediates (yellow arrowhead). (**B**) *run* mRNA in the nucleus of *l(1)ts148* embryos after shifting to 33°C for 15 minutes. (**C**) Many more particles of *run* mRNA are detected in the nucleus of *l(1)ts148* after 30 minutes at 33°C.

Figure 6-2

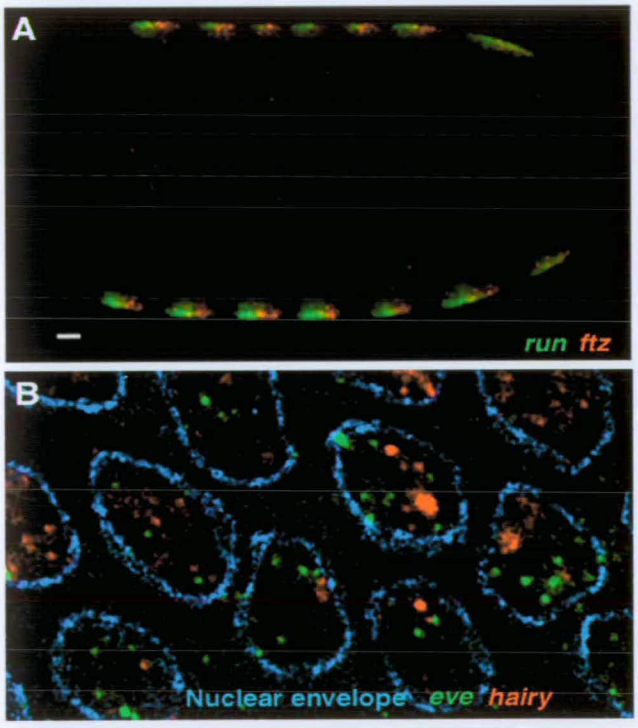

Figure 6-2. Covisualisation of Different Transcripts in the Blastoderm embryo. (**A**) Low power image of a wild type embryo in which *run* mRNA (green) and *ftz* mRNA (red) have been detected simultaneously. Bar = 20µm. (**B**) Higher power image of a *l(1)ts148* embryo, shifted to 33°C for 30 minutes, in which *eve* mRNA (green) and *h* mRNA (red) have been covisualised. The different transcripts accumulate in discrete particles within the nucleus, which do not overlap. The nuclear envelope was labelled with an anti-lamin antibody and detected with Cyanine-5, shown in blue.

RESULTS

Nuclear mRNA export is rapidly inhibited in *l(1)ts148* embryos

Mutations in other genes directly required for mRNA export have been found to have a rapid onset of nuclear mRNA accumulation, first visible 5-15 minutes after switching to restrictive conditions (Hurt et al., 2000; Strasser and Hurt, 1999). Therefore, to determine whether *l(1)ts148* was likely to disrupt a component of the nuclear mRNA export machinery directly, nuclear mRNA export was tested in embryos after shorter shifts to the restrictive temperature.

It was found that excess *run* mRNA was detectable in the nucleus after only 15 minutes at 33°C (Figure 6-1). In a time course of shifts to the restrictive temperature, greater numbers of mRNA particles were visualised in the nucleus after successively longer temperature shifts (Figure 6-1). Furthermore, it was observed that many of the particles of mRNA which accumulate within the nucleus at the restrictive temperature are similar in size and fluorescence intensity to cytoplasmic mRNA (Table 6a). Cytoplasmic mRNA particles were previously found to have identical intensities to nuclear mRNA export intermediates (Table 4a). Therefore, these results imply that transcription continues normally under restrictive conditions, but mRNA export intermediates are unable to exit the nucleus and accumulate throughout the nucleoplasm.

It is conceivable that the particles of mRNA which accumulate in the nucleus at the restrictive temperature might be gathering at nuclear sites involved in processing or degradation of all transcripts. To test this possibility, the transcripts of two different genes were covisualised in *l(1)ts148* embryos at the restrictive temperature. Some pair-rule genes such as *run* and *ftz*, or *eve* and *h*, are expressed in overlapping stripes at the

Figure 6-3

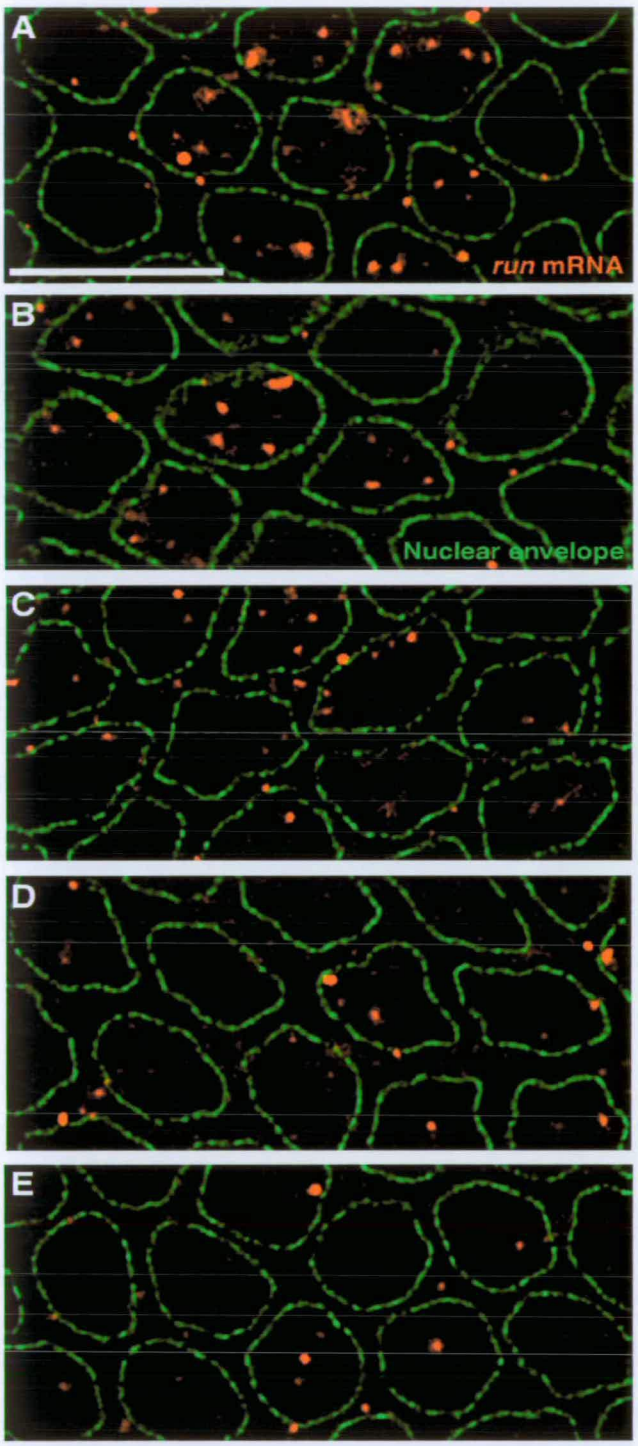

Figure 6-3 The mRNA accumulation phenotype of *l(1)ts148* is rapidly reversible. (**A**) *l(1)ts148* embryo shifted to 33°C for 60 minutes, showing excess nuclear *run* mRNA (red) Bar = 10μm. (**B-E**) *l(1)ts148* embryos shifted to 33°C for 60 minutes then shifted back to 18°C for (**B**) 1 minute (**C**) 2 minutes (**D**) 5 minutes (**E**) 10 minutes.

syncitial blastoderm stage (Figure 6-2), so are often expressed in the same nuclei. In *l(1)ts148* embryos, *h* and *eve* mRNA were found to accumulate in discrete nuclear particles which did not overlap significantly, demonstrating that specific transcripts accumulate at different sites at the restrictive temperature (Figure 6-2).

Furthermore, the mRNA export phenotype was found to be rapidly reversible. *l(1)ts148* embryos were incubated at 33°C for 60 minutes, then shifted back to 18°C for a range of different times (Figure 6-3). Embryos shifted back to 18°C for 10 minutes were indistinguishable from wild type, with little *run* mRNA in the nucleus outwith nascent transcript foci and abundant *run* mRNA localised in the apical cytoplasm. In contrast, embryos shifted back to the permissive temperature for 1-2 minutes showed large amounts of nuclear mRNA particles and very little *run* mRNA in the cytoplasm, similar to embryos which had not been shifted down. Nuclear mRNA levels were significantly reduced after 5 minutes at the permissive temperature. This result demonstrates that between 5-10 minutes after shifting back to the permissive temperature, the nuclear mRNA vanishes and correctly localised mRNA appears in the apical cytoplasm (Figure 6-3 and data not shown). This suggests that the accumulated nuclear mRNA can be exported and localised rapidly at the permissive temperature, and was therefore unlikely to be incorrectly processed or targeted for degradation.

Taken together, these results suggest that *l(1)ts148* disrupts an essential gene in the mRNA export pathway, causing intermediates in the mRNA export pathway to accumulate within the nucleus at the restrictive temperature. However, it is also possible that *l(1)ts148* might cause a defect in pre-mRNA splicing or nuclear protein import, indirectly causing a block in the nuclear export of mRNA.

Table 6a. Intensity of nuclear and cytoplasmic mRNA in *l(1)ts148* embryos

Region of embryo	Intensity
run nascent transcript foci	5,118,017 ± 127,912 (N=4)
run apical cytoplasmic mRNA	205,042 ± 37,134 (N=16)
run nuclear mRNA particles	214,662 ± 37,495 (N=19)

The fluorescence intensity of *run* nascent transcript foci, and other particles of *run* RNA in the nucleus and cytoplasm of *l(1)ts148* embryos after a 15 minute shift to 33°C. Measurements were made from a single embryo which displayed a typical mRNA export defect. Total integrated fluorescence intensity is measured in arbitrary units ± standard error. N = number of foci measured.

l(1)ts148 does not disrupt pre-mRNA splicing

It has been shown that the presence of splicing signals and introns prevents the nuclear export of pre-mRNA. Mature mRNA (but not excised introns) can be exported to the cytoplasm only after splicing is complete, and mutated pre-mRNA that cannot be spliced is retained inside the nucleus by the splicing machinery (Legrain and Rosbash, 1989). Mutations in the yeast *prp22* gene, or its mammalian homologue HRH1, inhibit pre-mRNA splicing and cause nuclear accumulation of unspliced transcripts (Lee and Silver, 1997). Interestingly, retroviruses have evolved mechanisms to overcome this regulatory step. Unspliced viral RNA must be exported to the cytoplasm to act as a template for viral protein synthesis and also for packaging into progeny virus particles. The Simian Type D retrovirus encodes a signal known as the constitutive transport element (CTE) which binds directly to the cellular TAP protein, targeting the unspliced viral genomic RNA for export via the normal mRNA export pathway (Braun et al., 1999; Gruter et al., 1998).

In order to determine if pre-mRNA splicing was disrupted in *l(1)ts148* embryos, nuclear mRNA was tested for the presence of intron sequences at the restrictive temperature. In wild type embryos, *in situ* hybridisation using a *h* intron probe gives a typical pair-rule expression pattern of seven stripes in the blastoderm embryo, except the signal is restricted to two foci within each nucleus that expresses *h* (Davis, 1990). This has previously been reported for the introns of other *Drosophila* genes such as *Ultrabithorax* (Shermoen and O' Farrell, 1991) and *Delta* (Kopczynski and Muskavitch, 1992). Intron RNA and mRNA from the *h* gene was covisualised by *in situ* hybridisation with two-colour fluorescent detection (Wilkie and Davis, 1998). In wild type embryos *h* intron RNA is only detected at nascent transcript foci (Figure 6-4), demonstrating that splicing occurs in close association with the transcription machinery as previously reported

Figure 6-4

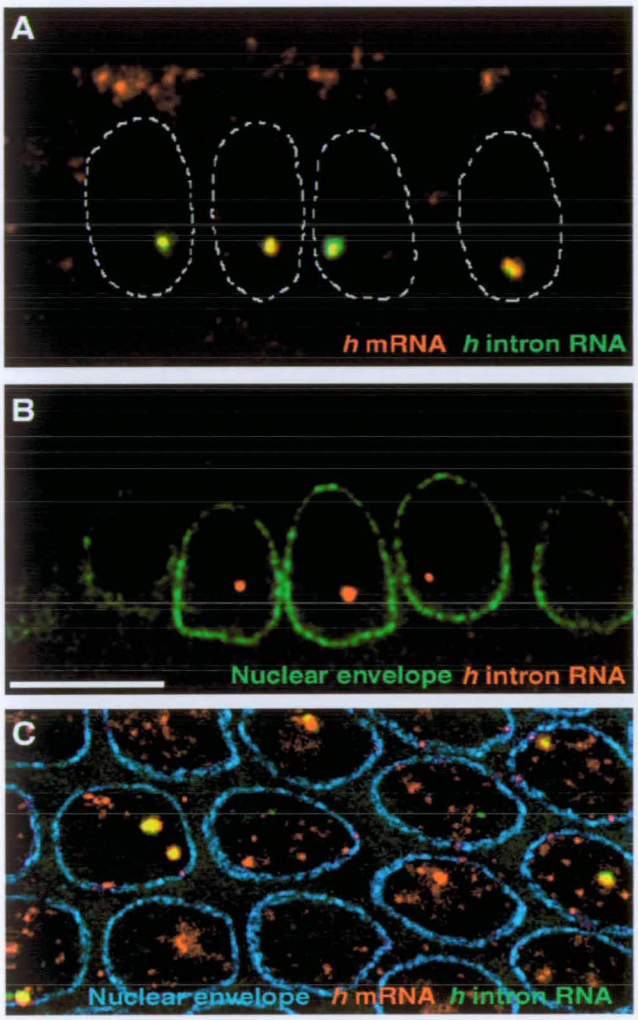

Figure 6-4 *l(1)ts148* does not disrupt pre-mRNA splicing (**A**) Wild type embryo in which *h* mRNA and intron RNA are labelled in red and green, respectively. The position of the nuclear membrane is represented by a dotted white line. *h* mRNA is detected at nascent transcripts and in the apical cytoplasm, whereas *h* intron RNA is visualised exclusively at nascent transcript foci. (**B**) *l(1)ts148* embryo after 30 minutes at 33°C. *h* intron RNA (red) is only detected at nascent transcript foci. Bar = 10μm. The nuclear envelope is labelled in green. (**C**) *l(1)ts148* embryo shifted to 33°C for 30 minutes in which *h* mRNA and intron RNA are covisualised in red and green, respectively. The nuclear envelope is labelled in blue. Excess nuclear particles of *h* mRNA do not contain detectable amounts of intron RNA, which remains confined to nascent transcript foci.

(Bauren and Wieslander, 1994; Beyer and Osheim, 1988; Custodio et al., 1999; LeMaire and Thummel, 1990; Tennyson et al., 1995). In *l(1)ts148* embryos, *h* intron RNA remains confined to nascent transcript foci, and the *h* mRNA particles which accumulate throughout the nucleus at the restrictive temperature lack detectable intron sequences (Figure 6-4). Although this result does not prove that the entire splicing pathway is functional in *l(1)ts148* embryos, it demonstrates *h* mRNA is not retained in the nucleus due to inefficient removal of this intron at the restrictive temperature.

Nuclear protein import is not disrupted in *l(1)ts148* embryos

Many mutations in some nuclear trafficking factors are known to disrupt both nuclear protein import and mRNA export. For example, mutations in some yeast nucleoporin genes cause poly(A)$^+$ RNA accumulation in the nucleus and also prevent the import of nuclear proteins (Fabre and Hurt, 1997). Dominant negative truncations of human importin-β protein have also been shown to inhibit both nuclear protein import and mRNA export in *Xenopus* oocytes and *Drosophila* embryos (Kutay et al., 1997)(Davis and Kumar, manuscript submitted). In order to determine whether nuclear protein import was disrupted by *l(1)ts148*, a sensitive nuclear protein import assay using nlsGFP was used to test import in living *l(1)ts148* embryos. Nuclear import of nlsGFP occurs by the 'classical' nuclear protein import pathway mediated by importin-α/β, and is abolished by known nuclear trafficking inhibitors such as RanQ69L (Palacios et al., 1996), or by excess cargo protein such as nlsBSA (Davis and Kumar, manuscript submitted).

Two independent insertions of the *nlsGFP* transgene on chromosomes 2 and 3 (Davis et al., 1995) were crossed into the *l(1)ts148* line to produce flies of genotype *l(1)ts148 ; nlsGFPM, nlsGFPN* (Ruth Kirby). Imaging GFP fluorescence in living *l(1)ts148* embryos showed that nlsGFP import was not disrupted when the temperature was

increased to 33°C using a temperature-controlled microscope stage (Ilan Davis, data not shown).

This result demonstrates that nuclear protein import of nls-containing proteins by importin-β is not affected by *l(1)ts148* at the restrictive temperature. The mRNA export phenotype is therefore unlikely to be caused by inhibition of nuclear protein import, unless a different nuclear import pathway (such as transportin mediated nuclear import) is defective in *l(1)ts148*.

l(1)ts148 does not disrupt nuclear ultrastructure

Many of the mRNA export mutants isolated in yeast have also been found to disrupt nuclear architecture at the ultrastructural level. Defects which have been described include fragmentation of the nucleolus (Goldstein et al., 1996; Kadowaki et al., 1994; Segref et al., 1997) clustering of NPC's on one side of the nuclear envelope (Gorsch et al., 1995; Heath et al., 1995) and herniations in the nuclear envelope which seal the NPC's under layers of membrane (Murphy et al., 1996; Wente and Blobel, 1993). Although it has been proposed in the case of *gle2* mutants that the clusters of herniated NPC's are secondary to the RNA export defect because they form subsequent to the poly(A)$^+$ RNA export block (Murphy et al., 1996), the significance of these defects in a number of other mRNA export mutants is not understood. It is possible in many cases that mRNA export could be blocked due to defects in the NPC or nuclear envelope, rather than as a direct consequence of disrupting part of the mRNA export machinery. In some mutants which disrupt mRNA export and also cause nucleolar fragmentation, poly(A)$^+$ RNA and nucleolar antigens colocalise in multiple foci throughout the nucleus (Kadowaki et al., 1994). In contrast, the fragmented nucleolus does not colocalise with

Figure 6-5

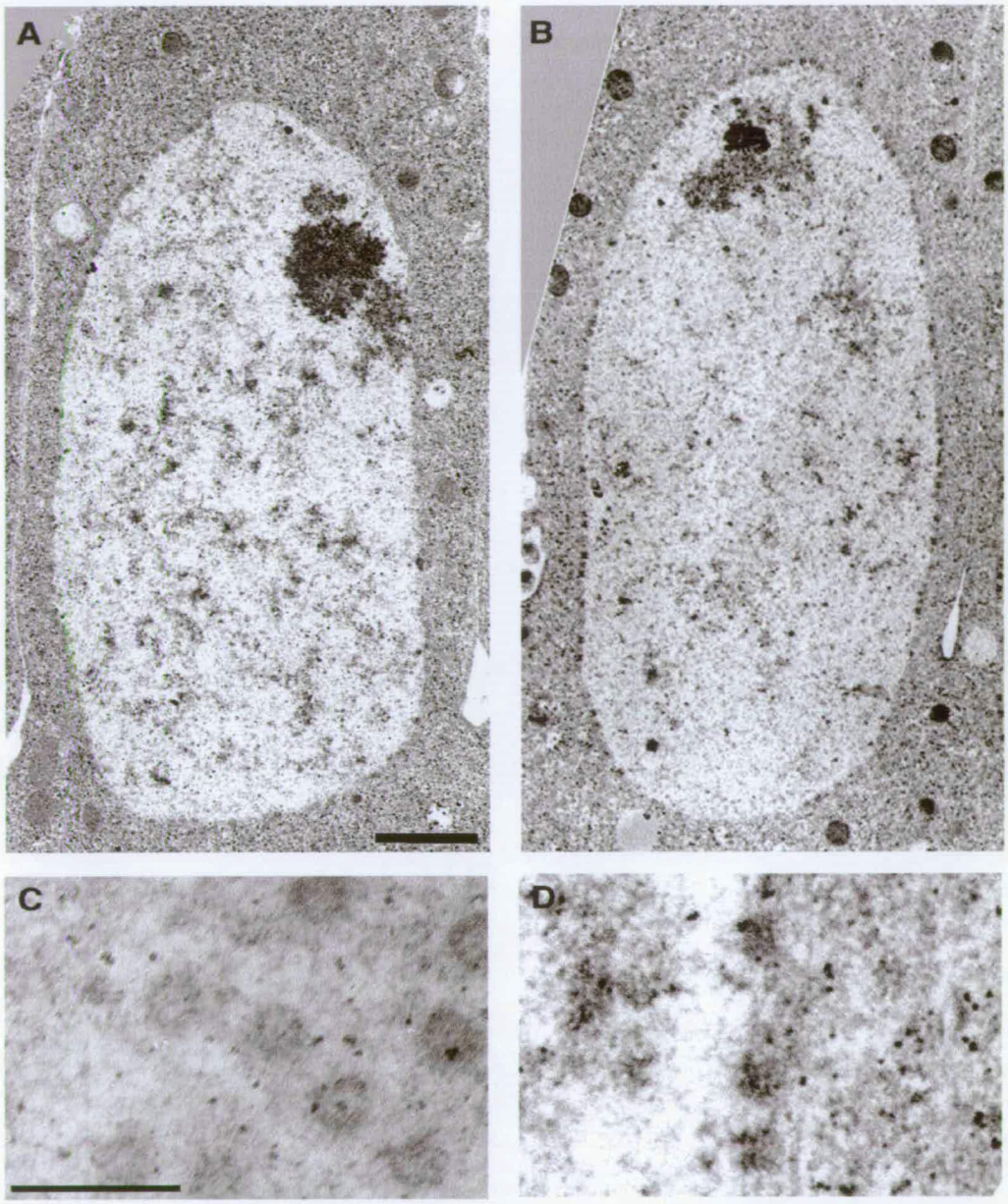

Figure 6-5 Nuclear Ultrastructure of *l(1)ts148* embryos (**A**) Ultrastructure of a single nucleus from a blastoderm stage *l(1)ts148* embryo at 18°C. Apical is up. Bar = 2μm. (**B**) Electron micrograph of a nucleus in a *l(1)ts148* embryo after 30 minutes at 33°C. (**C**) Nuclear pores in a section grazing the nuclear membrane in a *l(1)ts148* embryo at the restrictive temperature, shown at higher magnification. Bar = 100nm. (**D**) Section through the nuclear envelope in a *l(1)ts148* embryo at the restrictive temperature, showing three NPC's spanning the nuclear membrane. The nucleus on the left of the micrograph.

poly(A)$^+$ RNA in *mex67-5* mutant cells at the restrictive temperature (Segref et al., 1997).

To determine whether *l(1)ts148* exhibits morphological abnormalities in the nucleus at the ultrastructural level, thin-section transmission electron microscopy was used to examine wild type and *l(1)ts148* mutant embryos at the permissive and the restrictive temperature. At the permissive temperature, *l(1)ts148* embryos were found to have a similar nuclear ultrastructure to wild type embryos. Furthermore, ultrastructural defects were not observed in *l(1)ts148* embryos at the restrictive temperature. In *l(1)ts148* embryos which were shifted to 33°C for 30 minutes before fixation, NPC's were visible around the entire nucleus, and were not found in clusters (Figure 6-5). Furthermore, herniations in the NE were not observed, and the NPC's were not sealed within layers of nuclear membrane (Figure 6-5). At this level of magnification, the gross structure of NPC's were normal, with 8-fold rotational symmetry and clearly visible central transporters. Each nucleus contained a single nucleolous, visualised as an electron-dense region of the nucleoplasm on the apical side of the nucleus where rDNA genes are localised. The nucleolus was not fragmented in *l(1)ts148* embryos after 30 minutes at 33°C (Figure 6-5). As no nucleolar fragments were observed, and mRNA does not accumulate exclusively on the apical side of the nucleus where the nucleolus is located, it is not likely that the mRNA which accumulates in the nucleus in *l(1)ts148* embryos is associated with the nucleolus.

Thus, under restrictive conditions which cause the nuclear accumulation of mRNA throughout the nucleus, *l(1)ts148* embryos were not observed to have ultrastructural defects that could lead to a block in mRNA export. This suggests that *l(1)ts148* might

disrupt a factor directly required for the nuclear export of mRNA, rather than a factor involved in maintaining the structure and function of the NE and NPC.

CONCLUSIONS

l(1)ts148 causes the rapid nuclear accumulation of mRNA from all genes tested in distinct particles, which become distributed throughout the nucleoplasm at the restrictive temperature. The phenotype is rapidly reversible by shifting back to the permissive temperature, suggesting that the mRNA is competent for export and is not retained in the nucleus due to processing defects. *l(1)ts148* does not disrupt the removal of introns from pre-mRNA, or the nls-mediated import of proteins into the nucleus. The fluorescence intensity of the accumulated mRNA is similar to cytoplasmic mRNA particles, suggesting that *l(1)ts148* inhibits the nuclear exit of mRNA export intermediates. Furthermore, *l(1)ts148* does not cause defects in the ultrastructure of the nuclear envelope or the nucleolus, and does not affect the distribution, number or gross structure of NPC's at the restrictive temperature. Taken together, these results suggest that *l(1)ts148* disrupts the function of a gene which is directly involved in the export of mRNA from the nucleus.

7

l(1)ts148 ENCODES THE *DROSOPHILA* HOMOLOGUE OF HUMAN TAP

INTRODUCTION

In order to identify the gene that is mutated in *l(1)ts148*, use was made of the powerful array of genetic and molecular resources available in *Drosophila*. Transposon tagging, recombination with visible genetic markers and complementation with chromosomes containing mapped deletions and duplications are invaluable techniques for mapping and identifying genes. Use was also made of the vast collections of mapped mutations existing in *Drosophila* stock centres and the wealth of sequence information produced by the *Drosophila* EST and genome sequencing projects carried out by the BDGP, EDGP and Celera Genomics.

Table 7a. Mapping the genetic position of *l(1)ts148* by recombination analysis

Genetic marker	Map position	% Recombination	Position of *l(1)ts148*
singed	21.0	11.1	32.2
vermillion	33.0	1.8	31.2
minute	36.1	4.2	31.9
forked	56.7	23.7	33.0
outstretched	58.7	26.3	32.4

The recombination frequency of various genetic markers with *l(1)ts148*. Recombination frequencies were assayed in the progeny of female flies heterozygous for a multiply-marked X chromosome and *l(1)ts148*, at 29°C. The map position deduced for *l(1)ts148* from each genetic marker is shown.

Table 7b. Complementation of *l(1)ts148* with Deficiency and Duplication strains

Deficiency	Breakpoints	Complementation at 29°C
Df(1)C52	8E;9C-D	viable
Df(1)N110	9B3-4;9D1-2	viable
Df(1)v-L15	9B1-2;10A1-2	lethal
Df(1)RJ7	9B9;9E3-4	viable
Df(1)HC133	9B9;9F5	viable
Df(1)v-L11	9C4;10A1-2	lethal
Df(1)ras-V17	9D1-2;10A2-3	lethal
Df(1)ras203	9E1;10A11	lethal
Df(1)v64f	9E7;10A2	lethal
Df(1)Mec13	9F3;10A	lethal
Df(1)v-L4	9F5-6;10A1	lethal
Df(1)v-L3	9F10;10A7	viable
Df(1)v-L6	9F11;10A1-2	viable
Df(1)v-L2	9F13;10A1	viable
Df(1)v-L1	10A1;10A5	viable
Df(1)v-N48	10A1;10C3-3	viable
Df(1)RA37	10A6;10B15-17	viable
Df(1)GA112	10B1;10C2	viable
Df1)m259-4	10C2;10E2	viable
Duplication	**Breakpoints**	**Complementation at 29°C**
$Dp(1;2)v^{+75d}$	9A2;10C2	viable
$Dp(1;2)v^{+63i}$	9E1;10A11	viable
$Dp(1;Y)B^{S}v^{+}y^{+}$	9F3;10E3-4	viable
$Dp(1;Y)v^{+}y^{+}$	9F5;10C2	viable

The complementation of *l(1)ts148* with deficiency chromosomes containing mapped deletions, and duplication chromosomes containing mapped translocations of DNA from the X chromosome to other chromosomes. Complementation was assayed by measuring the survival of appropriate classes of progeny from crosses carried out at 29°C. In all cases, control crosses were carried out at 18°C and showed survival of all classes of progeny, indicating lethality was due to the t.s. lethal mutation in *l(1)ts148*.

RESULTS

Mapping the position of *l(1)ts148*

The first step towards identifying the *l(1)ts148* gene was to find the position of the t.s. lethal mutation on the *l(1)ts148* chromosome. To map the genetic position of *l(1)ts148* on the X chromosome, heterozygous female flies were generated with one *y,w,l(1)ts148* chromosome and one multiply marked X chromosome carrying the markers *singed*, *vermillion*, *minute*, *forked* and *outstretched*. The recombination frequency of the t.s. lethal mutation was calculated against each of these recessive genetic markers by scoring the male progeny of these females at 29°C (Ruth Kirby). The results of the recombination experiments (Table 7a) suggest that there is a single lethal t.s. mutation on the *l(1)ts148* chromosome which maps around position 32.1 on the genetic map. This position is almost halfway along the X chromosome, at around segment 9 of the cytological (polytene) map.

To further refine the position of *l(1)ts148*, the mutation was mapped by complementation with chromosomes containing mapped deletions and insertions of DNA from the X chromosome. It was found that seven different deficiencies removing DNA from segment 9 failed to complement *l(1)ts148* at 29°C, whilst producing viable flies at 21°C (Table 7b). Other deficiencies deleting DNA from most other parts of the X chromosome complemented *l(1)ts148* at 29°C (Ruth Kirby, data not shown). In addition to this, 4 different duplications of DNA from segment 9 to the 2nd chromosome or the Y chromosome rescued the lethality of *l(1)ts148* flies at 29°C. These results confirm that there is a single lethal mutation on the *l(1)ts148* chromosome which maps between 9F5-6 and 9F10 (Figure 7-1), a region containing roughly 50-100Kb of DNA.

Figure 7-1

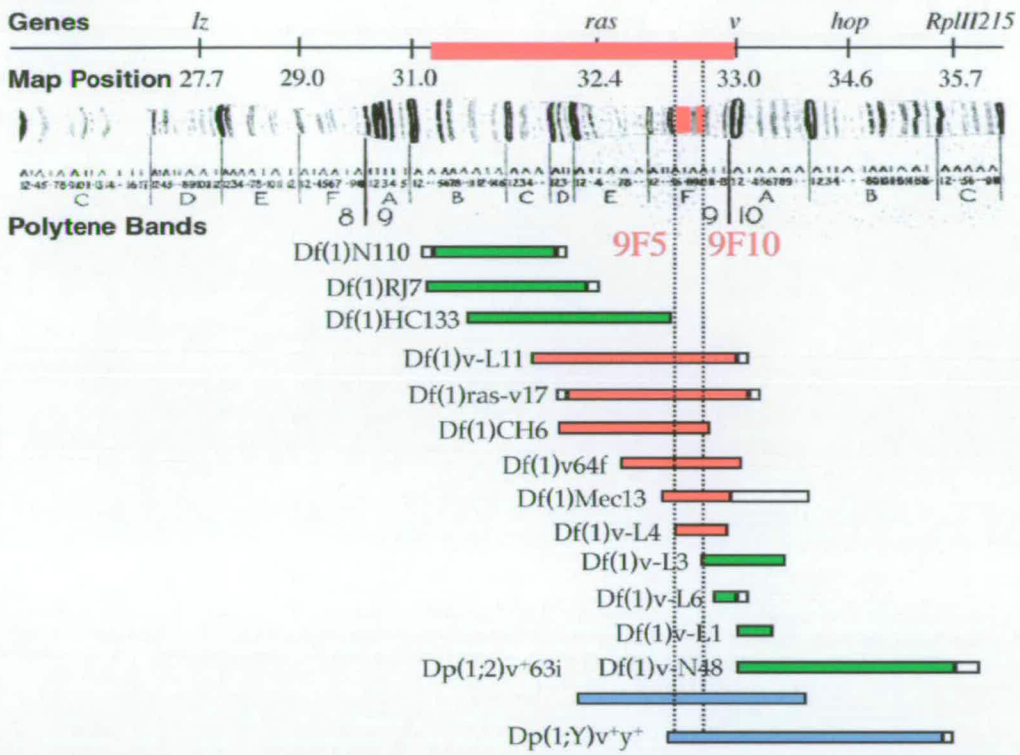

Figure 7-1 Map position of *l(1)ts148* on the X chromosome. Diagram of genetic and cytological markers in polytene chromosome bands 8-10. Top, *l(1)ts148* maps within the red area, near *ras* and *v*, by recombination analysis. Bottom, the breakpoints of deficiency and duplication chromosomes used to map *l(1)ts148* to polytene bands 9F5-10. Green deficiencies complement *l(1)ts148* at 29°C. Red deficiencies fail to complement and blue duplications rescue *l(1)ts148* at 29°C. White areas represent uncertainty in the mapping of breakpoints.

Figure 7-2

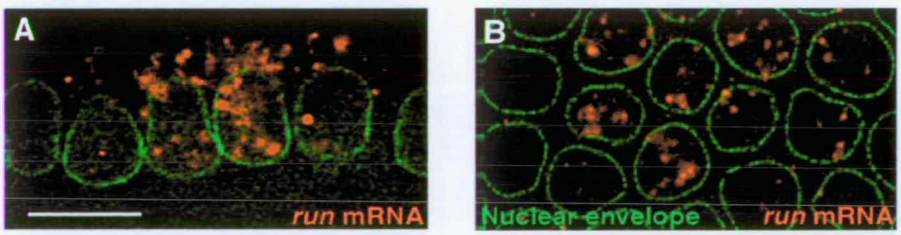

Figure 7-2 mRNA export is defective in heterozygous *l(1)ts148/Df* embryos. (**A**) *run* mRNA (red) in a *l(1)ts148/Df(1)v-L11* embryo shifted to 33°C for 30 minutes, imaged in nuclei at the edge of a blastoderm stage embryo. Bar = 10μm. (**B**) *run* mRNA in a *l(1)ts148/Df(1) Mec13* embryo shifted to 33°C for 30 minutes, imaged in a cross section of nuclei near the surface of the embryo. The nuclear envelope is labelled in green.

In order to show that the mRNA export phenotype is due to the t.s. lethal mutation in 9F5-10, and not due to another recessive mutation elsewhere in the genome, the phenotype was examined in embryos laid by females where one copy of the wild type *l(1)ts148*$^{+}$ gene was deleted by a deficiency, and all chromosomes were heterozygous. In *l(1)ts148/Df(1)v-L11* and *l(1)ts148/Df(1)Mec13* embryos, nuclear mRNA export is disrupted at the restrictive temperature, and the phenotype is indistinguishable from homozygous *l(1)ts148* embryos (Figure 7-2). A similar phenotype was observed in *l(1)ts148/Df(1)v-64f* and *l(1)ts148/Df(1)v-L4* embryos at the restrictive temperature (data not shown). This result confirms that the mRNA export defect is indeed due to the lethal t.s. mutation that maps between 9F5-10. In addition to this, this result suggests that the t.s. mutation in *l(1)ts148* acts as a strong loss of function (null) allele at the restrictive temperature, since the phenotype is not more severe when one copy of the mutant allele is deleted by a deficiency.

Isolating a P-element allele of *l(1)ts148*

One of the most straightforward ways to clone a gene in *Drosophila* is by transposon tagging. If a P-element induced allele of a gene can be found, then the genomic DNA flanking the P-element insertion site can be cloned by plasmid rescue. P-element insertions mapping to the 9F region were identified by searching all known P-element lines on flybase. The only P-elements mapping to the 9F area were three lines with insertions of an enhancer trap EP element containing a UAS driver in 9F2-3 (Rorth, 1996). EP(X)108, EP(X)109, EP(X)1207 are viable lines, and therefore the P-elements are not likely to disrupt an essential gene. These P-elements map quite far from *l(1)ts148*, and were found to complement *l(1)ts148* at 29°C. Therefore, none of these lines are likely to contain a P-element insertion in the *l(1)ts148* gene.

Figure 7-3

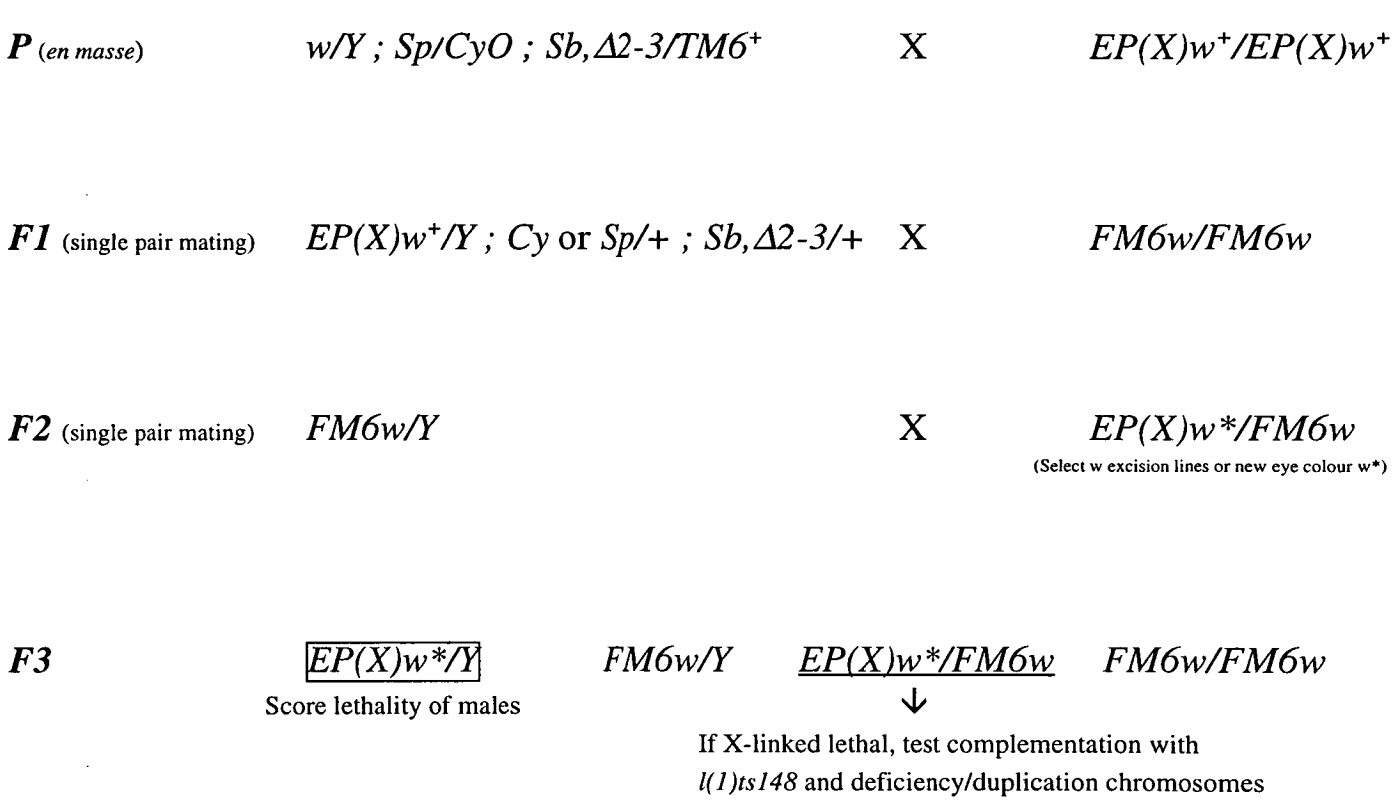

Figure 7-3 Scheme to generate new lethal insertions or excision derivatives of EP element.
EP(X) elements were mobilised with *Δ2-3* transposase. Transposition of the EP element occurs throughout somatic and germ cells in the F1 generation. The transposase was then crossed out, and F2 lines with new orange/red eye colours (new insertions) or white eyes (excisions) were scored for X-linked lethality by absence of males in the F3 generation. Suitable lines were tested for complementation with *l(1)ts148,* and mapped using deficiency and duplication chromosomes in 9F.

Having failed to find an existing allele of *l(1)ts148* induced by a P-element, an attempt was made to generate a P-element insertion in or near the *l(1)ts148* gene by mobilising the EP(X) elements located in 9F2-3. These P-elements do not encode their own source of transposase, so remain as stable insertions in the genome. However, P-elements can be mobilised by providing a source of transposase encoded by a separate transgene, allowing the P-element to excise and re-insert elsewhere in the genome. It has been demonstrated that P-elements tend to re-insert within approximately 50kb of their original insertion site, a phenomenon called local hopping (Tower et al., 1993). This technique is commonly used to hop a nearby P-element into a gene of interest to create a P-element induced mutant allele.

The EP(X) elements were mobilised by crossing in a *Sb, Δ2-3* transgene encoding the transposase. The EP(X) elements are marked with the *white* (*w*) gene, allowing them to be followed by eye colour. A scheme was designed to identify lethal insertions and deletions of the P-element (Figure 7-3). New P-element insertions can be identified as they tend to have distinct eye colours ranging from light orange to red, due to position effect variegation. Lines where the P-element has been excised (occasionally removing some genomic DNA and making a deletion) are visible by their white eyes.

A pilot screen was performed by screening 600 F2 lines (200 for each P element insertion line). Although 42% of the F2 lines had new eye colours due to transposition of the EP(X) element, only 1% of these lines had lethal insertions on the X chromosome. 6 lethal lines were isolated in total, 4 of which were new w^+ insertions. The remaining 2 lines were w^- and therefore likely to be caused by imprecise excision of the P-element. These lethal lines were tested for lesions in or near the *l(1)ts148* gene by complementation with deficiency chromosomes and *l(1)ts148*. All six of the lethal

insertion and excision lines were found to complement *l(1)ts148* at 29°C, and none of the lines had lethal insertions or deletions within 9F3-10A1. The local hopping approach using the EP(X) elements was therefore not successful in transposing a P-element into or near the *l(1)ts148* gene. Furthermore, this approach was not likely to work even when scaled up considerably because of the very low frequency of lethals generated.

An alternative approach made use of a new collection of over 500 lethal P-element insertions on the X chromosome from the laboratory of Herbert Jackle (Scheffer and Jackle, unpublished results). This collection was screened for insertions in *l(1)ts148* and for insertions in the 9F region by complementation with *l(1)ts148* and deficiencies in the 9F region. All 502 lethal P-element lines screened were found to complement *l(1)ts148* at the restrictive temperature, and although 15 lines were identified with insertions mapping between 9D1-9E7, and 2 further lines had insertions between 9E7 and 9F3, no lines were found with P-element insertions in the 9F3-10A1 region. The Jackle collection therefore did not contain any P-elements disrupting *l(1)ts148*, and no insertions were found to map near enough to *l(1)ts148* to use in further local hopping experiments.

Using two different approaches, a P-element induced allele of *l(1)ts148* was not identified. Local hopping may have failed either because the insertion site of the EP(X) elements was too far (more than 50kb) from *l(1)ts148*, or because not enough flies were screened. Alternatively, *l(1)ts148* may be one of the genes which are not readily mutable by P-elements in *Drosophila*. What defines whether a gene is mutable by P-elements is not known.

Identifying other alleles of *l(1)ts148*

In order to test whether *l(1)ts148* is an allele of a previously identified gene, mutant lines mapping to the 9F region were obtained and tested for complementation with *l(1)ts148* at the restrictive temperature. Two genes, *flightlessK* and *small bristles,* were identified as candidates to test for complementation as they had previously been mapped to the 9F5-10 region and mutant alleles of both genes were available from *Drosophila* stock centres and other laboratories.

The *flightlessK (fliK)* gene maps to 9F5, and the $fliK^1$ allele causes reduced flying and jumping ability in adult flies, and is also t.s. lethal at 29°C (Homyk et al., 1980). Since adult *l(1)ts148* flies also fail to jump and fly at 29°C, *l(1)ts148* was an excellent candidate for a novel allele of *fliK*. However, $fliK^1$ was found to complement *l(1)ts148* at 29°C, producing viable $fliK^1/l(1)ts148$ adult females which were fertile at 29°C, and displayed normal flying and jumping abilities. *l(1)ts148* and $fliK^1$ are therefore highly unlikely to be mutant alleles of the same gene.

The *small bristles* (*sbr*) gene maps to 9F5-8, and was originally defined by the sbr^1 mutation which causes missing scutellar bristles on the notum of the adult fly (Lindsley and Zimm, 1992). 19 different alleles of *sbr* have been reported to date (Lindsley and Zimm, 1992). Most alleles are recessive lethal mutations, but sbr^2 also affects scutellar bristles, and sbr^{17} disrupts fertility in male and female flies (Geer et al., 1983). The viable allele sbr^1, the lethal alleles sbr^5, sbr^6, sbr^{12} (Eeken et al., 1985; Zhimulev et al., 1987) and the lethal t.s. allele sbr^{10} (Arking, 1975) were obtained and tested for complementation with *l(1)ts148*. Complementation with *magellan (mgln)*, a novel *sbr* allele isolated in a screen for axon guidance defects (Korey and Van Vactor, unpublished results) was also tested.

Figure 7-4

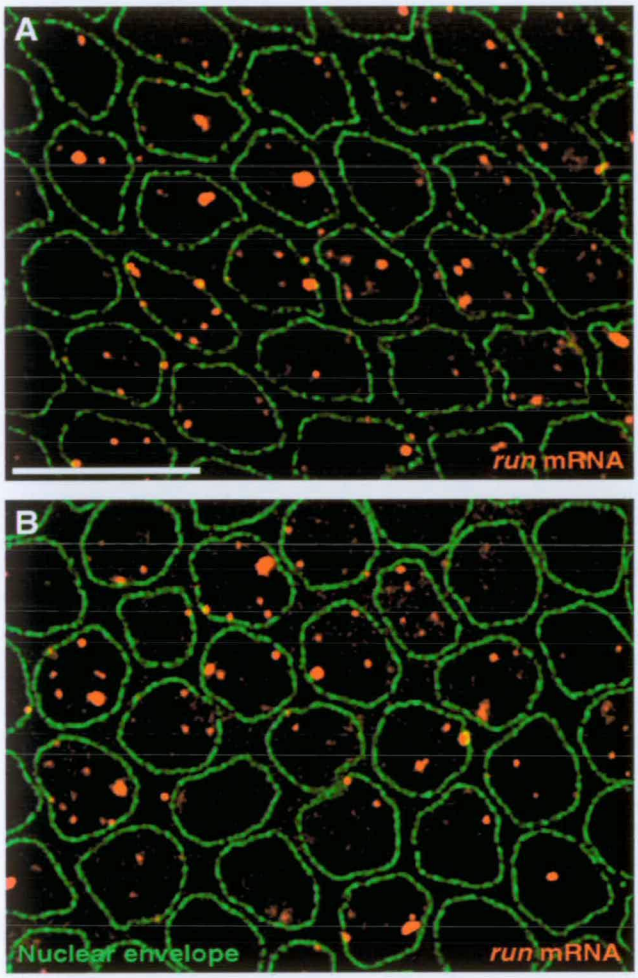

Figure 7-4 Nuclear mRNA export is disrupted in *sbr*^{10} and *l(1)ts148/sbr*^{10} embryos.
(**A**) Excess nuclear *run* mRNA (red) in a homozygous *sbr*^{10} embryo shifted to 33°C for 30 minutes. Bar = 10μm. (**B**) Particles of *run* mRNA accumulate in a similar manner within nuclei of a heterozygous *l(1)ts148/sbr*^{10} embryo shifted to 33°C for 30 minutes. The nuclear envelope is labelled in green.

sbr^{1} was found to complement *l(1)ts148* at 29°C and *sbr*^{1}*/l(1)ts148* females were viable and fertile and had no visible bristle defects at 29°C. However *mgln*, *sbr*^{5}, *sbr*^{6}, *sbr*^{10} and *sbr*^{12} failed to complement *l(1)ts148* at 29°C, strongly suggesting that *l(1)ts148* is an allele of *sbr*. To investigate this further, *sbr*^{10}*/sbr*^{10} and heterozygous *l(1)ts148/sbr*^{10} females were generated at the permissive temperature (21°C) and the phenotype of embryos laid by these flies was examined. Such embryos were found to have a mRNA export defect at the restrictive temperature, very similar to that found in homozygous *l(1)ts148* embryos (Figure 7-4). This strongly suggests that *sbr*^{10} and *l(1)ts148* are mutant alleles of the same gene. Since homozygous flies or embryos cannot easily be generated for the unconditional lethal alleles *mgln*, *sbr*^{5}, *sbr*^{6} or *sbr*^{12}, it is difficult to directly test these lines for defects in mRNA export. However, the complementation data is strong evidence that *l(1)ts148* is allelic to all these mutations.

The best way to determine whether *l(1)ts148* and the *sbr* mutants are alleles of the same or different genes would be to look for differences in the DNA sequences of the alleles and to construct an *sbr*$^{+}$ transgene to test for rescue of the phenotypes. Since *sbr* had not been cloned or sequenced, this was not possible. The discovery that *l(1)ts148* was likely to be a new allele of *sbr* did not therefore immediately lead to the identification of the molecular sequence of the *l(1)ts148* gene.

The Drosophila homologue of the TAP/Mex67 gene maps to 9F2-5

At this time, the *Drosophila* genome sequencing project was in its early stages, before the announcement by Celera Genomics that the company intended to sequence the entire *Drosophila* genome as a test for its whole-genome shotgun approach (later used to sequence the human genome). The X chromosome was being sequenced by members of the European *Drosophila* Genome Project (EDGP) by sequencing overlapping genomic

Table 7c. Hybridisation of nuclear trafficking EST's to genomic P1 clones

EST clone	Homologues	P1 hits	Map position
LD05914	RAE1/Gle2p	DS04000	57F4-57F10
		DS07844	57F8-58A2
LD11064	TAP/Mex67p	DS03615	9E7-9F6
GH01390	importin-β3	DS00373	5E5-5F1
		DS00253	5F1-5F5

The map position of genomic P1 clones which hybridised to labelled probes from different *Drosophila* EST clones. The vertebrate and yeast homologues of the EST sequences are shown.

Table 7d. Mapping the position of the dTAP EST LD11064

clone	Cytology	Hybridisation to EST
P1 DS00018	9F10-9F13	negative
P1 DS03615	9E7-9F6	positive
P1 DS06190	9E2-9F5	negative
cosmid 36A5	9F-10A	positive
cosmid 161H8	9E	negative
cosmid 186C8	9F	positive
cosmid 139F9	9E	negative

The map position of genomic DNA clones which contain the *Drosophila* dTAP EST sequence, detected by Southern hybridisation. The map position of genomic DNA clones was previously established by *in situ* hybridisation to polytene chromosomes by the European and Berkeley *Drosophila* Genome Projects.

clones, beginning in region 1A and progressing in order along the chromosome arm. This work was not expected to reach the 9F region, where *sbr* is located, for several years. However, Phase 1 of the *Drosophila* EST sequencing project, carried out by the Berkeley *Drosophila* Genome Project (BDGP) had recently completed the partial sequence of over 80,000 EST clones. Although the EST sequences were not mapped within the genome, they were found to represent almost 6000 genes, estimated to be around 50% of the genes expressed in *Drosophila*, and therefore provided a rich source of cDNA sequence information from previously unidentified fly genes (Rubin et al., 2000). In order to use a candidate gene approach to identify the wild type gene mutated in *l(1)ts148* and *sbr*, BLAST searches were performed with the EST database and a number of sequences with homology to yeast and human mRNA export factors were identified. The cytological positions of these EST clones were determined by hybridisation to a membrane containing an array of genomic P1 clone DNA by Vitaly Zimyanin, an undergraduate student working in our lab at the time. Since the map position of the P1 clones was previously established by *in situ* hybridisation to polytene chromosomes as part of the BDGP genome project, identification of genomic P1 clones containing a particular EST sequence allowed the map position of the EST sequence to be inferred. This approach is faster and less technically difficult than mapping genes by *in situ* hybridisation of short EST probes to polytene chromosomes, and also has the advantage of immediately isolating large genomic clones likely to contain the entire gene, allowing intron/exon structure to be examined.

The results of this work (Table 7c) show that an EST clone with high homology to human TAP hybridised strongly to a P1 clone from the 9F region (Vitaly Zimyanin). This suggests that the *Drosophila* TAP gene (dTAP) maps to the same area of the genome as *l(1)ts148*. This result was confirmed and the map position was further refined

Figure 7-5

Figure 7-5 Map of P1 clones in 9F which contain the dTAP EST. The dTAP sequence was detected in green, but not red, genomic P1 clones. Blue P1 clones were not tested. Gray squares represent unmapped STS sequences, which have been assigned arbitrary positions depending on their presence in different P1 clones. The yellow arrows show the maximum size of the region between STS sites in 9F2-5 which was deduced to contain the dTAP gene.

Figure 7-6

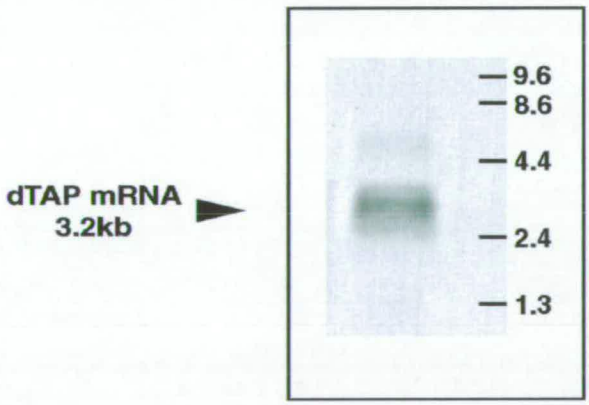

Figure 7-6 Northern Blot of the dTAP transcript. Northern Blot of total RNA from wild type flies, hybridised with a dTAP EST probe. The size of the major dTAP transcript, estimated from the position of RNA markers indicated on the blot was 3.2kb

by testing whether the dTAP EST sequence was contained in other P1 and cosmid clones from the 9F region. The dTAP EST sequence was found to hybridise to DNA from three independent genomic clones from the 9F region by Southern hybridisation (Table 7d), confirming that the *Drosophila* dTAP gene maps to 9F. As part of the *Drosophila* genome project, overlapping P1 clones were identified by STS analysis, allowing the tiling path of large contigs of P1 clones to be mapped along the chromosome arm. This information was used by the BDGP to produce a detailed map of P1 clones based on sequence and cytological information (Figure 7-5). Since the dTAP EST was detected in DS03615, but not in DS00018 or DS06190, the dTAP EST can be reliably mapped between 9F3-9F5.

Only short fragments of the EST clones (< 500bp) were originally sequenced during the *Drosophila* EST project. In order to determine the sequence of the complete *Drosophila* dTAP gene, the entire dTAP EST clone was sequenced. This clone was found to contain a 2kb insert which did not appear to represent a full-length cDNA, as no Methionine residues were identified near the start of the ORF and the protein encoded was much shorter than human TAP or yeast Mex67p. To obtain a full-length cDNA, a *Drosophila* embryo cDNA library was screened by plaque hybridisation with the dTAP EST probe (Vitaly Zimyanin). 4 independent cDNA clones were obtained, with a range of insert sizes from 0.7 to 2.5 kb. All clones were sequenced, and found to contain parts of an identical cDNA sequence, which encoded a protein rather shorter than human TAP or yeast Mex67p.

In order to determine the size of full-length dTAP cDNA, Northern hybridisation was used to detect the dTAP transcript in RNA isolated from wild type flies. 2 bands were consistently detected in both total RNA and poly(A)$^+$ RNA, but one band was much

Figure 7-7

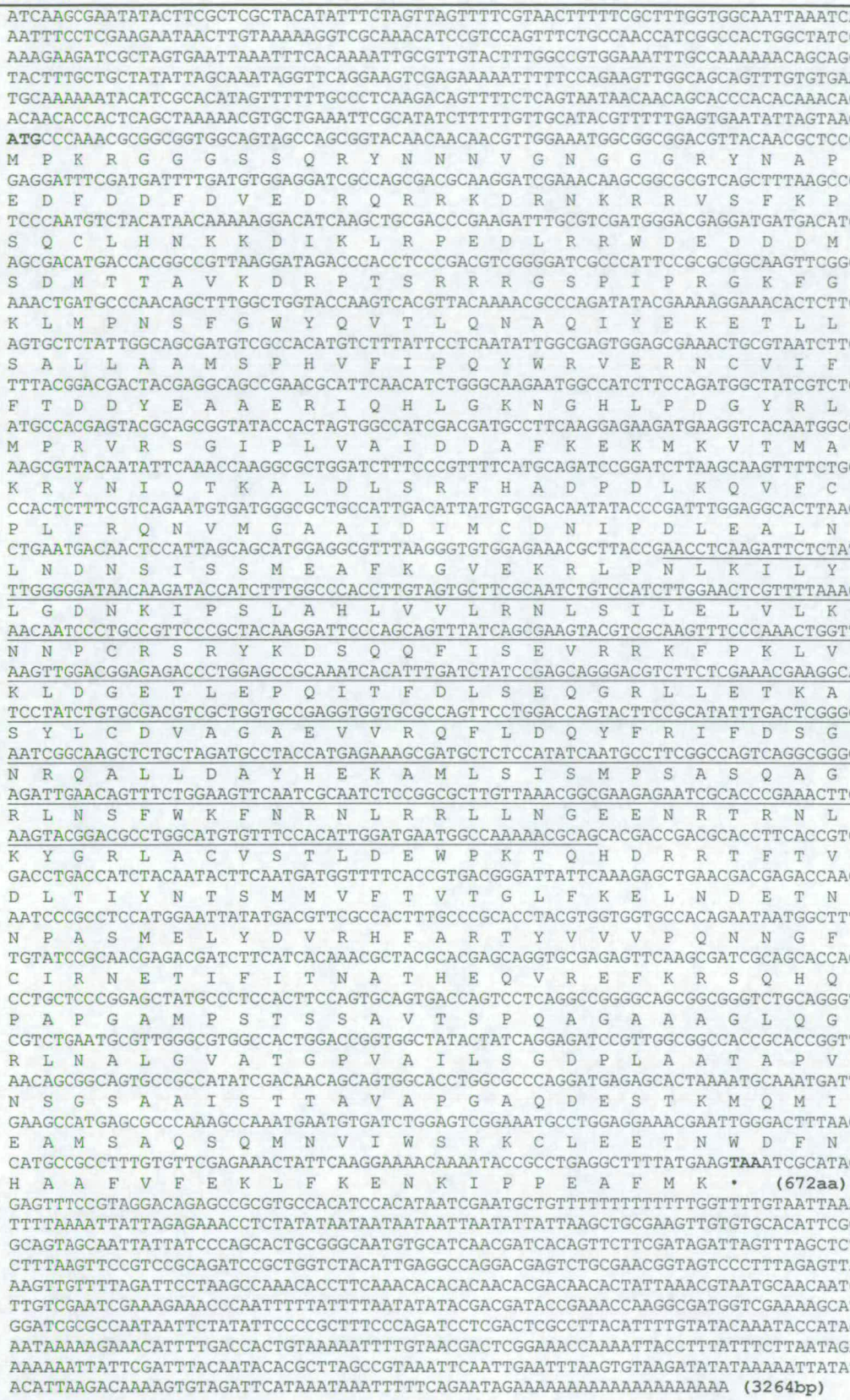

Figure 7-7. Complete sequence of dTAP showing nucleic acid sequence of cDNA and deduced amino acid sequence. The Genbank accession number for this data is AJ251947. The dTAP EST LD11064 corresponds to nucleotides 1309-1849, indicated by underlining.

stronger than the other (Figure 7-6). The fainter band migrated between 6-7kb and was not characterised further. The size of the band that hybridised most strongly to the EST probe was estimated to be 3.2kb in size. Approximately 900bp of sequence from the 5' end of the gene was therefore missing from the cDNA and EST clones. Two different approaches were taken to obtain the missing sequence. Firstly, 5' RACE was used in an attempt to amplify the 5' end of the dTAP gene from both total and poly(A)$^+$ *Drosophila* RNA. However, no specific bands were produced (data not shown). Since the missing sequence must be located in the genomic DNA upstream of the dTAP sequences already identified, 5kb of the genomic DNA upstream was sequenced directly from the genomic cosmid clone 36A5. However, no exons encoding any TAP-like sequence were identified in this genomic DNA, suggesting that there is a large intron in this region of the dTAP gene.

A full-length cDNA clone for the *Drosophila* dTAP gene was later isolated during independent work to identify the *magellan* gene (Korey and van Vactor, unpublished results). These researchers performed elaborate mapping experiments to identify expressed genes in the 9F area, and isolated a number of cDNA clones including a 3.2kb dTAP cDNA. At this time, these workers were not aware of our results, and therefore did not suspect that this clone might correspond to the wild type *magellan* gene. Later, our two labs exchanged fly lines and collaborated to show that *mgln* fails to complement all lethal alleles of *sbr*, including *l(1)ts148*, and therefore represents a novel *sbr* allele. Analysis of the dTAP cDNA clone isolated in the van Vactor lab by Christopher Korey indicated that the 3.2kb insert consisted of 2.5kb of sequence identical to the dTAP cDNA sequence already identified, but with an additional 830bp at the 5' end (Figure 7-7). Since this cDNA sequence was the same length as the dTAP transcript estimated by Northern analysis, and encoded a protein of 672 amino acids which could be completely

Figure 7-8

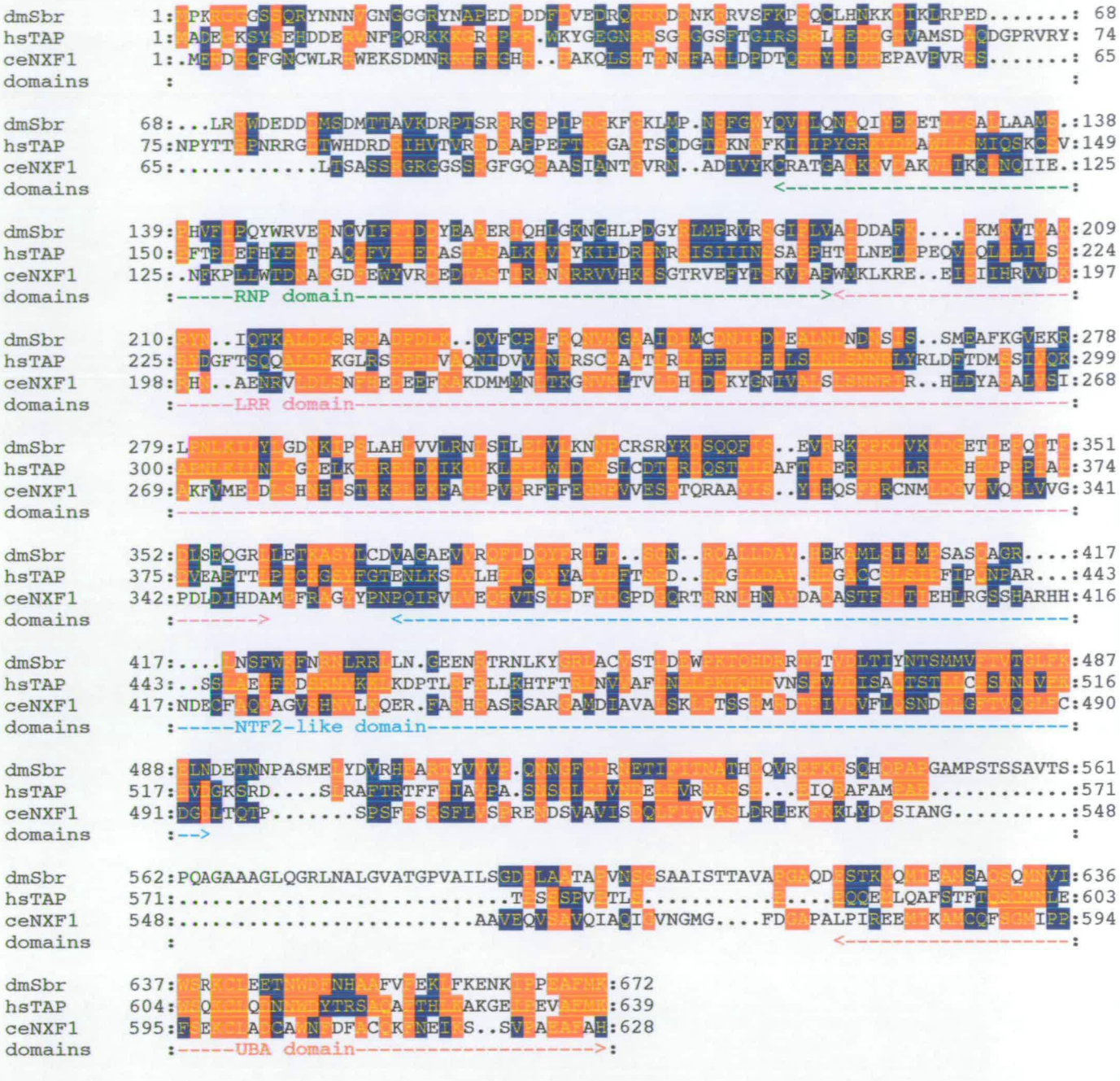

Figure 7-8 Multiple alignment of human and worm TAP/NXF1 proteins with *Drosophila* Sbr/dTAP. Spec initials and protein names are indicated in the first column, followed by the number of the first aligned residues each sequence. Identical residues in over 66% of sequences are indicated in red, while similar residues a highlighted in blue. The domains assigned to human TAP protein are indicated on the lower line in the follow colours:- **RNP domain (RNA binding)** **LRR domain** **NTF2-like domain (p15 binding)** **UBA domain (NUP bindin**

aligned to the entire human and worm TAP/NXF1 proteins and yeast Mex67p (Figure 7-8), it was assumed that this represented a full-length dTAP cDNA clone. Overall, dTAP has 32% identical and 50% similar residues to human TAP/NXF1, and is 23% identical/42% similar to yeast Mex67p. Of the four NXF proteins which have now been identified in *Drosophila*, dTAP is the most similar in sequence to human TAP/NXF1 (Figure 7-9) and (Herold et al., 2000).

The release of the complete *Drosophila* genome in March 2000 (Adams et al., 2000) allowed the genomic structure of the gene to be defined. Comparison of the dTAP cDNA sequence with this region of the *Drosophila* genome sequence indicates that the gene has a complex structure, consisting of 10 exons spanning 14.3kb of genomic DNA (Figure 7-10). The largest intron is 8.9kb in length. Several other ORF's and one EST sequence are located within introns in the dTAP gene, on the opposite strand to dTAP (data not shown). The *Drosophila* genome sequence also confirmed the mapping of the dTAP gene to 9F5.

Taken together, these results demonstrate that the *Drosophila* homologue of human TAP and yeast *MEX67*is encoded by a gene which maps to 9F5. This gene is therefore an excellent candidate for the gene encoded by *sbr/l(1)ts148,* which was previously mapped to 9F5-10.

l(1)ts148 encodes the *Drosophila* homologue of the TAP/*Mex67* gene.

Human TAP is thought to be involved in mRNA export (Gruter et al., 1998) and disruption of TAP homologues in *C. elegans* (Ce-NXF1) and yeast (Mex67p) cause nuclear accumulation of poly(A)$^+$ RNA (Hurt et al., 2000; Segref et al., 1997; Tan et al.,

Figure 7-9

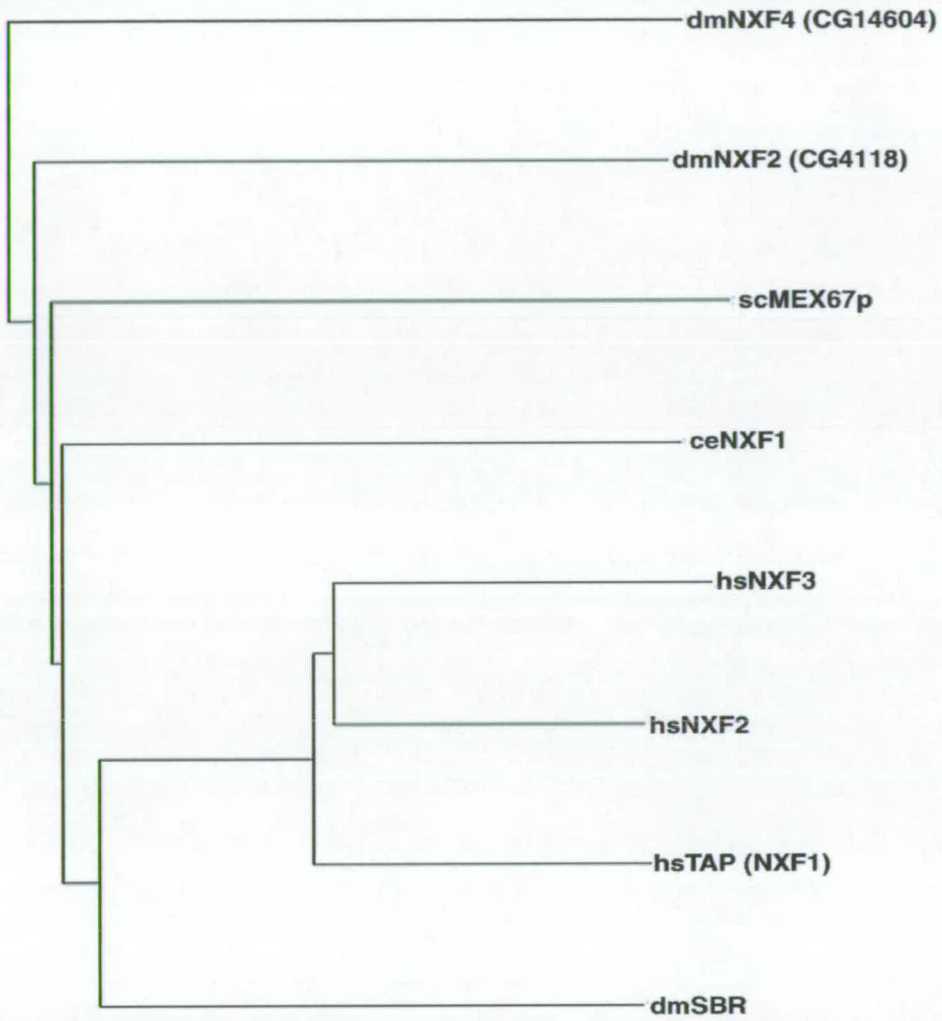

Figure 7-9 Phylogenetic Tree of NXF proteins. The relationship of *Drosophila* Sbr to other NXF proteins from *Drosophila* (dm), human (hs), *C. elegans* (ce) and *S. cerevisiae* (sc). Compared to other NXF proteins in *Drosophila*, Sbr is the closest homologue to human TAP/NXF1.

Figure 7-10

Figure 7-10 Intron-exon Structure of the *Drosophila sbr* gene. Exons are represented by solid black boxes, whilst introns, drawn to scale, are indicated by lines. Green and red triangles mark the positions of initiation and termination codons, respectively. The entire genomic region spans 14.3kb

2000). In order to test whether the mRNA export phenotypes of *l(1)ts148* and sbr^{10} are caused by mutations in the *Drosophila* dTAP gene, the entire coding sequence of the dTAP gene from *l(1)ts148* and sbr^{10} flies was amplified by PCR, then sequenced and compared to that obtained from yw^{67} and wild-type flies.

Both *l(1)ts148* and sbr^{10} were found to have mutations in the dTAP open reading frame which cause non-conservative amino acid substitutions in the dTAP protein. *l(1)ts148* has a T-A transition at position 461 in the open reading frame, which causes a change from valine to glutamic acid at residue 154 of the dTAP protein (Figure 7-11). This change was not present at the corresponding position in yw^{67}, the original strain which was mutagenised in the screen to produce *l(1)ts148*.

In sbr^{10}, a C at position 416 of the ORF is mutated to a to T, causing a change from proline to leucine at residue 139 (just 15 amino acids upstream of the mutation in *l(1)ts148*). sbr^{10} also has two conservative changes near the C-terminus, threonine to serine at position 493 and methionine to isoleucine at residue 499 (Figure 7-11). These additional mutations are likely to be polymorphisms, but this could not be confirmed because the original stock which was mutagenised to produce sbr^{10} is no longer available. These results are not unexpected as the sbr^{10} mutation was originally isolated in 1975 (Arking, 1975) and additional mutations would be likely to accumulate in the null allele of a balanced stock during this time.

In addition to the results described above, the *mgln* allele of *sbr* has also been found to have a mutation in the TAP ORF. This mutation is caused by an insertion near the start of exon 8 that introduces a premature stop codon, truncating the protein by more than 250 amino acids (Korey and van Vactor, unpublished data).

Figure 7-11

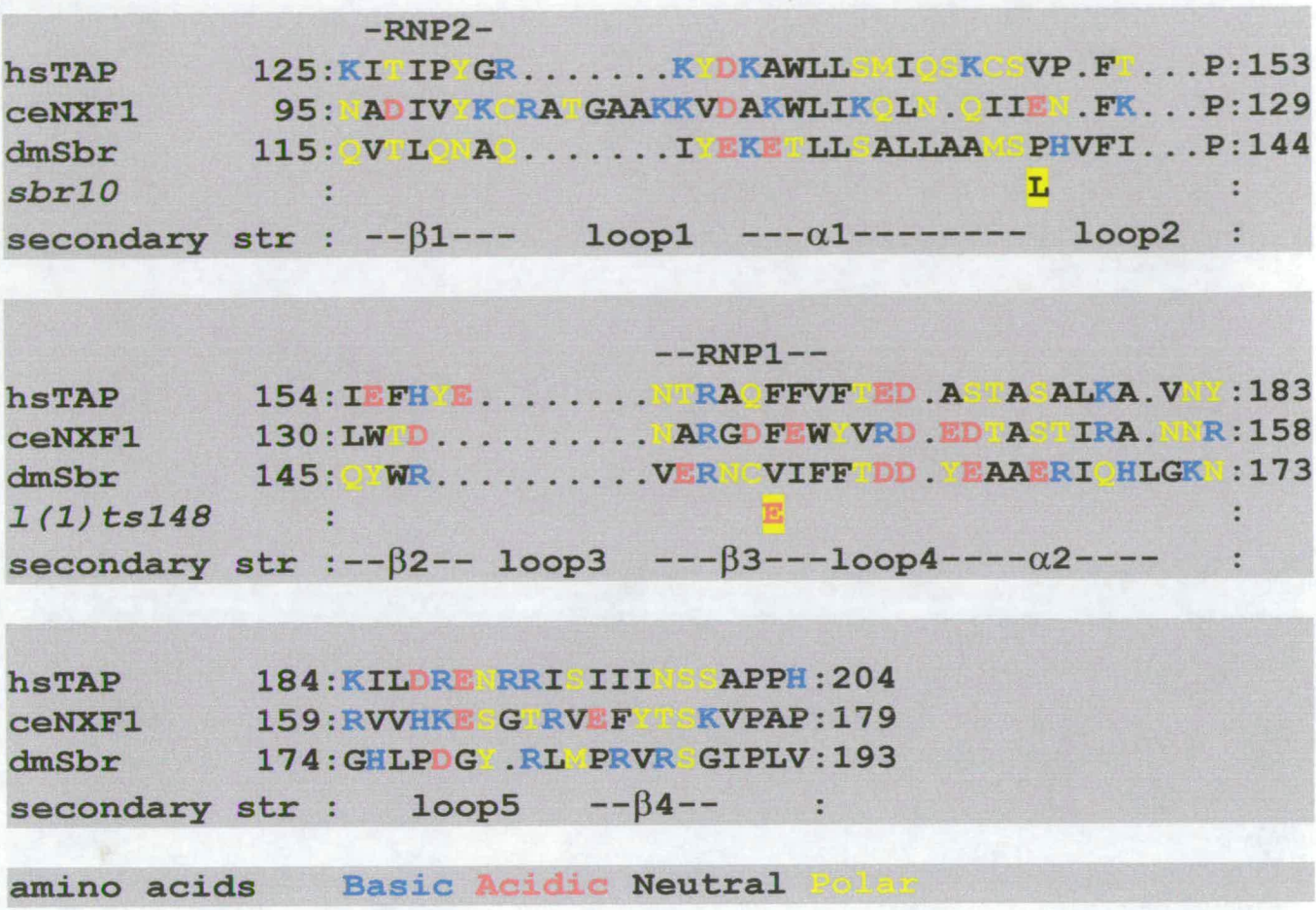

Figure 7-11 Mutations in *l(1)ts148* and *sbr^{10}* map to the RNA binding domain. A structure-based alignment of the RNP motif (RNA binding domain) of hsTAP, ceNXF1 and dmSbr, based on Liker *et al* (2000). The known secondary structural elements of hsTAP are shown on the lower line. Octameric RNP1 and hexameric RNP2 consensus domains are outlined in dark grey. Mutant residues of *sbr^{10}* and *l(1)ts148* are indicated by a yellow background. Basic amino acids are coloured blue, acidic residues are red, neutral residues are black and polar amino acids are coloured yellow.

The amino acid changes in the dTAP proteins encoded by both *l(1)ts148* and sbr^{10} are located in the region of the protein identified as the RNA-binding domain in human TAP (Bachi et al., 2000; Braun et al., 1999; Kang and Cullen, 1999). Strikingly, both mutations fall within a cryptic RNP domain recently identified in human TAP which can bind to RNA *in vitro* (Liker et al., 2000). The structure of this RNP domain (also sometimes referred to as an RRM or RBD domain) has been solved for human TAP by X-ray crystallography, (Liker et al., 2000), and the domain is also found in *Drosophila* Sbr protein (Herold et al., 2000). In *l(1)ts148*, the mutation V154E falls within the 8 residues which form the RNP1 motif essential for structural stability and RNA binding (Figure 7-11). The mutation P139L in sbr^{10} is in loop2 of the RNP structural domain. Both mutations are non-conservative changes, and are therefore likely to disrupt the structure of the RNP domain and could be predicted to abolish or reduce the RNA binding properties of the protein.

In summary, three independent alleles of *sbr* have been shown to have mutations within the dTAP ORF. These results strongly suggest that the mRNA export phenotype of *l(1)ts148* and sbr^{10} are caused by mutations in the *Drosophila* gene encoding the homologue of the vertebrate TAP/NXF1 and yeast *MEX67* gene.

CONCLUSIONS

l(1)ts148 was mapped to 9F5-10 by deficiency chromosome and recombination analysis. A P-element induced allele of *l(1)ts148* could not be generated, but five independent lethal alleles of the *sbr* gene failed to complement *l(1)ts148*, suggesting that *l(1)ts148* is a novel allele of *small bristles*. The finding that *l(1)ts148/sbr*^{10} and *sbr*^{10}*/sbr*^{10} embryos have a similar mRNA export defect is further strong evidence that *l(1)ts148* is a novel allele of *sbr*. The wild type *sbr* gene is likely to have a function in mRNA export in all tissues, since *l(1)ts148* disrupts the nuclear export of all transcripts tested at several different developmental stages, and the gene is essential for the survival of embryos, larvae, pupae and adult flies.

The *Drosophila* homologue of the vertebrate TAP/NXF1 and yeast *MEX67* genes was identified and mapped to 9F2-5. *l(1)ts148* and *sbr*^{10} were both found to have strong non-conservative mutations in the RNA binding domain of the *Drosophila* dTAP gene, demonstrating that the nuclear mRNA export defects observed in these lines is highly likely to be due to mutations in *Drosophila* dTAP. It can therefore be concluded that *l(1)ts148* is a mutation in the *sbr* gene which encodes the *Drosophila* homologue of vertebrate TAP/NXF1 and yeast Mex67p. Since *l(1)ts148* disrupts the nuclear export of many transcripts at different stages of development, these results suggest that *Drosophila* NXF2-4 do not have redundant functions in the nuclear export of most transcripts. Furthermore, these results show that disrupting TAP/NXF1 function in *Drosophila* leads to a specific defect in mRNA export, with no detectable effects on pre-mRNA splicing, nuclear protein import or nuclear ultrastructure.

8

APICAL mRNA LOCALISATION OCCURS BY ACTIVE TRANSPORT ALONG MICROTUBULES

INTRODUCTION

The results described in Chapter 4 demonstrate that vectorial export of pair-rule mRNA does not occur, but rather that these transcripts are exported from the nucleus in all directions. The apical localisation of these transcripts must therefore be achieved by a mechanism that operates in the cytoplasm. Three different cytoplasmic models were previously described for the mechanism of apical mRNA localisation (Davis et al., 1993; Francis-Lang et al., 1996). Transcripts could be degraded throughout the cytoplasm but specifically protected from degradation in the apical cytoplasm. Alternatively, transcripts could become selectively anchored in the apical cytoplasm after random diffusion through the cytoplasm. Finally, mRNA could be actively transported to the apical cytoplasm along microtubules or microfilaments. These models are not mutually exclusive and could all contribute to localisation. However, selective degradation is not thought to have a role in pair-rule mRNA localisation because *ftz* transcripts are short-lived in the blastoderm embryo, and stabilisation of mRNA by injection of cycloheximide leads to hyperaccumulation of *ftz* mRNA in the apical cytoplasm rather than unlocalised *ftz* mRNA (Edgar et al., 1986).

The requirement for the cytoskeleton in the apical localisation of pair-rule transcripts is currently uncertain. Previous experiments suggested that the cytoskeleton is not involved in the localisation of pair-rule mRNA as *h*, *eve* and *ftz* transcripts were found to be correctly localised on the apical side of internalised nuclei lacking detectable microtubules or microfilaments (Francis-Lang et al., 1996). However, other work has shown that microtubules are required for *ftz* mRNA localisation (Edgar et al., 1987; Lall et al., 1999). It therefore remains possible that pair-rule transcripts could be localised either by active transport along microtubules or microfilaments, by random diffusion followed by anchoring in the apical cytoplasm, or by some other mechanism yet to be identified.

In order to identify the mechanism of apical mRNA localisation in the *Drosophila* embryo, fluorescently labelled RNA was microinjected into blastoderm embryos and the movement of RNA localisation intermediates was studied by time-lapse fluorescence microscopy. These techniques led to the development of an *in vivo* assay to identify components required for localisation by pre-injecting embryos with drugs, toxins and antibodies, and by testing mutant embryos for correct localisation of injected RNA (Wilkie and Davis, 2001).

Figure 8-1

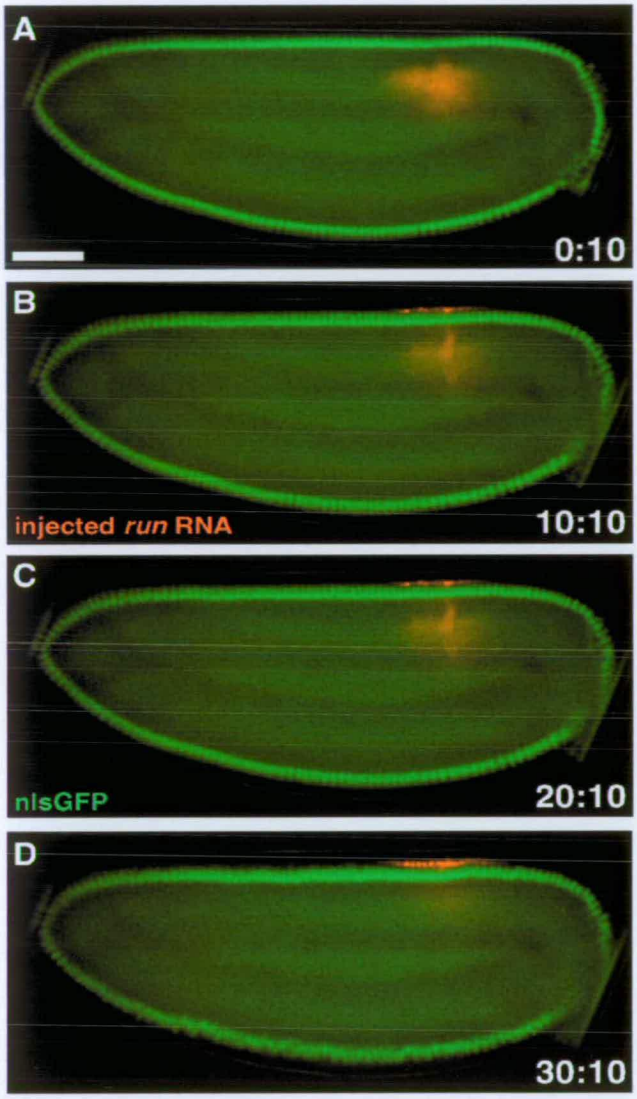

Figure 8-1 Injected Apically Targeted RNA Localises Rapidly to the Apical Cytoplasm in Living Blastoderm embryos. (**A–D**) Four snapshots from a time lapse movie of a living blastoderm embryo expressing nlsGFP (green nuclei) and injected with protein-free *run* RNA labelled with AlexaFluor546 (red). Time elapsed after injection is shown in the bottom right corner of each image. Within 20 min, the majority of injected *run* RNA localises correctly to the apical cytoplasm. Bar = 50μm.

RESULTS

Pair-rule and *wg* RNA is actively transported to the apical cytoplasm after microinjection into living *Drosophila* embryos

Previous methods used for the synthesis of fluorescently labelled RNA have relied on incorporation of aminoallyl-UTP into RNA, followed by chemical coupling of succinimidyl esters of fluorescein or rhodamine dye to the reactive aminoallyl groups (Glotzer et al., 1997; Lall et al., 1999). This protocol is time consuming and inefficient. To overcome these difficulties, an improved labelling method was devised to directly incorporate bright AlexaFluor UTP analogues into capped, polyadenylated RNA by *in vitro* transcription (Wilkie and Davis, 2001).

It was found that protein-free *ftz*, *run* and *wg* RNA synthesised by this improved labelling method rapidly becomes localised to the apical cytoplasm after microinjection into the basal cytoplasm or yolk of living blastoderm embryos (Figure 8-1 and Movie 1). In most time-lapse movies RNA first became visible in the apical cytoplasm, 20 to 80μm above the site of injection, within 30-120 seconds. Localisation appeared to continue for 10-30 minutes until very little RNA remained at the site of injection. The RNA did not appear to diffuse through the embryo and always became localised to the apical cytoplasm immediately above the injection site, suggesting that the injected RNA was localised by active transport rather than a diffusion and anchoring mechanism. To test the mechanism of localisation further, the injected RNA was imaged at higher resolution. Strikingly, it was observed that within 30 seconds after injection, the RNA assembled into bright particles which moved along straight paths to the apical cytoplasm (Figure 8-2 and Movie 2). The average speeds observed for the movement of *ftz*, *run* and

Figure 8-2

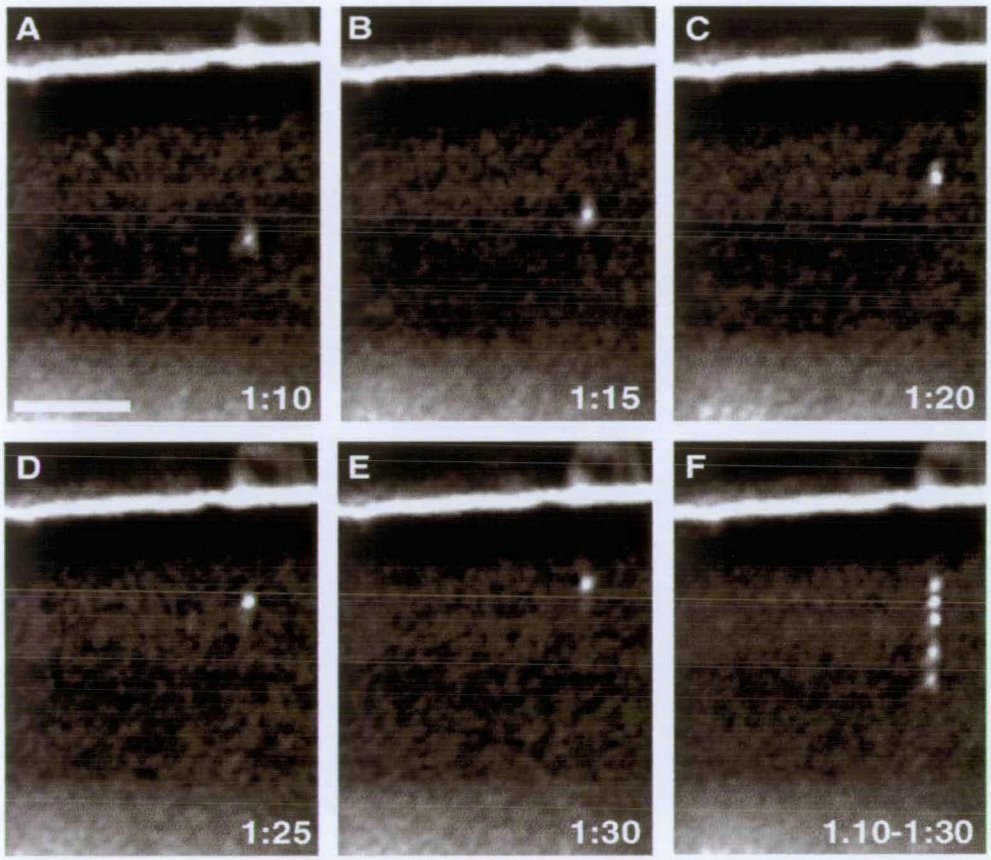

Figure 8-2 Injected RNA assembles into particles that localise to the apical cytoplasm along distinct tracks. (**A-E**) Five snapshots from a time lapse movie showing the movement of a typical particle of injected *run* RNA to the apical cytoplasm. The site of injection is below the bottom of the image. (**F**) A composite image of (A)–(E) showing the RNA particle moving directly apically at an average speed of approximately 0.5 μm/sec. The time in minutes and seconds after injection is shown on the bottom right. Bar = 10μm.

wg RNA particles towards the apical cytoplasm were 0.46, 0.49 and 0.41 μm/s respectively (see Table 9b). The maximum speed observed for any particle was 2.13 μm/s.

These results demonstrate that apical localisation of injected *run*, *ftz* and *wg* RNA in the blastoderm embryo occurs by active transport from the basal cytoplasm to the apical cytoplasm along direct tracks, rather than by diffusion and anchoring of mRNA. The speeds of the RNA particles and the directional nature of their movement are consistent with motor-driven transport along cytoskeletal filaments.

Apically targeted RNA is localised in particles similar to endogenous localisation intermediates

It was important to determine whether the bright particles of RNA which assemble from the highly concentrated injected RNA and move to the apical cytoplasm are related to endogenous mRNA localisation intermediates. To test this, embryos were fixed 2-10 minutes after injection with fluorescent *run* RNA, enabling high resolution 3D imaging techniques to be used which are more challenging to employ in living embryos. The vast majority of injected RNA in fixed material was present in particles. In addition to some bright particles of RNA, many small particles of RNA were visualised between the site of injection and the apical cytoplasm, which are likely to represent localisation intermediates (Figure 8-3). Living embryos were later imaged at high magnification after injection of fluorescent *wg* RNA. In these time-lapse movies, numerous small particles of RNA were visualised moving towards the apical cytoplasm in addition to a few bright particles, confirming that the majority of injected RNA is transported in particles of varying size and RNA content (Ilan Davis, data not shown).

Figure 8-3

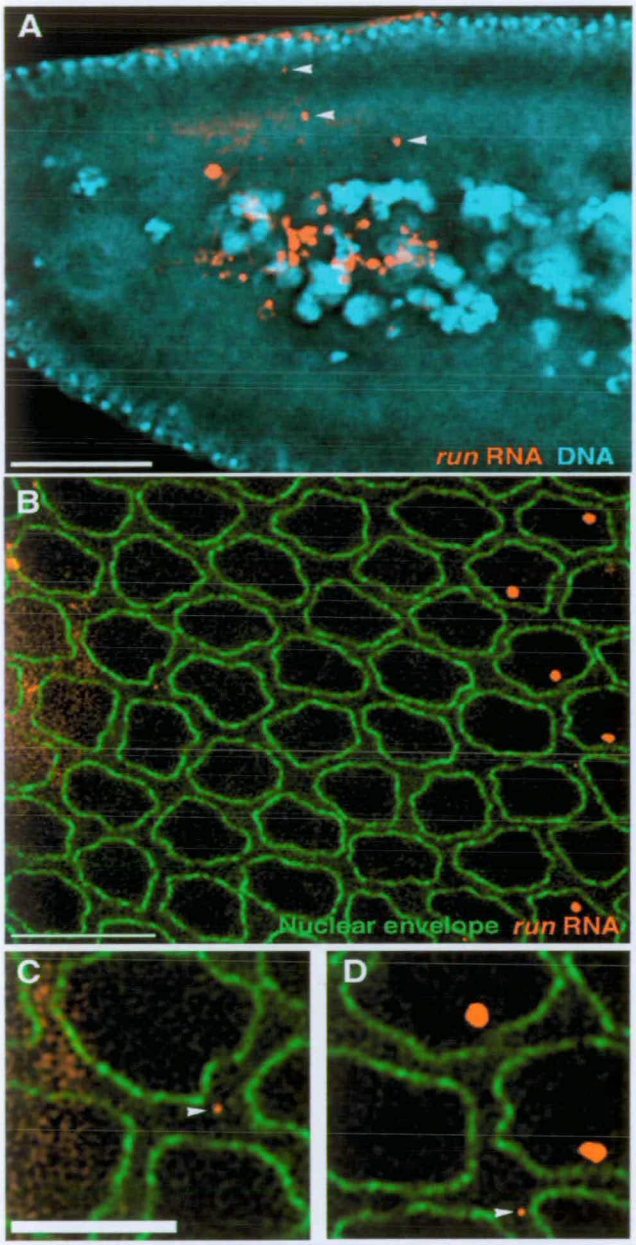

Figure 8-3 Injected RNA particles are similar to endogenous intermediates. (**A**) An embryo fixed 5 minutes after injection with AlexaFluor546-labelled *run* RNA (red). Nuclei were stained with DAPI, shown in cyan. Particles of *run* RNA in transit to the apical cytoplasm are indicated with arrowheads. Bar = 20μm (**B**) A section through nuclei at the surface of an embryo injected with *run* RNA labelled with AlexaFluor488 (not shown), then fixed 5 minutes later. The site of injection was just off the left edge of the image, at a deeper focal plane. All the *run* RNA in the embryo was detected by *in situ* hybridisation with Cy-3 TSA detection (shown in red). *run* RNA on the right is endogenous expression stripe 1. The nuclear envelope was detected with an anti-lamin antibody, visualised with Cy-5 (shown in green). Bar = 10μm (**C**) High powered view of an injected RNA localisation intermediate (arrowhead). Bar = 5μm. (**D**) High powered view of an endogenous RNA localisation intermediate (arrowhead).

To compare the particles of injected RNA with endogenous transcripts, embryos were fixed 1-5 minutes after injection with *run* RNA labelled with AlexaFluor488. All the *run* RNA in these embryos was then detected by *in situ* hybridisation with a *run* antisense probe, and visualised with fluorescent Cyanine 3 tyramides. The injected RNA can be distinguished from the endogenous *run* transcripts as the injected RNA is labelled in both green (AlexaFluor488) and red (Cyanine 3), while the stripes of *run* mRNA transcribed in the embryo are labelled exclusively in red (Figure 8-3). Although some particles of injected RNA are very bright, particles of RNA can be visualised near the site of injection which have similar intensities to export and localisation intermediates in the expression stripes, indicating that they contain similar amounts of RNA (Figure 8-3 and Table 8a). This result suggests that some particles of injected RNA are equivalent to endogenous mRNA localisation intermediates.

Apical localisation intermediates can contain several different apically targeted RNAs, but not basal or unlocalised RNA.

To determine whether different apical transcripts can assemble in the same particles or localise in different particles, apically targeted RNA was synthesised with different fluorescent labels, and embryos were co-injected with mixtures of *ftz* with *run* and *wg* with *run*. Surprisingly, it was found that although many particles consist of predominately one or other transcript, different transcripts can often assemble and be localised together within the same particles. Some particles in transit to the apical cytoplasm were observed to contain both injected *ftz* and *run* RNA while other localisation intermediates contained both *wg* and *run* RNA (Figure 8-4 and Movie 3). This suggests that different pair-rule and *wg* transcripts localise in functionally equivalent particles. Control coinjections carried out with *run* RNA labelled with

Figure 8-4

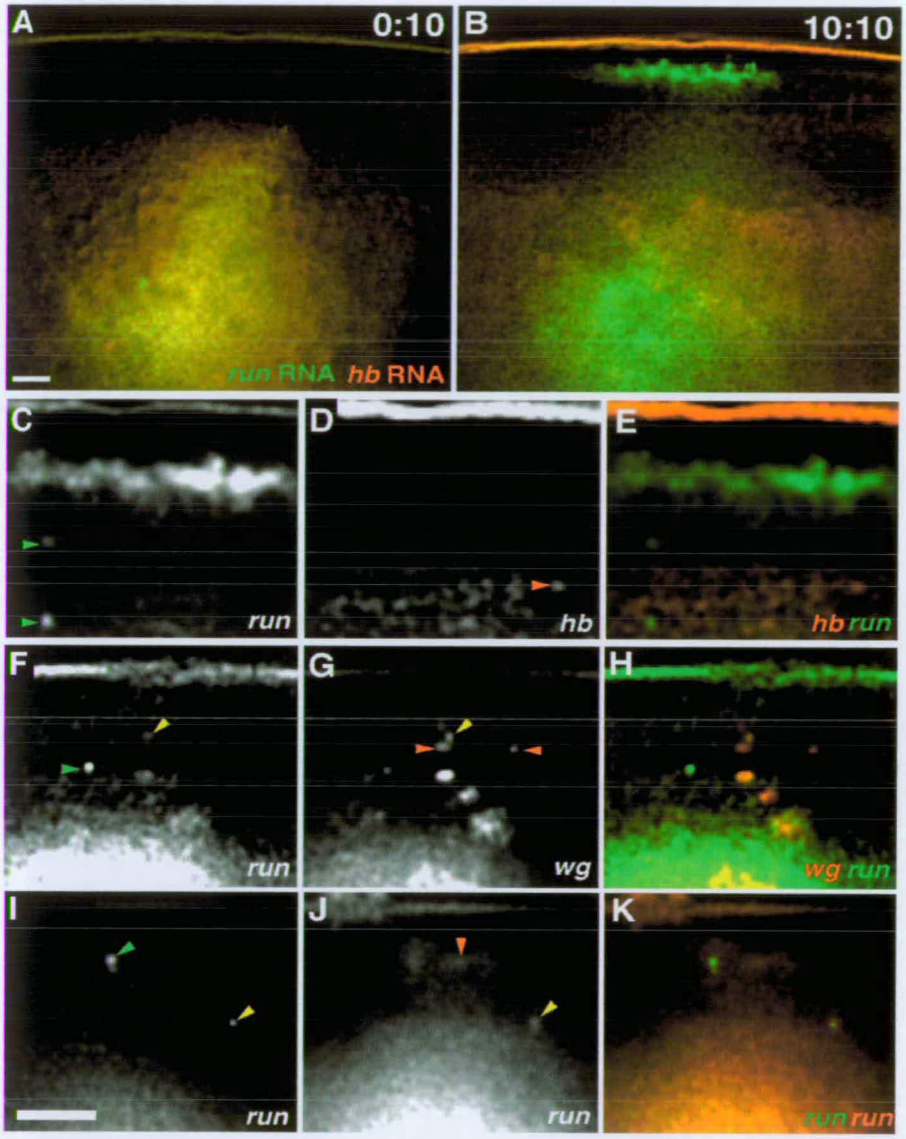

Figure 8-4 Apical localisation intermediates can contain more than one apically-targeted transcript, but lack basal or unlocalised RNA. (**A**) Image of an embryo 10 seconds after coinjection of AlexaFluor488-labelled *run* RNA (green) and AlexaFluor546-labelled *hb* RNA (red). (**B**) After 10 minutes, the *run* RNA has localised to the apical cytoplasm but the *hb* has diffused from the site of injection. (**C-E**) Two time points (10 seconds apart and superimposed into one) from a time lapse movie of an embryo coinjected with *run* and *hb* RNA, showing that *run* particles move apically and do not contain *hb* RNA, whereas *hb* particles do not move and do not contain *run* RNA. (**F-H**) Single time point from an embryo coinjected with *run* and *wg* RNA, showing particles can consist either of *run*, *wg* or a mixture of both types of RNA. (**I-K**) Single time point from a control embryo injected with a mixture of green and red *run* RNA, showing that differently labelled RNA can assemble in the same particles, but often does not. Scale Bars = 10μm. The colour of arrowheads pointing to particles indicates which RNA they contain.

AlexaFluor488 and AlexaFluor546 showed a similar mixture of green, red and yellow particles (Figure 8-4). These results imply that the localisation particles contain a relatively small amount of RNA, otherwise more yellow particles would be observed in transit to the apical cytoplasm.

It was also important to determine whether the localisation of injected RNA is specific to apically targeted transcripts, or whether any type of RNA injected into embryos can be localised to the apical cytoplasm. To test this, labelled *hb* and *stg* RNA was synthesised and microinjected into blastoderm embryos. It was found that neither *hb* nor *stg* RNA became localised after injection into blastoderm embryos. Both transcripts were observed to diffuse away from the site of injection in all directions (Figure 8-4 and Movies 4,5). It was rather surprising that the *stg* RNA did not become localised, since endogenous *stg* mRNA is mainly localised to the basal cytoplasm. To investigate whether *stg* RNA can localise basally from other sites of injection, attempts were made to microinject *stg* RNA directly into the apical cytoplasm. However, this was technically difficult to achieve without damaging the plasma membrane or peripheral nuclei around the site of injection, causing RNA to leak into other regions of the embryo.

To compare the movement of apically targeted RNA and unlocalised RNA, *run* and *hb* RNA were labelled in different fluorescent channels and coinjected into embryos. Whilst the green *run* RNA (labelled with AlexaFluor488) rapidly formed particles which became localised to the apical cytoplasm above the site of injection, the red (AlexaFluor546 labelled) *hb* RNA formed some particles which did not show directed movement. Furthermore, particles of *run* RNA in transit to the apical cytoplasm did not contain detectable amounts of *hb* RNA (Figure 8-4 and Movie 6).

Table 8a. Fluorescence intensity of injected and endogenous RNA particles

Type of RNA	Source of signal	Average intensity	N
Endogenous	Nascent transcripts	2,294,715 ± 356,784	8
Endogenous	Nuclear export intermediates	56,450 ± 8,210	8
Endogenous	Cytoplasmic intermediates	61,795 ± 12,919	14
Injected	Cytoplasmic -bright	256,326 ± 57,484	14
Injected	Cytoplasmic -faint	87,192 ± 15,479	12

A comparison of the fluorescence intensity of endogenous and injected RNA localisation intermediates. Injected and endogenous *run* RNA were detected simultaneously within the same embryo. Injected *run* RNA was labelled with AlexaFluor488. In situ hybridisation was performed using *run* antisense probes detected with Cy3-TSA. Total integrated fluorescence intensity is measured in arbitrary units ± standard error. N = number of foci measured.

Table 8b. Injection of Colcemid inhibits apical RNA Localisation

Reagent	RNA	% Localisation	N
Control injection buffer	*wg*	88%	17
	run	94%	17
	ftz	92%	12
Cytochalasin B	*run*	91%	23
	wg	80%	10
Colcemid	*wg*	10%	29
	run	8%	52
	ftz	13%	30
Colcemid followed by UV light	*run*	100%	6

The proportion of embryos that correctly localise injected RNAs to the apical cytoplasm are shown for embryos pre-injected with cytoskeletal inhibitors. Drugs or control buffer were injected approximately 10 minutes before apically-targeted RNA. N= number of embryos tested.

Taken together, these results show that apically-targeted RNA is specifically localised to the apical cytoplasm upon microinjection into blastoderm embryos. In contrast, RNA which is not destined for the apical cytoplasm does not become localised, but instead diffuses throughout the embryo. Different apically-targeted transcripts can be localised within the same particles, suggesting that *run*, *ftz* and *wg* transcripts use similar machinery for localisation in the blastoderm embryo.

Microtubules are required for localisation of RNA to the apical cytoplasm

The movement of apically targeted particles occurs along distinct, straight paths from the site of injection to the apical cytoplasm (Figure 8-2 and Movie 2) suggesting that the particles are transported along cytoskeletal filaments. To directly test whether microtubules or actin microfilaments are required for localisation, embryos were pre-injected with cytoskeletal inhibitors 10 minutes before injection of fluorescent RNA.

It was found that the actin filament inhibitor cytochalasin B does not disrupt the localisation of injected *run* and *wg* RNA to the apical cytoplasm, compared to control embryos preinjected with buffer (Table 8b, and Figure 8-5). Identical results were obtained with cytochalasin D (data not shown). Cytochalasin B was injected at an identical concentration to a previous study which showed that this drug disrupts the organisation of actin filaments, inhibiting membrane invagination and causing many nuclei to fall away from the cortical cytoplasm into the yolk (Edgar et al., 1987). Similar effects were observed on membrane furrow progression and position of nuclei in the cortical cytoplasm in this work (data not shown). This suggests that actin function is indeed disrupted by cytochalasin treatment, but that this does not inhibit localisation of

Figure 8-5

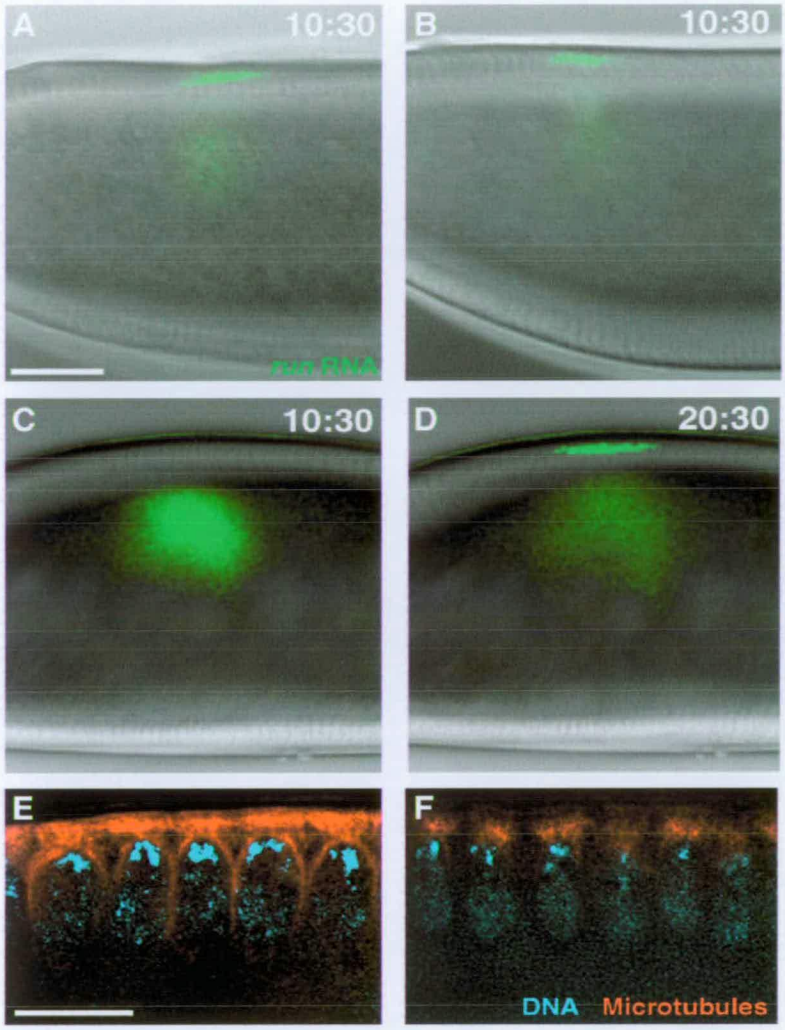

Figure 8-5 Apical localisation of Injected RNA requires Microtubules, but not Microfilaments. (**A**) Dual DIC/fluorescence image of a control living embryo pre-injected with buffer, then injected with AlexaFluor488-labelled *run* RNA (green) 10 minutes later. After a further 10 minutes, the majority of the injected *run* RNA has become localised to the apical cytoplasm. Bar = 50μm (**B**) Pre-injection of cytochalasin B does not inhibit localisation of injected *run* RNA. (**C**) Colcemid pre-injection disrupts apical localisation of *run* RNA. (**D**) Localisation of injected RNA occurs normally following U.V. irradiation which inactivates colcemid. (**E**) Control embryo showing normal organisation of microtubules (red) in an apical basket with long microubules extending between nuclei into the yolk. Nuclei were visualised by DAPI staining (cyan). Bar = 10μm. (**F**) A similar embryo that was injected with colcemid then fixed after 10 minutes, showing fewer apical microtubules and no microtubules between the nuclei or in the basal cytoplasm. Time after injection of RNA is indicated in upper right corner.

apically targeted mRNA, as previously reported for *ftz* RNA (Edgar et al., 1987; Lall et al., 1999).

To determine if apical localisation requires microtubules, embryos were pre-injected with colcemid, a potent inhibitor of microtubule growth. It was found that colcemid strongly disrupts the localisation of injected *run*, *ftz* and *wg* RNA (Figure 8-5). In control embryos pre-injected with buffer, an average of 91% of embryos which were tested correctly localised injected RNA to the apical cytoplasm. In contrast, only 10% of embryos pre-injected with colcemid correctly localised injected *run*, *ftz* and *wg* RNA to the apical cytoplasm (Table 8b). In most embryos pre-injected with colcemid, the injected RNA remained at the site of injection and later diffused to all parts of the embryo (Movie 7). Furthermore, when the colcemid was inactivated by exposure to U.V. light allowing microtubules to repolymerise, it was found that *run* RNA which had remained at the site of injection due to colcemid treatment began localisation within 2 minutes, and became fully localised at normal rates in 100% (N=6) of U.V. irradiated embryos (Figure 8-5 and Movie 7).

To determine the effects of colcemid on the microtubule cytoskeleton, embryos were fixed 5-10 minutes after injection of colcemid, and microtubules were visualised by indirect immunofluorescence. It was found that the dose of colcemid used inhibits the growth of microtubules which extend between nuclei to reach the basal cytoplasm and yolk whilst having less effect on the apical caps of microtubules in most embryos (Figure 8-5). Taken together, these results suggest that microtubules, but not microfilaments, are required for the apical localisation of pair-rule and *wg* mRNA.

CONCLUSIONS

Capped, polyadenylated RNA was synthesised using a modified protocol to directly incorporate fluorescent UTP analogues into RNA by *in vitro* transcription. Protein-free RNA synthesised by this method rapidly formed particles after injection which often consisted of a small number of RNA molecules, similar to endogenous localisation intermediates. Particles of *hb* and *stg* RNA, which are not targeted to the apical cytoplasm, displayed random diffusional movement. In contrast, particles of *ftz*, *run* and *wg* RNA were transported to the apical cytoplasm along direct paths, at velocities consistent with motor driven transport along the cytoskeleton. These results demonstrate that apical localisation of injected *run*, *ftz* and *wg* RNA in the blastoderm embryo occurs by active transport of RNA particles from the basal to the apical cytoplasm, rather than by diffusion and anchoring of mRNA. In addition, these results show that proteins required for localisation of the injected RNA can be efficiently recruited in the cytoplasm, and that pre-incubation of the RNA in nuclear extracts or hnRNPA1 (Squid) protein is not an absolute requirement for localisation, in contrast to previous reports (Lall et al., 1999).

Colcemid treatment was found to inhibit apical localisation, and was also shown to cause depolymerisation of microtubules reaching the basal cytoplasm and yolk. Furthermore, it was demonstrated that pre-injection of buffer does not inhibit localisation and that colcemid treatment is reversible by exposure to U.V. light, which inactivates the drug. While the drug injection experiments do not exclude the possibility that actin microfilaments might have a minor role in localisation or anchoring in the apical cytoplasm, the results strongly suggest that the transport of RNA occurs on

microtubules which are nucleated in the apical cytoplasm and extend between nuclei to reach the basal cytoplasm and yolk.

9

CYTOPLASMIC DYNEIN IS REQUIRED FOR APICAL LOCALISATION OF mRNA.

INTRODUCTION

There is increasing evidence that some transcripts are localised by transport along polarised cytoskeletal filaments by specific molecular motors. For example, the localisation of Ash1 mRNA to the bud of a dividing yeast cell depends on transport along actin filaments by Myo4p, a class V myosin motor (Jansen et al., 1996; Munchow et al., 1999; Takizawa et al., 1997) and *oskar* mRNA localisation to the posterior of the *Drosophila* oocyte requires the plus end directed microtubule motor Kinesin I (Brendza et al., 2000). Cytoplasmic dynein, a minus end directed microtubule motor, has also been suggested to have a role in transcript localisation (Nasmyth and Jansen, 1997; Schnorrer et al., 2000) but direct evidence implicating dynein in mRNA localisation has not been reported.

Microtubules in the blastoderm embryo are arranged with their minus ends in the apical cytoplasm above the nuclei, where the centrosomes are located. The microtubules which extend between nuclei are organised with their plus ends in the basal cytoplasm and yolk (Foe et al., 1993). Transcripts which move to the apical cytoplasm along these microtubules are therefore likely to be transported by a minus end directed microtubule motor.

The only minus end directed microtubule motors which have been characterised in *Drosophila* to date are cytoplasmic dynein (Hays et al., 1994; McGrail et al., 1994) and non-claret disjunction (McDonald et al., 1990; Walker et al., 1990). The *Drosophila* genome does not appear to encode additional minus end directed microtubule motors (Goldstein and Gunawardena, 2000).

Cytoplasmic dynein is a large multisubunit protein complex known to participate in a variety of cellular transport events in flies including fast axonal transport, mitosis and lipid droplet transport (Gross et al., 2000; Martin et al., 1999; Robinson et al., 1999; Sharp et al., 2000a; Sharp et al., 2000b). Dynein has been shown to transport an even wider array of cargoes in other organisms (Habermann et al., 2001; Karki and Holzbaur, 1999) and the average speed of the dynein motor, measured *in vitro* at 0.7 ± 0.1 μm/s (King and Schroer, 2000) is in the correct range to drive the transport of RNA particles. Furthermore, cytoplasmic dynein has been detected on interphase microtubules in the blastoderm embryo (Hays et al., 1994) and lipid droplets transported by dynein in *Drosophila* embryos have been measured *in vivo* at speeds ranging from 0.15 to 2.0 μm/s (average speed 0.45 μm/s) which are remarkably similar to the speeds of RNA particles (Gross et al., 2000).

Non-claret disjunctional (ncd) is a C-terminal kinesin motor which translocates to microtubule minus ends and functions in chromosome segregation during meiosis and mitosis (Endow et al., 1994; Endow and Komma, 1996; Walker et al., 1990). ncd is a poor candidate for the motor responsible for apical localisation of mRNA as it is localised to centrosomes and spindles during mitosis and meiosis rather than interphase microtubules, and levels of the protein become greatly diminished during interphase14 in blastoderm embryos (Endow et al., 1994). Furthermore the motility characteristics of

the ncd motor, measured at 0.06 - 0.16 μm/s (average 0.1 ± 0.007 μm/s) in microtubule gliding assays (Chandra et al., 1993; Endow et al., 1994) is too low to account for the transport of RNA particles observed in transit to the apical cytoplasm.

Figure 9-1

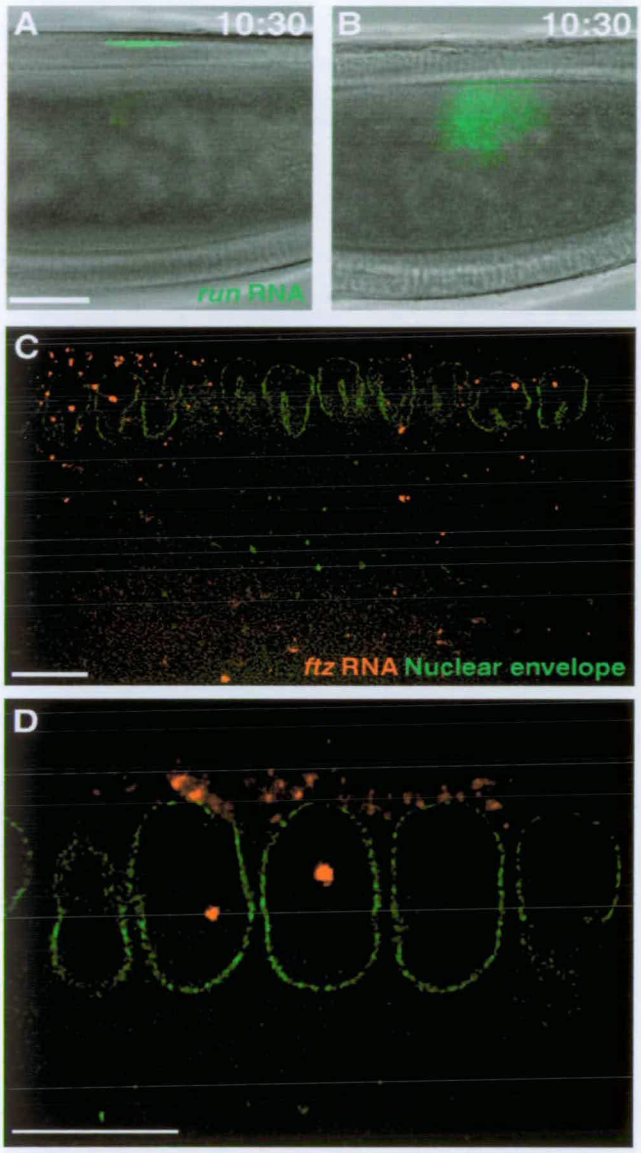

Figure 9-1 Localisation of Apically targeted RNA requires dynein (**A**) Dual DIC/fluorescence image of a living embryo pre-injected with control monoclonal antibody 12CA5 against HA, then injected with AlexaFluor488-labelled *run* RNA 10 minutes later. After a further 10 minutes, the majority of the injected *run* RNA has become localised to the apical cytoplasm. Scale Bar = 50μm. (**B**) An embryo that was pre-injected with a *Drosophila* anti-dhc monoclonal antibody, which inhibits localisation of injected *run* RNA. (**C**) *In situ* hybridisation of *ftz* mRNA in an embryo injected with an anti-dhc antibody 20-30 minutes before fixation. *ftz* mRNA becomes unlocalised in expression stripes near the site of injection, and is detected in the basal cytoplasm and yolk. (**D**) *In situ* hybridisation to detect *ftz* mRNA in a $Dhc64C^{6-6}/Dhc64C^{6-8}$ mutant embryo, showing normal apical localisation of *ftz* mRNA. Scale Bars in (C) and (D) represent 10μm.

RESULTS

Anti-dynein antibodies disrupt the apical localisation of injected and endogenous transcripts

To test the requirement for cytoplasmic dynein in apical RNA localisation, embryos were pre-injected with antibodies against *Drosophila* cytoplasmic dynein heavy chain (dhc). It was found that two different monoclonal anti-dhc antibodies (McGrail and Hays, 1997; Sharp et al., 2000a) consistently inhibited the localisation of injected *run*, *ftz* and *wg* RNA (Table 9a and Figure 9-1). In most embryos pre-injected with anti-dhc antibodies, RNA diffused away from the site of injection (Movie 8) in a similar manner to embryos injected with colcemid. In contrast, pre-injection of embryos with a control monoclonal antibody did not disrupt the ability of injected RNA to localise correctly to the apical cytoplasm (Table 9a and Figure 9-1).

To determine if inhibition of cytoplasmic dynein also has an effect on the localisation of endogenous transcripts, embryos were fixed 15-30 minutes after injection with anti-dhc antibodies, and the endogenous *ftz* mRNA was detected by *in situ* hybridisation. *ftz* mRNA was visualised in the basal cytoplasm and yolk of expression stripes near the site of anti-dhc antibody injection (Figure 9-1). Given that the half life of *ftz* mRNA is 6-8 minutes in the blastoderm embryo (Edgar et al., 1986), the unlocalised *ftz* transcripts detected in the basal cytoplasm and yolk are likely to have been synthesised after the injection of anti-dhc antibodies into the embryo.

Taken together, these results suggest that cytoplasmic dynein is required for the localisation of both endogenous and injected transcripts to the apical cytoplasm.

Table 9a. Injection of anti-dynein antibodies inhibits apical localisation

Reagent	RNA	% Localisation	N
Control monoclonal antibody against HA	*wg*	89%	18
	run	90%	30
	ftz	90%	21
Monoclonal antibody P1H4 against N-terminal residues 128-422 of *Drosophila* dhc (Tom Hays)	*wg*	21%	14
	run	12%	33
	ftz	7%	15
Monoclonal antibody against HUV fragment of *Drosophila* dhc (David Sharp)	*wg*	0%	22
	ftz	0%	14

The proportion of embryos that correctly localise injected RNAs to the apical cytoplasm are shown for embryos pre-injected with anti-dhc antibodies. Monoclonal antibodies to *Drosophila* dhc, or control 12CA5 anti-HA antibodies were injected approximately 10 minutes before apically-targeted RNA. N = number of embryos tested.

Table 9b. RNA particle speed in wild type and dhc mutant embryos

Genotype	RNA	% localisation	particle speed (μm/s)	max speed (μm/s)	*P* value
wild type	*wg*	88% (N=17)	0.41 ± 0.03 (N=32)	0.67	0.10 [a]
	run	94% (N=17)	0.49 ± 0.04 (N=34)	1.01	0.60 [b]
	ftz	92% (N=12)	0.46 ± 0.03 (N=29)	0.84	0.24 [c]
$Dhc64C^{8\text{-}1}/Dhc64C^{6\text{-}10}$	*wg*	89% (N=19)	0.16 ± 0.008 (N=37)	0.27	5.7×10^{-9}
	run	95% (N=22)	0.19 ± 0.008 (N=69)	0.35	4.4×10^{-9}
	ftz	86% (N=22)	0.19 ± 0.009 (N=72)	0.34	4.0×10^{-9}
$Dhc64C^{6\text{-}6}/Dhc64C^{6\text{-}8}$	*wg*	92% (N=12)	0.13 ± 0.01 (N=64)	0.41	2.7×10^{-10}
	run	86% (N=14)	0.15 ± 0.01 (N=55)	0.37	2.7×10^{-10}
	ftz	88% (N=22)	0.14 ± 0.01 (N=60)	0.46	3.9×10^{-11}

The speeds of apical localisation particles in wild type and mutant cytoplasmic dynein embryos. The average ± standard error and maximum speeds of movement of N particles. Speeds were measured from the distance in μm between successive positions of injected RNA particles at 10 second intervals while in transit to the apical cytoplasm. The *P* values represent the probability of the speed measurements being derived from the same population as the appropriate controls. [a] compared to *run* RNA. [b] compared to *ftz* RNA. [c] compared to *wg* RNA. The proportion of embryos that correctly localise injected RNAs to the apical cytoplasm are also shown for each condition (N = number of embryos tested).

Mutations in the gene for cytoplasmic dynein heavy chain decrease the speed of RNA localisation intermediates

To further test the requirement for cytoplasmic dynein in apical RNA localisation, fluorescent RNA was injected into embryos where dynein function was impaired genetically by mutations in *Dhc64C*, the gene encoding the cytoplasmic dynein heavy chain in *Drosophila* (Hays et al., 1994). Cytoplasmic dynein is required for mitosis, axonal transport, organelle transport and other essential processes, and all known mutations in *Dhc64C* are homozygous lethal (Gepner et al., 1996). However, due to the fact that the dynein complex contains a dimer of heavy chains, transheterozygous combinations of certain *Dhc64C* mutant alleles are viable and can support development to fertile adults due to intragenic complementation (Gepner et al., 1996).

Apical localisation of mRNA was analysed in *Dhc64C* mutant embryos laid by transheterozygous mutant females of genotype $Dhc64C^{6\text{-}6}/Dhc64C^{6\text{-}8}$ and $Dhc64C^{8\text{-}1}/Dhc64C^{6\text{-}10}$ (Gepner et al., 1996). It was found that apically targeted RNA is able to localise in *Dhc64C* mutant embryos. Detection of endogenous *ftz* mRNA in *Dhc64C* mutant embryos by *in situ* hybridisation showed that the majority of *ftz* mRNA was correctly localised in the apical cytoplasm, with only a few localisation intermediates in the basal cytoplasm (Figure 9-1), as found for wild type embryos (Wilkie and Davis, 2001). Furthermore, it was found that injected apically-targeted RNA is also localised in *Dhc64C* mutant embryos. On average, 89% of *Dhc64C* mutant embryos correctly localised injected *ftz*, *run* or *wg* RNA to the apical cytoplasm (Table 9b). However, when the speed of movement of injected RNA particles was measured in *Dhc64C* mutant embryos, it was found to be significantly reduced. The average and maximum speeds of *run*, *ftz* and *wg* RNA particles in transit to the apical cytoplasm were around 60% lower in both mutant combinations of *Dhc64C*, compared to wild type embryos (*P*

$< 4.0 \times 10^{-9}$, see Table 9b). The slower moving RNA particles in *Dhc64C* mutants are evident in time-lapse movies (Movie 9). These results complement the anti-dhc antibody injections, providing further evidence that cytoplasmic dynein has a role in the apical localisation of mRNA.

Disruption of the dynactin complex reduces the speed of RNA particle movement

Dynactin is a protein complex which is involved in co-ordinating the activities of cytoplasmic dynein, and is thought to be required for all forms of dynein-based transport in the cell (Karki and Holzbaur, 1999). Dynactin is thought to regulate the binding of some cargoes to cytoplasmic dynein (Karki and Holzbaur, 1999; Waterman-Storer et al., 1997) and has also been shown to control the processivity of the cytoplasmic dynein motor (King and Schroer, 2000). p50/dynamitin is a subunit of dynactin that has been widely used as an agent to disrupt the dynactin complex and demonstrate dynein-dependent motility (Ahmad et al., 1998; Burkhardt et al., 1997; King and Schroer, 2000; Sharp et al., 2000b; Waterman-Storer et al., 1997). Treatment of cultured cells, *Xenopus* extracts or purified dynactin complexes with excess p50/dynamitin has been shown to break up the dynactin complex into several subcomplexes (Echeverri et al., 1996; Eckley et al., 1999; Karki et al., 1998; Wittmann and Hyman, 1999).

To test whether dynactin is required for apical RNA localisation, embryos were pre-injected with an excess of purified human recombinant GST-p50/dynamitin protein. It was found that p50/dynamitin does not inhibit the localisation of injected RNA to the apical cytoplasm, as 92% of embryos pre-injected with excess GST-p50/dynamitin correctly localised *run*, *wg* and *ftz* RNA to the apical cytoplasm. However, as found for the *Dhc64C* mutant embryos, the average speed of RNA particles in transit from the site

Table 9c. RNA particle speed in p50/dynamitin-injected embryos

Agent	RNA	% localisation	particle speed (μm/s)	max speed (μm/s)	*P* value
No pre-injection (Wild type)	*wg*	88% (N=17)	0.41 ± 0.03 (N=32)	0.67	0.10 [a]
	run	94% (N=17)	0.49 ± 0.04 (N=34)	1.01	0.60 [b]
	ftz	92% (N=12)	0.46 ± 0.03 (N=29)	0.84	0.24 [c]
GST	*wg*	90% (N=11)	0.40 ± 0.02 (N=46)	0.86	0.80
	run	92% (N=13)	0.42 ± 0.04 (N=34)	0.97	0.23
GST-p50/dynamitin	*wg*	90% (N=20)	0.18 ± 0.03 (N=44)	0.59	4.67×10^{-8}
	run	92% (N=26)	0.16 ± 0.03 (N=45)	0.66	9.28×10^{-7}
	ftz	94% (N=16)	0.21 ± 0.03 (N=44)	0.83	1.7×10^{-5} [d]

The speeds of apical localisation particles in wild type embryos, and embryos pre-injected with excess recombinant GST-p50/dynamitin protein or GST alone. The average ± standard error and maximum speeds of movement of N particles. Speeds were measured from the distance in μm between successive positions of injected RNA particles at 10 second intervals while in transit to the apical cytoplasm. The *P* values represent the probability of the speed measurements being derived from the same population as the appropriate controls. [a] compared to *run* RNA. [b] compared to *ftz* RNA. [c] compared to *wg* RNA. [d] compared to embryos injected with GST and then *wg* RNA. The proportion of embryos that correctly localise injected RNAs to the apical cytoplasm are also shown for each condition (N = number of embryos tested).

Table 9d. RNA particle motion in embryos pre-injected with p50/dynamitin

Pre-injection	Minus End	Plus End	Paused	Average particle speed (μm/s)	Minus end particle speed (μm/s)	Plus end particle speed (μm/s)
Buffer	82%	6%	12%	0.42 ± 0.03 (N=210)	0.53 ± 0.03 (N=174)	0.19 ± 0.02 (N=13)
GST-p50/dynamitin	63%	17%	20%	0.19 ± 0.01 (N=665)	0.37 ± 0.02 (N=421)	0.20 ± 0.008 (N=136)

The average, apical (minus end) and basal (plus end) speeds of apical localisation particles in embryos pre-injected with excess recombinant GST-p50/dynamitin protein, or buffer alone. The average speeds of movement ± standard error are shown for N particle movements. Speeds were measured from the distance in μm between successive positions of injected RNA particles at 2 second intervals, whilst undergoing bidirectional movement during transit to the apical cytoplasm. The proportion of time which RNA particles spent paused, or moving in the apical or basal direction is also shown.

of injection to the apical cytoplasm was reduced from an average of 0.45 μm/s to 0.23 μm/s (Table 9c), an overall change which was found to be highly significant ($P = 5.16 \times 10^{-15}$). In contrast, pre-injection of control GST protein did not significantly change the speed of RNA localisation intermediates ($P < 0.8$), showing that the effect on the speed of localisation intermediates is specifically caused by the presence of excess p50/dynamitin protein. These results strongly suggest that dynactin is involved in the apical localisation of RNA, providing further evidence that apical mRNA localisation is mediated by cytoplasmic dynein.

Excess p50/dynamitin causes increased pausing and plus-end directed motion of apical RNA localisation intermediates.

Mutations in *Dhc64C* and pre-injection of p50/dynamitin both reduce the average speed of RNA particles in transit to the apical cytoplasm. However, one apparent difference is that the maximum speed of RNA particles does not appear to be affected by pre-injection of p50/dynamitin but is reduced in *Dhc64C* mutant embryos (Tables 9b, 9c). To examine this in more detail, injected RNA was filmed at higher time resolution in wild type embryos and embryos pre-injected with excess p50/dynamitin.

Time-lapse movies in which images were acquired every 2 seconds revealed that the movement of localisation particles in wild type embryos is very dynamic. While the average velocity of injected *wg* RNA particles was 0.42 μm/s towards the apical cytoplasm (minus end of microtubules) it was found that the RNA particles frequently stopped moving (pause) and occasionally moved in the plus end direction (towards the basal cytoplasm). The average plus end speed was 0.19 μm/s and the maximum plus end particle speed observed was 0.46 μm/s. In addition to pauses and changes in direction, the RNA particles also displayed rapid changes in speed, often reaching speeds of over 2

μm/s then slowing to under 0.2 μm/s or pausing between successive time frames (data not shown).

Tracking RNA particles at higher time resolution in embryos pre-injected with p50/dynamitin confirmed that this treatment causes a reduction in the average speed of injected RNA particles towards the apical cytoplasm. However, this time-lapse data also showed that excess p50/dynamitin significantly changes the characteristics of the particle motion ($P = 3.4 \times 10^{-15}$). In embryos pre-injected with p50/dynamitin, injected RNA localisation intermediates can reach minus end speeds of up to 1.6 μm/s but spend a greater proportion of time paused or moving towards the plus end of microtubules compared to embryos pre-injected with control buffer (Table 9d and Movie 10). The average plus end particle speed is not affected by pre-injection of p50/dynamitin.

These results show that pre-injection of p50/dynamitin causes increased pausing and plus end directed motion of RNA localisation intermediates, reducing the average speed of RNA particles towards the apical cytoplasm. These results are consistent with previous work showing that the dynactin complex is required for processivity of the dynein motor (King and Schroer, 2000), and provide further evidence for the involvement of cytoplasmic dynein in mRNA localisation.

CONCLUSIONS

Tracking individual RNA particles revealed that localisation intermediates move bidirectionally, suggesting that they are transported in a complex containing multiple minus and plus end directed motors.

It was found that anti-dynein antibodies, mutations in the gene for dynein heavy chain and excess p50/dynamitin all disrupt apical RNA localisation. Whilst this data does not address the question of which plus end directed motor(s) might be involved in bidirectional movement, or completely exclude the possibility that ncd might contribute to localisation, these results strongly suggest that cytoplasmic dynein and its associated dynactin complex are required for the localisation of pair-rule and *wg* mRNA to the minus ends of microtubules in the apical cytoplasm.

10

DISCUSSION AND FUTURE PERSPECTIVES

INTRODUCTION

In this thesis, the entire path of movement taken by specific transcripts has been followed from their site of synthesis within the nucleus to their final site of localisation in the cytoplasm of *Drosophila* embryos. The intranuclear sites of transcription, movement of mRNA through the nucleoplasm, export of mRNA from the nucleus and apical localisation of specific transcripts have been analysed, and the mechanisms responsible investigated.

NUCLEAR EXPORT OF mRNA

Nuclear export requires long range transport of mRNA through the nucleoplasm

Using a new, highly sensitive method for the fluorescent detection of mRNA (Wilkie and Davis, 1998), specific transcripts were covisualised with the nuclear envelope in *Drosophila* blastoderm embryos. This technique allowed transcripts in the nucleus or cytoplasm to be clearly distinguished and imaged at high resolution. Mapping the nuclear position of nascent transcripts demonstrated that transcription can take place throughout the nucleoplasm and that genes are often transcribed in the nuclear interior.

Therefore, newly synthesised transcripts must frequently travel significant distances through the nucleoplasm to reach the nuclear envelope for export.

In this study, intermediates in the nuclear export of mRNA were detected both in the nuclear interior and in close association with the nuclear envelope. It was proposed that these signals represent intermediates in the nuclear export of mRNA since the number of these particles found in individual nuclei is related to the intensity of nascent transcripts (level of expression). Furthermore, these signals were 5-10 times brighter than background fluorescence, were absent in transcript null embryos and were found to have a similar intensity to particles of mRNA in the cytoplasm.

Specific transcripts move through the nucleoplasm by diffusion

Intermediates in the nuclear export of all transcripts examined were found at random positions in the nucleoplasm and nuclear envelope, compatible with diffusion away from nascent transcript foci after completion of synthesis and processing. This result is in agreement with other work suggesting that movement of specific transcripts and poly(A)$^+$ RNA through the nucleoplasm is based mainly on diffusion (Pante et al., 1997; Politz et al., 1998; Politz et al., 1999; Singh et al., 1999; Zachar et al., 1993). Furthermore, the phenotype of *sbr* mutants which disrupt mRNA export is also consistent with a diffusional mechanism for the intranuclear movement of mRNA. In *l(1)ts148* and *sbr*^{10} mutant embryos, specific transcripts accumulate at random positions throughout the nucleus at the restrictive temperature, suggesting that when mRNA export is blocked, RNA export intermediates diffuse from nascent transcripts to all parts of the nucleus. This phenotype was also observed in embryos when mRNA export was disrupted by injection of dominant negative fragments of human importin-β protein,

which bind irreversibly to nuclear pores and rapidly inhibit both nuclear protein import and mRNA export (Kutay et al., 1997)(Davis and Kumar, manuscript submitted).

Export intermediates consist of a small number of transcripts

Previous work using different methods has led to variable estimates for the amount of RNA contained in nuclear export intermediates. Incorporation of nucleotide analogues into nascent RNA, which allowed export intermediates to be detected by immunogold labelling and visualised in the electron microscope, suggested that mRNA is transported through the nucleus in groups of 5 transcripts (Iborra et al., 1998). In contrast, detection of intermediates in the export of *β-actin* mRNA by hybridisation with fluorescent oligonucleotide probes has shown directly that transcripts in the nucleus and cytoplasm are likely to be single molecules of RNA (Femino et al., 1998).

The export intermediates, localisation intermediates and cytoplasmic particles of mRNA observed in this work were all found to have similar intensities, suggesting that they are each likely to consist of similar amounts of RNA. However, the detection methods used here do not allow direct quantitation of RNA in images, only relative measurements of fluorescence intensity. A comparison of the average intensity of nascent transcripts with RNA particles in the export and localisation pathway suggests that these intermediates may contain 20-50 times less RNA than nascent transcript foci in strongly expressing regions of the embryo (Table 4a). Nascent transcript foci are thought to consist of 5-50 nascent RNA chains, and contain more RNA in strongly-expressing nuclei (Table 3a), suggesting that export and localisation intermediates consist of 1-5 particles of RNA. Intermediates in all parts of the export and localisation pathway were generally found to have around a five-fold range of different intensities, suggesting that they contain variable amounts of mRNA. This is consistent with the results of RNA injection, which

demonstrated that localisation particles could consist of more than one RNA molecule or even different apically-targeted transcripts. Taken together, these results suggest that mRNA export and localisation intermediates contain a small amount of mRNA, probably between one to five molecules. The resolution of this issue awaits more quantitative detection methods for mRNA in fixed *Drosophila* tissues.

Nuclear Export of mRNA requires TAP/Sbr

Although there is increasing evidence suggesting that TAP might function as a receptor for the nuclear export of mRNA in higher eukaryotes, none of this data is absolutely conclusive (reviewed in (de Castilla and Rout, 1999). Recently, RNA interference experiments in *C. elegans* have shown that disrupting the TAP orthologue Ce-NXF-1 causes nuclear accumulation of Poly(A)$^+$ RNA in embryos and adult nematodes (Tan et al., 2000). However, since the integrity of other nuclear transport pathways was not investigated after RNAi, the nuclear poly(A)$^+$ export defect could be an indirect effect of disrupting Ce-NXF-1 expression.

The most direct demonstration that TAP is required for nuclear mRNA export has been achieved in lower eukaryotes. In *S. cerevisiae*, mutations in the essential yeast gene *MEX67*, which encodes the sole yeast homologue of TAP, render the cell unable to export mRNA (Hurt et al., 2000; Segref et al., 1997). Mex67p interacts with Mrt2p, forming a complex which binds RNA and interacts with nucleoporins (Santos-Rosa et al., 1998; Strasser et al., 2000). The finding that human TAP, when co-expressed with its human cofactor p15, can rescue the lethality of a *mex67,mtr2* double knockout yeast strain is highly significant and suggests that NXF proteins have been conserved across evolution and have similar functions in nuclear mRNA export (Katahira et al., 1999). However, there are at least four additional NXF proteins in the human genome and three

further *Drosophila* NXF proteins in addition to Sbr (Herold et al., 2000). The function of these other NXF proteins are not known, but it is interesting to speculate that they might have tissue-specific functions or specialised roles such as regulating the nuclear export of specific transcripts. Alternatively, the NXF proteins might have redundant functions in the nuclear export of mRNA. Early indications are that some NXF proteins may have different functions, since human NXF2 and NXF3 proteins display different abilities to bind RNA and nucleoporins (Herold et al., 2000). However, the most conclusive method of testing these possibilities and analysing the function of different NXF proteins is mutational analysis.

This thesis describes the first genetic evidence that TAP/NXF1 functions directly in the nuclear export of mRNA in a multicellular higher eukaryote. Two independent t.s. lethal mutations in *sbr*, which encodes the strongest homologue of TAP/NXF1 in *Drosophila*, cause a defect in the nuclear export of all transcripts tested in the embryo. These mutations are lethal throughout the *Drosophila* life cycle, and it will be important to determine if they inhibit mRNA export at all stages of development (Ilan Davis, experiments in progress). However, the fact that mutations in *sbr* are lethal and cause a defect in mRNA export demonstrates that *Drosophila* NXF2-4 cannot replace the function of Sbr in nuclear mRNA export. This suggests that NXF proteins are not functionally redundant, and that NXF2-4 may have much more restricted roles in mRNA export or indeed a different function all together.

In the future, it may be informative to find genes or proteins that interact with *sbr*, for example by carrying out genetic modifier and two hybrid screens, or co-immunoprecipitation experiments with purified proteins. These approaches would be likely to identify other factors required for nuclear mRNA export and could also be used

to test whether the different NXF factors interact with each other and with p15 homologues at the genetic or biochemical level.

It is exciting to note that different mutations in the *sbr* gene cause specific defects during *Drosophila* development. Although most mutations in *sbr* are recessive lethal alleles, sbr^{1}, sbr^{2}, sbr^{18} and sbr^{19} are viable lead to bristle defects in the adult fly (Lindsley and Zimm, 1992; Schalet, 1986; Zhimulev and Ilyina, 1980) whilst sbr^{17} causes male and female sterility (Geer et al., 1983). Furthermore, *magellan*, a novel allele of *sbr*, causes specific defects in motor axon guidance and muscle formation (C. Korey and D. van Vactor, personal communication). These results suggest that *sbr* may have specific functions in *Drosophila* development. Alternatively, this data may reveal the sensitivity of tissues with a high demand on mRNA export which are especially sensitive to hypomorphic mutations in *sbr* that marginally disrupt mRNA export. This issue could be resolved by defining the mutations in the other *sbr* alleles at the DNA sequence level, and analysing the defects these cause in the *sbr* gene product. Furthermore, mRNA export could be tested in nervous system tissues in sbr^{1} and *magellan* mutants to determine whether the bristle and axon defects are likely to be caused by a defect in nuclear mRNA export.

Both the *l(1)ts148* and sbr^{10} alleles of *sbr* which disrupt mRNA export were found to encode non-conservative amino acid substitutions in the same region of the protein, just 15 residues apart. Importantly, the corresponding region of human TAP has been identified as the substrate or RNA binding domain in a number of different studies (Bachi et al., 2000; Braun et al., 1999; Kang and Cullen, 1999). Furthermore, a cryptic RNP domain (also sometimes called RRM or RBD domain) was recently identified this region of human TAP, and shown to have a characteristic secondary structure consisting

of four antiparallel β-sheets packed against two perpendicular α-helices. Two short RNP consensus motifs are located on the 1st and 3rd β-strands (Liker et al., 2000). Strikingly, the mutation V154E in *l(1)ts148* falls at the 6th position within the 8 amino acids that form the RNP1 motif. It has previously been shown that the residues at positions 4, 6 and 8 of the RNP1 motif point to the interior of the domain and are crucial for the structural integrity of the fold, as they pack against the residues of the helices in the hydrophobic core of the domain (reviewed in (Liker et al., 2000). Therefore, the substitution of an uncharged residue with an acidic amino acid at this position in *l(1)ts148* may disrupt the structural stability of the RNP domain, leading to the temperature sensitive mRNA export phenotype.

In sbr^{10}, the mutation P139L is located in a short loop between the first helix and the second β-strand of the RNP domain. This non-conservative amino acid substitution is likely to disrupt the structure of the RNP domain, and may also lead to an unstable temperature-dependent topology within the RNA-binding domain. Since a 102 amino acid fragment of human TAP/NXF1 protein containing the RNP domain can bind to RNA *in vitro* (Liker et al., 2000) it would be very interesting to examine the RNA binding properties of this region of the Sbr protein, and determine whether the mutations in *l(1)ts148* and sbr^{10} abolish binding of RNA. This could be tested by performing gel shift assays with labelled RNA and fragments of wild type and mutant Sbr protein synthesised by *in vitro* translation. Such studies might reveal new information about TAP/NXF1 function and RNA-protein interactions when combined with structural modelling predictions on the RNP domain. Furthermore, if the mutant Sbr proteins are indeed unable to bind mRNA under restrictive conditions as suggested above, this would suggest that TAP is required for docking of mRNA at nuclear pores, since mRNA does not accumulate at the nuclear envelope in *l(1)ts148* and sbr^{10} mutant embryos at the

restrictive temperature. This idea is consistent with the finding that Mex67p and TAP proteins specifically bind to nucleoporins, and that this interaction is required for the nuclear export of mRNA (Bachi et al., 2000; Strasser et al., 2000).

The phenotype of *l(1)ts148* is consistent with many aspects of the phenotype of mutations in the yeast *MEX67* gene which were described previously. Conditional t.s. alleles of *mex67* which inhibit nuclear mRNA export do not disrupt pre-mRNA splicing or nuclear protein import at the restrictive temperature (Segref et al., 1997), as found for *l(1)ts148*. Furthermore neither *mex67* nor *l(1)ts148* cause defects in nuclear envelope such as clustering of nuclear pores or herniations in the nuclear envelope at the restrictive temperature. One apparent difference was that the nucleolus can become fragmented in thermosensitive *mex67-5* cells, but only after a 2 hour shift to the restrictive temperature (Segref et al., 1997). Nucleolar fragmentation was not observed in *l(1)ts148* embryos, but ultrastructural studies were carried out on embryos which were fixed after 30 minutes at the restrictive temperature. It is therefore possible that the nucleolus could become fragmented after longer shifts to the restrictive temperature in *l(1)ts148* mutant embryos.

sbr^{10} was previously reported to have a defect in heat shock protein synthesis at the post-transcriptional level (Evgen'ev and Denisenko, 1990). This could be explained if the transcripts encoding heat shock proteins (HSP's) accumulate in the nucleus under heat shock conditions, preventing them from being translated. This has been shown to occur in a t.s. allele of the yeast *MEX67* gene. In *mex67-5* cells, HSP's are not synthesised under temperature stress conditions because heat shock transcripts *SSA1,2 and 3* are not exported from the nucleus and therefore cannot be translated (Hurt et al., 2000). However, HSP synthesis begins in these cells after a shift back to the cooler permissive

temperature (at which HSP's would not normally be produced) because the nuclear pool of *SSA* transcripts accumulated during the restrictive temperature shift are released into the cytoplasm at permissive temperature (Hurt et al., 2000). This is also likely to occur in *Drosophila*, as sbr^{10} mutants were previously reported to undergo prolonged synthesis of HSP proteins after heat shock compared to wild type (Mamon and Kutskova, 1993). These findings are consistent with the discovery that the nuclear mRNA accumulation phenotype in *l(1)ts148* is rapidly reversible on shifting back to the permissive temperature, and could be examined further by carrying out *in situ* hybridisation to test whether heat shock transcripts accumulate in the nuclei of *sbr* mutants at the restrictive temperature.

LOCALISATION OF mRNA TO THE APICAL CYTOPLASM

Apically targeted transcripts are localised by a cytoplasmic mechanism

Gene gating mechanisms were previously proposed, suggesting transcripts could be localised to the apical cytoplasm by vectorial nuclear export (Davis et al., 1993; Francis-Lang et al., 1996). However, the nascent transcripts for genes with apically targeted mRNA are not found on the apical side of the nucleus but rather at more basal nuclear positions correlated with their position on chromosome arms. This result demonstrates that direct gene gating is not responsible for localisation of transcripts to the apical cytoplasm. Furthermore, nuclear export intermediates for these transcripts were visualised at random positions throughout the nucleoplasm and were also found in all parts of the nuclear envelope, indicating that they are exported to the cytoplasm in all directions. These findings are consistent with the visualisation of localisation intermediates in the basal cytoplasm of wild type embryos, and conclusively demonstrate that vectorial nuclear export of pair-rule mRNA does not occur. Instead, these results strongly suggest that pair-rule and *wg* transcripts are localised by a mechanism operating in the cytoplasm such as diffusion and anchoring of mRNA or active transport to the apical cytoplasm along cytoskeletal tracks (Davis et al., 1993). This results are consistent with previous reports that *ftz* RNA is able to localise when injected into the basal cytoplasm, but only when pre-incubated with squid hnRNP protein (Lall et al., 1999).

Fluorescently labelled synthetic RNA is actively localised to the apical cytoplasm in particles similar to endogenous mRNA localisation intermediates

It was found that direct incorporation of different fluorescent UTP analogues into RNA by *in vitro* transcription did not disrupt its localisation. *run*, *ftz* and *wg* RNA labelled with AlexaFluor488, AlexaFluor546, cyanine-3 or cyanine-5 dyes became rapidly localised to the apical cytoplasm after microinjection into the basal cytoplasm or yolk of living blastoderm embryos. Before injection, this RNA was extracted with phenol/chloroform, precipitated and resuspended in purified water or injection buffer and therefore contained no proteins. The difference between these results and previous experiments showing that fluorescent *ftz* RNA is not localised unless pre-incubated in nuclear extracts or squid protein (Lall et al., 1999) are likely to be due to the different methods used to label the RNA. Incorporation of aminoallyl-UTP into RNA, followed by chemical coupling of succinimidyl fluorescein dye esters disrupts the ability of *ftz* RNA to localise (S. Bullock and D. Ish-Horowicz, personal communication). The hnRNPA1 protein Squid appears to restore the competence of this RNA to be localised, either through its direct functions in mRNA localisation as suggested in other work (Cote et al., 1999; Hoek et al., 1998; Norvell et al., 1999) or possibly by allowing the labelled RNA to be folded correctly and enabling the localisation signals in the 3'UTR to be recognised. The results reported here do not address the question of whether hnRNP proteins such as sqd have specific roles in mRNA localisation, but they demonstrate that proteins required for localisation can be effectively recruited in the cytoplasm.

Fluorescent RNA was often observed to form bright particles after microinjection into living embryos. Strikingly, time-lapse microscopy showed that particles of *run*, *ftz* or *wg*

RNA were transported to the apical cytoplasm along direct paths, whereas other transcripts not targeted to the apical cytoplasm formed particles which displayed random movement. Many injected localisation intermediates were intensely fluorescent, suggesting that they contain more RNA than endogenous mRNA particles. This result is not unexpected, since the injected RNA is highly concentrated compared to endogenous transcript levels in the embryo. Despite this, some particles of injected RNA were found to have similar intensities to endogenous localisation intermediates, suggesting that they contain equivalent amounts of RNA.

Taken together, these results demonstrate that the localisation of pair-rule and *wg* mRNA occurs by active transport of RNA particles to the apical cytoplasm, rather than by diffusion and anchoring of mRNA.

Apical mRNA localisation is mediated by dynein dependent transport of RNA particles to the minus ends of microtubules

Pre-injection of cytoskeletal depolymerising drugs suggested that actin filaments are not required for apical mRNA localisation, but revealed a direct role for microtubules in the transport of pair-rule and *wg* transcripts to the apical cytoplasm. This data does not completely exclude some role for actin microfilaments in localisation, for example in short range transport or anchoring of mRNA in the apical cytoplasm. However, these results are in complete agreement with previous work showing that microtubules, but not microfilaments, are required for apical localisation of *ftz* mRNA (Edgar et al., 1987; Lall et al., 1999).

In addition, a number of different lines of evidence were presented which implicate cytoplasmic dynein in the localisation of pair-rule and *wg* mRNA to microtubule minus

ends in the apical cytoplasm. It was found that two different anti-dynein antibodies inhibited the localisation of injected and endogenous RNA. Furthermore, two distinct combinations of *Dhc64C* mutant alleles or an excess of p50/dynamitin were each sufficient to significantly reduce the speed of apical RNA localisation particles. Whilst it cannot be completely excluded that the injection of anti-dhc antibodies might inhibit localisation by disrupting microtubules, the effect of the antibodies is likely to be more specific as both were shown to recognise a single band corresponding to dynein heavy chain on Western blots (McGrail and Hays, 1997; Sharp et al., 2000a). Furthermore, injection of one of the antibodies was reported to cause specific defects in spindle pole separation and spindle elongation during mitosis in *Drosophila* embryos (Sharp et al., 2000a), an effect mirrored by injection of excess p50/dynamitin (Sharp et al., 2000b).

The dynactin complex is thought to be involved in recruitment of dynein to its various cargoes (Karki and Holzbaur, 1999; Vallee and Sheetz, 1996), and has also been shown to increase the processivity of the dynein motor *in vitro* (King and Schroer, 2000). Many studies using excess p50/dynamitin to disrupt the dynactin complex have reported that this treatment completely inhibits transport of cargo (Ahmad et al., 1998; Presley et al., 1997; Valetti et al., 1999). The finding that p50/dynamitin reduces the speed of apical RNA transport by increasing the frequency of pausing of RNA particles is consistent with the role of dynactin in dynein processivity, and supports a role for dynein in apical mRNA localisation. The fact that p50/dynamitin does not completely inhibit apical localisation suggests that dynactin is not essential for binding of apically-targeted RNA to dynein. However, since recombinant human p50/dynamitin was used rather than fly dynamitin, and these proteins are only well-conserved near the N-terminus (Valetti et al., 1999), this result could also reflect a reduced activity of the human protein in *Drosophila*.

All known mutations in *Dhc64C* are lethal, and clonal analysis indicates that dynein function is essential for cell viability in *Drosophila* (Gepner et al., 1996). It is therefore not possible to analyse RNA localisation in a dynein null genetic background in the embryo. This problem was overcome by using combinations of *Dhc64C* mutations that retain partial dynein function due to intragenic complementation. The discovery that apical localisation of RNA particles is slowed down, but not abolished, in such *Dhc64C* mutant embryos is consistent with the partial loss of dynein function previously reported in these mutants. Furthermore, the reduction in particle speed is excellent evidence for the involvement of dynein in apical localisation, since null dynein mutants could inhibit localisation by indirect means.

Although the molecular nature of the *Dhc64C* mutant alleles is not known, their lethality is fully rescued by dhc^{+} transgenes (Gepner et al., 1996) and some defects have been identified in mutants. For example, oocyte differentiation fails in $Dhc64C^{6\text{-}12}/Dhc64C^{3\text{-}2}$ mutant egg chambers due to a defect in spindle orientation during the asymmetric divisions in the germline cyst (McGrail and Hays, 1997). Furthermore, $Dhc64C^{6\text{-}6}/Dhc64C^{6\text{-}8}$ embryos have defects in centrosome migration and spindle attachment leading to highly aberrant mitotic events (Robinson et al., 1999). The results of investigating localisation of RNA particles are remarkably similar to previous work studying the movement of lipid droplets in living *Drosophila* embryos (Gross et al., 2000). The lipid droplets accumulate in the yolk during cycle 14 by plus end directed transport, then become redistributed to the apical cytoplasm at the onset of gastrulation by minus end directed transport. When the lipid droplets were imaged using Video-Enhanced DIC microscopy techniques at 30 frames per second, they were seen to move bidirectionally. The average minus end speed was around 0.45 μm/s and the droplets spent 9-11% of the time studied in a paused state, almost identical results to those found

for RNA particles. In *Dhc64C*$^{8\text{-}1}$/*Dhc64C*$^{6\text{-}10}$ embryos, the lipid droplets moved at an average minus end speed of 0.33 μm/s and were observed to pause more frequently (total time paused increased to 22%). The similarity of these results to the movement of RNA particles strongly suggests that RNA particles and lipid droplets are transported by the same mechanism. Whilst the RNA particles described here are not bright enough to allow acquisition of such frequent time points as those obtained using VE-DIC microscopy, optimising the imaging conditions would be likely to allow RNA particles to be filmed at 4 frames per second or higher. This ought to provide enough time resolution to study finer details of the particle movement and identify differences in particle run length and pause duration caused by mutations in *Dhc64C* or pre-injection of p50/dynamitin, allowing the precise defects in movement to be identified and compared. This would be likely to reveal new aspects of dynein function and RNA particle movement.

Increased resolution of time-lapse data would also allow the bidirectional nature of RNA particle movement to be studied in greater detail. In *Drosophila*, strong genetic interactions have been found between mutations in *Dhc64C* and *Glued* (a subunit of dynactin) with mutations in genes encoding the heavy and light chains of kinesin (Martin et al., 1999). Lipid droplets and RNA particles are observed to move bidirectionally, and therefore are likely to be transported in a complex containing a functional plus end motor such as kinesin in addition to dynein. The significance of this observation is not completely understood, but it has been shown that the transport of lipid droplets is determined by a balance between plus and minus end directed transport, and that a switch controls the net direction of travel (Gross et al., 2000; Welte et al., 1998). It is possible that many cargoes could be transported by complexes containing multiple plus and minus end motors, which would allow efficient and rapid cycling of

motor complexes between opposite ends of microtubules to participate in multiple rounds of cargo transport. Imaging bidirectional cargoes such as lipid droplets or RNA particles in kinesin mutant embryos could reveal if kinesin is the motor responsible for the plus end directed movements. However, the regulatory factors which control the net travel direction and cargo binding await future genetic or biochemical characterisation.

The *in vivo* injection assay is likely to provide a valuable tool to define and analyse RNA localisation elements. Restriction enzymes or PCR could be used to generate DNA fragments which can easily and quickly be transcribed and injected to test for functional localisation, bypassing the need to construct transgenic reporter constructs. Furthermore, this assay could be adapted to study the localisation of transcripts at other stages of development, or in different systems such as cultured cells. The importance of analysing RNA particle movement in living tissues is illustrated by the fact that endogenous *grk* and *osk* mRNA was previously reported to be correctly localised in fixed $Dhc64C^{6-6}/Dhc64C^{6-12}$ egg chambers, leading to the conclusion that dynein was unlikely to play a role in the localisation of these transcripts (McGrail and Hays, 1997). However, recent observations suggest that dynein is likely to play an important role in mRNA localisation during oogenesis in *Drosophila* (Nina Ehrenberg, unpublished data).

Given that localised transcripts have been found in many species and cell types, including *Xenopus*, echinoderm and ascidian oocytes, zebrafish embryos and polarised somatic cells such as insect and mammalian neurones (Bashirullah et al., 1998), it is likely that these results will be applicable to many different systems. Cytoplasmic dynein is highly conserved in most eukaryotes, and is therefore a good candidate for the motor responsible for transporting other transcripts to microtubule minus ends. However, a major goal for the future will be the identification of the factors which link

mRNA cargoes to motor proteins and control binding and release of mRNA cargoes at their origins and destinations. When these processes are more completely understood, and the mechanisms that link these events to the anchoring and translational activation of mRNA at the site of localisation are better characterised, we will finally be able to describe the entire pathway of mRNA movement within the cell.

11

REFERENCES

Adams, M. D., Celniker, S. E., Holt, R. A., Evans, C. A., Gocayne, J. D., Amanatides, P. G., Scherer, S. E., Li, P. W., Hoskins, R. A., Galle, R. F., George, R. A., Lewis, S. E., Richards, S., Ashburner, M., Henderson, S. N., Sutton, G. G., Wortman, J. R., Yandell, M. D., Zhang, Q., Chen, L. X., Brandon, R. C., Rogers, Y. H., Blazej, R. G., Champe, M., Pfeiffer, B. D., Wan, K. H., Doyle, C., Baxter, E. G., Helt, G., Nelson, C. R., Gabor, G. L., Abril, J. F., Agbayani, A., An, H. J., Andrews-Pfannkoch, C., Baldwin, D., Ballew, R. M., Basu, A., Baxendale, J., Bayraktaroglu, L., Beasley, E. M., Beeson, K. Y., Benos, P. V., Berman, B. P., Bhandari, D., Bolshakov, S., Borkova, D., Botchan, M. R., Bouck, J., and et al. (2000). The genome sequence of *Drosophila melanogaster*. Science *287*, 2185-95.

Ahmad, F. J., Echeverri, C. J., Vallee, R. B., and Baas, P. W. (1998). Cytoplasmic dynein and dynactin are required for the transport of microtubules into the axon. J Cell Biol *140*, 391-401.

Alberts, B., Bray, D., Lewis, J., Raff, M., Roberts, K., and Watson, J. D. (1989). The Cell Nucleus. In Molecular Biology of the Cell (New York: Garland), pp. 481-549.

Alzhanova-Ericsson, A. T., Sun, X., Visa, N., Kiseleva, E., Wurtz, T., and Daneholt, B. (1996). Protein Of the SR Family Of Splicing Factors Binds Extensively to Exonic Balbiani Ring Pre-Messenger-RNA and Accompanies the RNA From the Gene to the Nuclear Pore. Genes & Development *10*, 2881-2893.

Amberg, D. C., Goldstein, A. L., and Cole, C. N. (1992). Isolation and Characterization Of *RAT1* - an Essential Gene Of *Saccharomyces cerevisiae* Required For the Efficient Nucleocytoplasmic Trafficking Of Messenger RNA. Genes & Development *6*, 1173-1189.

Andrulis, E. D., Neiman, A. M., Zappulla, D. C., and Sternglanz, R. (1998). Perinuclear localization of chromatin facilitates transcriptional silencing. Nature *394*, 592-5.

Arking, R. (1975). Temperature sensitive cell-lethal mutants of *Drosophila*: Isolation and characterization. Genetics *80*, 519--537.

Arts, G. J., Fornerod, M., and Mattaj, I. W. (1998). Identification of a nuclear export receptor for tRNA. Current Biology *8*, 305-314.

Bachi, A., Braun, I. C., Rodrigues, J. P., Pante, N., Ribbeck, K., von Kobbe, C., Kutay, U., Wilm, M., Gorlich, D., Carmo-Fonseca, M., and Izaurralde, E. (2000). The C-terminal domain of TAP interacts with the nuclear pore complex and promotes export of specific CTE-bearing RNA substrates. RNA *6*, 136-58.

Bailer, S. M., Siniossoglou, S., Podtelejnikov, A., Hellwig, A., Mann, M., and Hurt, E. (1998). Nup116p and nup100p are interchangeable through a conserved motif which constitutes a docking site for the mRNA transport factor gle2p. EMBO J *17*, 1107-19.

Baker, N. E. (1988). Embryonic and imaginal requirements for *wingless*, a segment-polarity gene in Drosophila. Dev Biol *125*, 96-108.

Bashirullah, A., Cooperstock, R. L., and Lipshitz, H. D. (1998). RNA localization in development. Annu Rev Biochem *67*, 335-94.

Bashirullah, A., Halsell, S. R., Cooperstock, R. L., Kloc, M., Karaiskakis, A., Fisher, W. W., Fu, W., Hamilton, J. K., Etkin, L. D., and Lipshitz, H. D. (1999). Joint action of two RNA degradation pathways controls the timing of maternal transcript elimination at the midblastula transition in Drosophila melanogaster. EMBO J *18*, 2610-20.

Bauren, G., and Wieslander, L. (1994). Splicing of Balbiani ring 1 gene pre-mRNA occurs simultaneously with transcription. Cell *76*, 183-92.

Bear, J., Tan, W., Zolotukhin, A. S., Tabernero, C., Hudson, E. A., and Felber, B. K. (1999). Identification of Novel Import and Export Signals of Human TAP, the Protein That Binds to the Constitutive Transport Element of the Type D Retrovirus mRNAs. Mol Cell Biol *19*, 6306-6317.

Bergsten, S. E., and Gavis, E. R. (1999). Role for mRNA localization in translational activation but not spatial restriction of nanos RNA. Development *126*, 659-69.

Beyer, A. L., and Osheim, Y. N. (1988). Splice site selection, rate of splicing, and alternative splicing on nascent transcripts. Genes Dev *2*, 754-65.

Bharathi, A., Ghosh, A., Whalen, W. A., Yoon, J. H., Pu, R., Dasso, M., and Dhar, R. (1997). The human RAE1 gene is a functional homologue of *Schizosaccharomyces pombe rae1* gene involved in nuclear export of Poly(A)+ RNA. Gene *198*, 251-8.

Blobel, G. (1985). Gene gating: A hypothesis. Proceedings of the National Academy of Sciences of the United States of America *82*, 8527-9.

Bobola, N., Jansen, R. P., Shin, T. H., and Nasmyth, K. (1996). Asymmetric accumulation of Ash1p in postanaphase nuclei depends on a myosin and restricts yeast mating-type switching to mother cells. Cell *84*, 699-709.

Bornfleth, H., Edelmann, P., Zink, D., Cremer, T., and Cremer, C. (1999). Quantitative motion analysis of subchromosomal foci in living cells using four-dimensional microscopy. Biophys J *77*, 2871-86.

Braun, I. C., Herold, A., Rode, M., Conti, E., and Izaurralde, E. (2001). Overexpression of TAP/p15 heterodimers bypasses nuclear retention and stimulates nuclear mRNA export. J Biol Chem *19*, 19.

Braun, I. C., Rohrbach, E., Schmitt, C., and Izaurralde, E. (1999). TAP binds to the constitutive transport element (CTE) through a novel RNA-binding motif that is sufficient to promote CTE-dependent RNA export from the nucleus. EMBO J *18*, 1953-1965.

Brendza, R. P., Serbus, L. R., Duffy, J. B., and Saxton, W. M. (2000). A function for kinesin I in the posterior transport of *oskar* mRNA and staufen protein. Science *289*, 2120-2.

Bridger, J. M., Herrmann, H., Munkel, C., and Lichter, P. (1998). Identification of an interchromosomal compartment by polymerization of nuclear-targeted vimentin. J Cell Sci *111*, 1241-53.

Brodsky, A. S., and Silver, P. A. (2000). Pre-mRNA processing factors are required for nuclear export. RNA *6*, 1737-49.

Brown, J. A., Bharathi, A., Ghosh, A., Whalen, W., Fitzgerald, E., and Dhar, R. (1995). A mutation in the Schizosaccharomyces pombe rae1 gene causes defects in poly(A)+ RNA export and in the cytoskeleton. J Biol Chem *270*, 7411-9.

Brown, K. E., Guest, S. S., Smale, S. T., Hanm, K., Merkenschlager, M., and Fisher, A. G. (1997). Association of transcriptionally silent genes with Ikaros complexes at centromeric heterochromatin. Cell *91*, 845-854.

Burkhardt, J. K., Echeverri, C. J., Nilsson, T., and Vallee, R. B. (1997). Overexpression of the dynamitin (p50) subunit of the dynactin complex disrupts dynein-dependent maintenance of membrane organelle distribution. J Cell Biol *139*, 469-84.

Carson, J. H., Worboys, K., Ainger, K., and Barbarese, E. (1997). Translocation of myelin basic protein mRNA in oligodendrocytes requires microtubules and kinesin. Cell Motil Cytoskeleton *38*, 318-28.

Castagnetti, S., Hentze, M. W., Ephrussi, A., and Gebauer, F. (2000). Control of *oskar* mRNA translation by Bruno in a novel cell-free system from *Drosophila* ovaries. Development *127*, 1063-1068.

Chandra, R., Endow, S. A., and Salmon, E. D. (1993). An N-terminal truncation of the ncd motor protein supports diffusional movement of microtubules in motility assays. J Cell Sci *104*, 899-906.

Chang, D. D., and Sharp, P. A. (1989). Regulation by HIV Rev depends upon recognition of splice sites. Cell *59*, 789-95.

Cheng, Y., Dahlberg, J. E., and Lund, E. (1995). Diverse effects of the guanine nucleotide exchange factor RCC1 on RNA transport. Science *267*, 1807-10.

Chou, T. B., and Perrimon, N. (1992). Use of a yeast site-specific recombinase to produce female germline chimeras in *Drosophila*. Genetics *131*, 643-53.

Clark, I., Giniger, E., Ruohola-Baker, H., Jan, L. Y., and Jan, Y. N. (1994). Transient posterior localization of a kinesin fusion protein reflects anteroposterior polarity of the *Drosophila* oocyte. Current Biology *4*, 289-300.

Clark, I. E., Jan, L. Y., and Jan, Y. N. (1997). Reciprocal localization of Nod and kinesin fusion proteins indicates microtubule polarity in the *Drosophila* oocyte, epithelium, neuron and muscle. Development *124*, 461-470.

Clemson, C. M., McNeil, J. A., Willard, H. F., and Lawrence, J. B. (1996). Xist RNA Paints the Inactive X-Chromosome At Interphase - Evidence For a Novel RNA Involved In Nuclear Chromosome Structure. J Cell Biol *132*, 259-275.

Cockerill, P. N., and Garrard, W. T. (1986). Chromosomal loop anchorage of the kappa immunoglobulin gene occurs next to the enhancer in a region containing topoisomerase II sites. Cell *44*, 273-82.

Connelly, S., and Manley, J. L. (1988). A functional mRNA polyadenylation signal is required for transcription termination by RNA polymerase II. Genes Dev *2*, 440-52.

Cordes, V. C., Reidenbach, S., Rackwitz, H. R., and Franke, W. W. (1997). Identification of protein p270/Tpr as a constitutive component of the nuclear pore complex-attached intranuclear filaments. J Cell Biol *136*, 515-29.

Cote, C. A., Gautreau, D., Denegre, J. M., Kress, T. L., Terry, N. A., and Mowry, K. L. (1999). A Xenopus protein related to hnRNP I has a role in cytoplasmic RNA localization. Mol Cell *4*, 431-7.

Craymer, L., and Roy, E. (1980). Report of New Mutants - *Drosophila melanogaster*. D. I. S. *55*, 200-204.

Cremer, T., Kurz, A., Zirbel, R., Dietzel, S., Rinke, B., Schrock, E., Speicher, M. R., Mathieu, U., Jauch, A., Emmerich, P., Scherthan, H., Ried, T., Cremer, C., and Lichter, P. (1993). Role Of Chromosome Territories In the Functional Compartmentalization Of the Cell-Nucleus. Cold Spring Harbor Symposia On Quantitative Biology *58*, 777-792.

Croft, J. A., Bridger, J. M., Boyle, S., Perry, P., Teague, P., and Bickmore, W. A. (1999). Differences in the Localization and Morphology of Chromosomes in the Human Nucleus. J Cell Biol*145*, 1119-1131.

Cullen, B. R. (2000). Connections between the processing and nuclear export of mRNA: evidence for an export license? PNAS USA *97*, 4-6.

Custodio, N., Carmo-Fonseca, M., Geraghty, F., Pereira, H. S., Grosveld, F., and Antoniou, M. (1999). Inefficient processing impairs release of RNA from the site of transcription. EMBO J *18*, 2855-66.

Dahanukar, A., Walker, J. A., and Wharton, R. P. (1999). Smaug, a novel RNA-binding protein that operates a translational switch in *Drosophila*. Mol Cell *4*, 209-18.

Daneholt, B. (1997). A look at messenger RNP moving through the nuclear pore. Cell *88*, 585-588.

Davis, I. (1990). Intracellular Message Localisation in *Drosophila melanogaster* (PhD Thesis: Oxford University).

Davis, I. (2000). Visualising fluorescence in *Drosophila* - optimal detection in thick specimens. In Protein Localisation by Fluorescence Microscopy: A Practical Approach, V. J. Allan, ed. (Oxford: OUP), pp. 131-162.

Davis, I., Francis-Lang, H., and Ish Horowicz, D. (1993). Mechanisms of intracellular transcript localization and export in early *Drosophila* embryos. Cold Spring Harbor Symposia On Quantitative Biology *58*, 793-798.

Davis, I., Girdham, C. H., and O Farrell, P. H. (1995). A nuclear GFP that marks nuclei in living *Drosophila* embryos - maternal supply overcomes a delay in the appearance of zygotic fluorescence. Developmental Biology *170*, 726-729.

Davis, I., and Ish-Horowicz, D. (1991). Apical localization of pair-rule transcripts requires 3' sequences and limits protein diffusion In the *Drosophila* blastoderm embryo. Cell *67*, 927-940.
e Castilla, C. S., and Rout, M. P. (1999). TAPping into transport. Nature Cell Biol. *1*, 31-33.

Degraaf, A., Vanhemert, F., Linnemans, W. A. M., Brakenhoff, G. F. J., Dejong, L., Vanrenswoude, J., and Vandriel, R. (1990). 3-Dimensional Distribution Of Dnase I-Sensitive Chromatin Regions In Interphase Nuclei Of Embryonal Carcinoma-Cells. European J Cell Biol *52*, 135-141.

Del Priore, V., Snay, C. A., Bahr, A., and Cole, C. N. (1996). The product of the *Saccharomyces cerevisiae RSS1* gene, identified as a high-copy suppressor of the *rat7-1* temperature-sensitive allele of the RAT7/NUP159 nucleoporin, is required for efficient mRNA export. Mol Biol Cell *7*, 1601-21.

Dernburg, A. F., Broman, K. W., Fung, J. C., Marshall, W. F., Philips, J., Agard, D. A., and Sedat, J. W. (1996). Perturbation Of Nuclear Architecture By Long-Distance Chromosome Interactions. Cell *85*, 745-759.

Deshler, J. O., Highett, M. I., Abramson, T., and Schnapp, B. J. (1998). A highly conserved RNA-binding protein for cytoplasmic mRNA localization in vertebrates. Curr Biol *8*, 489-96.

Dirks, R. W., Daniel, K. C., and Raap, A. K. (1995). RNAs radiate from gene to cytoplasm as revealed by fluorescence in situ hybridization. J Cell Sci *108*, 2565-2572.

Doye, V., and Hurt, E. (1997). From nucleoporins to nuclear pore complexes. Current Opinion In Cell Biology *9*, 401-411.

Driever, W., and Nüsslein-Volhard, C. (1988). A gradient of bicoid protein in *Drosophila* embryos. Cell *54*, 83-93.

Dubowy, J., and Macdonald, P. M. (1998). Localization of mRNAs to the oocyte is common in *Drosophila* ovaries. Mech Dev *70*, 193-5.

Echeverri, C. J., Paschal, B. M., Vaughan, K. T., and Vallee, R. B. (1996). Molecular characterization of the 50-kD subunit of dynactin reveals function for the complex in chromosome alignment and spindle organization during mitosis. J Cell Biol *132*, 617-33.

Eckley, D. M., Gill, S. R., Melkonian, K. A., Bingham, J. B., Goodson, H. V., Heuser, J. E., and Schroer, T. A. (1999). Analysis of dynactin subcomplexes reveals a novel actin-related protein associated with the arp1 minifilament pointed end. J Cell Biol *147*, 307-20.

Edgar, B. A., and O'Farrell, P. H. (1990). The 3 postblastoderm cell-cycles of *Drosophila* embryogenesis are regulated in G2 by string. Cell *62*, 469-480.

Edgar, B. A., Odell, G. M., and Schubiger, G. (1987). Cytoarchitecture and the patterning of *fushi tarazu* expression in the *Drosophila* blastoderm. Genes Dev *1*, 1226-37.

Edgar, B. A., Weir, M. P., Schubiger, G., and Kornberg, T. (1986). Repression and turnover pattern of *fushi tarazu* RNA in the early *Drosophila* embryo. Cell *47*, 747-54.

Eeken, J. C., Sobels, F. H., Hyland, V., and Schalet, A. P. (1985). Distribution of MR-induced sex-linked recessive lethal mutations in *Drosophila melanogaster*. Mutat. Res. *150*, 261-275.

Endow, S. A., Chandra, R., Komma, D. J., Yamamoto, A. H., and Salmon, E. D. (1994). Mutants of the *Drosophila* ncd microtubule motor protein cause centrosomal and spindle pole defects in mitosis. J Cell Sci *107*, 859-67.

Endow, S. A., and Komma, D. J. (1996). Centrosome and Spindle Function Of the *Drosophila* Ncd Microtubule Motor Visualized In Live Embryos Using Ncd-GFP Fusion Proteins. J Cell Sci *109*, 2429-2442.

Ephrussi, A., Dickinson, L. K., and Lehmann, R. (1991). Oskar organizes the germ plasm and directs localization of the posterior determinant *nanos*. Cell *66*, 37-50.

Erdelyi, M., Michon, A. M., Guichet, A., Glotzer, J. B., and Ephrussi, A. (1995). Requirement for *Drosophila* cytoplasmic tropomyosin in *oskar* mRNA localization. Nature *377*, 524-7.

Evgen'ev, M. B., and Denisenko, O. N. (1990). The effect of ts-mutation on expression of genes induced by heat shock in *Drosophila* melanogaster. Genetika, Moscow *26*, 266--271.

Fabre, E., and Hurt, E. (1997). Yeast genetics to dissect the nuclear pore complex and nucleocytoplasmic trafficking. Annual Review Of Genetics *31*, 277-313.

Fabre, E., and Hurt, E. C. (1994). Nuclear Transport. Current Opinion in Cell Biology *6*, 335-342.

Fahrenkrog, B., Hurt, E. C., Aebi, U., and Pante, N. (1998). Molecular architecture of the yeast nuclear pore complex: localization of Nsp1p subcomplexes. J Cell Biol *143*, 577-88.

Fay, F. S., Taneja, K. L., Shenoy, S., Lifshitz, L., and Singer, R. H. (1997). Quantitative digital analysis of diffuse and concentrated nuclear distributions of nascent transcripts, SC35 and poly(A). Experimental Cell Research *231*, 27-37.

Feldherr, C. M., Kallenbach, E., and Schultz, N. (1984). Movement of a karyophilic protein through the nuclear pores of oocytes. J Cell Biol *99*, 2216-22.

Femino, A., Fay, F. S., Fogarty, K., and Singer, R. H. (1998). Visualization of single RNA transcripts in situ. Science *280*, 585-590.

Ferrandon, D., Elphick, L., Nüsslein-Volhard, C., and St Johnston, D. (1994). Staufen protein associates with the 3'UTR of *bicoid* mRNA to form particles that move in a microtubule-dependent manner. Cell *79*, 1221-32.

Foe, V. E., and Alberts, B. M. (1983). Studies of nuclear and cytoplasmic behaviour during the five mitotic cycles that precede gastrulation in *Drosophila* embryogenesis. J Cell Sci *61*, 31-70.

Foe, V. E., Odell, G. M., and Edgar, B. A. (1993). Mitosis and morphogenesis in the *Drosophila* embryo: Point and counterpoint. In The development of *Drosophila melanogaster*, M. Bate and A. Martinez-Arias, eds. (New York: Cold Spring Harbour Laboratory Press), pp. 149-300.

Fornerod, M., Ohno, M., Yoshida, M., and Mattaj, I. W. (1997). CRM1 is an export receptor for leucine-rich nuclear export signals. Cell *90*, 1051-1060.

Francis-Lang, H., Davis, I., and Ish-Horowicz, D. (1996). Asymmetric localization of *Drosophila* pair-rule transcripts from displaced nuclei - evidence for directional nuclear export. EMBO J *15*, 640-649.

Fung, J. C., Marshall, W. F., Dernburg, A., Agard, D. A., and Sedat, J. W. (1998). Homologous chromosome pairing in *Drosophila melanogaster* proceeds through multiple independent initiations. J Cell Biol *141*, 5-20.

Gall, J. G., Bellini, M., Wu, Z., and Murphy, C. (1999). Assembly of the nuclear transcription and processing machinery: Cajal bodies (coiled bodies) and transcriptosomes. Mol Biol Cell *10*, 4385-402.

Gavis, E. R., and Lehmann, R. (1994). Translational Regulation Of Nanos By RNA Localization. Nature *369*, 315-318.

Geer, B. W., Lischwe, T. D., and Murphy, K. G. (1983). Male Fertility in *Drosophila melanogaster*: Genetics of the *vermillion* region. Journal of Experimental Zoology *225*, 107-118.

Gemkow, M., Verveer, P., and Arndt-Jovin, D. (1998). Homologous association of the Bithorax-Complex during embryogenesis: consequences for transvection in *Drosophila melanogaster*. Development *125*, 4541-4552.

Gepner, J., Li, M., Ludmann, S., Kortas, C., Boylan, K., Iyadurai, S. J., McGrail, M., and Hays, T. S. (1996). Cytoplasmic dynein function is essential in *Drosophila melanogaster*. Genetics *142*, 865-78.

Gergen, J. P., and Butler, B. A. (1988). Isolation of the *Drosophila* segmentation gene runt and analysis of its expression during embryogenesis. Genes Dev *2*, 1179-93.

Glotzer, J. B., Saffrich, R., Glotzer, M., and Ephrussi, A. (1997). Cytoplasmic flows localize injected *oskar* RNA in *Drosophila* oocytes. Current Biology *7*, 326-337.

Goldberg, M. W., Wiese, C., Allen, T. D., and Wilson, K. L. (1997). Dimples, pores, star-rings, and thin rings on growing nuclear envelopes: evidence for structural intermediates in nuclear pore complex assembly. J Cell Sci *110*, 409-20.

Goldstein, A. L., Snay, C. A., Heath, C. V., and Cole, C. N. (1996). Pleiotropic Nuclear Defects Associated With a Conditional Allele Of the Novel Nucleoporin Rat9p/Nup85p. Mol Biol Cell *7*, 917-934.

Goldstein, L. S., and Gunawardena, S. (2000). Flying through the *Drosophila* cytoskeletal genome. J Cell Biol *150*, F63-8.

Gonzalez, I., Buonomo, S. B., Nasmyth, K., and von Ahsen, U. (1999). ASH1 mRNA localization in yeast involves multiple secondary structural elementsand ash1 protein translation. Curr Biol *9*, 337-40.

Gonzalez-Reyes, A., Elliott, H., and St Johnston, D. (1995). Polarization of both major body axes in *Drosophila* by Gurken-Torpedo signaling. Nature *375*, 654-658.

Gonzalez-Reyes, A., and St Johnston, D. S. (1998). Patterning of the follicle cell epithelium along the anterior-posterior axis during *Drosophila* oogenesis. Development *125*, 2837-2846.

Gorlich, D. (1997). Nuclear protein import. Current Opinion In Cell Biology *9*, 412-419.

Gorlich, D., Kostka, S., Kraft, R., Dingwall, C., Laskey, R. A., Hartmann, E., and Prehn, S. (1995). Two different subunits of importin cooperate to recognize nuclear localization signals and bind them to the nuclear envelope. Current Biology *5*, 383-92.

Gorlich, D., and Kutay, U. (1999). Transport between the cell nucleus and the cytoplasm. Annu Rev Cell Dev Biol *15*, 607-60.

Gorsch, L. C., Dockendorff, T. C., and Cole, C. N. (1995). A Conditional Allele Of the Novel Repeat-Containing Yeast Nucleoporin *rat7/nup159* Causes Both Rapid Cessation Of Messenger-RNA Export and Reversible Clustering Of Nuclear Pore Complexes. J Cell Biol *129*, 939-955.

Gross, S. P., Welte, M. A., Block, S. M., and Wieschaus, E. F. (2000). Dynein-mediated cargo transport in vivo. A switch controls travel distance. J Cell Biol *148*, 945-56.

Gruter, P., Tabernero, C., vonKobbe, C., Schmitt, C., Saavedra, C., Bachi, A., Wilm, M., Felber, B. K., and Izaurralde, E. (1998). TAP, the human homolog of Mex67p, mediates CTE-dependent RNA export from the nucleus. Molecular Cell *1*, 649-659.

Gunkel, N., Yano, T., Markussen, F. H., Olsen, L. C., and Ephrussi, A. (1998). Localization-dependent translation requires a functional interaction between the 5' and 3' ends of *oskar* mRNA. Genes Dev *12*, 1652-64.

Habermann, A., Schroer, T. A., Griffiths, G., and Burkhardt, J. K. (2001). Immunolocalization of cytoplasmic dynein and dynactin subunits in cultured macrophages: enrichment on early endocytic organelles. J Cell Sci *114*, 229-240.

Hama, C., Ali, Z., and Kornberg, T. B. (1990). Region-specific recombination and expression are directed by portions of the *Drosophila* engrailed promoter. Genes Dev. *4*, 1079--1093.

Hansen, K., Birse, C. E., and Proudfoot, N. J. (1998). Nascent transcription from the *nmt1* and *nmt2* genes of *Schizosaccharomyces pombe* overlaps neighbouring genes. EMBO J *17*, 3066-77.

Havin, L., Git, A., Elisha, Z., Oberman, F., Yaniv, K., Schwartz, S. P., Standart, N., and Yisraeli, J. K. (1998). RNA-binding protein conserved in both microtubule- and microfilament- based RNA localization. Genes Dev *12*, 1593-8.

Hays, T. S., Porter, M. E., McGrail, M., Grissom, P., Gosch, P., Fuller, M. T., and McIntosh, J. R. (1994). A cytoplasmic dynein motor in *Drosophila*: identification and localization during embryogenesis. J Cell Sci *107*, 1557-69.

Heath, C. V., Copeland, C. S., Amberg, D. C., Delpriore, V., Snyder, M., and Cole, C. N. (1995). Nuclear Pore Complex Clustering and Nuclear Accumulation Of Poly(A)+ RNA Associated With Mutation Of the *Saccharomyces cerevisiae rat2/nup120* Gene. J Cell Biol *131*, 1677-1697.

Hellmuth, K., Lau, D. M., Bischoff, F. R., Kunzler, M., Hurt, E., and Simos, G. (1998). Yeast Los1p has properties of an exportin-like nucleocytoplasmic transport factor for tRNA. Mol Cell Biol *18*, 6374-86.

Herold, A., Suyama, M., Rodrigues, J. P., Braun, I. C., Kutay, U., Carmo-Fonseca, M., Bork, P., and Izaurralde, E. (2000). TAP (NXF1) belongs to a multigene family of putative RNA export factors with a conserved modular architecture. Mol Cell Biol *20*, 8996-9008.

Hochstrasser, M., Mathog, D., Gruenbaum, Y., Saumweber, H., and Sedat, J. W. (1986). Spatial organization of chromosomes in the salivary gland nuclei of *Drosophila melanogaster*. J Cell Biol *102*, 112-23.

Hodge, C. A., Colot, H. V., Stafford, P., and Cole, C. N. (1999). Rat8p/Dbp5p is a shuttling transport factor that interacts with Rat7p/Nup159p and Gle1p and suppresses the mRNA export defect of *xpo1-1* cells. EMBO J *18*, 5778-88.

Hoek, K. S., Kidd, G. J., Carson, J. H., and Smith, R. (1998). hnRNP A2 selectively binds the cytoplasmic transport sequence of myelin basic protein mRNA. Biochemistry *37*, 7021-9.

Homyk, T., Szidonya, J., and Suzuki, D. T. (1980). Behavioral mutants of *Drosophila melanogaster*. III. Isolation and mapping by direct visual observations of behavioral phenotypes. Molec. Gen. Genet. *177*, 553--565.

Hood, J. K., and Silver, P. A. (1998). Cse1p is required for export of Srp1p/importin-alpha from the nucleus in Saccharomyces cerevisiae. J Biol Chem *273*, 35142-6.

Huang, S., and Spector, D. L. (1996). Dynamic Organization Of Pre-Messenger-RNA Splicing Factors. J Cell Biochem *62*, 191-197.

Huber, J., Cronshagen, U., Kadokura, M., Marshallsay, C., Wada, T., Sekine, M., and Luhrmann, R. (1998). Snurportin1, an m3G-cap-specific nuclear import receptor with a novel domain structure. EMBO J *17*, 4114-26.

Hulskamp, M., Pfeifle, C., and Tautz, D. (1990). A morphogenetic gradient of hunchback protein organizes the expression of the gap genes *Kruppel* and *knirps* in the early *Drosophila* embryo. Nature *346*, 577-80.

Hulskamp, M., and Tautz, D. (1991). Gap Genes and Gradients - the Logic Behind the Gaps. Bioessays *13*, 261-268.

Hurt, E., Strasser, K., Segref, A., Bailer, S., Schlaich, N., Presutti, C., Tollervey, D., and Jansen, R. (2000). Mex67p mediates nuclear export of a variety of RNA polymerase II transcripts. J Biol Chem *275*, 8361-8.

Hutchison, N., and Weintraub, H. (1985). Localization of DNAseI-sensitive sequences to specific regions of interphase nuclei. Cell *43*, 471-482.

Iborra, F., Pombo, A., Jackson, D., and Cook, P. (1996). Active RNA polymerases are localized within discrete transcription 'factories' in human nuclei. J Cell Sci *109*, 1427-1436.

Iborra, F. J., Jackson, D. A., and Cook, P. R. (2000). The path of RNA through nuclear pores: apparent entry from the sides into specialized pores. J Cell Sci *113 Pt 2*, 291-302.

Iborra, F. J., Jackson, D. A., and Cook, P. R. (1998). The path of transcripts from extra-nucleolar synthetic sites to nuclear pores: transcripts in transit are concentrated in discrete structures containing SR proteins. J Cell Sci *111*, 2269-2282.

Izaurralde, E., Kutay, U., vonKobbe, C., Mattaj, I. W., and Gorlich, D. (1997). The asymmetric distribution of the constituents of the Ran system is essential for transport into and out of the nucleus. EMBO J *16*, 6535-6547.

Izaurralde, E., Lewis, J., Gamberi, C., Jarmolowski, A., McGuigan, C., and Mattaj, I. W. (1995). A Cap-Binding Protein Complex Mediating U snRNA Export. Nature *376*, 709-712.

Jackson, D. A., Hassan, A. B., Errington, R. J., and Cook, P. R. (1993). Visualization of focal sites of transcription within human nuclei. EMBO J *12*, 1059-65.

Jakel, S., and Gorlich, D. (1998). Importin beta, transportin, RanBP5 and RanBP7 mediate nuclear import of ribosomal proteins in mammalian cells. EMBO J *17*, 4491-4502.

Jansen, R. P., Dowzer, C., Michaelis, C., Galova, M., and Nasmyth, K. (1996). Mother cell-specific HO expression in budding yeast depends on the unconventional myosin myo4p and other cytoplasmic proteins. Cell *84*, 687-97.

Jarmolowski, A., Boelens, W. C., Izaurralde, E., and Mattaj, I. W. (1994). Nuclear Export Of Different Classes Of RNA Is Mediated By Specific Factors. J Cell Biol *124*, 627-635.

Jeanmougin, F., Thompson, J. D., Gouy, M., Higgins, D. G., and Gibson, T. J. (1998). Multiple sequence alignment with Clustal X. Trends Biochem Sci *23*, 403-5.

Joseph, E. M., and Melton, D. A. (1998). Mutant Vg1 ligands disrupt endoderm and mesoderm formation in Xenopus embryos. Development *125*, 2677-85.

Jullien, D., Gorlich, D., Laemmli, U. K., and Adachi, Y. (1999). Nuclear import of RPA in Xenopus egg extracts requires a novel protein XRIPalpha but not importin alpha. EMBO J *18*, 4348-58.

Kadowaki, T., Goldfarb, D., Spitz, L. M., Tartakoff, A. M., and Ohno, M. (1993). Regulation of RNA processing and transport by a nuclear guanine nucleotide release protein and members of the Ras superfamily. EMBO J *12*, 2929-37.

Kadowaki, T., Hitomi, M., Chen, S. P., and Tartakoff, A. M. (1994). Nuclear Messenger-RNA Accumulation Causes Nucleolar Fragmentation In Yeast *mtr2* Mutant. Mol Biol Cell *5*, 1253-1263.

Kadowaki, T., Zhao, Y., and Tartakoff, A. M. (1992). A conditional yeast mutant deficient in mRNA transport from nucleus to cytoplasm. PNAS USA *89*, 2312-6.

Kang, Y., and Cullen, B. R. (1999). The human tap protein is a nuclear mRNA export factor that contains novel RNA-binding and nucleocytoplasmic transport sequences. Genes Dev *13*, 1126-1139.

Karki, S., and Holzbaur, E. L. (1999). Cytoplasmic dynein and dynactin in cell division and intracellular transport. Curr Opin Cell Biol *11*, 45-53.

Karki, S., LaMonte, B., and Holzbaur, E. L. (1998). Characterization of the p22 subunit of dynactin reveals the localization of cytoplasmic dynein and dynactin to the midbody of dividing cells. J Cell Biol *142*, 1023-34.

Katahira, J., Str##er, K., Podtelejnikov, A., Mann, M., Jung, J. U., and Hurt, E. (1999). The Mex67p-mediated nuclear mRNA export pathway is conserved from yeast to human. EMBO J *18*, 2593-2609.

Kataoka, N., Yong, J., Kim, V. N., Velazquez, F., Perkinson, R. A., Wang, F., and Dreyfuss, G. (2000). Pre-mRNA splicing imprints mRNA in the nucleus with a novel RNA-binding protein that persists in the cytoplasm. Mol Cell *6*, 673-82.

Kelley, R. L. (1993). Initial organization of the *Drosophila* dorsoventral axis depends on an RNA-binding protein encoded by the squid gene. Genes Dev. *7*, 948--960.

Kilchherr, F., Baumgartner, S., Bopp, D., Frei, E., and Noll, M. (1986). Isolation of the *paired* gene of *Drosophila* and its spatial expression during early embryogenesis. Nature *321*, 493-499.

Kim-Ha, J., Kerr, K., and Macdonald, P. M. (1995). Translational regulation of *oskar* mRNA by Bruno, an ovarian RNA-binding protein, is essential. Cell *81*, 403--412.

Kim-Ha, J., Smith, J. L., and MacDonald, P. M. (1991). *oskar* mRNA is localized to the posterior pole of the *Drosophila* oocyte. Cell *66*, 23-35.

King, S. J., and Schroer, T. A. (2000). Dynactin increases the processivity of the cytoplasmic dynein motor. Nat Cell Biol *2*, 20-4.

Kiseleva, E., Goldberg, M. W., Allen, T. D., and Akey, C. W. (1998). Active nuclear pore complexes in Chironomus: visualization of transporter configurations related to mRNP export. J Cell Sci *111*, 223-236.

Kislauskis, E. H., Zhu, X. C., and Singer, R. H. (1997). Beta-actin messenger RNA localization and protein synthesis augment cell motility. J Cell Biol *136*, 1263-1270.

Kislauskis, E. H., Zhu, X. C., and Singer, R. H. (1994). Sequences Responsible For Intracellular-Localization Of Beta-Actin Messenger-RNA Also Affect Cell Phenotype. J Cell Biol *127*, 441-451.

Klingler, M., Soong, J., Butler, B., and Gergen, J. P. (1996). Disperse versus compact elements for the regulation of *runt* stripes in *Drosophila*. Developmental Biology *177*, 73-84.

Koepp, D. M., and Silver, P. A. (1996). A GTPase controlling nuclear trafficking: running the right way or walking RANdomly? Cell *87*, 1-4.

Kohler, M., Speck, C., Christiansen, M., Bischoff, F. R., Prehn, S., Haller, H., Gorlich, D., and Hartmann, E. (1999). Evidence for distinct substrate specificities of importin alpha family members in nuclear protein import. Mol Cell Biol *19*, 7782-91.

Kopczynski, C. C., and Muskavitch, M. A. (1992). Introns excised from the Delta primary transcript are localized near sites of *Delta* transcription. J Cell Biol*119*, 503-12.

Kosova, B., Pante, N., Rollenhagen, C., Podtelejnikov, A., Mann, M., Aebi, U., and Hurt, E. (2000). Mlp2p, a component of nuclear pore attached intranuclear filaments, associates with nic96p. J Biol Chem *275*, 343-50.

Kraemer, D., and Blobel, G. (1997). mRNA binding protein mrnp 41 localizes to both nucleus and cytoplasm. PNAS USA *94*, 9119-9124.

Krystosek, A., and Puck, T. T. (1990). The Spatial-Distribution Of Exposed Nuclear-DNA In Normal, Cancer, and Reverse-Transformed Cells. PNAS USA *87*, 6560-6564.

Ku, M., and Melton, D. A. (1993). Xwnt-11: a maternally expressed Xenopus wnt gene. Development *119*, 1161-73.

Kunzler, M., and Hurt, E. C. (1998). Cse1p functions as the nuclear export receptor for importin alpha in yeast. FEBS Letters *433*, 185-190.

Kurz, A., Lampel, S., Nickolenko, J. E., Bradl, J., Benner, A., Zirbel, R. M., Cremer, T., and Lichter, P. (1996). Active and Inactive Genes Localize Preferentially In the Periphery Of Chromosome Territories. J Cell Biol *135*, 1195-1205.

Kutay, U., Bischoff, F. R., Kostka, S., Kraft, R., and Gorlich, D. (1997). Export of importin alpha from the nucleus is mediated by a specific nuclear transport factor. Cell *90*, 1061-1071.

Kutay, U., Izaurralde, E., Bischoff, F. R., Mattaj, I. W., and Gorlich, D. (1997). Dominant-negative mutants of importin-beta block multiple pathways of import and export through the nuclear pore complex. EMBO J *16*, 1153-1163.

Kutay, U., Lipowsky, G., Izaurralde, E., Bischoff, F., Schwarzmaier, P., Hartmann, E., and Gorlich, D. (1998). Identification of a tRNA-Specific Nuclear Export Receptor. Molecular Cell *1*, 359-369.

Lall, S., Francis-Lang, H., Flament, A., Norvell, A., Schupbach, T., and Ish-Horowicz, D. (1999). Squid hnRNP protein promotes apical cytoplasmic transport and localization of *Drosophila* pair-rule transcripts. Cell *98*, 171-80.

Lamond, A., and Earnshaw, W. (1998). Structure and Function in the Nucleus. Science *280*, p547-553.

Lantz, V. A., Clemens, S. E., and Miller, K. G. (1999). The actin cytoskeleton is required for maintenance of posterior pole plasm components in the *Drosophila* embryo. Mech Dev *85*, 111-22.

Lawrence, J. B., Carter, K. C., and Xing, X. (1993). Probing Functional-Organization Within the Nucleus - Is Genome Structure Integrated With RNA-Metabolism. Cold Spring Harbor Symposia On Quantitative Biology *58*, 807-818.

Lawrence, J. B., Singer, R. H., and Marselle, L. M. (1989). Highly localized tracks of specific transcripts within interphase nuclei visualized by in situ hybridization. Cell *57*, 493-502.

Lee, M. S., and Silver, P. A. (1997). RNA movement between the nucleus and the cytoplasm. Curr Op Gen Dev *7*, 212-219.

Lefevre, G. (1969). The eccentricity of vermilion deficiencies in *Drosophila melanogaster*. Genetics *63*, 589--600.

Legrain, P., and Rosbash, M. (1989). Some Cis-Acting and Trans-Acting Mutants For Splicing Target Pre- Messenger RNA to the Cytoplasm. Cell *57*, 573-583.

Lehmann, R., and Ephrussi, A. (1994). Germ plasm formation and germ cell determination in *Drosophila*. Ciba Foundation Symposia *182*, 282-296.

Lehmann, R., and Tautz, D. (1994). In situ hybridization to RNA. Methods In Cell Biology *44*, 575-598.

Leitch, A. R., Mosgoller, W., Schwarzacher, T., Bennett, M. D., and Heslop-Harrison, J. S. (1990). Genomic in situ hybridization to sectioned nuclei shows chromosome domains in grass hybrids. J Cell Sci *95*, 335-41.

LeMaire, M. F., and Thummel, C. S. (1990). Splicing precedes polyadenylation during *Drosophila* E74A transcription. Mol Cell Biol *10*, 6059-63.

Lewis, J. D., and Tollervey, D. (2000). Like attracts like: getting RNA processing together in the nucleus. Science *288*, 1385-9.

Li, P., Yang, X. H., Wasser, M., Cai, Y., and Chia, W. (1997). Inscuteable and staufen mediate asymmetric localization and segregation of *prospero* RNA during *Drosophila* neuroblast cell divisions. Cell *90*, 437-447.

Lie, Y. S., and Macdonald, P. M. (1999). Translational regulation of *oskar* mRNA occurs independent of the cap and poly(A) tail in *Drosophila* ovarian extracts. Development *126*, 4989-96.

Liker, E., Fernandez, E., Izaurralde, E., and Conti, E. (2000). The structure of the mRNA export factor TAP reveals a cis arrangement of a non-canonical RNP domain and an LRR domain. EMBO J *19*, 5587-98.

Lindsley, D. L., and Zimm, G. G. (1992). The Genome of *Drosophila melanogaster* (San Diego: Academic Press, Inc.).

Lipshitz, H. D., and Smibert, C. A. (2000). Mechanisms of RNA localization and translational regulation. Curr Opin Genet Dev *10*, 476-88.

Logan, J., Falck-Pedersen, E., Darnell, J. E., Jr., and Shenk, T. (1987). A poly(A) addition site and a downstream termination region are required for efficient cessation of transcription by RNA polymerase II in the mouse beta-globin gene. PNAS USA *84*, 8306-10.

Long, R. M., Chartrand, P., Gu, W., Meng, X. H., Schaefer, M. R., and Singer, R. H. (1997). Characterization of transport and localization of ASH1 mRNA in yeast. Mol Biol Cell *8*, 2060-2060.

Long, R. M., Singer, R. H., Meng, X. H., Gonzalez, I., Nasmyth, K., and Jansen, R. P. (1997). Mating type switching in yeast controlled by asymmetric localization of ASH1 mRNA. Science *277*, 383-387.

Luo, M. J., and Reed, R. (1999). Splicing is required for rapid and efficient mRNA export in metazoans. PNAS USA *96*, 14937-42.

Macdonald, P. M., Ingham, P., and Struhl, G. (1986). Isolation, structure, and expression of *even-skipped*: a second pair- rule gene of *Drosophila* containing a homeo box. Cell *47*, 721-34.

MacDougall, N., Lad, Y., Wilkie, G., Francis-Lang, H., Sullivan, W., and Davis, I. (2001). Merlin, the *Drosophila* homologue of Neurofibromatosis-2, is specifically required in posterior follicle cells for axis formation in the oocyte. Development *128*, 665-673.

Mahowald, A. P., and Kambysellis, M. P. (1980). Oogenesis. In The genetics and biology of *Drosophila*, M. Ashburner and T. R. F. Wright, eds. (London: Academic Press), pp. 141-224.

Mamon, L. A., and Kutskova, Y. A. (1993). The role of the heat-shock proteins in recovery of cell proliferation following high temperature treatment of *Drosophila melanogaster*. Genetika, Moscow *29*, 791-798.

Marshall, W. F., Dernburg, A. F., Harmon, B., Agard, D. A., and Sedat, J. W. (1996). Specific interactions of chromatin with the nuclear-envelope: positional determination within the nucleus in *Drosophila* melanogaster. Mol Biol Cell *7*, 825-842.

Marshall, W. F., Fung, J. C., and Sedat, J. W. (1997). Deconstructing the nucleus: Global architecture from local interactions. Curr Op Gen Dev *7*, 259-263.

Marshall, W. F., and Sedat, J. W. (1999). Nuclear architecture. In Genomic Imprinting, An Interdisciplinary Approach, R. Ohlsson, ed. (Berlin, Heidelberg: Springer-Verlag), pp. 283-301.

Marshall, W. F., Straight, A., Marko, J. F., Swedlow, J., Dernburg, A., Belmont, A., Murray, A. W., Agard, D. A., and Sedat, J. W. (1997). Interphase chromosomes undergo constrained diffusional motion in living cells. Current Biology *7*, 930-939.

Martin, M., Iyadurai, S. J., Gassman, A., Gindhart, J. G., Jr., Hays, T. S., and Saxton, W. M. (1999). Cytoplasmic dynein, the dynactin complex, and kinesin are interdependent and essential for fast axonal transport. Mol Biol Cell *10*, 3717-28.

Martinez-Arias, A. (1993). Development and Patterning of the Larval Epidermis of *Drosophila*. In The development of *Drosophila melanogaster*, M. Bate and A. Martinez-Arias, eds. (New York: Cold Spring Harbour Laboratory Press).

Mathog, D., Hochstrasser, M., Gruenbaum, Y., Saumweber, H., and Sedat, J. (1984). Characteristic Folding Pattern Of Polytene Chromosomes In *Drosophila* Salivary Gland Nuclei. Nature *308*, 414-421.

Mattaj, I. W., and Englmeier, L. (1998). Nucleocytoplasmic transport: the soluble phase. Annu Rev Biochem *67*, 265-306.

Mattern, K. A., van Goethem, R. E., de Jong, L., and van Driel, R. (1997). Major internal nuclear matrix proteins are common to different human cell types. J Cell Biochem *65*, 42-52.

McDonald, H. B., Stewart, R. J., and Goldstein, L. S. (1990). The kinesin-like ncd protein of Drosophila is a minus end-directed microtubule motor. Cell *63*, 1159-65.

McGrail, M., Gepner, J., Li, M. G., Ludmann, S., Boylan, K., Iyadurai, S., and Hays, T. S. (1994). A mutational analysis of cytoplasmic dynein function in *Drosophila*. Molec. Biol. Cell *5*, 131a.

McGrail, M., and Hays, T. S. (1997). The microtubule motor cytoplasmic dynein is required for spindle orientation during germline cell divisions and oocyte differentiation in *Drosophila*. Development *124*, 2409-19.

McKnight, S., and Miller, O., Jr. (1976). Ultrastructural Patterns of RNA Synthesis during Early Embryogenesis of *Drosophila melanogaster*. Cell *8*, 305-319.

Melcak, I., Cermanova, S., Jirsova, K., Koberna, K., Malinsky, J., and Raska, I. (2000). Nuclear pre-mRNA compartmentalization: trafficking of released transcripts to splicing factor reservoirs. Mol Biol Cell *11*, 497-510.

Michael, W. M., Eder, P. S., and Dreyfuss, G. (1997). The K nuclear shuttling domain: a novel signal for nuclear import and nuclear export in the hnRNP K protein. EMBO J *16*, 3587-98.

Micklem, D. R., Adams, J., Grunert, S., and St Johnston, D. (2000). Distinct roles of two conserved Staufen domains in *oskar* mRNA localization and translation. EMBO J *19*, 1366-77.

Mirkovitch, J., Mirault, M. E., and Laemmli, U. K. (1984). Organization of the higher-order chromatin loop: specific DNA attachment sites on nuclear scaffold. Cell *39*, 223-32.

Munchow, S., Sauter, C., and Jansen, R. P. (1999). Association of the class V myosin Myo4p with a localised messenger RNA in budding yeast depends on She proteins. J Cell Sci *112*, 1511-8.

Murphy, R., Watkins, J. L., and Wente, S. R. (1996). GLE2, a Saccharomyces cerevisiae homologue of the Schizosaccharomyces pombe export factor RAE1, is required for nuclear pore complex structure and function. Mol Biol Cell *7*, 1921-37.

Murphy, R., and Wente, S. R. (1996). An RNA-export mediator with an essential nuclear export signal. Nature *383*, 357-60.

Nasmyth, K., and Jansen, R. P. (1997). The cytoskeleton in mRNA localization and cell differentiation. Current Opinion In Cell Biology *9*, 396-400.

Nelson, W. G., Pienta, K. J., Barrack, E. R., and Coffey, D. S. (1986). The role of the nuclear matrix in the organization and function of DNA. Annu Rev Biophys Biophys Chem *15*, 457-75.

Neri, L. M., Raymond, Y., Giordano, A., Capitani, S., and Martelli, A. M. (1999). Lamin A is part of the internal nucleoskeleton of human erythroleukemia cells. J Cell Physiol *178*, 284-95.

Neugebauer, K. M., and Roth, M. B. (1997). Distribution of pre-mRNA splicing factors at sites of RNA polymerase II transcription. Genes & Development *11*, 1148-59.

Neuman-Silberberg, F. S., and Schüpbach, T. (1994). Dorsoventral axis formation in *Drosophila* depends on the correct dosage of the gene gurken. Development *120*, 2457-2463.

Neuman-Silberberg, F. S., and Schüpbach, T. (1993). The *Drosophila* dorsoventral patterning gene *gurken* produces a dorsally localized RNA and encodes a TGF alpha-like protein. Cell *75*, 165-174.

Nickerson, J. A., Krockmalnic, G., Wan, K. M., and Penman, S. (1997). The nuclear matrix revealed by eluting chromatin from a cross-linked nucleus. PNAS USA *94*, 4446-50.

Nierras, C. R., Liebman, S. W., and Warner, J. R. (1997). Does *Saccharomyces* need an organized nucleolus? Chromosoma *105*, 444-51.

Noble, S. M., and Guthrie, C. (1996). Identification of novel genes required for yeast pre-mRNA splicing by means of cold-sensitive mutations. Genetics *143*, 67-80.

Nogami, M., Kohda, A., Taguchi, H., Nakao, M., Ikemura, T., and Okumura, K. (2000). Relative locations of the centromere and imprinted snRNP gene within chromosome 15 territories during the cell cycle in HL60 cells. J Cell Sci *113*, 2157-65.

Norvell, A., Kelley, R. L., Wehr, K., and Schüpbach, T. (1999). Specific isoforms of Squid, a *Drosophila* hnRNP, perform distinct roles in *gurken* localization during oogenesis. Genes Dev *13*, 864-876.

Nüsslein-Volhard, C., and Wieschaus, E. (1980). Mutations affecting segment number and polarity in *Drosophila*. Nature *287*, 795--801.

Ohtsubo, M., Okazaki, H., and Nishimoto, T. (1989). The RCC1 protein, a regulator for the onset of chromosome condensation locates in the nucleus and binds to DNA. J Cell Biol *109*, 1389-97.

Osheim, Y. N., Miller, O. L., Jr., and Beyer, A. L. (1985). RNP particles at splice junction sequences on *Drosophila* chorion transcripts. Cell *43*, 143-51.

Osheim, Y. N., Proudfoot, N. J., and Beyer, A. L. (1999). EM visualization of transcription by RNA polymerase II: downstream termination requires a poly(A) signal but not transcript cleavage. Mol Cell *3*, 379-87.

Palacios, I., Weis, K., Klebe, C., Mattaj, I. W., and Dingwall, C. (1996). Ran/Tc4 mutants identify a common requirement for snRNP and protein import into the nucleus. J Cell Biol *133*, 485-494.

Pankratz, M. J., and Jackle, H. (1993). Blastoderm Segmentation. In The development of *Drosophila melanogaster*, M. Bate and A. Martinez-Arias, eds. (New York: Cold Spring Harbour Laboratory Press).

Pante, N., Jarmolowski, A., Izaurralde, E., Sauder, U., Baschong, W., and Mattaj, I. W. (1997). Visualizing nuclear export of different classes of RNA by electron microscopy. RNA *3*, 498-513.

Pederson, T. (2000). Half a century of "the nuclear matrix". Mol Biol Cell *11*, 799-805.

Phair, R. D., and Misteli, T. (2000). High mobility of proteins in the mammalian cell nucleus. Nature *404*, 604-9.

Pokrywka, N. J., and Stephenson, E. C. (1995). Microtubules are a general component of mRNA localization systems in *Drosophila* oocytes. Dev. Biol. *167*, 363-370.

Pokrywka, N. J., and Stephenson, E. C. (1991). Microtubules mediate the localization of *bicoid* RNA during *Drosophila* oogenesis. Development *113*, 55-66.

Politz, J. C., Browne, E. S., Wolf, D. E., and Pederson, T. (1998). Intranuclear diffusion and hybridization state of oligonucleotides measured by fluorescence correlation spectroscopy in living cells. PNAS USA *95*, 6043–6048.

Politz, J. C., Tuft, R. A., Pederson, T., and Singer, R. H. (1999). Movement of nuclear poly(A) RNA throughout the interchromatin space in living cells. Current Biology *9*, 285-291.

Pollard, V. W., Michael, W. M., Nakielny, S., Siomi, M. C., Wang, F., and Dreyfuss, G. (1996). A Novel Receptor-Mediated Nuclear-Protein Import Pathway. Cell *86*, 985-994.

Pombo, A., and Cook, P. R. (1996). The localization of sites containing nascent RNA and splicing factors. Experimental Cell Research *229*, 201-203.

Presley, J. F., Cole, N. B., Schroer, T. A., Hirschberg, K., Zaal, K. J., and Lippincott-Schwartz, J. (1997). ER-to-Golgi transport visualized in living cells. Nature *389*, 81-5.

Pritchard, C. E., Fornerod, M., Kasper, L. H., and van Deursen, J. M. (1999). RAE1 is a shuttling mRNA export factor that binds to a GLEBS-like NUP98 motif at the nuclear pore complex through multiple domains. J Cell Biol *145*, 237-54.

Raap, A. K., Vandecorput, M. P. C., Vervenne, R. A. W., Vangijlswijk, R. P. M., Tanke, H. J., and Wiegant, J. (1995). Ultra-Sensitive Fish Using Peroxidase-Mediated Deposition Of Biotin- Tyramide or Fluorochrome-Tyramide. Human Molecular Genetics *4*, 529-534.

Rabl, C. (1885). Uber Zelltheilung. Morphol. Jahrb. *10*, 214-330.

Ramos, A., Grunert, S., Adams, J., Micklem, D. R., Proctor, M. R., Freund, S., Bycroft, M., St Johnston, D., and Varani, G. (2000). RNA recognition by a Staufen double-stranded RNA-binding domain. EMBO J *19*, 997-1009.

Ripoll, P., and Garcia-Bellido, A. (1979). Viability of homozygous deficiencies in somatic cells of *Drosophila melanogaster*. Genetics *91*, 443-453.

Robinson, J. T., Wojcik, E. J., Sanders, M. A., McGrail, M., and Hays, T. S. (1999). Cytoplasmic dynein is required for the nuclear attachment and migration of centrosomes during mitosis in *Drosophila*. J Cell Biol *146*, 597-608.

Rodrigues, J. P., Rode, M., Gatfield, D., Blencowe, B., Carmo-Fonseca, M., and Izaurralde, E. (2001). REF proteins mediate the export of spliced and unspliced mRNAs from the nucleus. PNAS USA *98*, 1030-5.

Rorth, P. (1996). A Modular Misexpression Screen In *Drosophila* Detecting Tissue- Specific Phenotypes. PNAS USA *93*, 12418-12422.

Ross, A. F., Oleynikov, Y., Kislauskis, E. H., Taneja, K. L., and Singer, R. H. (1997). Characterization of a beta-actin mRNA zipcode-binding protein. Molecular and Cellular Biology *17*, 2158-2165.

Rout, M. P., Aitchison, J. D., Suprapto, A., Hjertaas, K., Zhao, Y., and Chait, B. T. (2000). The yeast nuclear pore complex: composition, architecture, and transport mechanism. J Cell Biol *148*, 635-51.

Rubin, G. M., Hong, L., Brokstein, P., Evans-Holm, M., Frise, E., Stapleton, M., and Harvey, D. A. (2000). A Drosophila complementary DNA resource. Science *287*, 2222--2224.

Sabri, N., and Visa, N. (2000). The Ct-RAE1 protein interacts with Balbiani ring RNP particles at the nuclear pore. RNA *6*, 1597-609.

Sambrook, J., Fritsch, E. F., and Maniatis, T. (1989). Molecular Cloning : A Laboratory Manual, 2 Edition (New York: Cold Spring Harbour Laboratory Press).

Santos-Rosa, H., Moreno, H., Simos, G., Segref, A., Fahrenkrog, B., Pante, N., and Hurt, E. (1998). Nuclear mRNA export requires complex formation between Mex67p and Mtr2p at the nuclear pores. Mol Cell Biol *18*, 6826-38.

Saunders, C., and Cohen, R. S. (1999). The role of oocyte transcription, the 5'UTR, and translation repression and derepression in *Drosophila gurken* mRNA and protein localization. Molecular Cell *3*, 43-54.

Schalet, A. (1986). The distribution of and complementation relationships between spontaneous X-linked recessive lethal mutations recovered from crossing long-term laboratory stocks of *Drosophila* melanogaster. Mutat. Res. *163*, 115--144.

Schalet, A. (1969). A Y chromosorae carrying the v+ to dy+ region of the X. D. I. S. *44*, 123.

Schlenstedt, G., Saavedra, C., Loeb, J. D., Cole, C. N., and Silver, P. A. (1995). The GTP-bound form of the yeast Ran/TC4 homologue blocks nuclear protein import and appearance of poly(A)+ RNA in the cytoplasm. PNAS USA *92*, 225-9.

Schmitt, C., von Kobbe, C., Bachi, A., Pante, N., Rodrigues, J. P., Boscheron, C., Rigaut, G., Wilm, M., Seraphin, B., Carmo-Fonseca, M., and Izaurralde, E. (1999). Dbp5, a DEAD-box protein required for mRNA export, is recruited to the cytoplasmic fibrils of nuclear pore complex via a conserved interaction with CAN/Nup159p. EMBO J *18*, 4332-47.

Schmitt, C., von Kobbe, C., Bachi, A., Pante, N., Rodrigues, J. P., Boscheron, C., Rigaut, G., Wilm, M., Seraphin, B., Carmo-Fonseca, M., and Izaurralde, E. (1999). Dbp5, a DEAD-box protein required for mRNA export, is recruited to the cytoplasmic fibrils of nuclear pore complex via a conserved interaction with CAN/Nup159p. EMBO J *18*, 4332-47.

Schnorrer, F., Bohmann, K., and Nüsslein-Volhard, C. (2000). The molecular motor dynein is involved in targeting swallow and bicoid RNA to the anterior pole of *Drosophila* oocytes. Nat Cell Biol *2*, 185-90.

Schul, W., Groenhout, B., Koberna, K., Takagaki, Y., Jenny, A., Manders, E. M., Raska, I., van Driel, R., and de Jong, L. (1996). The RNA 3' cleavage factors CstF 64 kDa and CPSF 100 kDa are concentrated in nuclear domains closely associated with coiled bodies and newly synthesized RNA. EMBO J. *15*, 2883-2892.

Schüpbach, T., and Roth, S. (1994). Dorsoventral patterning in *Drosophila* oogenesis. Curr Opin Genet Dev *4*, 502-507.

Segref, A., Sharma, K., Doye, V., Hellwig, A., Huber, J., Luhrmann, R., and Hurt, E. (1997). Mex67p, a novel factor for nuclear mRNA export, binds to both poly(A)(+) RNA and nuclear pores. EMBO J *16*, 3256-3271.

Seksek, O., Biwersi, J., and Verkman, A. S. (1997). Translational diffusion of macromolecule-sized solutes in cytoplasm and nucleus. J Cell Biol *138*, 131-42.

Sharp, D. J., Brown, H. M., Kwon, M., Rogers, G. C., Holland, G., and Scholey, J. M. (2000a). Functional coordination of three mitotic motors in *Drosophila* embryos. Mol Biol Cell *11*, 241-253.

Sharp, D. J., Rogers, G. C., and Scholey, J. M. (2000b). Cytoplasmic dynein is required for poleward chromosome movement during mitosis in *Drosophila* embryos. Nat Cell Biol *2*, 922-30.

Shermoen, A. W., and O' Farrell, P. H. (1991). Progression of the cell-cycle through mitosis leads to abortion of nascent transcripts. Cell *67*, 303-310.

Simmonds, A. J., dosSantos, G., Livne-Bar, I., and Krause, H. M. (2001). Apical Localization of *wingless* Transcripts Is Required for Wingless Signaling. Cell *105*, 197–207.

Singer, R. H., and Green, M. R. (1997). Compartmentalization of eukaryotic gene expression: Causes and effects. Cell *91*, 291-294.

Singh, O. P., Bjorkroth, B., Masich, S., Wieslander, L., and Daneholt, B. (1999). The intranuclear movement of Balbiani ring pre-messenger ribonucleoprotein particles. Exp Cell Res *251*, 135-46.

Smibert, C. A., Lie, Y. S., Shillinglaw, W., Henzel, W. J., and Macdonald, P. M. (1999). Smaug, a novel and conserved protein, contributes to repression of *nanos* mRNA translation in vitro. RNA *5*, 1535-47.

Smith, K., Moen, P., Wydner, K., Coleman, J., and Lawrence, J. (1999). Processing of Endogenous Pre-mRNAs in Association with SC-35 Domains Is Gene Specific. J Cell Biol*144*, 617-629.

SnayHodge, C. A., Colot, H. V., Goldstein, A. L., and Cole, C. N. (1998). Dbp5p/Rat8p is a yeast nuclear pore-associated DEAD-box protein essential for RNA export. EMBO J *17*, 2663-2676.

Solsbacher, J., Maurer, P., Bischoff, F. R., and Schlenstedt, G. (1998). Cse1p is involved in export of yeast importin alpha from the nucleus. Molecular and Cellular Biology *18*, 6805-6815.

Spector, D. L. (1993). Macromolecular Domains Within the Cell-Nucleus. Annual Review Of Cell Biology *9*, 265-315.

Speel, E. J. M., Ramaekers, F. C. S., and Hopman, A. H. N. (1997). Sensitive multicolor fluorescence in situ hybridization using catalyzed reporter deposition (CARD) amplification. Journal Of Histochemistry & Cytochemistry *45*, 1439-1446.

Spradling, A. C. (1993). Developmental genetics of oogenesis. In The development of *Drosophila melanogaster*, M. Bate and A. M. Martinez Arias, eds. (New York: Cold Spring Harbour Laboratory Press), pp. 1-70.

St Johnston, D. (1995). The intracellular localization of messenger RNAs. Cell *81*, 161-170.

St Johnston, D., Beuchle, D., and Nüsslein-Volhard, C. (1991). *staufen*, a Gene Required to Localize Maternal RNAs In the Drosophila Egg. Cell *66*, 51-63.

Stephenson, E. C., Chao, Y.C., Fackelthal, J.D. (1988). Molecular analysis of the *swallow* gene of *Drosophila melanogaster*. Genes Dev. *2*, 1655-1665.

Stoffler, D., Fahrenkrog, B., and Aebi, U. (1999). The nuclear pore complex: from molecular architecture to functional dynamics. Current Opinion in Cell Biology *11*, 391-401.

Strambio-de-Castillia, C., Blobel, G., and Rout, M. P. (1999). Proteins connecting the nuclear pore complex with the nuclear interior. J Cell Biol *144*, 839-55.

Strasser, K., Bassler, J., and Hurt, E. (2000). Binding of the Mex67p/Mtr2p heterodimer to FXFG, GLFG, and FG repeat nucleoporins is essential for nuclear mRNA export. J Cell Biol *150*, 695-706.

Strasser, K., and Hurt, E. (1999). Nuclear RNA export in yeast. FEBS Letters *452*, 77-81.

Strasser, K., and Hurt, E. (2000). Yra1p, a conserved nuclear RNA-binding protein, interacts directly with Mex67p and is required for mRNA export. EMBO J *19*, 410-20.

Stutz, F., Bachi, A., Doerks, T., Braun, I. C., Seraphin, B., Wilm, M., Bork, P., and Izaurralde, E. (2000). REF, an evolutionary conserved family of hnRNP-like proteins, interacts with TAP/Mex67p and participates in mRNA nuclear export. RNA *6*, 638-50.

Stutz, F., and Rosbash, M. (1998). Nuclear RNA export. Genes Dev *12*, 3303-19.

Stuurman, N., de Graaf, A., Floore, A., Josso, A., Humbel, B., de Jong, L., and van Driel, R. (1992). A monoclonal antibody recognizing nuclear matrix-associated nuclear bodies. J Cell Sci *101*, 773-84.

Sun, X., Alzhanova-Ericsson, A. T., Visa, N., Aissouni, Y., Zhao, J., and Daneholt, B. (1998). The hrp23 protein in the balbiani ring pre-mRNP particles is released just before or at the binding of the particles to the nuclear pore complex. J Cell Biol *142*, 1181-93.

Sundell, C. L., and Singer, R. H. (1990). Actin mRNA localizes in the absence of protein synthesis. J Cell Biol *111*, 2397-2403.

Sundell, C. L., and Singer, R. H. (1991). Requirement for microfilaments in sorting of actin mRNA. Science *253*, 1275-1277.

Suyama, M., Doerks, T., Braun, I. C., Sattler, M., Izaurralde, E., and Bork, P. (2000). Prediction of structural domains of TAP reveals details of its interaction with p15 and nucleoporins. EMBO rep *1*, 53-8.

Suzuki, T. (1970). Temperature-Sensitive mutations in *Drosophila melanogaster*. Science *170*, 695-706.

Takizawa, P. A., Sil, A., Swedlow, J. R., Herskowitz, I., and Vale, R. D. (1997). Actin-dependent localization of an RNA encoding a cell-fate determinant in yeast. Nature *389*, 90-3.

Takizawa, P. A., and Vale, R. D. (2000). The myosin motor, Myo4p, binds Ash1 mRNA via the adapter protein, She3p. PNAS USA *97*, 5273-8.

Tan, W., Zolotukhin, A. S., Bear, J., Patenaude, D. J., and Felber, B. K. (2000). The mRNA export in *Caenorhabditis elegans* is mediated by Ce-NXF-1, an ortholog of human TAP/NXF and *Saccharomyces cerevisiae* Mex67p. RNA *6*, 1762-72.

Tautz, D., and Pfeifle, C. (1989). A non-radioactive in situ hybridization method for the localization of specific RNAs in *Drosophila* embryos reveals translational control of the segmentation gene *hunchback*. Chromosoma *98*, 81-85.

Tautz, D., and Pfeifle, C. (1989). A non-radioactive in situ hybridization method for the localization of specific RNAs in *Drosophila* embryos reveals translational control of the segmentation gene *hunchback*. Chromosoma *98*, 81-5.

Tennyson, C. N., Klamut, H. J., and Worton, R. G. (1995). The human dystrophin gene requires 16 hours to be transcribed and is cotranscriptionally spliced. Nat Genet *9*, 184-90.

Tetzlaff, M. T., Jackle, H., and Pankratz, M. J. (1996). Lack of *Drosophila* cytoskeletal tropomyosin affects head morphogenesis and the accumulation of *oskar* mRNA required for germ cell formation. EMBO J *15*, 1247-54.

Theurkauf, W. E., Alberts, B. M., Jan, Y. N., and Jongens, T. A. (1993). A central role for microtubules in the differentiation of *Drosophila* oocytes. Development *118*, 1169-1180.

Theurkauf, W. E., and Hazelrigg, T. I. (1998). In vivo analyses of cytoplasmic transport and cytoskeletal organization during *Drosophila* oogenesis: Characterization of a multi-step anterior localization pathway. Development *125*, 3655-66.

Theurkauf, W. E., Smiley, S., Wong, M. L., and Alberts, B. M. (1992). Reorganization of the cytoskeleton during *Drosophila* oogenesis - implications for axis specification and intercellular transport. Development *115*, 923-936.

Thio, G. L., Ray, R. P., Barcelo, G., and Schüpbach, T. (2000). Localization of gurken RNA in *Drosophila* oogenesis requires elements in the 5' and 3' regions of the transcript. Dev. Biol. *221*, 435-46.

Tower, J., Karpen, G. H., Craig, N., and Spradling, A. C. (1993). Preferential Transposition of *Drosophila* P-Elements to Nearby Chromosomal Sites. Genetics *133*, 347-359.

Trapp, B. D., Moench, T., Pulley, M., Barbosa, E., Tennekoon, G., and Griffin, J. (1987). Spatial segregation of mRNA encoding myelin-specific proteins. PNAS USA *84*, 7773-7.

Tseng, S. S. L., Weaver, P. L., Liu, Y., Hitomi, M., Tartakoff, A. M., and Chang, T. H. (1998). Dbp5p, a cytosolic RNA helicase, is required for poly(A)+ RNA export. EMBO J *17*, 2651-2662.

Valetti, C., Wetzel, D. M., Schrader, M., Hasbani, M. J., Gill, S. R., Kreis, T. E., and Schroer, T. A. (1999). Role of dynactin in endocytic traffic: effects of dynamitin overexpression and colocalization with CLIP-170. Mol Biol Cell *10*, 4107-20.

Vallee, R. B., and Sheetz, M. P. (1996). Targeting of motor proteins. Science *271*, 1539-44.

Visa, N., Alzhanovaericsson, A. T., Sun, X., Kiseleva, E., Bjorkroth, B., Wurtz, T., and Daneholt, B. (1996). A Pre-mRNA Binding Protein Accompanies the RNA From the Gene Through the Nuclear Pores and Into Polysomes. Cell *84*, 253-264.

Visa, N., Izaurralde, E., Ferreira, J., Daneholt, B., and Mattaj, I. W. (1996). A Nuclear Cap-Binding Complex Binds Balbiani Ring Pre-mRNA Cotranscriptionally and Accompanies the Ribonucleoprotein Particle During Nuclear Export. J Cell Biol *133*, 5-14.

Walker, R. A., Salmon, E. D., and Endow, S. A. (1990). The *Drosophila* claret segregation protein is a minus-end directed motor molecule. Nature *347*, 780-2.

Wang, J., Cao, L. G., Wang, Y. L., and Pederson, T. (1991). Localization of pre-messenger RNA at discrete nuclear sites. PNAS USA *88*, 7391-5.

Warrell, R. P., Jr., de The, H., Wang, Z. Y., and Degos, L. (1993). Acute promyelocytic leukemia. N Engl J Med *329*, 177-89.

Waterman-Storer, C. M., Karki, S. B., Kuznetsov, S. A., Tabb, J. S., Weiss, D. G., Langford, G. M., and Holzbaur, E. L. (1997). The interaction between cytoplasmic dynein and dynactin is required for fast axonal transport. PNAS USA *94*, 12180-5.

Watkins, J. L., Murphy, R., Emtage, J. L. T., and Wente, S. R. (1998). The human homologue of Saccharomyces cerevisiae Gle1p is required for poly(A)(+) RNA export. PNAS USA *95*, 6779-6784.

Webster, P. J., Liang, L., Berg, C. A., Lasko, P., and Macdonald, P. M. (1997). Translational repressor bruno plays multiple roles in development and is widely conserved. Genes Dev *11*, 2510-21.

Weeks, D. L., and Melton, D. A. (1987). A maternal mRNA localized to the vegetal hemisphere in *Xenopus* eggs codes for a growth factor related to TGF-beta. Cell *51*, 861-7.

Welte, M. A., Gross, S. P., Postner, M., Block, S. M., and Wieschaus, E. F. (1998). Developmental regulation of vesicle transport in *Drosophila* embryos: Forces and kinetics. Cell *92*, 547-57.

Wente, S. R., and Blobel, G. (1993). A Temperature-Sensitive Nup116 Null Mutant Forms a Nuclear-Envelope Seal Over the Yeast Nuclear-Pore Complex Thereby Blocking Nucleocytoplasmic Traffic. J Cell Biol *123*, 275-284.

Wilkie, G., and Davis, I. (1998). High resolution and sensitive mRNA in situ hybridisation using fluorescent tyramide signal amplification. Elsevier Trends Journals Technical Tips Online *t01458 (http://www.biomednet.com/db/tto)*.

Wilkie, G., Shermoen, A., O'Farrell, H., and Davis, I. (1999). Transcribed genes are localized according to chromosomal position within polarized *Drosophila* embryonic nuclei. Current Biology *9*, 1263-1266.

Wilkie, G. S., and Davis, I. (2001). *Drosophila wingless* and Pair-Rule Transcripts Localize Apically by Dynein-Mediated Transport of RNA Particles. Cell *105*, 209–219.

Wittmann, T., and Hyman, T. (1999). Recombinant p50/dynamitin as a tool to examine the role of dynactin in intracellular processes. Methods Cell Biol *61*, 137-43.

Xing, Y., and Lawrence, J. B. (1993). Nuclear RNA tracks: structural basis for transcription and splicing. Trends in Cell Biology *3*, 346-353.

Xing, Y. G., Johnson, C. V., Dobner, P. R., and Lawrence, J. B. (1993). Higher Level Organization Of Individual Gene Transcription and RNA Splicing. Science *259*, 1326-1330.

Xing, Y. G., Johnson, C. V., Moen, P. T., McNeil, J. A., and Lawrence, J. B. (1995). Nonrandom Gene Organization - Structural Arrangements Of Specific Pre-mRNA Transcription and Splicing With SC-35 Domains. J Cell Biol *131*, 1635-1647.

Yisraeli, J. K., Sokol, S., and Melton, D. A. (1990). A two-step model for the localization of maternal mRNA in *Xenopus* oocytes: involvement of microtubules and microfilaments in the translocation and anchoring of Vg1 mRNA. Development *108*, 289-98.

Zachar, Z., Kramer, J., Mims, I. P., and Bingham, P. M. (1993). Evidence for channeled diffusion of pre-mRNAs during nuclear RNA transport in metazoans. J Cell Biol *121*, 729-742.

Zeng, C., Kim, E., Warren, S. L., and Berget, S. M. (1997). Dynamic relocation of transcription and splicing factors dependent upon transcriptional activity. EMBO J *16*, 1401-12.

Zhimulev, I. F., and Ilyina, O. V. (1980). Localisation and some characteristics of *sbr* in *D. melanogaster*. Drosophila Information Service *55*, 146.

Zhimulev, I. F., Pokholkova, G. V., Bgatov, A. B., Umbetova, G. H., Solovjeva, I. V., and Khudyakov, Y. E. (1987). Fine cytogenetical analysis of the band 10A1-2 and adjoining regions in the *Drosophila melanogaster* X-chromosome. Biol. Zentbl. *106*, 699-719.

Zhou, Z., Luo, M. J., Straesser, K., Katahira, J., Hurt, E., and Reed, R. (2000). The protein Aly links pre-messenger-RNA splicing to nuclear export in metazoans. Nature *407*, 401-5.

Zirbel, R. M., Mathieu, U. R., Kurz, A., Cremer, T., and Lichter, P. (1993). Evidence for a nuclear compartment of transcription and splicing located at chromosome domain boundaries. Chromosome Res *1*, 93-106.

12

APPENDIX

A. *DROSOPHILA* STOCKS

The fly stocks used in this work are listed below. The wild type strain used throughout was *Oregon R* or yw^{67} unless stated otherwise. All genetic markers and balancer chromosomes have been described previously (Lindsley and Zimm, 1992).

Oregon R	Umea Drosophila Stock Centre, U-#W0670
sbr^{1}	Bloomington Drosophila Stock Centre, B-#94
sbr^{5} *(l(1)K4)*	(Zhimulev et al., 1987)
sbr^{6} *(l(1)K5)*	(Zhimulev et al., 1987)
sbr^{10} *(l(1)ts403)*	(Arking, 1975)
sbr^{12} *(24/45A)*	(Eeken et al., 1985)
magellan	Chris Korey and David Van Vactor
v^{24}	Umea Drosophila Stock Centre, U-#30170
yw; nlsGFPM; nlsGFPN	(Davis et al., 1995)
EP(X)108	(Rorth, 1996)
EP(X)109	(Rorth, 1996)
EP(X)1207	(Rorth, 1996)
$FliK^{1}$	(Homyk et al., 1980)
$Dhc64C^{6\text{-}6}$	(Gepner et al., 1996)
$Dhc64C^{6\text{-}8}$	(Gepner et al., 1996)
$Dhc64C^{6\text{-}10}$	(Gepner et al., 1996)
$Dhc64C^{8\text{-}1}$	(Gepner et al., 1996)

Aberrations around *sbr*

Aberration	Cytology	Reference
Df(1)C52	8E4; 9C1-4	(Lindsley and Zimm, 1992)
Df(1)N110	9B3-4; 9D1-2	(Lindsley and Zimm, 1992)
Df(1)HC133	9B9; 9F4	(Lindsley and Zimm, 1992)
Df(1)v-L15	9B1; 10A1	(Lefevre, 1969)
Df(1)v-L11	9C4; 10A1-2	(Lefevre, 1969)
Df(1)v-64f	9E7-8; 10A2	(Lefevre, 1969)
Df(1)Mec13	9F3-10A	Madeleine Nivard
Df(1)v-L4	9F5-6; 10A1	(Lefevre, 1969)
Df(1)v-L3	9F12; 10A7	(Lefevre, 1969)
Df(1)v-L1	9F13; 10A5	(Lefevre, 1969)
Df(1)v73	10A2; 10A5	(Ripoll and Garcia-Bellido, 1979)
Df(1)RA37	10A7; 10B17	(Lindsley and Zimm, 1992)
Dp(1;Y)v$^+$y$^+$	9F3; 10C2; h1-h25B	(Craymer and Roy, 1980)
Dp(1;Y))v$^+$y$^+$#3	9F4; 10E3-4; h1-h25	(Schalet, 1969)
Dp(1;2)v$^+$63i	9E1;10A11;56A	(Lefevre, 1969)

Temperature sensitive stock collection

The temperature sensitive (t.s.) lethal *Drosophila* lines were generated in a mutagenesis scheme that takes advantage of the fact that males are hemizygous for the X chromosome (H. Francis-Lang and W. Sullivan, unpublished information and (MacDougall et al., 2001). Mutations were induced by EMS treatment of male flies of the genotype *y^1,Df(1)w^{67}/Y* (*y,w*) which were then crossed *en masse* to viable homozygous *FM7a,B,y^{31d},w^a,v^{Of}* (*FM7a*) balancer females. Virgin female progeny of genotype *y,w/FM7a* were then pair mated to *FM7a/Y* males to create individual balanced mutant lines. 10,000 mutant lines were screened for mutations which were lethal to *y,w/Y* males at 29°C but which showed viable *y,w/Y* males at 29°C. This yielded 180 lines with lethal t.s. mutations on the *y,w* X chromosome. These lines were balanced over the female sterile *FM7c,B,y^{31d},w^a,v^{Of}* chromosome (*FM7c*) to create stable stocks of the genotype *y,w,l(1)t.s./FM7c*.

Homozygous t.s. lines were created by maintaining the balanced *y,w,l(1)t.s./FM7c* stocks at 18°C or 21°C for a few generations, then crossing individual *y,w,l(1)t.s./Y* males to homozygous virgin *y,w,l(1)t.s* females. 100 homozygous viable t.s. lines were created in this way and maintained at the permissive temperature (18°C or 21°C).

B. Primers used for PCR and Sequencing

Primers for amplification *hairy* intron 1

These primers were used to amplify intron 1 of the hairy gene from genomic DNA, and incorporate T3 and T7 RNA polymerase promoters into the PCR product

GW1 AATTAACCCT CACTAAAGGG ATCCGTCGGG TAAGTTTCTT TCG
GW2 AATTAACCCT CACTAAAGGG ATCCGAAGCG AACCAAACCG AG
GW3 TAATACGACT CACTATAGGG TACCGGGTCT TCAATTGGAT TGG
GW4 TAATACGACT CACTATAGGG TACCATACGG CTTTTGCACG GC

Primers used to amplify and sequence *sbr*

GW13 GGAAGTTCAA TCGCAATCTC CG
GW14 ACTGCCCGAA TGTGCACACA AC
GW16 GGTTAAGTGC CTCCAAATCG GG
GW17 TGCGAAGCAC TACAAGGTGG G
GW18 GACATCGCTG CCAATAGAGC
GW19 CCATTAGACG TCGTCTGTCG
GW20 CGACAGACGA CGTCTAATGG
GW21 TCCTGGACCA GTACTTCCGC
GW22 TCCTGATAGT ATAGCCACCG G
GW23 CCTCAATGTA GACCAGCG
GW24 GGAGCAGTCT TATCATTCAAGCC
GW25 GCTATGCGTG GAACTCATCA CC
GW26 CGAACGCATT CAACATCTGG GC
GW27 AGGCGGGATT GTTGGTCTCG
GW28 GTCACAGCAC ACATCTAGCC C
GW29 CACTACCCAC TTATCCATCC CG
GW30 CTTGAGTGCT CTATTGGCAG CG
GW31 GCCGAACGCA TTCAACATCT GG
GW32 GATCGGATTT GACATTCTCG GG
GW33 CCACAGACAA CAATGGCAGC C
GW34 CGAGGAGACC AAGAATGG
GW35 CTAACAAGTG AACACCACAT CG
GW36 GGAAACTTGC GACGTACTTC GC
GW37 CTTCGTTTCG AGAAGACGTC CC
GW38 GTGGAGAAAC GCTTACCGAA CC
GW39 GCGCCTGAAT TTCAATATCG
GW40 CGTGAGTCTG TTGTGAGTGT GT
GW41 CACTCTTGAG TGCTCTATTG G
GW42 TTCGGTGTCA GAGGAAGTGG
GW43 CGCCCAGATA TACGAAAAGG
GW44 TCTATTGGCA GCGATGTCGC
GW45 ACATCTGGCA TGCGAGCAAC C
GW46 AAATATGTCT CAGCCAGCGA GC
GW47 TTGCGTATCG CTGACCTTCG
GW48 GGTAATTTTG GTTTCCGAGT CG
GW49 TCGACCATCG CCTTGGTTTC G
GW50 AAGCCATGAG CGCCCAAAGC
GW51 TATCGACAAC AGCAGTGGCA CC
GW52 TTCATCACAA ACGCTACGCA CG
GW53 CCAGATGTTG AATGCGTTCG GC
GW54 GGATGGATAA GTGGGTAGTG GG
GW55 CCTCTGACAC CGAAGGTCAG
GW56 CGAATGCGAG TACTGGCTGG C
GW57 GTATGTAGGT TGCTCGCATG CC

C. PUBLICATIONS.

Wilkie, G. S., and Davis, I. (2001). *Drosophila wingless* and Pair-Rule Transcripts Localize Apically by Dynein-Mediated Transport of RNA Particles. Cell *105*, 209–219.

MacDougall, N., Lad, Y., **Wilkie, G. S.** , Francis-Lang, H., Sullivan, W., and Davis, I. (2001). Merlin, the *Drosophila* homologue of Neurofibromatosis-2, is specifically required in posterior follicle cells for axis formation in the oocyte. Development *128*, 665-673.

Wilkie, G. S., Shermoen, A., O'Farrell, H., and Davis, I. (1999). Transcribed genes are localized according to chromosomal position within polarized *Drosophila* embryonic nuclei. Current Biology *9*, 1263-1266.

Wilkie, G. S., and Davis, I. (1998). High resolution and sensitive mRNA *in situ* hybridisation using fluorescent tyramide signal amplification. Elsevier Trends Journals Technical Tips Online *t01458 (http://www.biomednet.com/db/tto)*.

Cell, Vol. 105, 209–219, April 20, 2001, Copyright ©2001 by Cell Press

Drosophila wingless and Pair-Rule Transcripts Localize Apically by Dynein-Mediated Transport of RNA Particles

Gavin S. Wilkie and Ilan Davis*
Wellcome Trust Centre for Cell Biology
ICMB
University of Edinburgh
King's Buildings
Edinburgh EH9 3JR
Scotland, United Kingdom

Summary

Asymmetric mRNA localization targets proteins to their cytoplasmic site of function. We have elucidated the mechanism of apical localization of *wingless* and pair-rule transcripts in the *Drosophila* blastoderm embryo by directly visualizing intermediates along the entire path of transcript movement. After release from their site of transcription, mRNAs diffuse within the nucleus and are exported to all parts of the cytoplasm, regardless of their cytoplasmic destinations. Endogenous and injected apical RNAs assemble selectively into cytoplasmic particles that are transported apically along microtubules. Cytoplasmic dynein is required for correct localization of endogenous transcripts and apical movement of injected RNA particles. We propose that dynein-dependent movement of RNA particles is a widely deployed mechanism for mRNA localization.

Introduction

Asymmetric mRNA localization is a common posttranscriptional method of targeting proteins efficiently to their site of function (St. Johnston, 1995; Lipshitz and Smibert, 2000). It is estimated that 10% of all mRNAs in the *Drosophila* oocyte (Dubowy and Macdonald, 1998), and probably in other organisms, are localized asymmetrically. However, the mechanism of localization is still poorly understood in most cases. Examples include actin mRNA localization that targets actin filaments to the distal lamellae of chicken embryo fibroblasts (Sundell and Singer, 1990), an essential process for cell motility (Kislauskis et al., 1997). In *Xenopus* oocytes, Vg1 mRNA is localized to the vegetal hemisphere and may play a role in mesoderm induction (Weeks and Melton, 1987; Joseph and Melton, 1998). In *Saccharomyces cerevisiae*, *Ash1* mRNA is localized to the bud of a dividing cell (Long et al., 1997), ensuring that Ash1p suppresses mating type switching only in the daughter cell (Bobola et al., 1996).

In *Drosophila*, transcript localization plays an important role in development. The anteroposterior and dorsoventral axes of the embryo are specified in the oocyte through the localization of three mRNAs. *gurken* (*grk*) mRNA localization targets the Grk TGFα-like signal to specific groups of follicle cells, thus establishing the embryonic axes (Neuman-Silberberg and Schüpbach, 1993; Gonzalez-Reyes et al., 1995). *bicoid* (*bcd*) mRNA is localized to the anterior of the oocyte, forming a long-range anteroposterior gradient of nuclear protein in the embryo (Berleth et al., 1988). *oskar* (*osk*) mRNA is localized at the posterior, targeting Osk protein to the posterior and specifying germ plasm formation (Ephrussi et al., 1991).

mRNA localization is also important in the *Drosophila* syncytial blastoderm embryo, which consists of a monolayer of 6000 nuclei that are coaligned along the cortex. The nuclei and surrounding cytoplasm have a pronounced apical-basal polarity with most microtubules (MTs) lying apical of the nuclei where their minus ends and centrosomes are located. Most MT plus ends are found in the basal cytoplasm and in the yolk (Foe et al., 1993). There are three alternate patterns of mRNA distributions in the cytoplasm surrounding each nucleus. The segment polarity transcript *wingless* (*wg*) and pair-rule transcripts such as *fushi tarazu* (*ftz*), *hairy* (*h*), and *runt* (*run*) are apically localized. However, *string* (*stg*) mRNA, which encodes the *Drosophila* homolog of CDC25 (Edgar and O'Farrell, 1990), is basally localized. Gap transcripts such as *hunchback* (*hb*) and *Kruppel* (*Kr*) are unlocalized (Davis and Ish-Horowicz, 1991), probably allowing these nuclear proteins to diffuse and form short-range gradients in the embryo (Hulskamp et al., 1990). In contrast, the apical localization of pair-rule transcripts is thought to restrict the lateral diffusion of the nuclear transcription factors they encode (Davis and Ish-Horowicz, 1991; Davis et al., 1993). The apical localization of *wg* mRNA is required to target the Wnt-like Wg secreted protein to the apical membrane (Simmonds et al., 2001 [this issue of *Cell*]).

Four models have been proposed for the mechanism of apical mRNA localization (Francis-Lang et al., 1996) and all other asymmetrically localized transcripts (Lipshitz and Smibert, 2000). RNA could be exported directly from the apical side of the nucleus. Alternatively, unlocalized RNA could be selectively degraded in the basal cytoplasm, or could diffuse freely and become anchored in the apical cytoplasm. Finally, mRNA could be transported actively within the cytoplasm. While the precise mechanism and path of localization of most transcripts is uncharacterized, *cis*-acting sequences in the 3′ UTR usually determine the site of localization (St. Johnston, 1995). However, the identity and function of the factors that bind to these signals are mostly unknown.

There is increasing evidence that MTs are important for long distance localization processes, while actin has a role over short distances. Actin mRNA localization in fibroblast cells is dependent on actin microfilaments (Sundell and Singer, 1991), while *bcd* (Pokrywka and Stephenson, 1991), Vg1 (Yisraeli et al., 1990), and pair-rule mRNA localization are MT dependent (Edgar et al., 1987; Lall et al., 1999). Interestingly, *osk* mRNA localization is actin and MT dependent (Theurkauf et al., 1993; Erdelyi et al., 1995; Glotzer et al., 1997). Furthermore, some mRNAs are thought to localize by motor-mediated transport along actin or MTs. Ash1 mRNA localization

*To whom correspondence should be addressed (e-mail: ilan.davis@ed.ac.uk).

in yeast requires myosin and actin (Takizawa et al., 1997). *osk* mRNA localization requires the plus end directed motor, Kinesin I (Brendza et al., 2000). *bcd* localization depends on *swallow* (*swa*) (Stephenson et al., 1988), a putative linker to the minus end directed MT motor cytoplasmic dynein (Schnorrer et al., 2000). *bcd* mRNA localization also requires *exuparentia* (*exu*) (St Johnston et al., 1989), a protein that has been visualized moving within particles in an MT-dependent manner in living egg chambers (Theurkauf and Hazelrigg, 1998), suggesting that *bcd* mRNA may move in Exu-containing particles along MTs with Swa and dynein. However, Exu particles do not contain *bcd* mRNA (Wilhelm et al., 2000) and *bcd* mRNA localization has not been shown directly to require dynein. Furthermore, dynein has not yet been shown directly to be required for any mRNA localization process, despite its involvement in the movement of many other cytoplasmic components (Vallee and Sheetz, 1996).

Here we use a combination of highly sensitive in situ hybridization in fixed embryos and time-lapse imaging of fluorescently tagged RNA in living embryos to observe intermediates in the movement of apically targeted transcripts in blastoderm embryos. We have followed the movement of apical mRNAs from their site of transcription to their final site of apical localization in the cytoplasm. Apical, basal, and unlocalized mRNAs reach the nuclear envelope by diffusion, and are exported in all directions. Apically targeted transcripts selectively assemble into particles that move rapidly to the apical cytoplasm by dynein-mediated movement along MTs. Our observations explain the speed and polarity of apical mRNA localization in the blastoderm embryo and suggest a similar mechanism of localization for other transcripts.

Results

Specific mRNAs Diffuse from Their Site of Transcription to the Nuclear Periphery and Are Exported in All Directions

Previous studies showed that the transcription of most mRNAs in the blastoderm embryo occurs at nuclear nascent transcript foci, usually in the nuclear interior (O'Farrell et al., 1989; Davis and Ish-Horowicz, 1991; Wilkie et al., 1999). To test whether different transcripts move along distinct paths after release from the site of transcription, we used high resolution and sensitive fluorescent in situ hybridization (Wilkie and Davis, 1998). Probes against apical, basal, and unlocalized transcripts detect punctate nuclear sites of hybridization in addition to brighter nascent transcript foci (Figure 1) (Wilkie et al., 1999) and abundant cytoplasmic mRNA (Figure 1). The fainter punctate signal is found only in regions of the embryo where the gene is expressed, which is almost exclusively within stripes (Figure 2A). Mutant embryos that lack both copies of the *ftz* gene show no nuclear or cytoplasmic staining above background (Figure 2B), whereas sibling embryos from the same collection are indistinguishable from wild-type embryos (data not shown). We conclude that the punctate nuclear signal represents export intermediates en route from the site of transcription and processing to the nuclear envelope for export to the cytoplasm.

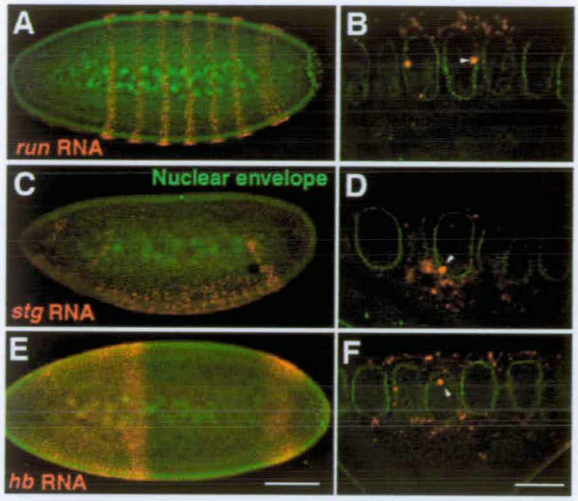

Figure 1. Apical, Basal, and Unlocalized mRNAs in *Drosophila* Blastoderm Embryos

High resolution and sensitivity in situ hybridization on interphase 14 syncytial blastoderm embryos showing mRNA (red, cy3) and the nuclear envelope (green, Alexafluor488-Wheat Germ Agglutinin). (A, C, and E) Low-powered images showing the pattern of expression in embryo (anterior to the left). (B, D, and F) High-powered images showing bright nascent transcript foci (arrowheads) and the site of mRNA localization in the cytoplasm near the syncytial nuclei. (A and B) *run* mRNA is apical. (C and D) *stg* mRNA is predominantly basal. (E and F) *hb* mRNA is unlocalized. High-powered and low-powered images are shown at the same scale with scale bars 10 μm and 50 μm, respectively, in this and all subsequent figures, unless otherwise stated.

To determine whether export intermediates show any directionality in their movement, or diffuse freely within the nucleoplasm, we measured their intranuclear positions. The location of export intermediates was mapped along the apical-basal axis of the nucleus using stacks of optical sections captured at 0.2 μm intervals (Figures 2C–2L). Our results show that export intermediates for apically targeted transcripts (*run, ftz, and wg*) are distributed throughout the nucleoplasm and nuclear envelope (Figures 2G–2I). Basal *stg* and unlocalized (*Kr* and *hb*) transcripts show a similar even distribution (Figures 2J–2L). We conclude that, regardless of their final site of cytoplasmic localization, specific transcripts diffuse from their site of synthesis and are exported in all directions.

Injected *wg* and Pair-Rule RNAs Localize Rapidly and Directly in Particles Similar to Endogenous Localization Intermediates

In addition to export intermediates, we detect unlocalized punctate cytoplasmic signal with a similar range of intensities, approximately 4-fold greater than background fluorescence in the embryo (data not shown). The cytoplasmic signal represents localization intermediates, as it is found only in regions of the embryo where the gene is expressed (Figures 1 and 2A), and is not present in mutant embryos that lack both copies of the *ftz* gene (Figure 2B).

To determine how cytoplasmic intermediates move within the cytoplasm to their final site of localization,

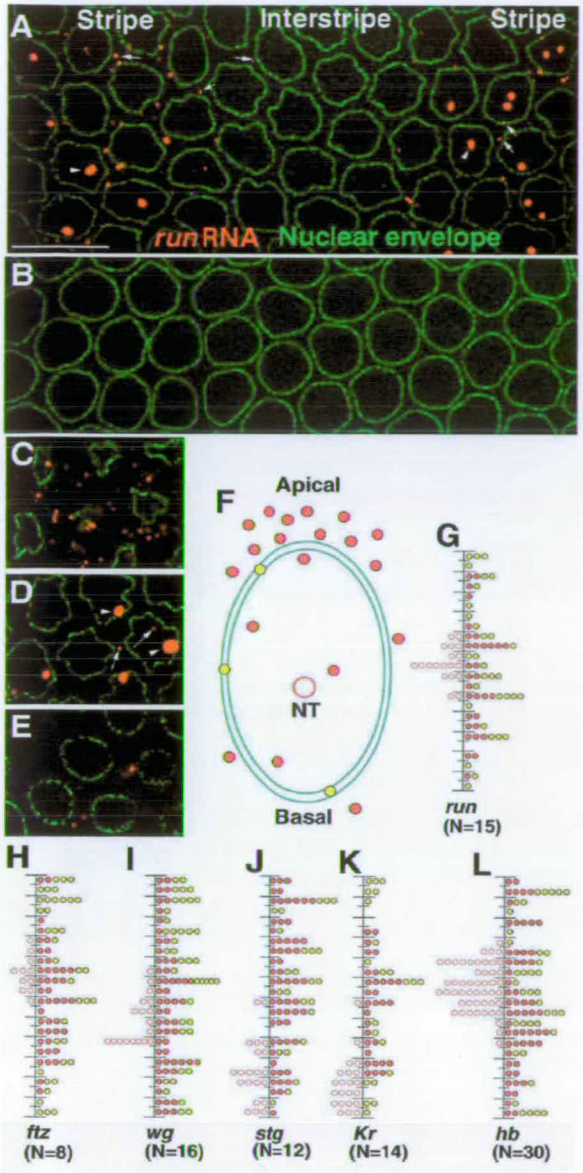

Figure 2. The Distribution of Intermediates in Nuclear Movement and Export of *run* mRNA

(A) Stripes 1 and 2 of *run* mRNA (red) visible within nuclei as bright nascent transcript foci (arrowheads) and fainter signal in the nucleus and cytoplasm (arrows), which are sometimes colocalized with the nuclear envelope (green). mRNA is only rarely detected in the interstripe region (arrows).

(B) In situ hybridization to detect *ftz* mRNA in a mutant that lacks the *ftz* gene, showing no detectable signal above background.

(C) A section through the apical part of nuclei showing punctate *run* mRNA (red) in the apical cytoplasm and some nuclear intermediates.

(D and E) Sections through the middle and basal part, respectively, of the same nucleus as (C) showing bright nascent transcripts and fainter intermediates within nuclei and cytoplasm.

(F) A diagram representing an interphase 14 nucleus showing a nascent transcript focus (NT, open red circle) and localization intermediates in the nucleoplasm and cytoplasm (red circles) and in the nuclear envelope (yellow circles).

(G–L) Positions of nascent transcripts (open red circles), mRNA particles in the nucleus (red circles) or on the nuclear envelope (yellow circles) from N nuclei within a single or two embryos. Each line represents the apical-basal axis of the nucleus and each graduation represents 0.5 μm. Nascent transcript foci are localized according to their chromosomal position in the apical-basal axis (as previously described), but localization intermediates are in all parts of the nucleoplasm and nuclear envelope.

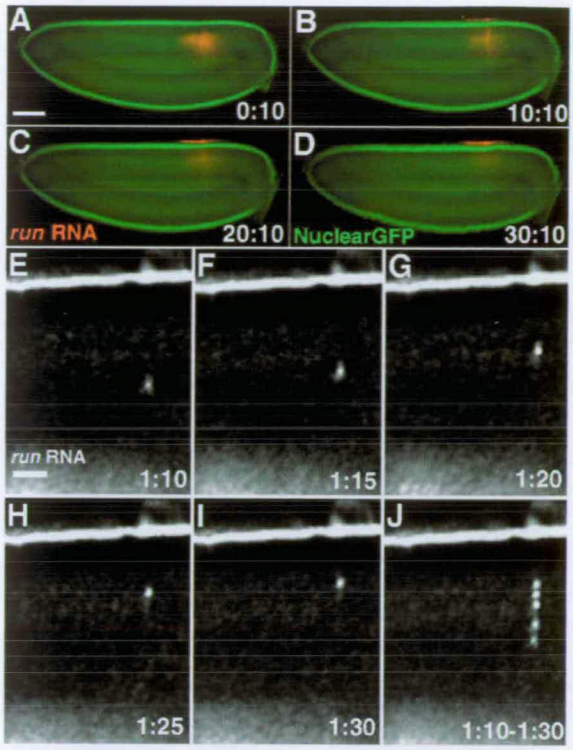

Figure 3. Injected Apically Targeted RNA Assembles into Particles that Localize Apically in Living Blastoderm Embryos

(A–D) Four snapshots from a time lapse movie of a blastoderm embryo expressing nlsGFP (green nuclei) and injected with AlexaFluor546-labeled protein-free *run* RNA (red). Within 20 min, the majority of injected *run* RNA localizes to the apical cytoplasm.

(E–J) Higher power view of six snapshots from a similar time lapse movie showing the movement of a typical particle of injected *run* RNA. (J) A composite image of (E)–(I) showing an RNA particle moving directly apically at an average speed of approximately 0.5 μm/sec. The time in minutes and seconds after injection is shown on the bottom right.

we studied the localization of injected RNA in real time in living embryos. We used direct incorporation of bright AlexaFluor dyes, rather than previous indirect methods of labeling RNA with Fluorescein (Glotzer et al., 1997; Lall et al., 1999). We found that capped, protein-free *run*, *ftz*, and *wg* transcripts become apically localized when injected into the basal cytoplasm or yolk (Figures 3A–3D; Movies 1 and 2 [see Supplemental Data below]). Our results are similar to the localization of amino-allyl FITC-labeled *ftz* mRNA preincubated with the hnRNPA1 homolog Squid and observed in fixed embryos (Lall et al., 1999). However, by imaging RNA in living embryos, we observed that approximately 30 s after injection, *run*, *ftz*, and *wg* RNAs assemble into bright particles that move rapidly and directly to the apical cytoplasm at approximately 0.5 μm/sec (Figures 3E–3J and Movie 2 [see Supplemental Data below]). We conclude that the

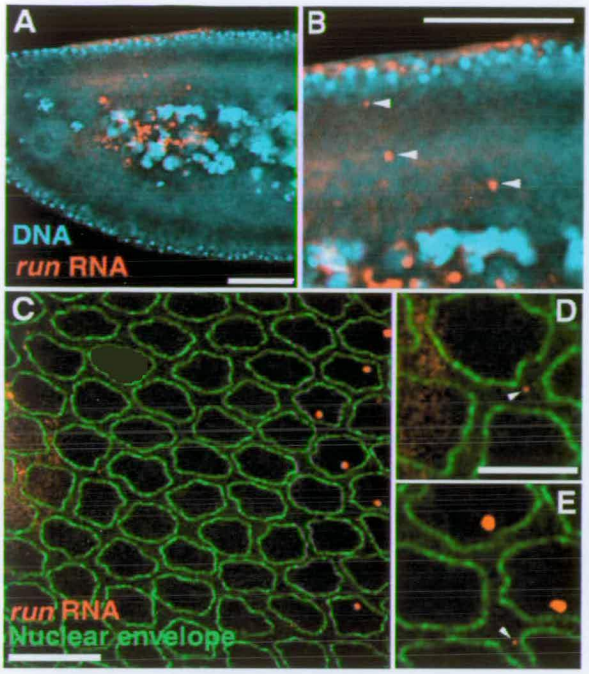

Figure 4. Rapidly Moving Particles in Living Embryos Are Equivalent to Endogenous mRNA Localization Intermediates

(A) Low-powered section through a blastoderm embryo fixed 5 min after injection with AlexaFluor546 *run* RNA (red). DAPI staining of DNA (cyan), highlighting cortical and yolk nuclei.

(B) Magnified view of part of (A), showing some RNA particles at the site of injection, apically localized RNA, and three particles in transit (arrowheads).

(C) Section through nuclei near the surface of an embryo that was injected with AlexaFluor488 *run* RNA and fixed after 5 min. Endogenous and injected *run* RNA were simultaneously detected by in situ hybridization with Cy3-TSA (red) and covisualised with the nuclear envelopes (green). The site of injection was off the left edge of the panel, near the anterior and at a much deeper focal plane. *run* mRNA on the right is endogenous stripe 1.

(D) High-powered view of a localization intermediate of injected RNA (arrowhead).

(E) High-powered view of endogenous localization intermediates (arrowhead). Many endogenous and injected intermediates show similar fluorescence intensity, indicating equivalent amounts of RNA. Scale bars are 20 μm in (A) and (B), 10 μm in (C), and 5 μm in (D) and (E).

apical localization of mRNA in the blastoderm embryo occurs by active transport to the apical cytoplasm.

To determine whether the RNA particles that assemble from highly concentrated injected RNA are similar to endogenous intermediates, we covisualized the injected and endogenous RNAs in fixed embryos. This allowed us to compare directly the intensities of endogenous and injected localization intermediates. We injected *run* RNA labeled with AlexaFluor488-UTP incorporation (green) and fixed the embryos 1 to 5 min after injection. Both endogenous and injected RNA particles were detected within the same embryos by fluorescent in situ hybridization (red). The results show that some RNA particles that assembled from injected RNA have similar intensities to endogenous localization intermediates (Figure 4 and data not shown). As expected, endogenous and injected RNAs were not colocalized within the same particles since the two types of particles assemble in different locations. We also found that high-powered imaging of injected RNA in living and fixed material showed that the majority of the RNA was present in particles of variable intensities (data not shown). We conclude that injected RNA particles are genuine localization intermediates similar to those of endogenous apical transcripts.

Apical Localization Intermediates Can Contain Several Different Apically Targeted RNAs, But Not Basal or Unlocalized RNA

To test whether RNA particle movement is specific to apically localized transcripts, we coinjected apically targeted RNA with either unlocalized or basal RNA. Our results show that injected *hb* RNA (Figures 5A–5E) and *stg* RNA (data not shown) partly diffuse away from the site of injection and do not become apically or basally localized. Unlocalized and basal RNAs can form bright particles, but these lack apical RNA and do not move apically (Figures 5C–5E). We conclude that the particles of RNA we observe moving to the apical cytoplasm are specific apical localization intermediates.

To determine whether different apical transcripts assemble within the same or distinct particles, we coinjected two different apically localized transcripts, *wg* with *run* (Figures 5F–5H) and *ftz* with *run* (data not shown). Our results show that both can assemble within the same particles, but some particles consist of predominantly one or the other RNA. Control coinjection experiments were performed with AlexaFluor488 *run* and AlexaFluor546 *run* RNA showing a similar mixture of red, green, and yellow particles (Figures 5I–5K). These results suggest that the localization particles contain a relatively small number of RNA molecules and that *wg* and different pair-rule transcripts localize using a similar mechanism.

Apical RNA Particles Move toward the Minus Ends of MTs Using Cytoplasmic Dynein and Dynactin

To study the mechanism of apical localization, we tested whether actin and/or MTs are necessary for localization of injected RNA by preinjecting cytoskeletal inhibitors 10 min before injecting the RNA. We found that preinjection of Cytochalasin B, at concentrations that disrupt the organization of actin filaments (Edgar et al., 1987), has no affect on *run* RNA localization (Table 1). However, we observed a similar disruption of nuclear position in the cortical cytoplasm (data not shown) as previously reported (Edgar et al., 1987). In contrast, preinjection of colcemid, which destabilizes blastoderm MTs (Edgar et al., 1987), disrupts *run*, *wg*, and *ftz* RNA localization almost entirely (Figure 6A, Table 1). Control embryos preinjected with buffer showed correct apical localization of injected *run*, *wg*, and *ftz* RNA (Table 1). Furthermore, when colcemid was inactivated by a 10 s UV exposure, the injected *run* RNA started localizing a few minutes later and became fully localized in all cases (Table 1, Figure 6B, and Movie 3 [see Supplemental Data below]). To confirm that colcemid disrupted MTs, we fixed embryos and visualized MTs, approximately 10 min after injection with colcemid. In agreement with previous studies, we found that colcemid causes the disappear-

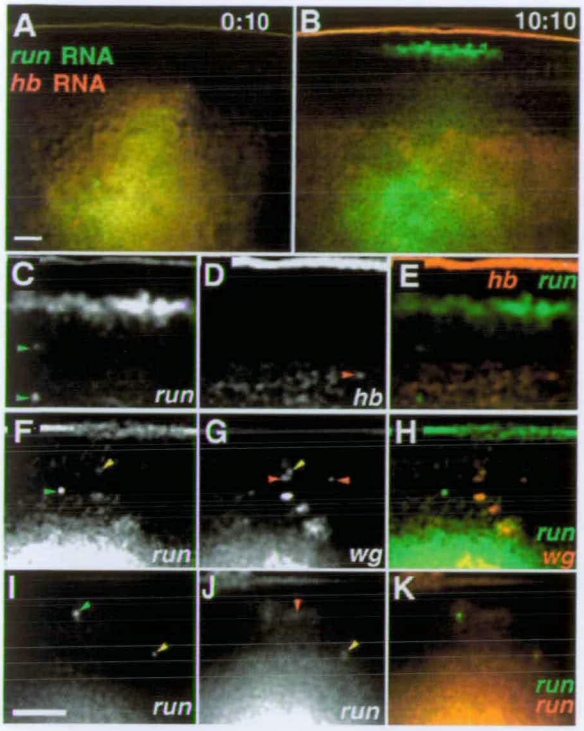

Figure 5. Apical Particles Often Contain More Than One Type of Apical RNA, But Lack Basal and Unlocalized RNAs

Snap shots from time lapse movies of coinjected apical and unlocalized RNAs. (A and B) Embryo coinjected with AlexaFluor488-labeled *run* RNA (green) and AlexaFluor546-labeled *hb* RNA (red). *run* RNA becomes apically localized but *hb* remains unlocalized. *run* RNA that has not yet localized does not diffuse, *hb* RNA diffuses away from the site of injection. The lines above the apical cytoplasm are due to auto-fluorescence and reflection of light by the vitelline membrane. In (B), the line is red because the red channel is enhanced (relative to [A]) to show the diffuse *hb* RNA. (C–E) Two time points (10 s apart and superimposed into one) from living embryo coinjected with *run* and *hb* RNA showing that *run* particles move apically and do not contain *hb* RNA, but *hb* particles do not move or contain *run* RNA. (C) *run*. (D) *hb*. (E) Merged image. (F–H) Single time point from living embryo coinjected with green *run* RNA and red *wg* RNA. (F) *run*. (G) *wg*. (H) Merged image. Particles contain either *run* or *wg* RNA, or a mixture of both. Arrowheads point to particles, all of which can be seen to move apically in other time points . (I–K) Single time point from a control embryo coinjected with green *run* RNA and red *run* RNA showing that differently labeled RNA can assemble in the same particles, but often do not. (I) Green *run* RNA. (J) Red *run* RNA. (K) Merged image. The color of the arrowheads indicates which RNA the particles contain. Time after injection is shown in minutes and seconds at the top right.

ance of MTs that reach the yolk and basal cytoplasm leaving some apical MTs unaffected (Figures 6C and 6D). We conclude that an intact MT cytoskeleton is required for apical localization of injected RNA and that actin does not play a major role in the process. However, we cannot exclude some minor role for actin in apical localization of RNA.

We next tested whether the localization of injected RNA occurs by minus end directed MT-dependent motor movement by preinjecting embryos with antibodies against *Drosophila* cytoplasmic dynein heavy chain (dhc). Our results show that two independently raised monoclonal antibodies against dhc (McGrail and Hays, 1997; Sharp et al., 2000a) are each sufficient to inhibit *run*, *ftz*, and *wg* RNA apical localization in most, or all, embryos (Figure 6E and Table 1). In contrast, embryos preinjected with a control IgG monoclonal antibody showed normal *wg*, *ftz*, and *run* RNA localization (Figure 6F and Table 1). We also found that either anti-dynein antibody or colcemid injections were each sufficient to cause apical RNA to partly diffuse away from the site of injection (Movie 4) in a similar manner to embryos injected with *hb* RNA alone (Figures 5A and 5B). Injected apical RNA does not diffuse in the absence of anti-dynein antibodies or Colcemid preinjections (Figure 3 and Movie 4). These results suggest that apical RNA is tethered to MTs by dynein and that dynein is required for the transport of RNA particles.

To further test the involvement of cytoplasmic dynein in apical transcript localization, we injected RNA into mutant cytoplasmic dynein heavy chain (*Dhc64C*) embryos. We found a marked reduction in the speed of movement of injected apical targeted RNAs in dynein mutants (Table 1). Cytoplasmic dynein is essential for many cellular processes, so strong mutations in *Dhc64C* are homozygous lethal in *Drosophila* and cannot be studied at the blastoderm stage (Gepner et al., 1996). Instead we used hypomorphic allelic combinations of *Dhc64C*, which are viable in trans due to intragenic complementation (Gepner et al., 1996) and have been shown to reduce the speed of dynein-dependent lipid droplet movement in embryos (Gross et al., 2000). We found that injected RNA particles move at 60% to 70% slower speeds in two different allelic combinations of *Dhc64C*, compared with wild-type (Table 1 and Movie 5). Staining *Dhc64C* mutant embryos with anti-tubulin antibodies showed that MT distribution was indistinguishable from wild-type (data not shown), indicating that the reduced speed of localization is not due indirectly to a disruption of the MTs. Instead, the reduction in speed is likely to show a direct requirement for dynein in particle transport.

To test whether cytoplasmic dynein is also required for apical localization of endogenous transcripts, we determined the effects of *Dhc64C* hypomorphic mutants and anti-dhc antibodies on the apical localization of endogenous *ftz* transcripts by in situ hybridization. As expected, hypomorphic *Dhc64C* mutants showed no detectable effects on *ftz* apical mRNA localization (data not shown) since injected RNA localizes correctly, but more slowly (Table 1 and Movie 5). In contrast, injection of anti-dhc antibody disrupts endogenous *ftz* localization, leading to unlocalized stripes of *ftz* mRNA 20–30 min after injection (Figure 6G). Given that *ftz* mRNA has a half-life of 6 min in the blastoderm (Edgar et al., 1986), the *ftz* transcripts we observed are likely to have been synthesized after the injection. We conclude that endogenous apical mRNA localization is also dynein dependent.

Dynactin is a protein complex that is involved in coordinating the activities of cytoplasmic dynein, and is thought to be required for most forms of dynein-based transport (Karki and Holzbaur, 1999). To test whether dynactin is also required for apical RNA localization, we preinjected a large excess of p50/dynamitin into embryos 10 min before injecting apically targeted RNA. p50/dynamitin causes a significant reduction in the

Table 1. Disruption of Microtubules or Cytoplasmic Dynein Inhibits Apical Localization of Injected *run*, *ftz*, and *wg* RNA

Genotype/Reagent	RNA	Localization	Particle Speed (μm/s)	Probability Value
Cytochalasin B preinjected into wild-type	*run*	91% (N = 23)		
	wg	80% (N = 10)		
Colcemid preinjected into wild-type	*wg*	10% (N = 29)		
	run	8% (N = 52)		
	ftz	13% (N = 30)		
Colcemid followed by UV	*run*	100% (N = 6)		
Control monoclonal antibody against HA	*wg*	89% (N = 18)		
	run	90% (N = 30)		
	ftz	90% (N = 21)		
Monoclonal antibody P1H4 against N-terminal residues 128–422 of *Drosophila* dhc (Tom Hays)	*wg*	21% (N = 14)		
	run	12% (N = 33)		
	ftz	7% (N = 15)		
Monoclonal antibody against HUV fragment of *Drosophila* dhc (David Sharp)	*wg*	0% (N = 22)		
	ftz	0% (N = 14)		
Buffer preinjected into wild-type	*wg*	88% (N = 17)	0.41 ± 0.03 (N = 32)	0.10 (*wg* & *run*)
	run	94% (N = 17)	0.49 ± 0.04 (N = 33)	0.60 (*run* & *ftz*)
	ftz	92% (N = 12)	0.46 ± 0.03 (N = 29)	0.24 (*ftz* & *wg*)
$Dhc64C^{6-1}/Dhc64C^{6-10}$	*wg*	89% (N = 19)	0.16 ± 0.008 (N = 37)	5.7×10^{-9}
	run	95% (N = 22)	0.19 ± 0.008 (N = 69)	4.4×10^{-9}
	ftz	86% (N = 22)	0.19 ± 0.009 (N = 72)	4.0×10^{-9}
$Dhc64C^{6-6}/Dhc64^{6-8}$	*wg*	92% (N = 12)	0.13 ± 0.01 (N = 64)	2.7×10^{-10}
	run	86% (N = 14)	0.15 ± 0.01 (N = 55)	2.7×10^{-10}
	ftz	88% (N = 22)	0.14 ± 0.01 (N = 60)	3.9×10^{-11}
GST preinjected into wild-type	*wg*	90% (N = 11)	0.40 ± 0.02 (N = 46)	0.80[a]
	run	92% (N = 13)	0.42 ± 0.04 (N = 34)	0.23[a]
GST-p50/dynamitin preinjected into wild-type	*wg*	90% (N = 20)	0.18 ± 0.03 (N = 43)	4.67×10^{-8}
	run	92% (N = 26)	0.16 ± 0.03 (N = 44)	9.28×10^{-7}
	ftz	94% (N = 16)	0.21 ± 0.03 (N = 44)	1.7×10^{-5}[b]

The effects of colcemid treatment, cytoplasmic dynein antibodies and mutants, and p50/dynamitin on apical RNA localization.
The proportion of embryos that localize injected RNAs and the speeds of movement of apical particles are shown for various treatments, mutations, and controls. Particle speeds represent the mean ± standard error of the speed of N particle movements towards the minus ends of microtubules. Speeds were measured from the distance in μm between successive positions of particles at 10 s intervals. The *P* values represent the probability of the speed measurements being derived from the same population as the appropriate controls.
[a] Compared with buffer preinjected into wild-type.
[b] Compared with embryos preinjected with GST and then injected with *wg* RNA.

speed of RNA particle movement (Table 1) whereas preinjection of control GST protein has no effect (Table 1). p50/dynamitin is a subunit of dynactin whose overexpression is a widely used method of disrupting the dynactin complex and demonstrating conclusively dynein-dependent motility (Echeverri et al., 1996). Dynactin is required for some cargo binding (Karki and Holzbaur, 1999) and for dynein processivity (King and Schroer, 2000). We conclude that apical transcript localization in the blastoderm embryo occurs by cytoplasmic dynein- and dynactin-mediated transport along MTs toward their minus ends.

Discussion

We have visualized the entire path of movement of apically targeted mRNAs from the site of transcription to their final site of localization in the apical cytoplasm of syncytial blastoderm embryos. Intermediates in the nuclear export and cytoplasmic localization of all transcripts studied are evenly distributed and contain a small number of mRNA molecules. Our in vivo injection data shows that protein-free fluorescent apical RNAs specifically assemble into particles that move toward the minus ends of MTs using the motor protein cytoplasmic dynein and its associated dynactin complex.

Intranuclear Movement and Export of mRNA

Using new techniques for visualizing RNA in situ and in living embryos, we have been able to study directly the path taken by different classes of transcripts in the blastoderm embryo and image mRNA export intermediates in the nucleus. In all cases studied, we find that export intermediates are evenly distributed within the nucleus and on the nuclear envelope, arguing against any directionality in their movement or export. Instead, all transcripts appear to diffuse freely within the nucleoplasm after release from the site of transcription and processing, are exported to the cytoplasm in all directions, and localize by a cytoplasmic mechanism. Our results are consistent with other studies using fluorescently tagged poly(A)$^+$ RNA (Politz et al., 1998, 1999), unspliced mRNA (Zachar et al., 1993), giant Balbiani Ring transcripts (Singh et al., 1999), and gold-labeled RNA injected into *Xenopus* oocyte nuclei (Pante et al., 1997), all of which were found to diffuse freely within the nucleus.

Apical mRNA Localization Involves Six Distinct Steps

There are three main cytoplasmic mechanisms that have been proposed for apical transcript localization (Francis-Lang et al., 1996) and other asymmetrically localized

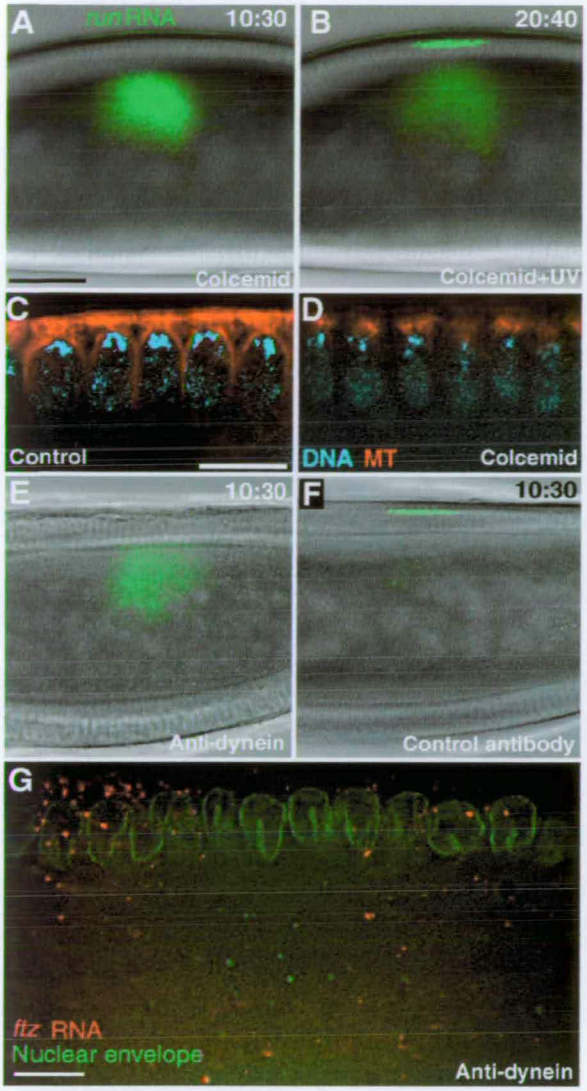

Figure 6. Localization of Injected Apically Targeted RNA Requires MTs and Dynein

(A) Snapshot taken 10 min after injection with AlexaFluor488 *run* RNA, which fails to localize because of prior (10 min earlier) injection of colcemid.

(B) A later snapshot of the same embryo 10min after 10 s irradiation with UV light (inactivates colcemid). The unlocalized *run* RNA rapidly localizes following the UV irradiation with similar kinetics to control injections with buffer (see Movie 3).

(C) Control embryo showing normal MT organization (red) and DNA (cyan). MTs are mainly apical but are also visualized between the nuclei and in the basal cytoplasm.

(D) A similarly treated embryo that was injected with colcemid and fixed 10 min later, showing fewer apical MTs and no MTs between the nuclei and in the basal cytoplasm.

(E) An embryo that was preinjected with an antibody against *Drosophila* cytoplasmic dynein heavy chain 10 min before injection with AlexaFluor488-labeled *run* RNA. The injected *run* RNA fails to localize, even an hour after injection (data not shown).

(F) Control embryo that was preinjected with an anti-HA IgG monoclonal antibody, under similar conditions to (E), showing normal localization of injected *run* RNA.

(G) In situ hybridization showing *ftz* mRNA in an embryo injected with anti-dynein antibody 20–30 min prior to fixation. *ftz* mRNA is unlocalized in expression stripes near the site of injection and is also detected in the yolk.

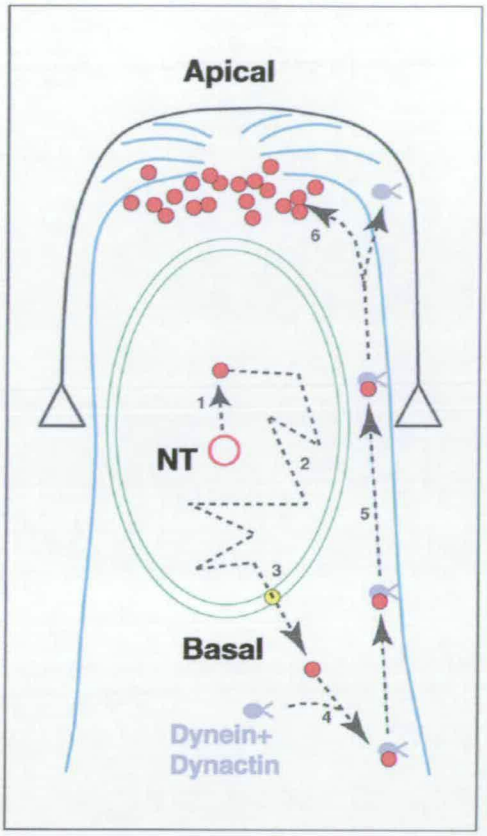

Figure 7. Stages in Apical mRNA Localization in the Blastoderm Embryo

A model representing the six steps in the movement of mRNA particles from the site of transcription at nascent transcript foci (NT) to its final site of localization in the apical cytoplasm. (1) Assembly into RNP complexes after release from the site of transcription and processing. (2) Diffusion throughout the nucleoplasm until particles encounter the nuclear envelope. (3) Export through NPCs. (4) Particle composition changes during and after export and cytoplasmic dynein and other proteins are recruited. (5) Dynein- and dynactin-mediated transport of particles along MTs to the apical cytoplasm. (6) Release and anchoring.

mRNAs (Lipshitz and Smibert, 2000). Unlocalized RNA could be selectively degraded or could diffuse freely and become anchored apically. Alternatively, transcripts could be actively transported within the cytoplasm to their final destinations. Our results and previous data (Francis-Lang et al., 1996) rule out selective degradation as the mechanism for apical mRNA localization. Our data also distinguish conclusively between the two remaining models for movement of apically targeted RNA in the cytoplasm by visualizing the dynein-dependent movement of apical RNA particles, which are inconsistent with diffusion. Furthermore, injected apically targeted mRNA is only able to diffuse when either MTs or dynein are disrupted, suggesting that mRNA destined to move to the apical cytoplasm is probably attached to MTs and dynein before the movement begins.

Considering our results in the context of other work (Daneholt, 1997; Lall et al., 1999; Norvell et al., 1999), export and localization of apical mRNA in the blastoderm embryo can be divided into six distinct steps (Figure

7). (1) During or after completion of transcription and processing, transcripts are assembled into particles, which contain various hnRNPs and export factors, some of which may form part of the cytoplasmic localization machinery. (2) mRNA particles diffuse freely after release from the site of transcription and processing until they reach NPCs on the nuclear periphery. (3) mRNA particles are exported through NPCs in all parts of the nuclear envelope. (4) The composition of the particles probably changes during export from the nucleus and in the cytoplasm to recruit dynein, dynactin, and associated proteins. (5) Particles attach to MTs and are actively transported to the apical cytoplasm. (6) Particle movement arrests in the apical cytoplasm, where they may associate with other particles and become anchored.

The first three steps of apical localization are thought to be common to most mRNAs, as they are essential universal processes in eukaryotic cells. However, the last three steps of the localization pathway are likely to vary amongst different kinds of transcripts, as the key determinant in sorting different mRNAs to their correct cytoplasmic destinations is presumably RNP particle composition in the cytoplasm. It is possible that some components required for cytoplasmic sorting are preassembled in the nucleus, as suggested by studies showing that the localization of injected *ftz* mRNA depends on preincubation with the hnRNPA1 protein Squid (Lall et al., 1999). Indeed, a requirement for hnRNPs has also been shown for *grk* mRNA localization in the oocyte (Norvell et al., 1999), for myelin basic protein mRNA in rat oligodendrocytes (Carson et al., 1998), and for Vg1 transcripts in *Xenopus* oocytes (Cote et al., 1999). However, our data show that injected protein-free apical RNA assembles in the cytoplasm into particles that localize correctly, arguing that all the factors needed to assemble competent localization particles can also be recruited in the cytoplasm. The differences between our results and those of Lall et al. are probably due to their method of labeling the RNA disrupting the competence of protein-free *ftz* RNA to localize (Bullock and Ish-Horowicz, personal communication). In contrast, labeling *ftz* RNA directly with various AlexaFlour dyes does not disrupt localization (this work and also Bullock and Ish-Horowicz, personal communication). Squid protein restores the ability of compromised *ftz* RNA to localize (Lall et al., 1999), possibly because RNP particles can be preassembled differently in the nucleus than in the cytoplasm (Kataoka et al., 2000).

Dynein/Dynactin-Mediated Transport of RNA Particles Is Likely to Be a Common Mechanism of mRNA Localization

We show that anti-dhc antibodies inhibit injected and endogenous transcript localization and that two different hypomorphic *Dhc64C* mutant combinations or an excess of p50/dynamitin are each sufficient to reduce significantly the speed of apical RNA particle movement. The reduction in speed of particle movement we observe in *Dhc64C* mutants is consistent with the fact that the *Dhc64C* allelic combinations have been shown to reduce the speed of dynein-dependent lipid droplet movement (Gross et al., 2000) and are semi-viable (Gepner et al., 1996). In these hypomorphic *Dhc64C* mutants, RNA particle movement is not abolished, but simply occurs more slowly. In contrast, the anti-dhc antibody treatments are equivalent to a genetic null as they abolish dynein function and apical RNA localization. The effects of the anti-dhc antibodies are likely to be specific as they were previously shown to recognize single bands on Western blots and to decorate MTs in oocytes (McGrail and Hays, 1997). In addition, injecting one of the antibodies specifically inhibits spindle pole separation during pro-metaphase and spindle elongation during anaphase B (Sharp et al., 2000a), as does p50/dynamitin (Sharp et al., 2000b), and these processes are thought to require dynein.

While we cannot completely exclude the possibility that dynein antibodies could disrupt apical RNA localization by affecting MT organization, the fact that excess p50/dynamitin reduces the speed of localization shows that dynein and dynactin are likely to be involved directly in transport of apical RNA. p50/dynamitin has been widely used to demonstrate the direct involvement of dynein and dynactin (reviewed in Karki and Holzbaur, 1999), and dynactin has been shown to be required for dynein processivity (King and Schroer, 2000), explaining why p50/dynamitin injections reduce the speed of apical RNA movement rather than abolishing localization entirely.

Dynein is involved in the transport of various other cytoplasmic components including the movement of lipid droplets in *Drosophila* embryos. Imaging lipid droplet movement at 30 frames/s has indicated that multiple minus end and plus end directed motors are assembled with each droplet (Gross et al., 2000). The average speeds of movement of the particles we observe are remarkably similar to those of lipid droplets, suggesting that the mechanism of movement may be similar. However, the particles we observe are not bright enough to allow acquisition of such frequent time points, so the question of whether plus end directed and minus end directed motors are coassembled in apical RNA transport particles is currently unresolved.

Dynein/dynactin complexes are good candidates for transporting other mRNAs that move to MT minus ends. These include the transport of various mRNAs from the nurse cells into the *Drosophila* oocyte, *grk* mRNA localization within the oocyte, and the apical localization of a number of transcripts in epithelial cells and neuroblasts (Fischer, 2000). It is also likely that other localized mRNAs assemble into similar particles to the ones we observe since RNA granules have been reported in many other cases (St. Johnston, 1995; Hazelrigg, 1998). However, in the absence of direct visualization of particle movement, the significance of these granules remains unknown. Nevertheless, we propose that the movement we see after assembly into particles is a widely deployed mechanism of localization of mRNA. This view is supported by the fact that Dynein is implicated, but not directly shown to be involved, in *bcd* mRNA localization during oogenesis (Schnorrer et al., 2000).

While dynein is unlikely to provide the specificity required for different RNAs to be sorted to their correct destinations, dynactin is thought to be involved in some cargo binding (reviewed in Karki and Holzbaur, 1999), so it could provide a link between RNA and dynein. Specificity is presumably provided by proteins that bind

localization signals in the 3′ UTR of the RNAs. However, such *trans*-acting factors remain unknown, with the probable exception of Swa, which may act as a linker between dynein and *bcd* mRNA (Schnorrer et al., 2000). Future characterization of the composition of the apical localization particles and the factors required for their assembly and movement will no doubt shed light on the specificity of apical mRNA localization in the blastoderm embryo and on the mechanism of movement of other mRNAs to the minus ends of MTs.

Experimental Procedures

Fly Strains

Stocks were raised on standard cornmeal-agar medium at 25°C. RNA was injected into embryos laid by Oregon R, wild-type, or a strain with four copies of the nlsGFP transgene (yw; nlsGFPM; nlsGFPN) (Davis et al., 1995). *Dhc64C* mutants were from T. Hays (Gepner et al., 1996) and Df(3)4SCB/TM3,Sb,Sr (uncovering the *ftz* gene) was from the Bloomington stock center.

In Situ Hybridization and Immunofluoresence

In situ hybridisation to detect mRNA with fluorescent tyramides (NEN LifeSciences) was performed as in Wilkie et al. (1999), the nuclear envelope visualized with AlexaFluor488 Wheat Germ Agglutinin (Molecular Probes). MTs were detected using a monoclonal antibody against β-tubulin (Amersham) and visualized using AlexaFluor568 coupled goat anti-mouse antibodies (Molecular Probes). For triple labeling experiments, the nuclear envelope was labeled with a monoclonal anti-lamin antibody (Yosef Gruenbaum) and visualized using Cy5 coupled donkey anti-mouse antibodies (Jackson).

Synthesis of Fluorescently Labeled, Capped RNA

RNA was transcribed in vitro using an mCAP RNA capping kit (Stratagene). Linearized plasmid DNA was transcribed for 2 hr at 37°C with T7 or T3 polymerase in a 50 μl reaction containing 0.4 mM ATP, 0.4 mM CTP, 0.36 mM UTP, 0.04 mM AlexaFluor488 or 546-UTP (Molecular Probes), 0.12 mM GTP, and 0.3 mM ^{7}mG(5′)pppG CAP analog. The reaction was incubated for 15 min with DNaseI and unincorporated nucleotides were removed using a Sephadex G50 RNA spin column (Roche) and the RNA extracted with phenol/$CHCl_3$, precipitated with NH_4OAc/EtOH and resuspended in water. The quality of the resulting RNA was assessed by electrophoresis and the yield and incorporation by spectrophotometry. Each molecule of *run* RNA was labeled by 16 molecules of AlexaFluor546 dye. This is equivalent to incorporation of 6.5 fluorochromes per kb of RNA, or one fluorochrome every 154 nucleotides on average.

Plasmids containing cDNA were gifts from David Ish-Horowicz (*ftz*), Bruce Edgar (*stg, hb*, and *Kr*), Peter Gergen (*run*), and Jean-Paul Vincent (*wg*).

Injection of RNA and Inhibitors

Embryos were prepared for injection with femtotip needles (Eppendorf), as previously described (Davis, 2000), and injected with 100 μg/ml Colcemid (Sigma) in water, 500 μg/ml Cytochalasin B (Sigma) in injection buffer (0.1 mM NaH_2PO_4, 5 mM KCl, pH 7.8) with 10% DMSO. A similar concentration of Cytochalasin B was previously shown to disrupt actin organization and actin-dependent processes in *Drosophila* (Edgar et al., 1987). Colcemid was inactivated by 10 s UV irradiation as previously described for oocytes (Theurkauf and Hazelrigg, 1998). Monoclonal antibodies: P1H4 from Tom Hays against a fragment of dhc from residues 128–422 near the N terminus (McGrail and Hays, 1997), anti-dhc antibody from David Sharp against the HUV fragment (Sharp et al., 2000a), and 12CA5 anti-HA (Yiota Kafasla and Joe Lewis) were spot dialyzed into injection buffer using 0.025 μm VSWP filters (Millipore) before injection. GST-p50/dynamitin or control GST protein were expressed in bacteria and purified over a glutathione-agarose column as previously described (Sharp et al., 2000b) and concentrated to 18 mg/ml in injection buffer using an Ultrafree protein concentrator (Millipore). A second injection with fluorescent RNA was typically made through the same point in the embryo within 10 min after the first injection. Injected embryos were either imaged in vivo, or fixed and devitelinized by hand using a fine hypodermic needle.

4-D Imaging and Deconvolution

Fixed embryos were mounted in Vectashield (Vector Laboratories) and living embryos were imaged directly on coverslips using a Sedat/Agard widefield microscope (Applied Precision Inc.) based on an Olympus IX70 inverted microscope with a 12 bit cooled PXL CCD camera (Photometrics) as previously described (Davis, 2000). Living embryos were imaged using an Olympus 20X/0.75NA lens and fixed embryos imaged with an Olympus 100X/1.4NA oil immersion lens. Out-of-focus light was reassigned to its original point source in 3-D image stacks captured from each time point using Sedat/Agard 3-D constrained iterative deconvolution algorithms. Combined DIC and green fluorescent images were captured using a dedicated dual DIC/GFP filter cube from Olympus.

The age of interphase 14 embryos was judged by the progression of the membrane furrows. The distance from the top of the nucleus to the positions of nascent transcript foci and RNA export intermediates were measured and plotted onto a 12 μm scale at 0.5 μm intervals, representing a nucleus 30 min after the start of interphase 14 (Figure 2).

Supplemental Data

Supplemental movies 1–5 are available online (http://www.cell.com/cgi/content/full/105/2/209/DC1).

Acknowledgments

We are indebted to David Ish-Horowicz, Adrian Bird, Hildegard Tekotte, Simon Bullock, Nina MacDougall, David Tollervey, Andreas Merdes, Kenneth Sawin, Joe Lewis, Jeremy Brown, Andrew Simmonds, and Henry Krause for constructive comments on the manuscript. We thank Andrew Jarman, Jeffrey Bond, Margarete Heck, Helena Davis, and Barrie Davis for help with statistics and Andrew Simmonds and Henry Krause as well as Simon Bullock and David Ish-Horowicz for allowing us to refer to their unpublished work. We are grateful to Tom Hays for providing *Dhc64C* mutant lines and anti-dhc antibodies, David Sharp for an independent anti-dhc antibody and a GST-p50/dynamitin expression clone, Yosef Gruenbaum for anti-lamin antibody, and Yiota Kafasla and Joe Lewis for control anti-HA antibody and GST protein. We also thank David Ish-Horowicz, Bruce Edgar, Peter Gergen, and Jean-Paul Vincent for sending cDNA clones. This work was supported by a Wellcome Trust career development fellowship and a Lister senior fellowship to I. D., and an MRC PhD studentship to G. W.

Received November 29, 2000; revised March 19, 2001.

References

Berleth, T., Burri, M., Thoma, G., Bopp, D., Richstein, S., Frigerio, G., Noll, M., and Nüsslein-Volhard, C. (1988). The role of localization of bicoid RNA in organizing the anterior pattern of the *Drosophila* embryo. EMBO J. *7*, 1749–1756.

Bobola, N., Jansen, R.P., Shin, T.H., and Nasmyth, K. (1996). Asymmetric accumulation of Ash1p in postanaphase nuclei depends on a myosin and restricts yeast mating-type switching to mother cells. Cell *84*, 699–709.

Brendza, R.P., Serbus, L.R., Duffy, J.B., and Saxton, W.M. (2000). A function for kinesin I in the posterior transport of *oskar* mRNA and staufen protein. Science *289*, 2120–2122.

Carson, J.H., Kwon, S., and Barbarese, E. (1998). RNA trafficking in myelinating cells. Curr. Opin. Neurobiol. *8*, 607–612.

Cote, C.A., Gautreau, D., Denegre, J.M., Kress, T.L., Terry, N.A., and Mowry, K.L. (1999). A Xenopus protein related to hnRNP I has a role in cytoplasmic RNA localization. Mol. Cell *4*, 431–437.

Daneholt, B. (1997). A look at messenger RNP moving through the nuclear pore. Cell *88*, 585–588.

Davis, I. (2000). Visualising fluorescence in *Drosophila*—optimal detection in thick specimens. In Protein Localization by Fluorescence

Microscopy: A Practical Approach, V.J. Allan, ed. (Oxford: OUP), pp. 131–162.

Davis, I., and Ish-Horowicz, D. (1991). Apical localization of pair-rule transcripts requires 3′ sequences and limits protein diffusion in the *Drosophila* blastoderm embryo. Cell *67*, 927–940.

Davis, I., Francis-Lang, H., and Ish Horowicz, D. (1993). Mechanisms of intracellular transcript localization and export in early *Drosophila* embryos. Cold Spring Harb. Symp. Quant. Biol. *58*, 793–798.

Davis, I., Girdham, C.H., and O'Farrell, P.H. (1995). A nuclear GFP that marks nuclei in living *Drosophila* embryos—maternal supply overcomes a delay in the appearance of zygotic fluorescence. Dev. Biol. *170*, 726–729.

Dubowy, J., and Macdonald, P.M. (1998). Localization of mRNAs to the oocyte is common in *Drosophila* ovaries. Mech. Dev. *70*, 193–195.

Echeverri, C.J., Paschal, B.M., Vaughan, K.T., and Vallee, R.B. (1996). Molecular characterization of the 50-kD subunit of dynactin reveals function for the complex in chromosome alignment and spindle organization during mitosis. J. Cell Biol. *132*, 617–633.

Edgar, B.A., and O'Farrell, P.H. (1990). The 3 postblastoderm cell-cycles of *Drosophila* embryogenesis are regulated in G2 by string. Cell *62*, 469–480.

Edgar, B.A., Weir, M.P., Schubiger, G., and Kornberg, T. (1986). Repression and turnover pattern of *fushi tarazu* RNA in the early *Drosophila* embryo. Cell *47*, 747–754.

Edgar, B.A., Odell, G.M., and Schubiger, G. (1987). Cytoarchitecture and the patterning of *fushi tarazu* expression in the *Drosophila* blastoderm. Genes Dev. *1*, 1226–1237.

Ephrussi, A., Dickinson, L.K., and Lehmann, R. (1991). Oskar organizes the germ plasm and directs localization of the posterior determinant nanos. Cell *66*, 37–50.

Erdelyi, M., Michon, A.M., Guichet, A., Glotzer, J.B., and Ephrussi, A. (1995). Requirement for *Drosophila* cytoplasmic tropomyosin in *oskar* mRNA localization. Nature *377*, 524–527.

Fischer, J.A. (2000). Molecular motors and developmental asymmetry. Curr. Opin. Genet. Dev. *10*, 489–496.

Foe, V.E., Odell, G.M., and Edgar, B.A. (1993). Mitosis and morphogenesis in the *Drosophila* embryo: point and counterpoint. In The Development of *Drosophila melanogaster*, M. Bate and A. Martinez Arias, eds. (Cold Spring Harbor, NY: Cold Spring Harbor Laboratory Press), pp. 149–300.

Francis-Lang, H., Davis, I., and Ish-Horowicz, D. (1996). Asymmetric localization of *Drosophila* pair-rule transcripts from displaced nuclei—evidence for directional nuclear export. EMBO J. *15*, 640–649.

Gepner, J., Li, M., Ludmann, S., Kortas, C., Boylan, K., Iyadurai, S.J., McGrail, M., and Hays, T.S. (1996). Cytoplasmic dynein function is essential in Drosophila melanogaster. Genetics *142*, 865–878.

Glotzer, J.B., Saffrich, R., Glotzer, M., and Ephrussi, A. (1997). Cytoplasmic flows localize injected *oskar* RNA in *Drosophila* oocytes. Curr. Biol. *7*, 326–337.

Gonzalez-Reyes, A., Elliott, H., and St. Johnston, D. (1995). Polarization of both major body axes in *Drosophila* by Gurken-Torpedo signaling. Nature *375*, 654–658.

Gross, S.P., Welte, M.A., Block, S.M., and Wieschaus, E.F. (2000). Dynein-mediated cargo transport in vivo. A switch controls travel distance. J. Cell Biol. *148*, 945–956.

Hazelrigg, T. (1998). The destinies and destinations of RNAs. Cell *95*, 451–460.

Hulskamp, M., Pfeifle, C., and Tautz, D. (1990). A morphogenetic gradient of hunchback protein organizes the expression of the gap genes *Kruppel* and *knirps* in the early *Drosophila* embryo. Nature *346*, 577–580.

Joseph, E.M., and Melton, D.A. (1998). Mutant Vg1 ligands disrupt endoderm and mesoderm formation in Xenopus embryos. Development *125*, 2677–2685.

Karki, S., and Holzbaur, E.L. (1999). Cytoplasmic dynein and dynactin in cell division and intracellular transport. Curr. Opin. Cell Biol. *11*, 45–53.

Kataoka, N., Yong, J., Kim, V.N., Velazquez, F., Perkinson, R.A., Wang, F., and Dreyfuss, G. (2000). Pre-mRNA splicing imprints mRNA in the nucleus with a novel RNA-binding protein that persists in the cytoplasm. Mol. Cell *6*, 673–682.

King, S.J., and Schroer, T.A. (2000). Dynactin increases the processivity of the cytoplasmic dynein motor. Nat. Cell Biol. *2*, 20–24.

Kislauskis, E.H., Zhu, X.C., and Singer, R.H. (1997). Beta-actin messenger RNA localization and protein synthesis augment cell motility. J. Cell Biol. *136*, 1263–1270.

Lall, S., Francis-Lang, H., Flament, A., Norvell, A., Schupbach, T., and Ish-Horowicz, D. (1999). Squid hnRNP protein promotes apical cytoplasmic transport and localization of *Drosophila* pair-rule transcripts. Cell *98*, 171–180.

Lipshitz, H.D., and Smibert, C.A. (2000). Mechanisms of RNA localization and translational regulation. Curr. Opin. Genet. Dev. *10*, 476–488.

Long, R.M., Singer, R.H., Meng, X.H., Gonzalez, I., Nasmyth, K., and Jansen, R.P. (1997). Mating type switching in yeast controlled by asymmetric localization of ASH1 mRNA. Science *277*, 383–387.

McGrail, M., and Hays, T.S. (1997). The microtubule motor cytoplasmic dynein is required for spindle orientation during germline cell divisions and oocyte differentiation in *Drosophila*. Development *124*, 2409–2419.

Neuman-Silberberg, F.S., and Schüpbach, T. (1993). The *Drosophila* dorsoventral patterning gene *gurken* produces a dorsally localized RNA and encodes a TGF alpha-like protein. Cell *75*, 165–174.

Norvell, A., Kelley, R.L., Wehr, K., and Schüpbach, T. (1999). Specific isoforms of Squid, a *Drosophila* hnRNP, perform distinct roles in *gurken* localization during oogenesis. Genes Dev. *13*, 864–876.

O'Farrell, P.H., Edgar, B.A., Lakich, D., and Lehner, C.F. (1989). Directing cell division during development. Science *246*, 635–640.

Pante, N., Jarmolowski, A., Izaurralde, E., Sauder, U., Baschong, W., and Mattaj, I.W. (1997). Visualizing nuclear export of different classes of RNA by electron microscopy. RNA *3*, 498–513.

Pokrywka, N.J., and Stephenson, E.C. (1991). Microtubules mediate the localization of *bicoid* RNA during *Drosophila* oogenesis. Development *113*, 55–66.

Politz, J.C., Browne, E.S., Wolf, D.E., and Pederson, T. (1998). Intranuclear diffusion and hybridization state of oligonucleotides measured by fluorescence correlation spectroscopy in living cells. Proc. Natl. Acad. Sci USA *95*, 6043–6048.

Politz, J.C., Tuft, R.A., Pederson, T., and Singer, R.H. (1999). Movement of nuclear poly(A) RNA throughout the interchromatin space in living cells. Curr. Biol. *9*, 285–291.

Schnorrer, F., Bohmann, K., and Nüsslein-Volhard, C. (2000). The molecular motor dynein is involved in targeting swallow and bicoid RNA to the anterior pole of *Drosophila* oocytes. Nat. Cell Biol. *2*, 185–190.

Sharp, D.J., Brown, H.M., Kwon, M., Rogers, G.C., Holland, G., and Scholey, J.M. (2000a). Functional coordination of three mitotic motors in *Drosophila* embryos. Mol. Biol. Cell *11*, 241–253.

Sharp, D.J., Rogers, G.C., and Scholey, J.M. (2000b). Cytoplasmic dynein is required for poleward chromosome movement during mitosis in *Drosophila* embryos. Nat. Cell Biol. *2*, 922–930.

Simmonds, A., dosSantos, G., Livne-Bar, I., and Krause, H. (2001). Apical localization of *wingless* transcripts is required for wingless signaling. Cell *105*, this issue, 197–207.

Singh, O.P., Bjorkroth, B., Masich, S., Wieslander, L., and Daneholt, B. (1999). The intranuclear movement of Balbiani ring pre-messenger ribonucleoprotein particles. Exp. Cell Res. *251*, 135–146.

Stephenson, E.C., Chao, Y.C., and Fackelthal, J.D. (1988). Molecular analysis of the swallow gene of Drosophila melanogaster. Genes Dev. *2*, 1655–1665.

St. Johnston, D. (1995). The intracellular localization of messenger RNAs. Cell *81*, 161–170.

St. Johnston, D., Driever, W., Berleth, T., Richstein, S., and Nüsslein-Volhard, C. (1989). Multiple steps in the localization of bicoid RNA to the anterior pole of the *Drosophila* oocyte. Development *107*, 13–19.

Sundell, C.L., and Singer, R.H. (1990). Actin mRNA localizes in the absence of protein synthesis. J. Cell Biol. *111*, 2397–2403.

Sundell, C.L., and Singer, R.H. (1991). Requirement for microfilaments in sorting of actin mRNA. Science *253*, 1275–1277.

Takizawa, P.A., Sil, A., Swedlow, J.R., Herskowitz, I., and Vale, R.D. (1997). Actin-dependent localization of an RNA encoding a cell-fate determinant in yeast. Nature *389*, 90–93.

Theurkauf, W.E., and Hazelrigg, T.I. (1998). In vivo analyses of cytoplasmic transport and cytoskeletal organization during *Drosophila* oogenesis: characterization of a multi-step anterior localization pathway. Development *125*, 3655–3666.

Theurkauf, W.E., Alberts, B.M., Jan, Y.N., and Jongens, T.A. (1993). A central role for microtubules in the differentiation of *Drosophila* oocytes. Development *118*, 1169–1180.

Vallee, R.B., and Sheetz, M.P. (1996). Targeting of motor proteins. Science *271*, 1539–1544.

Weeks, D.L., and Melton, D.A. (1987). A maternal mRNA localized to the vegetal hemisphere in *Xenopus* eggs codes for a growth factor related to TGF-beta. Cell *51*, 861–867.

Wilhelm, J.E., Mansfield, J., Hom-Booher, N., Wang, S., Turck, C.W., Hazelrigg, T., and Vale, R.D. (2000). Isolation of a ribonucleoprotein complex involved in mRNA localization in *Drosophila* oocytes. J. Cell Biol. *148*, 427–440.

Wilkie, G., and Davis, I. (1998). High resolution and sensitive mRNA in situ hybridisation using fluorescent tyramide signal amplification. Elsevier Trends Journals Technical Tips Online t01458 (http://www.biomednet.com/db/tto).

Wilkie, G., Shermoen, A., O'Farrell, H., and Davis, I. (1999). Transcribed genes are localized according to chromosomal position within polarized *Drosophila* embryonic nuclei. Curr. Biol. *9*, 1263–1266.

Yisraeli, J.K., Sokol, S., and Melton, D.A. (1990). A two-step model for the localization of maternal mRNA in *Xenopus* oocytes: involvement of microtubules and microfilaments in the translocation and anchoring of Vg1 mRNA. Development *108*, 289–298.

Zachar, Z., Kramer, J., Mims, I.P., and Bingham, P.M. (1993). Evidence for channeled diffusion of pre-mRNAs during nuclear RNA transport in metazoans. J. Cell Biol. *121*, 729–742.

Development 128, 665-673 (2001)
Printed in Great Britain © The Company of Biologists Limited 2001
DEV7846

Merlin, the *Drosophila* homologue of neurofibromatosis-2, is specifically required in posterior follicle cells for axis formation in the oocyte

Nina MacDougall[1], Yatish Lad[1,*], Gavin S. Wilkie[1], Helen Francis-Lang[2,‡], William Sullivan[2] and Ilan Davis[1,§]

[1]Wellcome Centre for Cell Biology, ICMB, King's Buildings, University of Edinburgh, Edinburgh EH9 3JR, UK
[2]Department of Molecular, Cell and Developmental Biology, 322 Sinsheimer Labs, University of California, Santa Cruz 95064, USA.
*Present address: Centre for Inflammation Research, Medical School, University of Edinburgh, Teviot Place, Edinburgh EH8 9AG, UK
‡Present address: Exelixis, 170 Harbor Avenue, PO Box 511, S. San Francisco, CA 94083-0511, USA
§Author for correspondence (e-mail: ilan.davis@ed.ac.uk)

Accepted 21 December 2000; published on WWW 7 February 2001

SUMMARY

In *Drosophila*, the formation of the embryonic axes is initiated by Gurken, a transforming growth factor α signal from the oocyte to the posterior follicle cells, and an unknown polarising signal back to the oocyte. We report that *Drosophila* Merlin is specifically required only within the posterior follicle cells to initiate axis formation. *Merlin* mutants show defects in nuclear migration and mRNA localisation in the oocyte. Merlin is not required to specify posterior follicle cell identity in response to the Gurken signal from the oocyte, but is required for the unknown polarising signal back to the oocyte. Merlin is also required non-autonomously, only in follicle cells that have received the Gurken signal, to maintain cell polarity and limit proliferation, but is not required in embryos and larvae. These results are consistent with the fact that human Merlin is encoded by the gene for the tumour suppressor neurofibromatosis-2 and is a member of the Ezrin-Radixin-Moesin family of proteins that link actin to transmembrane proteins. We propose that Merlin acts in response to the Gurken signal by apically targeting the signal that initiates axis specification in the oocyte.

Key words: *Drosophila* oogenesis, *Merlin*, *gurken*, *bicoid*, *oskar*, TGFα, mRNA localisation, Oocyte microtubules, Embryonic axis formation, Tumour suppressor, ERM, Cell signalling

INTRODUCTION

The embryonic axes of *Drosophila* are established during oogenesis through the localisation of specific mRNAs to different regions of the oocyte cytoplasm. This process is initiated through bi-directional signalling between the oocyte and the overlying follicle cells (Schüpbach, 1987). While the localised mRNAs and some of the signalling components have been studied in detail, many of the genes involved in these processes are still unknown (Nilson and Schüpbach, 1999; van Eeden and St Johnston, 1999).

grk mRNA is localised in early oocytes in a posterior crescent between the nucleus and the follicle cells (Neuman-Silberberg and Schüpbach, 1993), thus targeting the Grk transforming growth factor α (TGFα) signal only to the adjacent follicle cells. The Grk signal is probably the ligand for Torpedo/DER, an epidermal growth factor receptor (EGFR) (Gonzalez-Reyes et al., 1995; Neuman-Silberberg and Schüpbach, 1993). Grk instructs 200 terminal follicle cells to adopt posterior instead of default anterior fates (Gonzalez-Reyes and St Johnston, 1998). Posterior, anterior and main body follicle cells originate from the same group of cells that divides five or six times before stage 6 and has equivalent columnar epithelial morphology up to stage 9 (Gonzalez-Reyes and St Johnston, 1998). However, anterior and posterior follicle cells express distinct cell fate markers (Deng and Bownes, 1998; Fasano and Kerridge, 1988; Micklem et al., 1997).

Once the Grk signal is received, an unknown signal is sent from the posterior follicle cells back to the oocyte, repolarising the oocyte microtubules (MTs). MT organisation and polarity have been visualised in fixed material with anti-Tubulin antibodies (Theurkauf et al., 1992) and β-galactosidase (βgal) fusions to MT-dependent motor domains (Clark et al., 1994; Clark et al., 1997) as well as a TauGFP fusion in living oocytes (Micklem et al., 1997). Before stage 7, a microtubule organising centre (MTOC) is located at the posterior of the oocyte, where the minus ends of MTs are localised. At stage 7, the posterior MTOC disassembles, a diffuse anterior MTOC forms and plus ends of MTs are found at the posterior. The polarity of MTs determines the site of localisation of different mRNAs in the oocyte. *bicoid* (*bcd*) mRNA is localised to the anterior of the oocyte, leading to a morphogenetic gradient of Bcd protein in the embryo (Driever and Nüsslein-Volhard, 1988). *osk* mRNA is localised at the posterior of the oocyte and embryo and specifies the future germ cells (Ephrussi et al., 1991).

The Grk signal also initiates formation of the dorsoventral (DV) axis when the oocyte nucleus moves from the posterior to the dorsoanterior corner. *grk* transcripts then become tightly

localised near the nucleus, so that Grk signalling instructs only the overlying follicle cells to adopt dorsal fates (Nilson and Schüpbach, 1999; van Eeden and St Johnston, 1999). The specification of appropriate populations of follicle cells along the DV axis leads to the secretion of egg shell structures such as the dorsal appendages. Later in development the embryonic DV axis is formed by signalling from ventral follicle cells, which leads to the formation of a graded nuclear-cytoplasmic distribution of Dorsal protein (Anderson, 1998).

Although the posterior polarising signal remains unidentified, a number of known genes are required for the process. Protein kinase A (PKA) is likely to be part of the machinery that receives the signal in the oocyte (Lane and Kalderon, 1994; Perrimon, 1994) but is not specific to this process. Mago nashi (Mago) is required for oocyte repolarisation and has an independent function in *osk* mRNA localisation. However, Mago is a novel nuclear protein that is ubiquitous in the egg chamber, and its role in signalling is unknown (Micklem et al., 1997; Newmark et al., 1997). Notch-Delta signalling is required among the posterior follicle cells to limit the number of polar posterior follicle cells that express Fasciclin III; it is also required earlier in oogenesis (Larkin et al., 1996). Notch is required for the specification of posterior follicle cell identity (Gonzalez-Reyes and St Johnston, 1998), and is therefore required indirectly for the generation of the polarising signal to the oocyte (Ruohola et al., 1991), rather than being directly involved in the signal itself. Two other neurogenic proteins, Brainiac (Brn) and Egghead (Egh) are required in the oocyte for follicle cell integrity, and it has been suggested that both proteins may interact with Notch and EGF-signalling (Goode et al., 1996a; Goode et al., 1996b). However, it is not known whether they are required for the polarising signal. Laminin A is a component of the extracellular matrix that is expressed and required in the posterior follicle cells for the polarising signal (Deng and Ruohola-Baker, 2000). A better understanding of the events associated with the polarising signal awaits the identification of the signal itself.

Here, we identify a new allele of *Mer* by screening a collection of temperature sensitive (ts) lethal alleles for defects in *grk* mRNA localisation and we show that Merlin functions in axis specification during oogenesis. *Drosophila Mer* was previously cloned by degenerate PCR (McCartney and Fehon, 1996) and mutations isolated by reverse genetic methods (Fehon et al., 1997). The human homologue is a tumour suppressor called neurofibromatosis-2 (NF2), which encodes Merlin (Moesin Ezrin Radixin Related Protein) (McCartney and Fehon, 1996). Merlin and Ezrin-Radixin-Moesin (ERM) proteins are members of the 4.1 family of proteins thought to link actin to transmembrane proteins (Mangeat et al., 1999; Tsukita et al., 1994) and *Drosophila* Merlin is apically localised in follicle cells (McCartney and Fehon, 1996). We show that Merlin is required only within the posterior follicle cells for mRNA localisation and axis specification in the oocyte. Merlin functions downstream of the Grk signal from the oocyte, but is only required if the posterior follicle cells receive the Grk signal. Merlin has no role in Notch-Delta signalling between the follicle cells, but is required upstream of the unknown polarising signal back to the oocyte. Merlin is also required non-autonomously in posterior follicle cells to limit their proliferation and maintain their polarity. We propose that Merlin functions by apically targeting the unknown polarising signal that initiates axis specification.

MATERIALS AND METHODS

Fly stocks

The collection of ts lethals was generated by EMS mutagenesis and subsequent selecting for male lethality at 29°C and viability at 21° (H. F.-L. and W. S., unpublished observations). $Merlin^{ts1}$ (Mer^{ts1}) stocks (yw^{67g},Mer^{ts1}) were maintained at 18°C or 21°C, and mutant phenotypes analysed by shifting newly eclosed adult flies to 29°C on fresh food. For analysis of follicle cell and MT markers, Mer^{ts1} females were crossed to males from the following stocks: posterior follicle cell marker (*yw; 998/12/TM6b*: P. Deak, M. Bownes and D. Glover), border cell markers (*yw; 459/2/TM6b*: P. Deak, M. Bownes and D. Glover), anterior follicle cell marker (*L53b*: S. Kerridge), polar follicle cell *marker (w; P(w+)8523/CyO*: M. Heck, A. Spradling) and MT markers (*yw;Nod-lacZ* and *yw;Kin-lacZ, Tau-GFP*: D. St Johnston). The F_1 male progeny were then back crossed to Mer^{ts1} females.

Generation and detection of FRT/FLP follicle cell clones

Clones were induced by mitotic recombination at high frequency only in follicle cells using *en-Gal4,UAS-FLP* (Duffy et al., 1998) at 29°C in Mer^3,*FRT/nlsGFP,FRT* (Davis et al., 1995) (FRT19A from S. Luschnig). Mer^3 Clones were identified by the lack of nlsGFP expression.

X-ray-induced germline clones

To create homozygous Mer^{ts1} germline clones, $ovoD^1$ males were mated to homozygous yw^{67g},Mer^{ts1} females for two days and transferred to fresh food for 8 hours. The larvae (40-48 hours old) were exposed to 1000 rads of X-rays and allowed to recover at 21°C. 1000 surviving F1 females were crossed to yw^{67g} males in single pair matings, shifted to 29°C for three days, and their ovaries dissected, fixed and stored in methanol at –20°C. 10 females (1%) containing Mer^{ts1} germline clones were identified by the lack of male progeny, and their ovaries studied. 50 (5%) females with wild-type recombinant chromosomes were identified by the presence of male progeny and discarded.

In situ hybridisation

Ovaries were dissected and fixed in 3.7% formaldehyde in PBS with 0.1% Tween20 (PBT) and in situ hybridisation carried out using standard methods (Tautz and Pfeifle, 1989) with our previously described modifications (Wilkie and Davis, 1998; Wilkie et al., 1999). Mounting and imaging were performed as previously described (Davis, 2000).

X-Gal staining

For X-gal staining of the enhancer trap and other transgenic lines expressing βgal fusion proteins, ovaries were dissected and fixed in 0.05% glutaraldehyde in PBT for 15 minutes, and stained for 2 hours to overnight at 37°C using standard methodology.

Protein localisation

Actin

Ovaries were dissected and fixed without methanol and incubated in a 1:40 dilution of Texas-red-phalloidin (Molecular probes) in PBS overnight at 4°C and washed with PBT.

Centrosomes and spectrin

Ovaries were blocked in 2% BSA in PBS with 0.1% TritonX-100 (PBTX) for 2 hours at room temperature, washed several times in PBT and incubated with anti γ-tubulin monoclonal antibody (1:10,000

Sigma) or anti β_H-spectrin (1:200) in PBTX with 2% BSA overnight at 4°C, followed by AlexaFluor594- and AlexaFluor488-coupled secondary antibodies, respectively (Molecular Probes).

RESULTS

Identification of a temperature-sensitive mutation that disrupts mRNA localisation and oocyte nuclear migration

To identify new genes required for axis specification, we screened a collection of X-linked ts lethal mutations generated by selecting for male lethality at 29°C and viability at 21°C. We collected homozygous female progeny at 21°C from 73 viable ts lethal lines, shifted to 29°C for 3 days and performed *grk* RNA in situ hybridisation on ovaries. In wild type or yw^{67g} controls at 29°C or in all strains at 21°C, the oocyte nucleus migrates correctly to the antero-dorsal corner of the oocyte with *grk* mRNA localising between the nucleus and the overlying future dorsal follicle cells (Fig. 1A). In one line, yw^{67g},*l(1)ts594* {*l(1)ts594*}, 55% (n=89) of oocyte nuclei fail to migrate and *grk* mRNA localises at the posterior after stage 8 (Fig. 1B). The remaining 45% of cases were similar to wild type, *l(1)ts594* at 21°C (Fig. 1A) and the same genetic background yw^{67g} (*yw*) chromosome at 29°C. In all subsequent experiments, similar controls were carried out, showing that the phenotype was not due to the temperature shift itself or the genetic background.

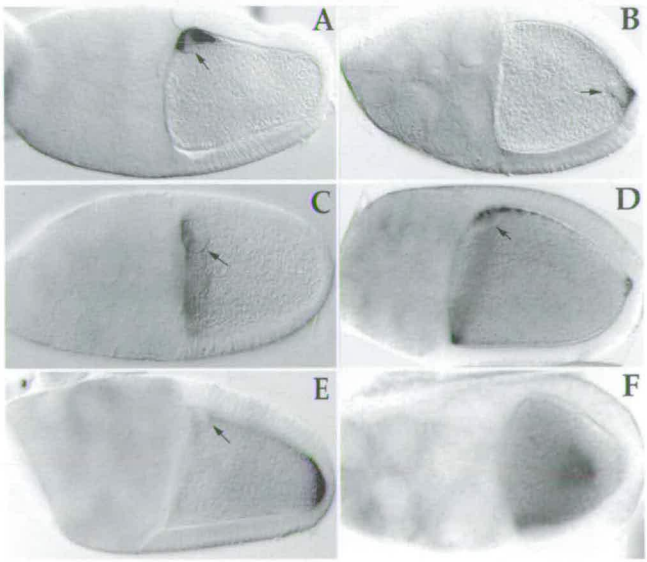

Fig. 1. Mutations in *Mer* disrupt mRNA localisation and nuclear migration in the oocyte. (A) Control showing the oocyte nucleus and *grk* mRNA at the dorso-anterior corner of the oocyte. (B) *Mer* mutant showing *grk* mRNA at the posterior near the oocyte nucleus (55% of cases). The other 45% of cases are the same as the control (not shown). (C) Control showing normal *bcd* mRNA localisation in an anterior ring. (D) *Mer* mutant showing some *bcd* mRNA abnormally localised at the posterior (83% of cases). (E) Control showing normal *osk* mRNA localisation at the posterior. (F) *Mer* mutant showing *osk* mRNA diffusely localised at the centre of the oocyte (89% of cases). The oocyte nucleus is in a different focal plane. (A,C,E) stage 10 Mer^{ts1} mutant 21°C, similar to wild type and *yw* strains at 29°C (not shown). (B,D) stage 10 and (F) stage 9 Mer^{ts1} mutants at 29°C. In situ hybridisation to detect *grk* (A,B), *bcd* (C,D) and *osk* (E,F) mRNA. Arrows indicate the oocyte nucleus.

We also performed in situ hybridisation on *l(1)ts594* ovaries to detect *bicoid* (*bcd*) and *oskar* (*osk*) mRNA. We found that in 83% (n=47) of stage 9 or 10A mutants at 29°C, *bcd* mRNA is localised at the posterior as well as its normal accumulation in an anterior ring (Fig. 1C,D). In 89% (n=32) of stage 9 and 10A mutants, *osk* mRNA is mislocalised at the centre of the oocyte (Fig. 1F) instead of its normal posterior localisation (Fig. 1E).

To test whether the defects in the oocyte are primarily due to a defect in MT organisation, we examined MT polarity. We used Kin:βgal, a plus end-directed MT motor fusion that leads to βgal accumulation at the posterior of the oocyte (Clark et al., 1994). We also used Nod:βgal, a MT motor fusion that leads to βgal accumulation at the anterior, where the minus ends of MTs are thought to localise (Clark et al., 1997). The βgal motor fusions indicate that prior to stage 7, there is an MTOC at the posterior (data not shown). In wild-type oocytes after stage 7, the posterior MTOC disassembles, a diffuse MTOC appears at the anterior (Fig. 2A) with MT plus ends at the posterior (Fig. 2C). Prior to stage 7, *l(1)ts594* mutant oocytes show a similar MT organization to wild type (data not shown), but after stage 7, the MTOC fails to disassemble at the posterior and a second diffuse MTOC forms at the anterior (Fig. 2B). This leads to a symmetric organization of MTs, with their plus ends at the centre of the oocyte (Fig. 2D) and minus ends at the anterior and posterior (Fig. 2B). We also examined the overall distribution of MTs using a maternally expressed TauGFP line showing the highest concentration of MTs at the anterior cortex of wild-type oocytes (Micklem et al., 1997). We observed a similar Tau-GFP distribution in *l(1)ts594* oocytes at 21°C (Fig. 2E). In *l(1)ts594* at 29°C Tau-GFP showed an abnormally high level at the posterior, consistent with a failure to disassemble the posterior MTOC (Fig. 2F). We conclude that the mislocalisation of mRNA and failure of the oocyte nucleus to relocate in *l(1)ts594* oocytes are due primarily to defects in MT organisation.

l(1)ts594 is a strong loss-of-function allele of *Mer*

In order to determine the gene mutated in *l(1)ts594*, we mapped the mutation. Complementation analysis against deficiencies showed that the mutation lies in one of two gaps in the available deficiencies on the X chromosome, 18A2-A5 or 18D1-18E1-2 and recombination mapping showed that the lethality and oocyte phenotype both map to 18D-18E. Complementation analysis with all the available alleles in the region showed that three lethal alleles of *Merlin* (Mer^1, Mer^2 *and* Mer^4) (LaJeunesse et al., 1998) failed to complement the lethality of *l(1)ts594* at 29°C. A fusion of the *Mer* full-length cDNA with GFP and a cosmid containing a genomic DNA fragment including *Mer* are both able to fully complement the lethality, oocyte nuclear migration defects and mRNA mislocalisation of *l(1)ts594* (data not shown), suggesting that *l(1)ts594* is a ts allele of *Mer*.

Mer is the closest *Drosophila* homologue of human Merlin, a member of the ERM/4.1 family encoded by the NF2 tumour suppressor (Mangeat et al., 1999). ERM proteins are thought to link actin with transmembrane proteins at the cell membrane (Turunen et al., 1998) and may play a role in signalling (Mangeat et al., 1999). We sequenced the entire coding regions

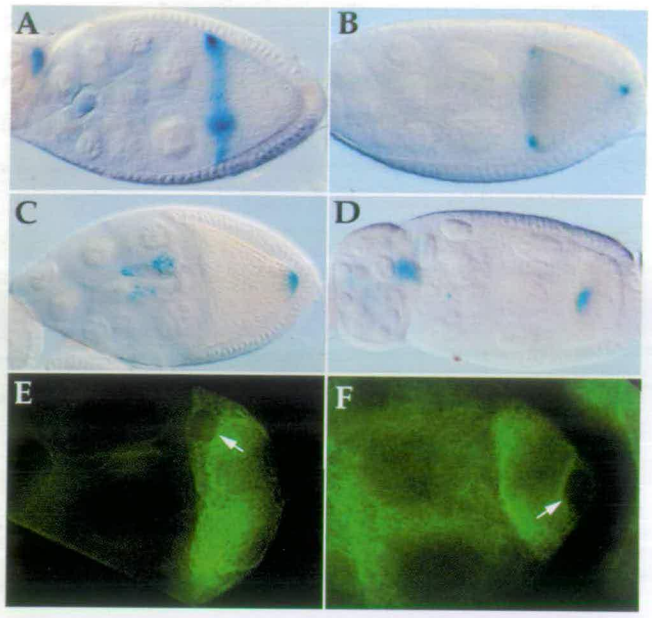

Fig. 2. Mutations in *Mer* disrupt microtubule (MT) organisation in the oocyte. (A,B) Minus ends of MTs visualised with Nod:βgal protein that marks the MT organising centre (MTOC). (A) Stage 9 control showing normal Nod:βgal localisation along the anterior cortex. (B) Stage 9 *Mer* mutant, showing Nod:βgal localisation at the posterior, owing to a failure of the posterior MTOC to disassemble. (C,D) Plus ends of MTs visualised with Kin:βgal expression. (C) Late stage 9 control showing Kin:βgal localised at the posterior of the oocyte. (D) Stage 9 *Mer* mutant showing abnormal Kin:βgal localisation in the centre of the oocyte. (E,F) MTs visualised in living egg chambers using Tau-GFP. Arrows indicate the nuclei. (E) Stage 9 control anterior-posterior gradient of MTs. (F) Stage 9 Mer^{ts1} mutant showing a symmetric array of MTs at the anterior and posterior cortex. (A,C,E) Mer^{ts1} 21°C. (B,D,F) Mer^{ts1} 29°C.

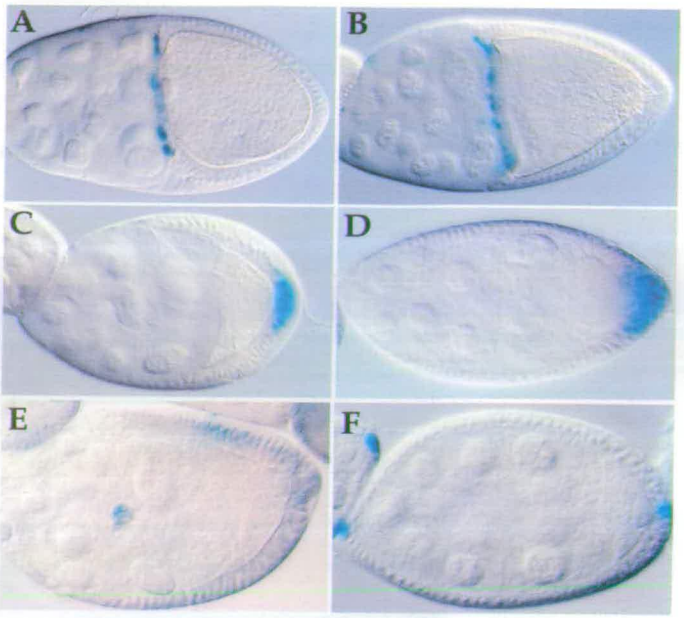

Fig. 3. Mutations in *Mer* do not disrupt follicle cell identity. (A-F) X-Gal staining of different *lacZ* lines crossed into control and Mer^{ts1} egg chambers. (A) Stage 10 control, expressing βgal protein in anterior follicle cells. (B) Mer^{ts1} egg chamber showing indistinguishable anterior follicle cells to A and no expression in posterior follicle cells. (C) Stage 9 control, expressing βgal in the posterior follicle cells. (D) Mer^{ts1} mutant showing normal posterior expression. Note the thicker layer of posterior follicle cells (also see Fig. 4) (E) Mer^{ts1} mutant showing normal expression of a border cell marker. (F) Mer^{ts1} mutant showing normal expression of polar posterior and polar anterior follicle cell marker.

of *Mer* in *l(1)ts594* and in the genetic background yw^{67g} chromosome. Two closely mapping non-conservative amino acid changes (F113L and I125F) were found in the conserved N-terminal domain involved in binding to transmembrane proteins (LaJeunesse et al., 1998). No modifications were detected in the C-terminal domain that has a putative regulatory role. We conclude that *l(1)ts594* is an allele of *Mer* and renamed it Mer^{ts1}.

To determine whether the phenotype we observed in Mer^{ts1} mutants was typical of existing loss-of-function *Mer* alleles, we studied the oogenesis phenotype of various other allelic combinations of *Mer*. We found similar defects in all the allelic combinations studied. Flies homozygous for Mer^{ts1}, and flies with Mer^{ts1} over a null allele (LaJeunesse et al., 1998) (Mer^{ts1}/Mer^{4}) showed almost identical phenotypes. Mer^{ts1} over a weak allele (Fehon et al., 1997) (Mer^{ts1}/Mer^{3}) showed a slightly reduced frequency of the oogenesis phenotype (data not shown). From these results, and the fact that a *Mer* transgene fully complements the Mer^{ts1} phenotype (data not shown), we conclude that Mer^{ts1} is a very strong loss-of-function allele, similar to a null.

Merlin is not required in the germline, or for Grk or Notch signalling

Merlin protein has previously been shown to be expressed in the oocyte and in posterior follicle cells (McCartney and Fehon, 1996), but its function was only studied later in development (LaJeunesse et al., 1998; McCartney et al., 2000). To determine where Merlin functions in egg chambers, we generated homozygous Mer^{ts1} germline clones using X-rays in females raised at the restrictive temperature (29°C). We analysed 10 Mer^{ts1} oocytes surrounded by $Mer^{ts1}/+$ follicle cells (see Materials and Methods), and they all showed normal mRNA localisation and lead to normal eggs (data not shown). We conclude that Merlin is not required in the germline derived nurse cells or oocyte.

To test whether Merlin is required within the somatically derived posterior follicle cells to receive the Grk signal from the oocyte, we studied the expression of different follicle cell markers in *Mer* egg chambers. The results show that Mer^{ts1} posterior follicle cells receive the Grk signal correctly, as they express posterior and not anterior markers (Fig. 3A-D). We conclude that Merlin is not required for any aspect of Grk signalling or its reception in the posterior follicle cells. Merlin is also not required for Notch signalling among the posterior follicle cells, which is required to specify the correct number of posterior cells (Gonzalez-Reyes and St Johnston, 1998).

We also tested whether Merlin is required for the formation or identity of other types of follicle cells by analysing markers for different follicle cell populations in Mer^{ts1}. These included a marker for border cells, stalk cells and polar follicle cells. Our results show that Merlin is not required for the correct

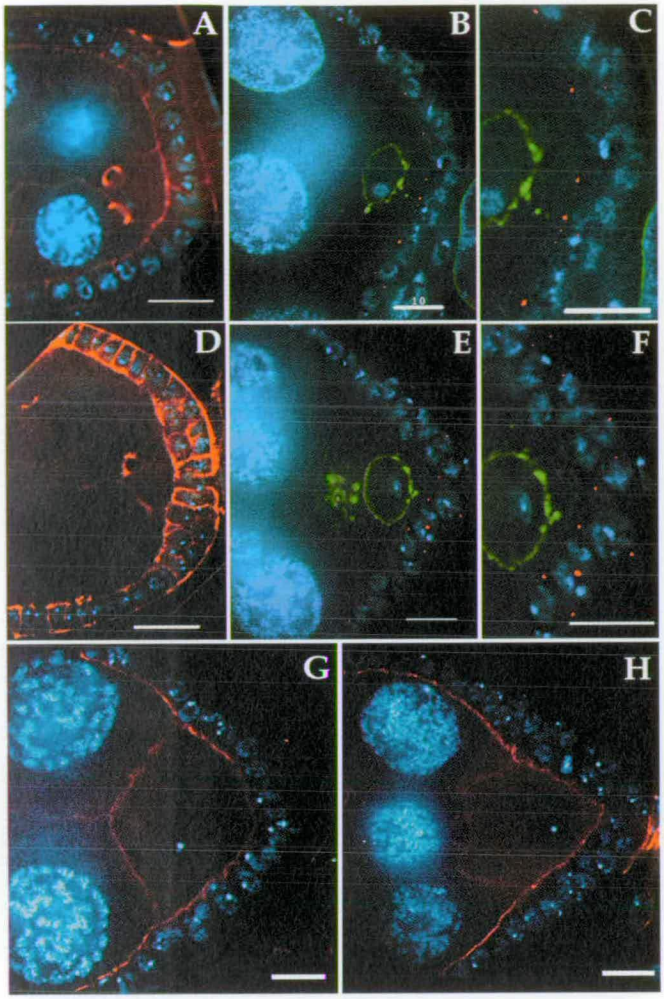

Fig. 4. *Mer* mutations disrupt posterior follicle cell organisation. (A,D) Follicle cell morphology visualised by phalloidin-rhodamine staining of actin (red) and DAPI staining of DNA (blue). (A) Control showing a columnar monolayer of follicle cells. (D) Mer^{ts1} mutant showing a double layer of follicle cells only at the posterior. (B,C,E,F) The polarity of follicle cells in control and Mer^{ts1} egg chambers showing centrosomes (γ-tubulin, red), the nuclear envelope (wheat germ agglutinin (WGA), green) and DNA (DAPI staining, blue). (B) Control showing that follicle cell centrosomes usually point to the apical surface, adjacent to the oocyte. (C) A higher magnification view of the posterior part of (B). (E) Mer^{ts1} egg chamber showing follicle cell centrosomes pointing both apically and basally. The oocyte nucleus has failed to migrate. WGA also stains the yolk particles, the boundary of the oocyte and outer edge of the follicle cells. (F) A higher magnification view of the posterior part of E. The centrosomes are not visible in some cells, as they are located in another focal plane. (G,H) Apical polarity visualised with anti-spectrin β heavy chain (β_H-spectrin) antibody (red) and DNA (blue). (G) Control showing apical localisation of β_H-spectrin in follicle cells. (H) Mer^{ts1} mutant showing normal apical β_H-spectrin in follicle cells adjacent to the oocyte, but no detectable β_H-spectrin in the outer layer of posterior follicle cells. Scale bars: 10 μm.

specification or development of any subgroup of follicle cells, and is not required for Notch signalling among the follicle cells, which limits the number of polar follicle cells to two (Fig. 3E,F). Merlin is therefore likely to be required for cell

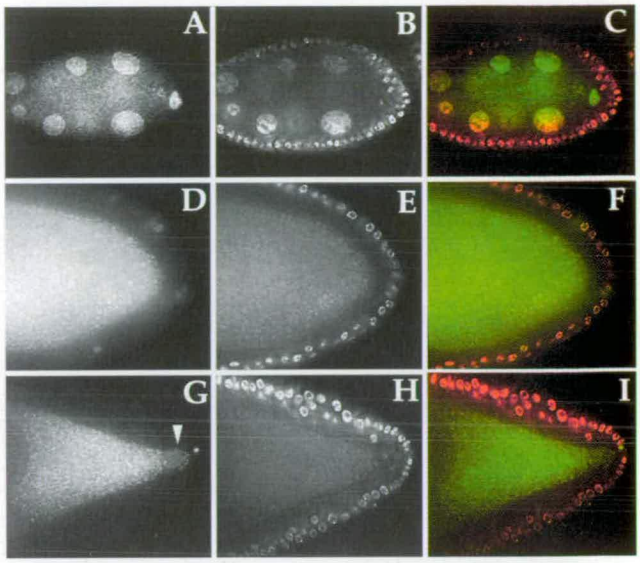

Fig. 5. Merlin is required non-autonomously in the posterior follicle cells to maintain their monolayer columnar morphology. (A-I) Examples of mosaic egg chambers with homozygous mutant *Mer* clones lacking nlsGFP expression. (A,D,G) nlsGFP expression (green in C,F,I). (B,E,H) DAPI staining showing all nuclei in the egg chambers (red in C,F,I). (A-C) Stage 8 in which all the follicle cells are Mer^3, but the germline is $Mer^3/+$, showing an identical phenotype to egg chambers from Mer^3 mothers. The nucleus has failed to migrate. (D-F) Stage 10 with four very small patches of $Mer^3/+$ follicle cells at the posterior in a homozygous Mer^3 mutant background. The few $Mer^3/+$ cells rescue the *Mer* mutant phenotype in all the neighbouring follicle cells and also rescue the nuclear migration phenotype. (G-I) Stage 10 with one $Mer^3/+$ follicle cell at the posterior in a Mer^3 mutant background. The single *Mer*/+ cell is able to rescue the mutant phenotype in the neighbouring follicle cells, but fails to rescue the nuclear migration phenotype. Arrowhead marks the oocyte nucleus.

communication between the follicle cells and oocyte, downstream of Grk and upstream of the unknown polarising signal from the posterior follicle cells to the oocyte.

Merlin acts as a tumour suppressor in posterior follicle cells and is required for their polarity

We observed that the posterior follicle cells in fixed (Figs 3D-F, 4D-F,H) and living (data not shown) *Mer* egg chambers often have a slightly disrupted morphology. To study these defects in more detail, we covisualised actin and DNA to highlight each cell and its boundaries (Fig. 4A,D). Posterior follicle cells in controls have a uniform columnar appearance characteristic of epithelial sheets (Fig. 4A). However, after stage 6, Mer^{ts1} egg chambers have a double layer of follicle cells only at the posterior where follicle cells are in contact with the oocyte (Fig. 4D). To determine whether the double layer of posterior follicle cells is due to overproliferation, we counted the number of cells using three-dimensional microscopy and found a twofold increase in the number of posterior follicle cells, but no changes in other follicle cells (data not shown).

To determine whether the overproliferation of posterior follicle cells is accompanied by polarity defects, we studied MT polarity by covisualising DNA, the nuclear envelope and centrosomes (Fig. 4B,C,E,F). In control egg chambers, most

centrosomes lie on the apical side of each nucleus, where the minus ends of MTs are found (Fig. 4B,C). In contrast, Mer^{ts1} posterior follicle cells mostly loose the apical-basal polarity of their MTs (Fig. 4E,F).

To investigate whether other aspects of the apical-basal polarity of the posterior follicle cells are also disrupted, we studied the distribution of β-spectrin heavy chain (β_H-spectrin) in *Mer* mutants (Fig. 4G,H). β_H-Spectrin is normally restricted to the apical side of follicle cells within a Spectrin-based membrane skeleton (Fig. 4G) (Zarnescu and Thomas, 1999). In Mer^{ts1} mutants β_H-spectrin is apically localised in the cells adjacent to the oocyte, but not detected in the second layer of follicle cells (Fig. 4H). These results suggest that in *Mer* mutants, the apical surface of posterior follicle cells contacts the oocyte correctly, and is probably competent to send and receive signals to the oocyte.

To determine whether the defects in cell proliferation and polarity in *Mer* egg chambers are dependent on receiving the Grk signal, we examined the follicle cells of *Mer, grk* double mutants. We found that even a hypomorphic allele of *grk* (grk^{2E12}) suppresses the *Mer* posterior follicle cell phenotype entirely (data not shown). We conclude that Merlin is required only in cells that receive the Grk signal and is not a constitutive factor required for cell polarity and proliferation.

Merlin is required non-autonomously in posterior follicle cells

To test directly whether Merlin is required only in posterior follicle cells, we used genetic mosaic analysis with the FRT/FLP system to make clones of homozygous *Mer* follicle cells located at posterior, anterior or central positions (Fig. 5A-I). We found that Merlin is required only in the posterior follicle cells for their correct morphology and migration of the oocyte nucleus. We produced *Mer* clones using Mer^3,FRT/*nlsGFP*,FRT; *en-Gal4,UASFLP* females. Mer^3 is a homozygous viable but sterile allele (Fehon et al., 1997) and *en-Gal4,UASFLP* expresses FLP recombinase at very high levels only in the follicle cells (Duffy et al., 1998). We examined a total of 43 egg chambers with Mer^3 clones, of which 29 were particularly revealing and analysed in detail. Of these, one egg chamber had follicle cells that were entirely Mer^3 (Fig. 5A-C), and three egg chambers had large mutant clones covering all the posterior (data not shown). These egg chambers showed a strong *Mer* phenotype indistinguishable from non-mosaic homozygous Mer^3 mutants. 21 egg chambers had large anterior or main body follicle cell clones without a *Mer* phenotype (data not shown). We conclude that Merlin is required only in posterior follicle cells.

To test whether Merlin is required cell autonomously to limit the proliferation and polarity of posterior follicle cells, we studied four egg chambers in which the follicle cells were Mer^3, except for one or more very small Mer^3/+ clones in the posterior follicle cells. Such egg chambers showed complete rescue of the Mer^3 phenotype when sufficient Mer^3/+ cells were present (Fig. 5D-F), indicating that Merlin acts cell non-autonomously among the posterior follicle cells. One of these clones had a single Mer^3/+ cell at the posterior tip surrounded by Mer^3 cells, showing that a single Mer^3/+ cell is able to rescue the overproliferation phenotype up to a distance of about six cell diameters (Fig. 5G-I). While the single Mer^3/+ cell was not able to rescue the oocyte nuclear migration defect, several small Mer^3/+ clones were sufficient to do so. We conclude that Merlin is required non-autonomously in the posterior follicle cells to limit their proliferation.

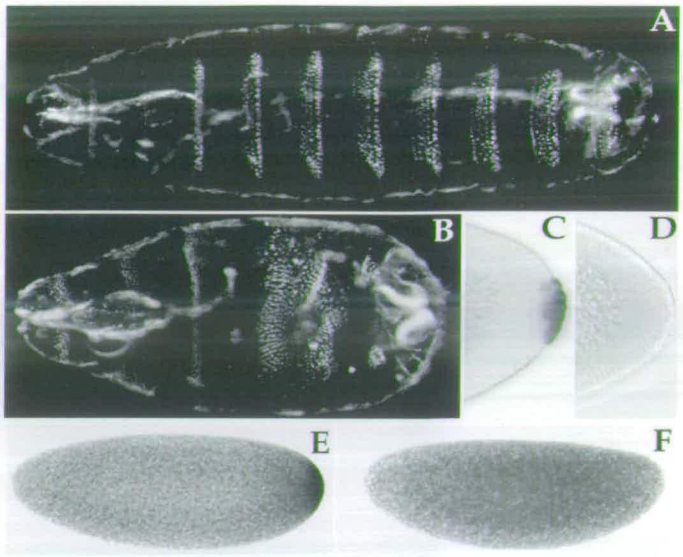

Fig. 6. *Mer* mutations disrupt *osk* mRNA localisation in some embryos, leading to abdominal defects and a lack of pole cells. (A,B) Cuticle preparations from Mer^{ts1} mutant eggs. (A) Normal cuticle of hatched eggs (79%). (B) Abdominal defects in unhatched eggs (21%). (C,D) Vasa antibody staining of pole cells in Mer^{ts1} embryos. (C) Normal numbers of pole cells (52% of cases). (D) Pole cells are absent (48% of cases). (E,F) *osk* mRNA localisation. (E) Control pre-blastoderm embryo showing normal posterior *osk* mRNA localisation. (F) Mer^{ts1} embryo showing unlocalised *osk* mRNA (50% of cases).

Merlin is not required during embryogenesis

To test whether Merlin is required for embryogenesis we analysed the hatch rate of eggs laid by Mer^{ts1} mothers. At 29°C, 74% of eggs (n=100) hatch and develop normally until third instar larvae, compared with a hatch rate of 94% for Mer^{ts1} at 21°C and yw^{67g} at 29°C (a difference of 21%). All the unhatched embryos have abdominal cuticle defects similar to *osk* alleles (Fig. 6B), while the eggs that hatch have normal cuticles (Fig. 6A). We found that *osk* mRNA is mislocalised in 51% of embryos (n=104) (Fig. 6F) and 48% of embryos (n=103) show missing pole cells (Fig. 6D), explaining why many of the resulting flies have few germ cells (data not shown). These results are consistent with the fact that *osk* alleles are known to disrupt pole cell formation more readily than abdominal patterning (Lehmann and Nüsslein-Volhard, 1986).

Initially, it was surprising that most *Mer* eggs hatch, since mislocalised *bcd* mRNA would be expected to disrupt AP axis specification and cause embryonic lethality. However, we found that *bcd* mRNA, which was mislocalised at the posterior, partially or completely relocalised in older egg chambers (Fig. 7A-D). Consequently, Mer^{ts1} embryos have completely normal *bcd* localisation (Fig. 7E,F). The near normal hatch rate of *Mer* eggs was also initially surprising because 55% (n=89) of *Mer* mutants have misplaced oocyte nuclei and mislocalised *grk* mRNA, which would lead to embryonic lethality. However, we

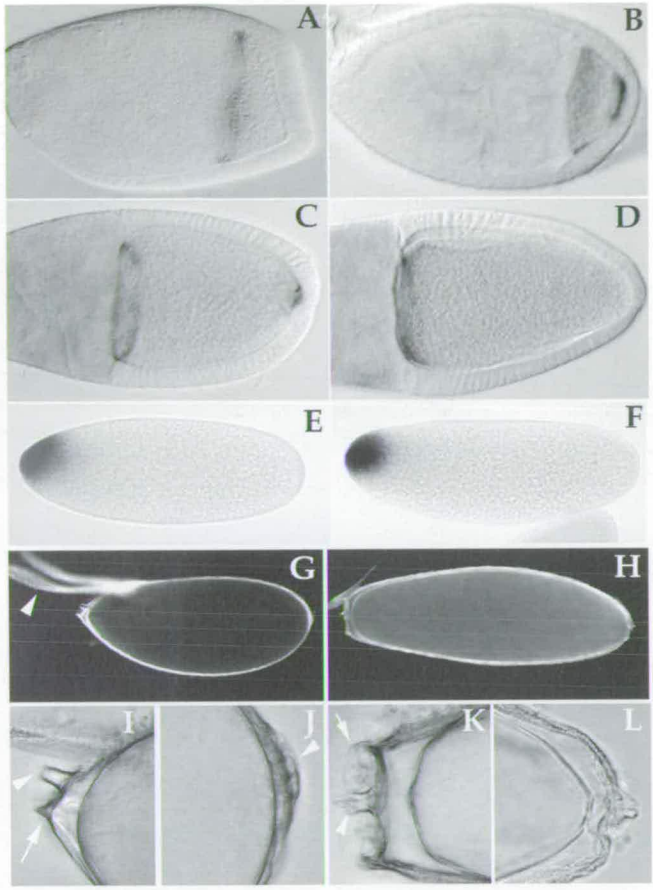

Fig. 7. Mutant *Mer* mothers lay eggs with normal *bcd* mRNA localisation, but some dorsoventral defects. (A-F) *bcd* mRNA in *Mer* and control egg chambers and embryos. (A) Stage 9 control showing normal *bcd* mRNA localisation in an anterior ring. (B) Stage 9 Mer^{ts1} mutant showing *bcd* mislocalisation at the posterior. (C) Stage 10B Mer^{ts1} mutant showing a reduced level of *bcd* mRNA at the posterior. (D) Stage 11 Mer^{ts1} mutant showing no *bcd* mRNA localisation at the posterior. (E) Control pre-blastoderm embryo showing *bcd* mRNA localisation at the anterior. (F) Pre-blastoderm Mer^{ts1} embryo showing indistinguishable anterior *bcd* mRNA localisation to controls. (G,I,J) Control Mer^{ts1} at 21°C showing the same structures as wild type eggs or *yw* eggs at 29°C (not shown). (G) Egg with dorsal appendages (arrowhead). (I) Higher power anterior view of dorsally positioned micropyle (arrowhead) and centrally placed operculum (arrow). (J) High power posterior view of dorsally placed aeropyle (arrowhead). (H,K,L) Egg from Mer^{ts1} female at 29°C. (H) Egg showing a lack of dorsal appendages and a torpedo-like shape (11% of cases). The other 89% are normal (not shown). Females retain many of the defective eggs (not shown). (K) High power anterior view showing a centrally located micropyle (arrowhead) and a symmetric ringed operculum (arrow). (L) High power posterior view showing an enlarged aeropyle.

found that only 11% (n=158) of eggs laid by Mer^{ts1} mothers have strong dorsoventral defects (Fig. 7H,K,L), and the other defective egg chambers degenerate in females after stage 10A (data not shown). It is likely that egg chambers with mislocalised *osk* mRNA also degenerate in the mothers, explaining why there is a lower percentage of *osk* mRNA localisation defects in embryos compared with oocytes.

We conclude that *Mer* eggs hatch at a slightly lower frequency than controls because of abdominal and dorsoventral defects that originate during oogenesis, rather than a direct requirement for Merlin in embryos. Therefore, Merlin is not required for embryogenesis and much of larval development.

DISCUSSION

We have shown that Merlin is required for the signal that initiates axis specification. Merlin is also required non-autonomously for signalling among the posterior follicle cells that limits their proliferation and maintains their polarity. Merlin is not required for other signals within the posterior follicle cells or in other parts of egg chambers and embryos.

Taking our data in the context of previous work, we propose that Merlin is involved in apical targeting of the unknown signal that initiates axis specification in the oocyte. Merlin is a member of the ERM/4.1 family of proteins and, in *Drosophila*, it is localised to the apical membrane of follicle cells and in the germline (McCartney and Fehon, 1996). ERM family members are thought to function as linkers between the cytoskeleton and the apical membrane, and they are probably required for apical targeting of signals, maintenance of epithelial adhesion, apical-basal polarity and to limit cell proliferation (Vaheri et al., 1997).

The overproliferation of the posterior follicle cells is consistent with overproliferation of mutant *Mer* cells seen in imaginal discs and with the function of human Merlin as a tumour suppressor causing neurofibromatosis-2. The changes in cell polarity we observe are also common in many other types of tumours. Interestingly, as in other *Drosophila* tissues (LaJeunesse et al., 1998), the *Mer* phenotypes we have studied are more similar in character to benign tumours seen in individuals with neurofibromatosis-2 than to the aggressive tumours produced in the mouse model (McClatchey et al., 1998). However, it is not known whether Merlin is required during mammalian oogenesis. We speculate that human Merlin may function in a similar non-autonomous manner in response to particular signals such as TGFα, which is known to be expressed in mammalian oocytes (Vaughan et al., 1992). Indeed, many parallels may exist between mammalian and fly oogenesis in respect of communication between the oocyte and follicle cells (Deng et al., 1997).

Is Merlin directly involved in signals that initiate axis specification?

We have shown that Merlin has a more specific and restricted function than previously thought, as it is required only in cells that receive the posterior Grk signal, despite being expressed more widely in egg chambers (McCartney and Fehon, 1996). Interestingly, the dorso-anterior follicle cells do not require Merlin, despite receiving the Grk signal.

Our data show that Merlin is required downstream of Grk but upstream of the unknown polarising signal. We propose that the effect of Merlin on the polarising signal is not indirectly due to the overproliferation and subtle changes in the polarity of the posterior follicle cells. β_H-Spectrin is correctly distributed in *Mer* follicle cells adjacent to the oocyte, despite the centrosomes being disorganised and the second layer of follicle cells showing mislocalised β_H-spectrin. Therefore, the inner layer of posterior follicle cells are probably competent to

send the polarising signal in *Mer* mutants. Furthermore, some *Mer* egg chambers were found in which the polarising signal was not received, despite the posterior follicle cells showing no apparent defects in their proliferation or polarity (data not shown). We also found that *brn* mutant egg chambers show a similar specific morphological disruption of posterior follicle cells to that seen in *Mer* mutants (Goode et al., 1996a; Goode et al., 1996b) but *brn* mutations do not lead to any defects in oocyte axis specification (data not shown). Therefore, the morphological disruption of the posterior follicle cells in itself is not likely to be responsible for perturbing the unknown signal to the oocyte. Instead, we propose that Merlin may have a more direct role in targeting the polarising signal to the apical surface of posterior follicle cells.

What signals are disrupted by *Mer* mutations?

Since many genes involved in signalling among the follicle cells and between the oocyte and follicle cells are unknown, it is difficult to be certain which signals might be disrupted by *Mer* mutations. Nevertheless, our data conclusively rule out a role for Merlin in a number of known signalling processes. Merlin is not required for receiving the Grk signal via Torpedo, an EGF-like receptor, by the posterior or dorso-anterior follicle cells. Merlin is also not required for lateral inhibition via Notch-Delta signalling among the posterior follicle cells, that determines the correct number of posterior, polar posterior follicle cells and stalk cells between egg chambers. Nor is Merlin required for many kinds of essential signalling pathways throughout embryogenesis. Merlin is unlikely to play a direct role in the presumptive Egh/Brn signal from the oocyte, as these proteins are required in the oocyte and not in the follicle cells. Nevertheless, it is intriguing that the posterior follicle cells of *N*, *brn* or *egh* mutant egg chambers all show a similar overproliferation phenotype to *Mer* egg chambers. While it is possible that N, Egh or Brn are in some way related in function to Merlin, further experiments will have to be performed to explore these issues.

Our results show that Merlin is required for two distinct processes involving signalling, but we cannot distinguish whether the two processes depend on a single signal or two distinct signals. For example, the restriction of posterior follicle cell proliferation could require the same unknown signal that initiates MT repolarisation in the oocyte. Both processes could depend on the same signal secreted into the space between the follicle cells and oocyte. Indeed, it is intriguing that *Merlin* egg chambers have MT polarity defects in both the oocyte and the posterior follicle cells. However, further progress awaits the identification of the signal or signals involved.

The identity of the polarising signal is unknown, but some genes are known to be required for the signal, including PKA (Lane and Kalderon, 1995), Mago (Micklem et al., 1997) and Laminin A. Merlin is unlikely to be required for PKA and Mago functions as they are required in the oocyte. In contrast, Laminin A is expressed and required in posterior follicle cells as a component of the extracellular matrix (Deng and Ruohola-Baker, 2000). It is tempting to speculate that Merlin and Laminin A could be functionally linked as specialised structural components required specifically in the posterior follicle cells for the transduction of the polarising signal.

It is interesting to ask how many additional components are required for axis specification in the oocyte but it is not possible to estimate this number from our results. However, the fact that we identified even one mutation required for this process out from only 73 ts alleles, strongly argues that there are many more unrecognised genes required for axis formation.

We thank Rick Fehon for discussions of unpublished observations. We also thank Catherine Rabouille, Rick Fehon, Andrew Jarman, Daniel St Johnston, Hildegard Tekotte and David Ish-Horowicz for comments on the manuscript, and Rick Fehon, Debiao Zhan and Mary Bownes, Peter Deak and David Glover, Stefan Luschnig, Margarete Heck and Alan Spradling, Daniel Kalderon, Graham Thomas, Daniel St Johnston and the Bloomington stock centre for fly stocks and antibodies. We thank Gill MacKay for unpublished observations. This work was supported by a Wellcome Trust career development fellowship and Lister senior fellowship to I. D., a Darwin Trust studentship to N. M., Wellcome Trust studentship to Y. L., MRC studentship to G. W., a Human Frontiers fellowship to H. F. L. and an NIH grant (GM46409) to W. S.

REFERENCES

Anderson, K. V. (1998). Pinning down positional information: dorsal-ventral polarity in the *Drosophila* embryo. *Cell* **95**, 439-442.

Clark, I., Giniger, E., Ruohola-Baker, H., Jan, L. Y. and Jan, Y. N. (1994). Transient posterior localization of a kinesin fusion protein reflects anteroposterior polarity of the *Drosophila* oocyte. *Curr. Biol.* **4**, 289-300.

Clark, I. E., Jan, L. Y. and Jan, Y. N. (1997). Reciprocal localization of Nod and kinesin fusion proteins indicates microtubule polarity in the *Drosophila* oocyte, epithelium, neuron and muscle. *Development* **124**, 461-470.

Davis, I. (2000). Visualising fluorescence in *Drosophila* – optimal detection in thick specimens. In *Protein Localisation by Fluorescence Microscopy: A Practical Approach*. Vol. 218 (ed. V. J. Allan), pp. 131-162. Oxford: Oxford University Press.

Davis, I., Girdham, C. H. and O Farrell, P. H. (1995). A nuclear GFP that marks nuclei in living *Drosophila* embryos – maternal supply overcomes a delay in the appearance of zygotic fluorescence. *Dev. Biol.* **170**, 726-729.

Deng, W. M., Zhao, D., Rothwell, K. and Bownes, M. (1997). Analysis of P[gal4] insertion lines of *Drosophila* melanogaster as a route to identifying genes important in the follicle cells during oogenesis. *Mol. Hum. Reprod.* **3**, 853-862.

Deng, W. M. and Bownes, M. (1998). Patterning and morphogenesis of the follicle cell epithelium during *Drosophila* oogenesis. *Int. J. Dev. Biol.* **42**, 541-552.

Deng, W. M. and Ruohola-Baker, H. (2000). Laminin A is required for follicle cell-oocyte signaling that leads to establishment of the anterior-posterior axis in *Drosophila*. *Curr. Biol.* **10**, 683-686.

Driever, W. and Nüsslein-Volhard, C. (1988). A gradient of bicoid protein in *Drosophila* embryos. *Cell* **54**, 83-93.

Duffy, J. B., Harrison, D. A. and Perrimon, N. (1998). Identifying loci required for follicular patterning using directed mosaics. *Development* **125**, 2263-2271.

Ephrussi, A., Dickinson, L. K. and Lehmann, R. (1991). Oskar organizes the germ plasm and directs localization of the posterior determinant nanos. *Cell* **66**, 37-50.

Fasano, L. and Kerridge, S. (1988). Monitoring positional information during oogenesis in adult *Drosophila*. *Development* **104**, 245-253.

Fehon, R. G., Oren, T., Lajeunesse, D. R., Melby, T. E. and McCartney, B. M. (1997). Isolation of mutations in the *Drosophila* homologues of the human Neurofibromatosis 2 and yeast CDC42 genes using a simple and efficient reverse-genetic method. *Genetics* **146**, 245-252.

Gonzalez-Reyes, A., Elliott, H. and St Johnston, D. (1995). Polarization of both major body axes in *Drosophila* by Gurken-Torpedo signaling. *Nature* **375**, 654-658.

Gonzalez-Reyes, A. and St Johnston, D. S. (1998). Patterning of the follicle cell epithelium along the anterior-posterior axis during *Drosophila* oogenesis. *Development* **125**, 2837-2846.

Goode, S., Melnick, M., Chou, T. B. and Perrimon, N. (1996a). The

neurogenic genes egghead and brainiac define a novel signaling pathway essential for epithelial morphogenesis during *Drosophila* oogenesis. *Development* **122**, 3863-3879.

Goode, S., Morgan, M., Liang, Y. P. and Mahowald, A. P. (1996b). brainiac encodes a novel, putative secreted protein that cooperates with Grk TGF alpha in the genesis of the follicular epithelium. *Dev. Biol.* **178**, 35-50.

LaJeunesse, D. R., McCartney, B. M. and Fehon, R. G. (1998). Structural analysis of *Drosophila* merlin reveals functional domains important for growth control and subcellular localization. *J. Cell Biol.* **141**, 1589-1599.

Lane, M. E. and Kalderon, D. (1994). RNA localization along the anteroposterior axis of the *Drosophila* oocyte requires PKA-mediated signal transduction to direct normal microtubule organization. *Genes Dev.* **8**, 2986-2995.

Lane, M. E. and Kalderon, D. (1995). Localization and functions of protein kinase A during *Drosophila* oogenesis. *Mech. Dev.* **49**, 191-200.

Larkin, M. K., Holder, K., Yost, C., Giniger, E. and Ruohola-Baker, H. (1996). Expression of constitutively active Notch arrests follicle cells at a precursor stage during *Drosophila* oogenesis and disrupts the anterior-posterior axis of the oocyte. *Development* **122**, 3639-3650.

Lehmann, R. and Nüsslein-Volhard, C. (1986). Abdominal segmentation, pole cell formation, and embryonic polarity require the localized activity of oskar, a maternal gene in *Drosophila*. *Cell* **47**, 141-152.

Mangeat, P., Roy, C. and Martin, M. (1999). ERM proteins in cell adhesion and membrane dynamics. *Trends Cell Biol.* **9**, 187-192.

McCartney, B. M. and Fehon, R. G. (1996). Distinct cellular and subcellular patterns of expression imply distinct functions for the *Drosophila* homologues of moesin and the neurofibromatosis 2 tumor suppressor, merlin. *J. Cell Biol.* **133**, 843-852.

McCartney, B. M., Kulikauskas, R. M., LaJeunesse, D. R. and Fehon, R. G. (2000). The neurofibromatosis-2 homologue, Merlin, and the tumor suppressor expanded function together in *Drosophila* to regulate cell proliferation and differentiation. *Development* **127**, 1315-1324.

McClatchey, A. I., Saotome, I., Mercer, K., Crowley, D., Gusella, J. F., Bronson, R. T. and Jacks, T. (1998). Mice heterozygous for a mutation at the NF2 tumor suppressor locus develop a range of highly metastatic tumors. *Genes Dev.* **12**, 1121-1133.

Micklem, D. R., Dasgupta, R., Elliott, H., Gergely, F., Davidson, C., Brand, A., Gonzalez-Reyes, A. and St Johnston, D. (1997). The *mago nashi* gene is required for the polarisation of the oocyte and the formation of perpendicular axes in *Drosophila*. *Curr. Biol.* **7**, 468-478.

Neuman-Silberberg, F. S. and Schüpbach, T. (1993). The *Drosophila* dorsoventral patterning gene gurken produces a dorsally localized RNA and encodes a TGF alpha-like protein. *Cell* **75**, 165-174.

Newmark, P. A., Mohr, S. E., Gong, L. and Boswell, R. E. (1997). *mago nashi* mediates the posterior follicle cell-to-oocyte signal to organize axis formation in *Drosophila*. *Development* **124**, 3197-3207.

Nilson, L. A. and Schüpbach, T. (1999). EGF receptor signaling in *Drosophila* oogenesis. *Curr. Top. Dev. Biol.* **44**, 203-243.

Perrimon, N. (1994). Signalling pathways initiated by receptor protein tyrosine kinases in *Drosophila*. *Curr. Opin. Cell Biol.* **6**, 260-266.

Ruohola, H., Bremer, K. A., Baker, D., Swedlow, J. R., Jan, L. Y. and Jan, Y. N. (1991). Role of neurogenic genes in establishment of follicle cell fate and oocyte polarity during oogenesis in *Drosophila*. *Cell* **66**, 433-449.

Schüpbach, T. (1987). Germ line and soma cooperate during oogenesis to establish the dorsoventral pattern of egg shell and embryo in *Drosophila melanogaster*. *Cell* **49**, 699-707.

Tautz, D. and Pfeifle, C. (1989). A non-radioactive in situ hybridization method for the localization of specific RNAs in *Drosophila* embryos reveals translational control of the segmentation gene hunchback. *Chromosoma* **98**, 81-85.

Theurkauf, W. E., Smiley, S., Wong, M. L. and Alberts, B. M. (1992). Reorganization of the cytoskeleton during *Drosophila* oogenesis – implications for axis specification and intercellular transport. *Development* **115**, 923-936.

Tsukita, S., Oishi, K., Sato, N., Sagara, J. and Kawai, A. (1994). ERM family members as molecular linkers between the cell surface glycoprotein CD44 and actin-based cytoskeletons. *J. Cell Biol.* **126**, 391-401.

Turunen, O., Sainio, M., Jaaskelainen, J., Carpen, O. and Vaheri, A. (1998). Structure-function relationships in the ezrin family and the effect of tumor-associated point mutations in neurofibromatosis 2 protein. *Biochim. Biophys. Acta* **1387**, 1-16.

Vaheri, A., Carpen, O., Heiska, L., Helander, T. S., Jaaskelainen, J., Majander-Nordenswan, P., Sainio, M., Timonen, T. and Turunen, O. (1997). The ezrin protein family: Membrane-cytoskeleton interactions and disease associations. *Curr. Opin. Cell Biol.* **9**, 659-666.

van Eeden, F. and St Johnston, D. (1999). The polarisation of the anterior-posterior and dorsal-ventral axes during *Drosophila* oogenesis. *Curr. Opin. Genet. Dev.* **9**, 396-404.

Vaughan, T. J., James, P. S., Pascall, J. C. and Brown, K. D. (1992). Expression of the genes for TGF alpha, EGF and the EGF receptor during early pig development. *Development* **116**, 663-669.

Wilkie, G. and Davis, I. (1998). High resolution and sensitive mRNA in situ hybridisation using fluorescent tyramide signal amplification. *Tech. Tips Online* **t01458** (http://www.biomednet.com/db/tto).

Wilkie, G., Shermoen, A., O'Farrell, H. and Davis, I. (1999). Transcribed genes are localized according to chromosomal position within polarized *Drosophila* embryonic nuclei. *Curr. Biol.* **9**, 1263-1266.

Zarnescu, D. C. and Thomas, G. H. (1999). Apical spectrin is essential for epithelial morphogenesis but not apicobasal polarity in *Drosophila*. *J. Cell Biol.* **146**, 1075-1086.

Transcribed genes are localized according to chromosomal position within polarized *Drosophila* embryonic nuclei

Gavin S. Wilkie*, Antony W. Shermoen†, Patrick H. O'Farrell† and Ilan Davis*

When some genes are silenced, their positions within the nucleus can change dramatically [1,2]. It is unclear, however, whether genes move to new positions when they are activated [3]. The chromosomes within the polarized nuclei of the fruit fly *Drosophila* have a well-characterized apical–basal orientation (the Rabl configuration [4]). Using a high-resolution *in situ* hybridization method [5], we found that each of 15 transcribed genes was localized as predicted by their chromosomal position and by the known polarized organization of the chromosomes. We also found that, within their specific apical–basal plane, most nascent transcript foci could occupy any radial position. There was no correlation between the apical–basal position of the transcribed locus and the final cytoplasmic site of localization of the RNA along the apical–basal axis of the cell. There was also no relationship between the distance of loci from the nuclear periphery and the amount of nascent mRNA decorating the gene. Our results are consistent with the view that effective transcription can occur without major re-localization of the genes themselves.

Addresses: *Institute of Cell and Molecular Biology, University of Edinburgh, King's Buildings, Mayfield Road, Edinburgh EH9 3JR, Scotland, UK. †Department of Biochemistry and Biophysics, Box 0448, University of California San Francisco, San Francisco, California 94143, USA.

Correspondence: Ilan Davis
E-mail: ilan.davis@ed.ac.uk

Received: **21 June 1999**
Revised: **7 September 1999**
Accepted: **13 September 1999**

Published: **25 October 1999**

Current Biology 1999, 9:1263–1266

0960-9822/99/$ – see front matter

Results and discussion

Nascent transcript foci are consistently positioned in the apical–basal nuclear axis

It is unclear to what extent the intranuclear position of genes changes according to their differing transcriptional states in various parts of the *Drosophila* embryo. Such potential variation in nuclear localization would not necessarily be apparent in studies describing the average intranuclear position of genes throughout the entire embryo [6]. We used a recently developed high-resolution RNA *in situ* hybridization method [5] to examine the localization of 15 different transcribed genes. In addition to cytoplasmic mRNA, nascent transcripts are visible as one to four small fluorescent foci within each nucleus that expresses a gene, depending on the state of pairing and DNA replication. The positions of 19–52 individual nascent transcript foci from each gene were mapped in nuclei from optical sections through the middle of two to three embryos of similar age (Figure 1b). The apical–basal distribution of the nascent transcript foci on the X chromosome and chromosome arms 2R and 3R were determined by plotting all the data onto the outline of a single representative nucleus (Figure 1c and see Supplementary material).

We found that the position of each transcribed gene was restricted to a particular plane along the apical–basal nuclear axis as predicted by the cytological position of the gene and the apical–basal, Rabl conformation of chromosomes. Genes near the centromeres were located in the apical hemisphere and those near the telomeres localized towards the basal pole of the nucleus. Genes in other parts of the chromosomes lay in intermediate positions in the apical–basal axis (Figure 1c and Supplementary material). All of the genes we studied occupied distinct locations, including *fushi tarazu* (*ftz*) and *hunchback* (*hb*), which are separated by only 10 centimorgans (one-tenth of a chromosome arm) and have overlapping but distinguishable nuclear distributions (Figure 1c). Our results also show conclusively that the intranuclear position of transcribed genes is not related to the cytoplasmic distribution of the mRNA. These results complement and extend previous findings [7].

Within their constrained apical–basal position, transcribed genes do not adopt a consistent radial position

We also investigated whether nascent transcript foci are consistently positioned with respect to nuclear axes perpendicular to the apical–basal axis. Nascent transcript foci from 11 endogenous genes were examined within a cross section through many nuclei (Figure 2b–m). For each of these genes, we imaged 23–103 nascent transcript foci distributed among two to three embryos of similar age and plotted their positions onto a profile of a typical nucleus. In all but one case, we detected no restriction of the foci to particular radial positions nor any consistent preference or exclusion from the nuclear envelope (Figure 2b–m). The genes studied included *ftz* (Figure 2f), of which the intranuclear position is in agreement with previous studies of a large genomic region containing *ftz* [6]. In contrast, *paired* (*prd*) nascent transcript foci were found to localize

Figure 1

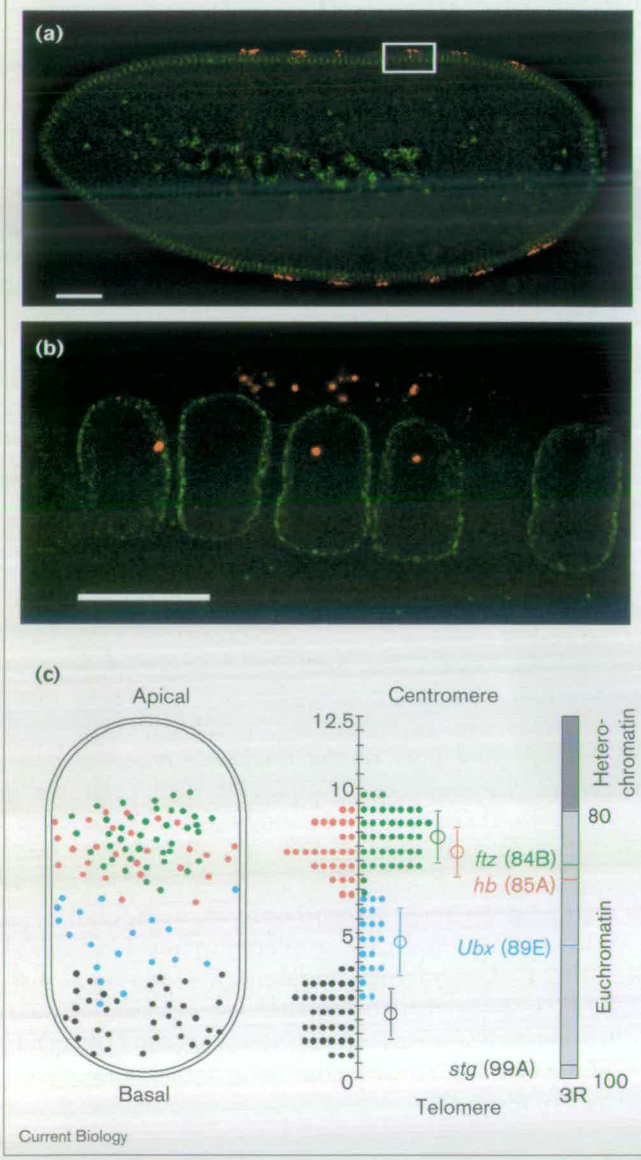

The position of nascent transcript foci along the apical–basal axis of embryonic nuclei. **(a,b)** Optical sections through the middle of a mid-interphase 14, blastoderm embryo expressing *ftz* mRNA (red) in seven stripes. AlexaFluor488-conjugated wheat germ agglutinin (AlexaWGA) marks the nuclear envelope (green). (a) A low-magnification view of the embryo. (b) A high-magnification view of the boxed area in (a). Note that *ftz* mRNA is exclusively localised in the apical cytoplasm above the nuclei and as nascent transcript foci within expressing nuclei [14]. The scale bar represents 50 μm in (a) and 10 μm in (b). **(c)** A map of the intranuclear positions of four transcribed genes *fushi tarazu* (*ftz*, green), hunchback (*hb*, red), *Ultrabithorax* (*Ubx*, blue) and *string* (*stg*, black) from the right arm of chromosome 3 (3R). Left, the observed nuclear positions plotted onto an average nucleus, 12.5 μm in length. Right, the cytological positions of the genes on a metaphase chromosome arm drawn to scale (based on [15]). Middle, a histogram drawn from the distribution of the nascent transcript foci that lie within 0.5 μm intervals. The average position is indicated by an open circle and the error bar represents the standard deviation.

mostly nearer the periphery (Figure 2e), in agreement with studies of a genomic region containing the *prd* gene, which is located near nuclear envelope attachment sites [6]. In conclusion, the intranuclear distribution of genes, within sub-regions of the embryo where they are expressed, simply follows the expected average position of their chromosomal sites over the entire embryo.

The intranuclear location of transcribed genes is independent of their level of expression

The perinuclear localization of chromatin helps to establish transcriptional silencing of some genes [8], and entire chromosomes can vary in their proximity to the nuclear periphery [9]. We tested whether the level of transcriptional activity of individual genes, in *Drosophila*, is related in any way to their proximity to the nuclear periphery. We first determined whether the intensity of fluorescence of a nascent transcript focus is a measure of the transcriptional activity of the gene. We measured the intensity of *run* nascent transcript foci in different parts of an embryo known to express *run* at different levels [10] (Figure 3a–c). Our results show that the intensity of the fluorescent signal is related to the level of expression of a gene (see Supplementary material). We then plotted, for a single embryo, the intensity of individual *run* nascent transcript foci against their distance from the nuclear periphery. Such plots were generated for a number of different transcribed genes and were reproducible from one embryo to another. In all cases that we studied, including different domains of *run* expression, a visual inspection of the plots showed that the intensity of nascent transcript foci was independent of their distance from the nuclear periphery (Figure 3d and Supplementary material). In all cases, linear regression analysis showed that the slope of the best-fit line was not significantly different from 0 (data not shown), confirming that the amount of nascent mRNA and the distance from the nuclear periphery were independent.

The intranuclear position of genes is not affected by abnormally abundant nascent mRNA

To test whether very large genes with abundant nascent mRNA are localized differently from the 11 shorter genes described above, we investigated the intranuclear distribution of *Ubx*, a 77 kb gene requiring 55 minutes to be transcribed completely [11]. *Ubx* nascent transcript foci were not specifically localized with respect to the nuclear periphery (Figure 4b), in agreement with studies that used DNA probes to the region surrounding *Ubx* [12].

To further test whether a large increase in the amount of nascent mRNA could influence the intranuclear position of a gene, we used transgenic flies expressing constructs lacking a polyadenylation signal. In these constructs, transcription continues past the end of the gene and into flanking sequences, increasing the number of nascent transcripts decorating the DNA. We first examined the

Figure 2

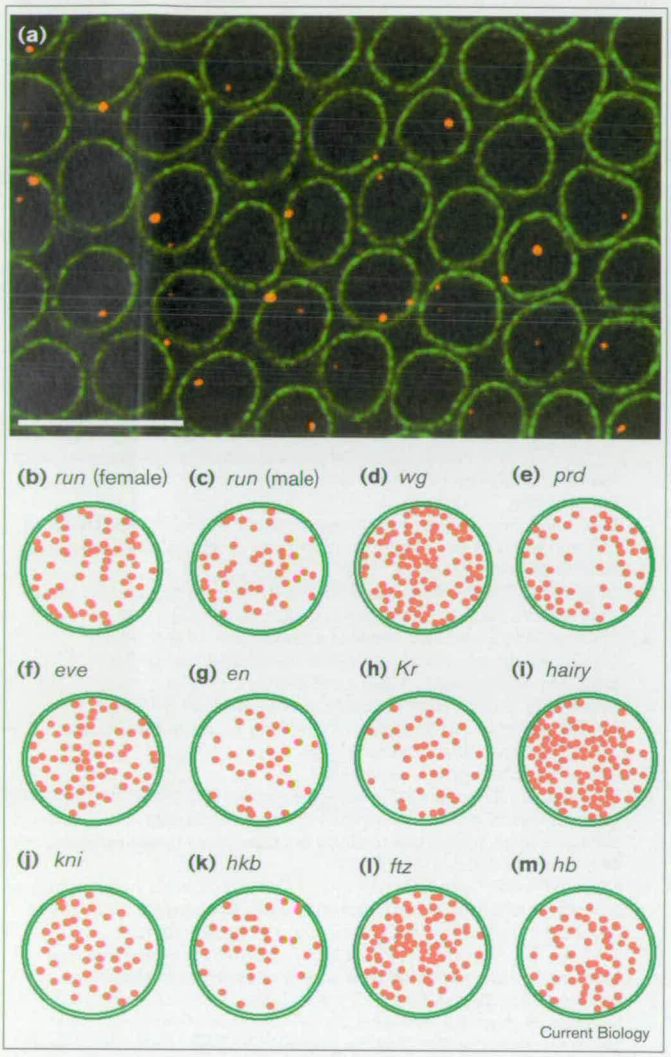

The position of transcribed genes in the plane perpendicular to the apical–basal axis of the nucleus. **(a)** Optical section through the layer of nuclei at the surface of the embryo, showing *hairy* (*h*) nascent transcript foci (red). AlexaWGA marks the nuclear envelope in green. The scale bar represents 10 μm. **(b–m)** Distribution of the nascent transcript foci of 11 genes plotted within average nuclear outlines. The distance to the nuclear envelope on the diagram is the same as the actual measured distance. Of the 11 genes, 10 had nascent transcript foci that could localize to any part of the nucleoplasm; *prd* showed some preference for the nuclear envelope, in accordance with the proximity of the gene to nuclear envelope attachment sites. No difference was observed between (b) female and (c) male embryos expressing *runt* (*run*), despite the different number of copies of the gene in the two sexes. Other gene abbreviations are: *en*, *engrailed*; *eve*, *even-skipped*; *hkb*, *huckebein*; *kni*, *knirps*; *Kr*, *Krüppel*; *wg*, *wingless*.

Figure 3

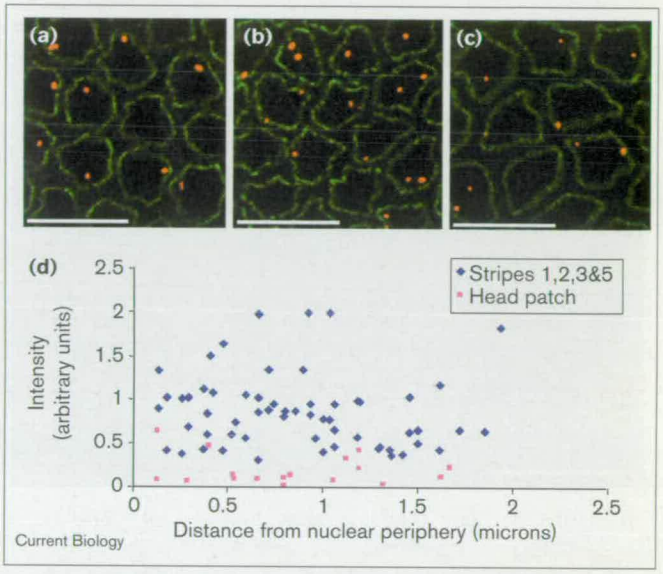

The intranuclear position and intensity of nascent transcript foci in different *run* expression domains. Representative optical sections through blastoderm nuclei used to quantify the relative fluorescence of nascent transcript foci in different *run* expression domains (red). AlexaWGA marks the nuclear envelope (green). The scale bars represent 10 μm. **(a–c)** The nascent transcript foci from stripe 1 of *run*, an X-linked gene, in (a) a male embryo, (b) a female embryo and (c) in the weakly expressed head patch of the embryo shown in (b). Each nucleus in (a) has only a single nascent transcript focus, but in (b) many nuclei contain a pair of nascent transcript foci, although some nuclei have a single nascent transcript focus due to pairing of homologous chromosomes. **(d)** A plot of the relative fluorescence intensity and distance from the nuclear periphery of individual *run* nascent transcript foci from different expression domains in a single embryo. The intensity and distance are unrelated whether in strongly expressing stripes (blue diamonds) or in the weaker head patch (pink squares).

nascent transcripts of *Xho25*, a *lacZ* fusion inserted in the *en* locus and lacking a polyadenylation signal ([13]; see Supplementary material). We found that *lacZ* and *en* genes have a similar distribution with respect to the nuclear envelope (Figure 4c,d), showing that increasing the number of nascent transcripts decorating the DNA does not alter its intranuclear localization. To test other cytological locations, in addition to *en*, we constructed *X44*, a fusion construct that lacks a polyadenylation signal. Transcription of *X44* is driven by the *hb* promoter and it contains 44 copies of a non-coding neutral sequence without a polyadenylation signal (see Supplementary material), leading to unusually bright nascent transcript foci (Figure 4a). The intranuclear distribution of nascent transcripts from the five most highly expressed lines showed no specific localization in cross sections of nuclei (Figure 4a,e–i). As in the case of smaller genes, the intensity of *X44* foci was unrelated to their distance from the nuclear periphery (see Supplementary material).

In summary, our results show that transcribed genes are distributed within the nucleus according to the known Rabl configuration of chromosomes and proximity of certain chromosomal sites to the nuclear periphery. We found that different transcribed genes have distinct intranuclear

Figure 4

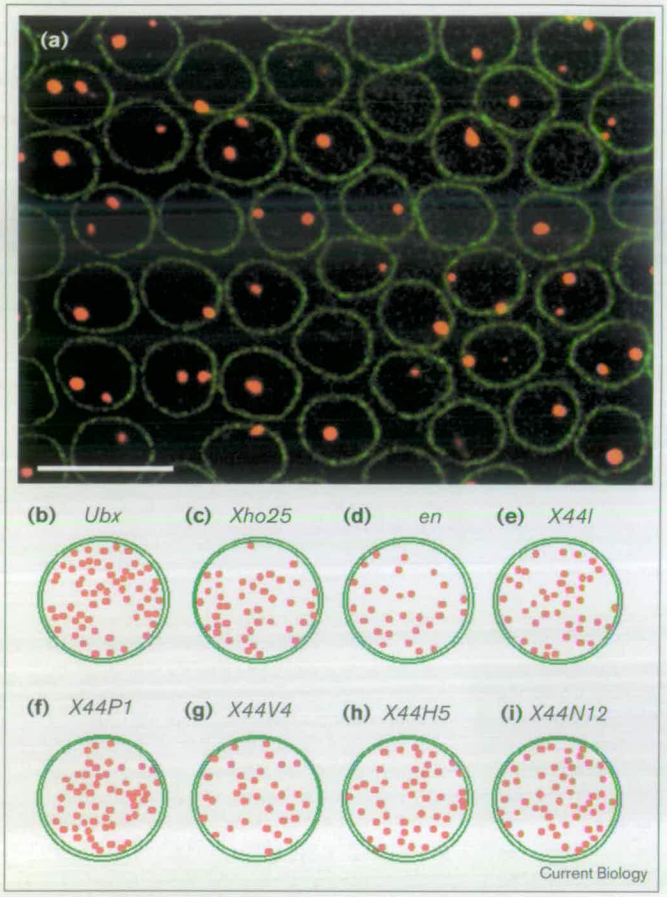

The intranuclear distribution of unusually abundant nascent transcript foci. **(a)** Nascent transcript foci (red) of the *X44* transgene, which lacks a polyadenylation signal (see Supplementary material). AlexaWGA marks the nuclear envelope (green). The scale bar represents 10 μm. **(b–i)** The intranuclear distribution of genes containing large nascent transcript foci viewed within a plane perpendicular to the apical–basal axis of the nucleus, showing no restrictions on their intranuclear position. (b) *Ubx*. (c,d) *Xho25* embryos stained with (c) a *lacZ* probe and (d) an *en* probe. (e–i) *X44* embryos from five of the strongest expressing transgenic lines stained with probes against the untranslated sequences in the construct.

distributions and their level of transcription is independent of their distance to the nuclear envelope. We interpret these results to mean that activation of transcription does not cause a major change in the intranuclear location of genes. If activated genes do move to new positions, then the distance moved must be small, and the sites to which they move must be numerous and evenly distributed. At least in *Drosophila* blastoderm nuclei, the distribution of actively transcribed genes is consistent with the possibility that transcriptional components are recruited to the site of the activated gene. These conclusions are likely to be general. Fundamental mechanisms such as recruitment of transcriptional components to genes and intranuclear transport of mRNA are unlikely to have evolved for a unique specialized role in the early *Drosophila* embryo. Indeed, there is evidence for a similar nuclear organization, and intranuclear transport of RNA in other systems [4].

Supplementary material

Supplementary material including additional methodological details and results is available at http://current-biology.com/supmat/supmatin.htm.

Acknowledgements

We thank David Ish-Horowicz, David Tollervey, Joe Lewis, Adrian Bird and Hildegard Tekotte for their useful comments on the manuscript, and Jeff Bond for help with statistical analysis of the data. The work was supported by a Wellcome Trust career development fellowship to I.D., an MRC studentship to G.S.W. and NSF and NIH grants to P.H.O.

References

1. Brown KE, Guest SS, Smale ST, Hanm K, Merkenschlager M, Fisher AG, *et al.*: **Association of transcriptionally silent genes with Ikaros complexes at centromeric heterochromatin.** *Cell* 1997, **91**:845-854.
2. Brown KE, Baxter J, Graf D, Merkenschlager M, Fisher AG: **Dynamic repositioning of genes in the nucleus of lymphocytes preparing for cell division.** *Mol Cell* 1999, **3**:207-217.
3. Singer RH, Green MR: **Compartmentalization of eukaryotic gene expression: causes and effects.** *Cell* 1997, **91**:291-294.
4. Marshall WF, Sedat JW: **Nuclear architecture.** In *Genomic Imprinting, An Interdisciplinary Approach.* Edited by Ohlsson R. Berlin: Springer-Verlag; 1999:283-301.
5. Wilkie GS, Davis I: **High resolution and sensitive mRNA *in situ* hybridisation using fluorescent tyramide signal amplification.** *Technical Tips Online* 1998, t01458 (http://www.biomednet.com/db/tto).
6. Marshall WF, Dernburg AF, Harmon B, Agard DA, Sedat JW: **Specific interactions of chromatin with the nuclear envelope: positional determination within the nucleus in *Drosophila melanogaster*.** *Mol Biol Cell* 1996, **7**:825-842.
7. Davis I, Francis-Lang H, Ish-Horowicz D: **Mechanisms of intracellular transcript localization and export in early *Drosophila* embryos.** *Cold Spring Harbor Symp Quant Biol* 1993, **58**:793-798.
8. Andrulis ED, Neiman AM, Zappulla DC, Sternglanz R: **Perinuclear localization of chromatin facilitates transcriptional silencing.** *Nature* 1998, **394**:592-595.
9. Croft JA, Bridger JM, Boyles S, Perry P, Teague P, Bickmore WA: **Differences in the localization and morphology of chromosomes in the human nucleus.** *J Cell Biol* 1999, **145**:1119-1131.
10. Klingler M, Soong J, Butler B, Gergen JP: **Disperse versus compact elements for the regulation of *runt* stripes in *Drosophila*.** *Dev Biol* 1996, **177**:73-84.
11. Shermoen AW, O'Farrell PH: **Progression of the cell-cycle through mitosis leads to abortion of nascent transcripts.** *Cell* 1991, **67**:303-310.
12. Gemkow M, Verveer P, Arndt-Jovin D: **Homologous association of the bithorax-complex during embryogenesis: consequences for transvection in *Drosophila melanogaster*.** *Development* 1998, **125**:4541-4552.
13. Hama C, Ali Z, Kornberg TB: **Region-specific recombination and expression are directed by portions of the *Drosophila engrailed* promoter.** *Genes Dev* 1990, **4**:1079-1093.
14. Davis I, Ish-Horowicz D: **Apical localization of pair-rule transcripts requires 3′ sequences and limits protein diffusion in the *Drosophila* blastoderm embryo.** *Cell* 1991, **67**:927-940.
15. Dernburg AF, Sedat JW: **Mapping three-dimensional chromosome architecture *in situ*.** *Meth Cell Biol* 1998, **53**:187.

Technical Tips Online

Simple History Results

Visualizing mRNA by *in situ* hybridization using 'high resolution' and sensitive tyramide signal amplification

Gavin S. Wilkie [a] and Ilan Davis [b] ilan.davis@ed.ac.uk

[a] Gavin S. Wilkie and [b]Ilan Davis are in the Institute of Cell and Molecular Biology, King's Buildings, Edinburgh University, Mayfield Road, Edinburgh EH9 3JR, Scotland.

Related fulltext articles on BioMedNet

Article Outline

Create new comment

Methods for analyzing the spatial distribution of mRNA by *in situ* hybridization have played a key role in studying development in *Drosophila* and other systems. The first methods for *in situ* hybridization made use of radioactive probes on wax sections (Ref. 1) or in whole mount (Ref. 2) followed by autoradiographic detection. This labour-intensive technique was slow and suffered from poor resolution. A substantially improved method involves the use of non-radioactive digoxigenin (DIG)-labelled probes in whole mount *in situ* hybridizations with highly sensitive alkaline phosphatase-based histochemical detection (Ref. 3, 4). However, the resulting dark stains are incompatible with fluorescent labelling and are visualized with much poorer spatial resolution than fluorescent markers.

One improvement in the resolution of histochemical detection has been to embed the whole-mount specimens in resin and section them using a microtome (Ref. 5). However, this variation is too labour intensive for general use and does not improve resolution sufficiently. Another solution has been to use alkaline phosphatase substrates that yield a red stain that is also fluorescent (Ref. 5). Unfortunately, the resulting stain slowly diffuses away from the site of enzyme activity, leading to poor spatial resolution and the need to analyze the samples immediately. In addition, the red stain emits mainly in the rhodamine channel but also partly in the fluorescein (FITC) channel, making it unsuitable for accurate double-fluorescence labelling. Some of these problems were recently solved by visualizing *Drosophila* mRNA with fluorescein-12-UTP labelled probes that are only barely detectable over background. The signal was improved by multiple antibody layers culminating in FITC-coupled antibodies (Ref. 6) or Cyanine-5 (Cy5)-coupled antibodies (G.S. Wilkie and I. Davis, unpublished). However, the fluorescent signal produced is fairly weak, making the technique practicable only for detecting a single highly abundant mRNA.

We have developed a new high-resolution fluorescence *in situ* hybridization protocol that overcomes the problems associated with previously described methods by using tyramide signal amplification (TSA). The technique depends on peroxidase-mediated deposition of fluorochrome-labelled tyramides at the location of the probe (Ref. 7). The detection is highly sensitive as it relies on enzymatic amplification of signal. High resolution is obtained because the reaction produces tyramide radicals that react covalently with proteins at the site of HRP activity, preventing appreciable diffusion of the signal (Ref. 8). Furthermore, the use of fluorescence allows quantitative high-resolution detection as well as double and triple labelling of different transcripts and other cell components.

Here, we use Cyanine-3 (Cy3) TSA to co-visualize *runt (run)* mRNA with the nuclear envelope at high resolution. *run* mRNA is exclusively localized to the apical cytoplasm, mainly in punctate dots (Fig. 1a). Nascent transcripts can be seen as two very intense foci of fluorescence in the nucleus, as previously reported in the case of other *Drosophila* transcripts using histochemical stains (Ref. 9, 10). In a separate experiment, we used the TSA technique to co-visualize the pair-rule transcripts *run* and *fushi tarazu* (*ftz*) with two different tyramide fluorochromes. *run* and *ftz* are expressed in a partially overlapping pattern in the embryo (Fig. 1b).

We have found that TSA has improved resolution compared with histochemical detection and is at least an order of magnitude more sensitive than fluorescent detection with secondary antibodies (Ref. 6). We anticipate that this technique could replace the existing methods for routine use in *Drosophila* and many other systems.

Protocol

:

Fixation

Wild type (Oregon R) *Drosophila melanogaster* embryos were dechorionated in 7% hypochlorite solution for two minutes, rinsed thoroughly with water and fixed in a two-phase mixture of 37% formaldehyde (Sigma) and heptane for five minutes with very gentle mixing. In addition to being faster than fixation in buffered 4% formaldehyde, this technique provides better preservation of microtubules in the embryo (Ref. 11). Fixed embryos were devitellinised in methanol, washed twice in methanol and stored at -20°C.

:

Prehybridization

Embryos were rehydrated for two minutes in 50% methanol : 50% PBT (1 ? PBS + 0.1% Tween20) , washed twice in PBT for two minutes and then post fixed for ten minutes in 4% formaldehyde in 1 ? PBS. Embryos were then washed five times for five minutes in PBT, followed by a five-minute wash in 50% PBT : 50% hybridization solution (HYB) and a further five-minute wash in HYB. Embryos were then prehybridized for at least one hour in HYB at 70°C. HYB consisted of 50% formamide, 5 ? SSC, 50 μg/ml heparin, 100 μg/ml *Escherichia coli* tRNA and 0.1% Tween20, and was adjusted to pH 6.5 with concentrated HCl.

:

Probe synthesis and hybridization

Antisense RNA probes, labelled with digoxygenin (Boehringer Mannheim) or FITC (Boehringer Mannheim), were synthesized as directed by the manufacturer by run-off transcription from restriction digested plasmids with SP6, T7 or T3 polymerases. *ftz* and *run* probes were 2 kb and 3 kb in length, respectively. Probes were used at a concentration of 0.5 ng/μl for hybridization overnight at 70°C.

:

Post-hybridization washes and antibody incubation

All washes (20 minutes each) were carried out at 70°C in a heat block with no agitation. Embryos were washed once in HYB, once in 50% HYB: 50% PBT, and four times in PBT. The embryos were then incubated for one hour in HRP-conjugated anti-digoxygenin IgG Sheep Fab fragment (Boehringer Mannheim), diluted 1/1000 in PBT, followed by three washes in PBT. When detecting very abundant transcripts we found that preabsorption of antibodies and blocking were not necessary. However, when detecting rarer transcripts, we found that non-specific background could be reduced by preabsorbing the antibody at a dilution of 1 : 100 overnight at 4°C with fixed and rehydrated (four ten-minute washes with PBT) embryos in PBT. The background can be reduced further by using a blocking step (0.5% non-fat milk powder or 2% bovine serum albumin) before antibody incubation and by adding 5% normal sheep serum to the antibody incubation step.

:

TSA Detection

The labelling was checked before TSA detection by developing a small sample of embryos with diaminobenzidine (Vector) (DAB) under standard conditions. DAB staining (brown/black) was visible within a few minutes under a dissecting stereo-microscope. Cyanine-3 (Cy3) tyramides (NEN Life Sciences, UK) or FITC tyramides (NEN Life Sciences, UK) from stock solutions were then diluted 1/50 in amplification diluent [TSA-Direct FISH (NEN Life Sciences, UK)] and added to embryos. Alternatively, the reagents could be used according to previously described methods of synthesising and using fluorescent tyramides (Ref. 7). The reaction was allowed to proceed for 2−10 minutes before washing three times for five minutes in PBT to remove unreacted substrate. The fluorescent tyramides were not visible in bright field microscopy, but the optimal reaction times were approximately the same with DAB and fluorescent tyramides. We were able to shorten the entire *in situ* hybridization procedure to a single day, at least in the case of abundant transcripts, by shortening the hybridization time to four hours and reducing each 20-minute wash to 10 minutes.

Co-visualization of two transcripts and of other cell components

To demonstrate the utility of the technique, we co-visualized two different mRNAs using Cy3-tyramine TSA to detect an FITC-labelled probe and FITC-tyramine TSA to detect a DIG-labelled probe. The first HRP-coupled antibody [anti-Fluorescein IgG Sheep Fab fragment (Boehringer Mannheim)] can be inactivated by a ten-minute incubation in 0.01M HCl (Ref. 8) or by a 15-minute incubation at 70°C (G.S. Wilkie and I. Davis, unpublished) before adding the second HRP-coupled antibody (anti-digoxygenin IgG Sheep Fab fragment).

Following TSA staining, the nuclear envelope was labelled by incubation in FITC-conjugated Wheat Germ Agglutinin (WGA) (Molecular Probes) at a concentration of 5 μg/ml in PBT for 1−4 hours. This decorates the nuclear pore complexes (NPCs). In other experiments (data not shown) we also co-visualised mRNA with microtubules by labelling with monoclonal anti β-tubulin antibody (Amersham) diluted 1/100 in PBT and then detected with Cy-5-conjugated F(ab')2 Donkey anti mouse IgG (H + L) antibodies (Jackson) at a concentration of 3 μg/ml (G.S. Wilkie and I. Davis, unpublished).

Mounting and imaging

Mounting and imaging

Embryos were mounted in vectashield (Vector Laboratories) and images were captured with a PXL-cooled CCD (Photometrics) camera on a Sedat/Agard widefield microscope (Applied Precision) based on an Olympus IX70 inverted microscope. Out-of-focus light was reassigned using Sedat/Agard 3-D deconvolution algorithms (Delta Vision software). Very similar results were obtained using a Leica laser scanning confocal microscope (data not shown).

Figure 1

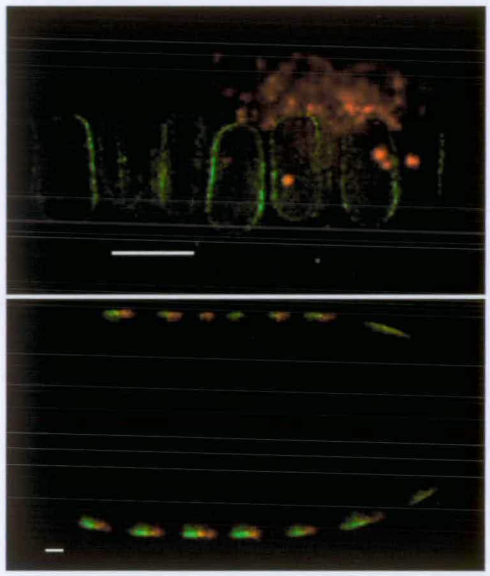

FIGURE 1.
Co-visualising ftz and run transcripts. (a) A high power (x 100 objective) view of run mRNA (Cy3-tyramide in red) and the nuclear envelope (WGA-FITC in green) in cross-section through a stage 5 blastoderm embryo. The edge of the embryo is oriented uppermost. The image represents 1 µm of focal depth, produced by projecting (superimposing) the maximum intensity of 5 adjacent 0.2 µm deconvolved Z sections into one image. run mRNA is visible in the apical cytoplasm as very bright red fluorescent dots and bright nascent transcripts within the nucleus. The scale bar represents 10 µm. (b) A low power (x 20 objective) co-visualisation of run mRNA (FITC-tyramide in green) and ftz mRNA (Cy3 tyramide in red) in cross-section through a stage 5 blastoderm embryo. The scale bar represents 20 µm.

Acknowledgements

We are grateful to Joe Lewis and Andrew Jarman for their helpful comments on the manuscript. This work was supported by the Wellcome Trust through a career development fellowship to I.D. (44878/Z/95/Z)

References

[1] Akam M.E. (1983) EMBO J. , 2:2075-2084.
[2] Edgar B.A. and Ofarrell P.H. (1989) Cell , 57:177-187.
[3] Lehmann R. and Tautz D. (1994) Methods Cell Biol. , 44:575-598.
[4] Tautz D. and Pfeifle C. (1989) Chromosoma , 98:81-85.
[5] Francis-Lang H., Davis I. and Ish-Horowicz D. (1996) EMBO J., 15:640-649.
[6] Hughes S.C., Saulierledrean B., Livnebar I. and Krause H.M. (1996) Biotechniques , 20:748-750.
[7] Raap A.K. et al. (1995) Hum. Mol. Genet., 4:529-534.
[8] Speel E.J.M., Ramaekers F.C.S. and Hopman A.H.N. (1997) J. Histochem. Cytochem. , 45:1439-1446.
[9] Davis I. and Ishhorowicz D. (1991) Cell , 67:927-940.
[10] Shermoen A.W. and Ofarrell P.H. (1991) Cell , 67:303-310.
[11] Theurkauf W.E. (1992) Dev. Biol., 154:205-217.

D. Supplementary Movie Legends

The supplementary time lapse movies are recorded on a CD placed inside the back cover of the thesis, and can be viewed using Quicktime Player or equivalent software.

Movie 1. Injected *run* RNA localises rapidly to the apical cytoplasm. Time lapse movie of apical localisation of *run* RNA (red) injected into the basal cytoplasm of a blastoderm embryo expressing a nuclear GFP (green). The images were captured at 20 second intervals for a total of 30 minutes.

Movie 2. Injected *wg* RNA localises as discrete particles. The site of injection was off the bottom of the image. Numerous particles of wg RNA form within 30 seconds of injection, and move directly to the apical cytoplasm (top of image) along straight paths. The images were captured at 10 second intervals for a total of 8 minutes.

Movie 3. Coinjection of different apically targeted transcripts. *run* RNA (green) and *ftz* RNA (red) were coinjected into the basal cytoplasm of a blastoderm embryo. Both types of RNA become localised to the apical cytoplasm. A mixture of red, green and yellow particles can be seen moving apically from the site of injection, showing that some particles consist exclusively of *run* or *ftz* RNA, whereas some particles contain both types of RNA.

Movie 4. *stg* RNA does not become localised to the apical cytoplasm after injection. Dual DIC/fluorescence movie of a living blastoderm embryo injected with *stg* RNA (green) in the basal cytoplasm. Some particles form from the injected *stg* RNA, but they do not show directed movement and no *stg* becomes localised to the apical cytoplasm above peripheral nuclei. The images were captured at 10 second intervals for a total of 8 minutes. After 1 hour, the *stg* RNA had diffused to all parts of the embryo (data not shown).

Movie 5. *hb* RNA does not become localised to the apical cytoplasm after injection. *hb* RNA was injected into the basal cytoplasm, and images were captured at 10 second intervals for 8 minutes. Particles of *hb* RNA do not display any directed movement. The apical cytoplasm is situated at the top of the image.

Movie 6. *run* localisation intermediates do not contain *hb* RNA. *run* RNA (green) and *hb* RNA (red) were coinjected into the basal cytoplasm of a blastoderm embryo. The *run* RNA becomes localised to the apical cytoplasm above the site of injection, whereas the *hb* RNA diffuses away from the site of injection in all directions. Particles of *run* RNA undergoing directed apical movement do not contain detectable amounts of *hb* RNA.

Movie 7. Pre-injection of colcemid inhibits apical localisation of injected *run* RNA. Dual DIC/fluorescence movie of two embryos injected with run RNA (green) in the basal cytoplasm. Preinjection of water does not disrupt apical localisation of injected RNA, whereas colcemid completely inhibits localisation. The effects of colcemid are reversed by 10 second exposure to UV which inactivates the drug, allowing microtubules to repolymerise.

Movie 8. Pre-injection of anti dhc antibody inhibits the apical localisation of *run* RNA. Anti dynein antibody injection also leads to the lateral diffusion of the RNA.

Movie 9. Hypomorphic mutations in cytoplasmic dynein heavy chain reduce the speed of apical movement of particles of injected RNA. RNA particles move more slowly in the $Dhc64C^{8-1}/Dhc64C^{6-10}$ mutant embryo on the right. Apical localisation of *run* RNA particles are shown in an equivalent wild type embryo for comparison on the left.

Movie 10. Excess p50/dynamitin causes frequent stalling and plus end directed movement of apically-targeted RNA. *ftz* RNA was injected into an embryo which was earlier injected with an excess of human recombinant GST-p50/dynamitin. The red cross marks a particle of *ftz* RNA which makes three long pauses during apical localisation. This *ftz* particle also moves back towards the basal cytoplasm (plus end directed movement) before continuing apical localisation. Images were captured at 10 second intervals.